The effect of gel structure on ionic conductance and capacitor impedance

The Effect of Gel Structure

on

Ionic Conductance and Capacitor Impedance

by

JULIAN HOLLOWAY, M.Sc.

A DOCTORAL THESIS

Submitted in partial fulfilment of the requirements

for the award of

Ph.D of the Loughborough University of Technology

February 1979

Supervisors: Prof. D.S. CAMPBELL.
Dr. N.A. HAMPSON.
Mr. N.F. JACKSON.
Dr. M.J. JAYCOCK.

SUMMARY.

The aim of this work was the determination of the effects of gelling the electrolytes used in electrolytic capacitors of the type Ta/Ta_2O_5/gel electrolyte/counter electrode. The investigation was divided between two main areas:- Firstly, the ionic conductivity of gel electrolytes was examined using Pt/Pt black electrodes. Secondly, the influence of various electrolytes on the properties of tantalum and Ta/Ta_2O_5 electrodes, and on the electrolytic capacitors was examined.

The conductivity of a series of gels prepared from fumed silica and 40% sulphuric acid showed a non linear dependence on silica content, but was sensitive to the method of preparation. A standard mixing technique was developed and the reproducible conductivity of gels prepared by this method showed a linear decrease with increasing silica content.

The conductance of gels prepared from a range of sulphuric acid and potassium chloride solutions with varying silica contents was measured at several temperatures. A linear decrease in conductance with increasing silica content was found for all gels except those prepared from 0.001D H_2SO_4 and 0.01D KCl which gave an increase in conductance. This change of slope is indicative of a change in conducting pathway and suggests that the surface conductance along the gel network swamped by the bulk conductance of the large excess of H^+ ion at higher concentrations has become the favoured pathway.

A method of predicting the linear decrease in the conductance of gels is described and the possible distributions of silica within the gel are discussed.

The differential capacitance of the tantalum electrode was measured in a series of aqueous solutions using conventional polarized AC bridges. Two types of solution were used: solutions containing simple inorganic ions; and oxalate solutions.

The results indicated that the tantalum pentoxide film invariably present on tantalum is extremely difficult to remove. However, there is some evidence that the oxide film is forced off the metal for a limited potential range in solutions containing oxalate as a complexant. It is not possible to determine the point of zero charge potential because the concentration dependent diffuse layer minimum could not be identified and must presumably lie outside the experimentally available range.

The breakdown processes of Ta/Ta_2O_5 were found to be inhibited by gelled sulphuric acid, but the electrical properties of oxide formed by anodization of tantalum foil in gelled sulphuric acid instead of the acid alone were unaffected, and no evidence of incorporation of silica into the oxide structure was found.

The effect of gelled electrolyte on the properties of capacitors was small. The improvement in stability to the effects of orientation and leakage through the seal for capacitors with gelled electrolyte has to be balanced against the lower $-55^{\circ}C$ impedance for capacitors with ungelled electrolyte.

To my parents

and Christine

ACKNOWLEDGEMENTS

I wish to express my appreciation to my four supervisors: Professor D.S. Campbell, Dr. N.A. Hampson, Mr. N.F. Jackson and Dr. M.J. Jaycock for their careful guidance, enthusiastic encouragement and patience during the course of this work.

I would also like to thank the Research Managers of the Tantalum Capacitor Division of the Plessey Co. Ltd: Mr. D. Haywood and Mr. R.A. Hancock, for their help with the Industrial aspects and for their contributions to the regular discussions.

I am grateful for the assistance given by members of the technical staff at the Loughborough University of Technology, the Allen Clark Research Centre, and the Tantalum Capacitor Division of the Plessey Co. Ltd.

Finally, financial support from the Science Research Council, the Loughborough University of Technology and the Plessey Co. Ltd. are acknowledged.

Declaration of Originality.

I am responsible for the work submitted in this Thesis. The original work is my own except as specified in acknowledgements or in footnotes. Neither the Thesis nor any of the original work contained within it have been previously submitted to any institution for a higher degree.

Julian Holloway

1979.

CONTENTS.

FIGURES.

TABLES.

GLOSSARY.

a_i	activity of species i
A	Area
AC	Alternating Current
C	Capacitance
C_a	Capacitance of anode
C_c	Capacitance of cathode
C_{cap}	Capacitance of a capacitor
C_g	Capacitance due to the diffuse layer
C_H	Capacitance due to the compact layer
C_p	Equivalent parallel Capacitance
C_s or C_{xs}	Equivalent series Capacitance
d	distance
d	loss angle
d'	intrinsic loss angle
D	Demal
E	Potential
E_{ecm}	Potential of the Electrocapillary Maximum
E_d	Differential Field Strength
f	frequency
F	Faraday
F	Formation Resistivity Factor
G	Conductance
I	Current
j	$\sqrt{-1}$
K	Conductivity
K_{cell}	Cell Constant

K_i	Conductivity of i
L_t	total inductance of a Capacitor
L	length
Leak.	Leakage current
M	Molecular weight
n	number of spherical primary silica particles
N_a	number of spherical primary silica particles in an aggregate
N_{cp}	number of close packed aggregates per unit volume
N_s	number of aggregates per gram of silica powder
P	sheer stress
P_k	static yield point
q	charge per unit area
r_a	radius of silica aggregate
r_p	radius of spherical primary silica particles
R	Gas Constant
R	Resistance
R_i	true ohmic resistance of electrolyte
R_{adl}	anode dielectric leakage resistance
R_{cdl}	cathode dielectric leakage resistance
R_e	electrolyte resistance
R_p	Equivalent parallel resistance
R_s or R_{xs}	Equivalent series resistance
S	constant (page 117)
S	Siemens
SCE	Standard Calomel Electrode
t	time

T	Temperature
T	Tortuosity
V	Void Volume
V	Voltage
w_i	weight of i
-W-	Warburg impedance
x	shape factor
y	axial ratio
<z>	mean distance of the net ion excesses from the electrode
z	electrochemical equivalent
z_i	impedance of i
α	thermal coefficient of conductivity
γ	Interfacial tension
ε_i	dielectric constant
ε	interfacial permittivity
θ	contact angle
ρ_i	density of i
ρ_i	resistivity of i
$\sigma_{\pm(z)}$	excess ion distribution
Γ	surface excess of adsorbed species
ϕ	phase angle, Cos ϕ = power factor
ϕ	porosity
ϕ	surface coverage
ϕ_i	volume fraction of i
ϕ_i	potential of i
ω	$2\pi f$ where f is the frequency

THE INTRODUCTION.

1. 1. The project was initiated by the Tantalum Capacitor Division of The Plessey Company Ltd. in an attempt to increase the basic understanding of the processes occuring within a tantalum electrolytic capacitor of the type:

Ta/Ta_2O_5/"gelled" sulphuric acid electrolyte/Ta counter electrode. A diagrammatic section through such a capacitor is given in fig 1. 1.

The most important part of any electrolytic capacitor is the oxide film produced on a metal by anodization, and acting as the dielectric. For this case the dielectric is a film of tantalum pentoxide. Although most metals will form an oxide during corrosion, there are a few which form a highly tenacious continuous oxide. The oxide forms a protective layer preventing further attack on the metal and normally reaches a limiting thickness. The thickness of the oxide may be enhanced by anodizing the metal in an electrolytic bath. The process of anodization, see Hoar (1959), Young (1961), or Campbell (1966, 1971) involves making the metal the anode of an electrode system and applying a potential across the electrodes. Metals in this category include zirconium, niobium, silicon, aluminium, and tantalum, the last two being widely used commercially in electrolytic capacitors. The thickness of the oxide after anodization is dependent on the potential applied. The maximum thickness for tantalum is approximately 1.1 μm, and a useful rule of thumb is that the oxide increases by 1.6 nm for each volt applied.

The tantalum pentoxide is a dense, relatively inert substance highly resistant to acids. It may only be brought into solution by fusing with alkali hydrogen sulphate, alkali carbonate, or hydroxide

Figure 1. 1.

TANTALUM CAPACITOR

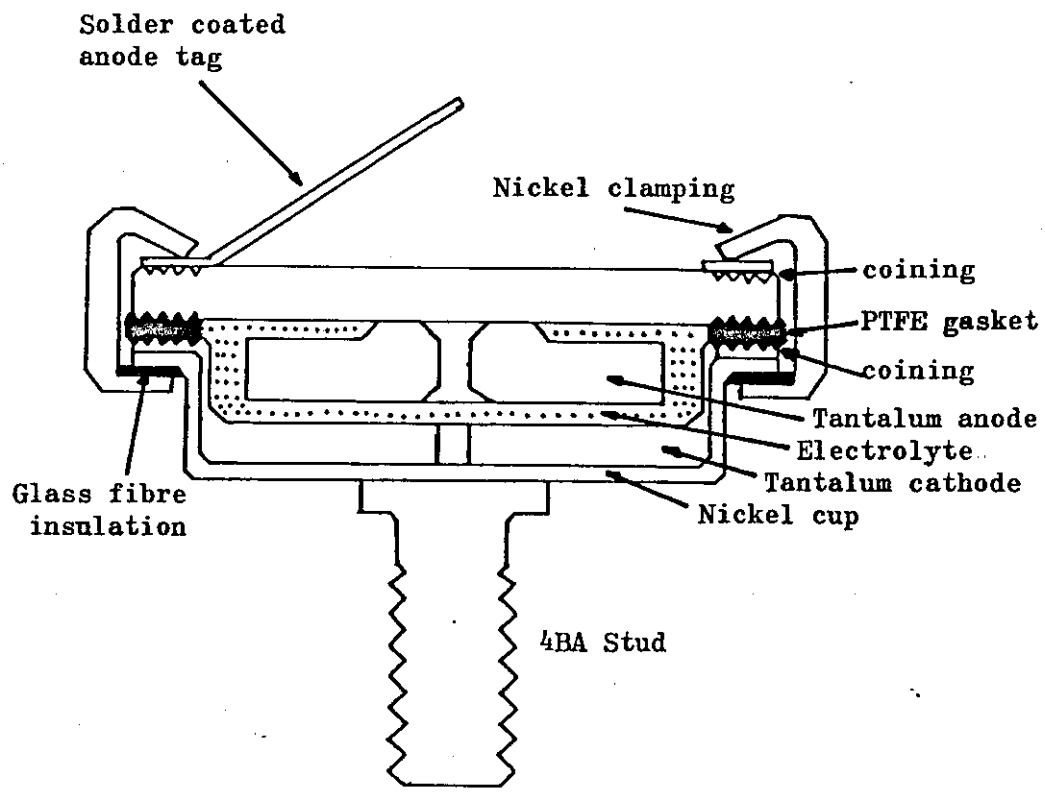

or by treatment with hydrofluoric acid. Tantalum is also very resistant to chemical attack because it is invariably covered with a thin protective layer of oxide. The best solvent is a mixture of nitric and hydrofluoric acids resulting in a solution containing fluoro complexes. Therefore tantalum capacitors are of special value in the demanding environments of avionics and military equipment.

Tantalum can be obtained in the form of a high quality (99.99%) powder with a particle size of 4-10 μm diameter, and of narrow particle size distribution. The powder may be sintered by heating to 2000°C, with the secondary advantage of removing impurities from the surface of the tantalum particles.

1. 2. The Manufacture of Tantalum Capacitors.

The anode of the tantalum capacitor is formed by pressing the powder mixed with a small quantity of wax as a binding agent into the desired shape around a tantalum support wire or cup. The powder body is heated under vacuum to remove the wax before the temperature is raised to 2000°C to give a porous sintered body of large surface area/unit volume. The porous body is anodized to form a tantalum pentoxide layer of the required thickness. By this method a capacitance of more than 7,000 $\mu F\ gm^{-1}$ is attainable which is equivalent to 7.47 $\mu F\ cm^{-2}$ for the 4 μm diameter particles.

The porous cathode, also of tantalum, is supported in a nickel cup, and is anodized at low voltage to give a thin oxide dielectric which gives the capacitor a partial protection under reverse voltage conditions.

Prior to assembly of the capacitor and the addition of a metered amount of "gelled" electrolyte, both anode and cathode are pre-soaked with a small amount of 40% by weight sulphuric acid.

If the gel electrolyte is added to the dry components, some of the acid is drawn into the porous bodies and the conducting path between the electrodes of the capacitor may be greatly reduced or broken due to air bubbles, causing the capacitor to fail.

The seal, designed for maximum electrolyte retention and to minimise vapour diffusion from the capacitor, comprises a PTFE gasket clamped between the coined plates of the anode and cathode by a work hardened nickel clamp ring. There is also glass fibre insulation between the cathode and the nickel clamp ring. This provides a very efficient seal of high reliability, essential because of the nature of the electrolyte and of advantage in severe environments.

The assembly requires a small air gap of ~ 15% of the volume available to the gelled electrolyte because of the need to rigidly exclude any acid or gelled electrolyte from the coined plates of the anode and cathode, see fig. 1.1. Failure in this respect leads to a high leakage current for the capacitor.

1. 3. Comparison of Electrolytic Capacitors.

In order to compare the performance of capacitors the capacitance and power factor are normally quoted. These parameters are based on the assumption that the equivalent circuit of the component is that of a resistor and capacitor in series. The equivalent series capacitance obtained using this assumption is not of necessity that of the anodic oxide dielectric alone.

Consider the double layer on a film-free metal in an electrolyte. This situation may be described in terms of the simple model of a layer of charge on the metal facing a layer of charge of the opposite sign

due to an excess of ions of one sign in the adjacent solution. The various models and theories of the double layer of the metal/solution interface are discussed in chapter 2. In a concentrated solution the two layers are as close as the physical size of the ions permits, thus producing a large capacitance per unit area of electrode. The capacitance, C, may be calculated using the simple Helmholtz expression for a parallel plate capacitor:

$$C = \frac{\mathcal{E}A}{4\pi d} \qquad 1.1.$$

where $\mathcal{E}$ = dielectric constant, $\hat{A}$ = area, and d = distance of separation.

The effect of an oxide film on tantalum may be considered to be that of an insulating dielectric causing a larger separation of the two layers of charge, and therefore a reduction in the capacitance. This simple model has support from the experimental observation that the reciprocal of the capacity is found to be very accurately linearly dependent on the film thickness (Young, 1961). Departure from this behaviour is due to flaws in the oxide film which provides leakage conductance.

The equivalent circuit for such a film is:

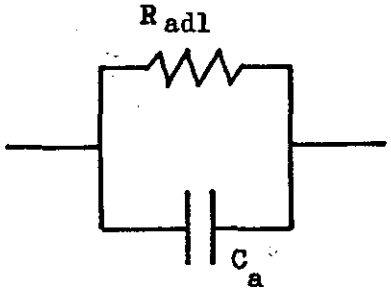

where R_{adl} is the anode dielectric leakage resistance and C_a is the capacitance of the anode.

The equivalent circuit for a fixed electrolytic capacitor has been represented in several ways:-

1. Mead (1962) used the circuit

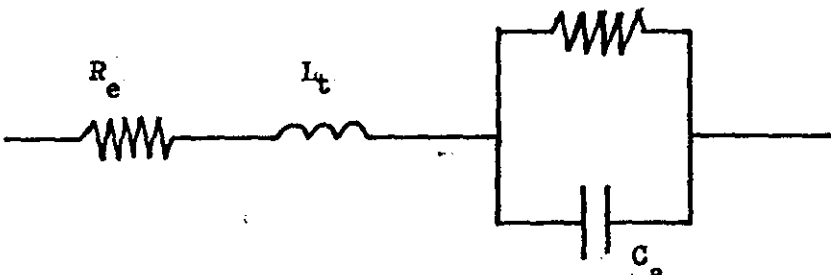

where R_e is the electrolyte resistance and L_t is the total inductance of the capacitor.

2. Harris (1974) in his review of trends in the design and performance of tantalum capacitors used:

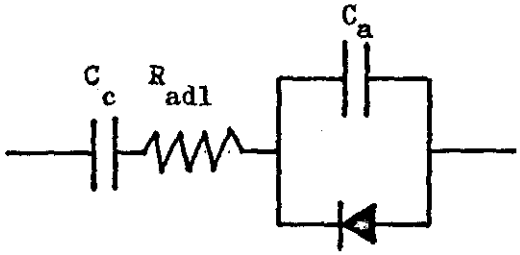

$$C_{cap} = \frac{C_a \cdot C_c}{C_a + C_c} \qquad 1.2.$$

$$\tan d = C_{cap} R \qquad 1.3.$$

3. A more complete equivalent circuit (after Campbell,1971) for a tantalum capacitor is:

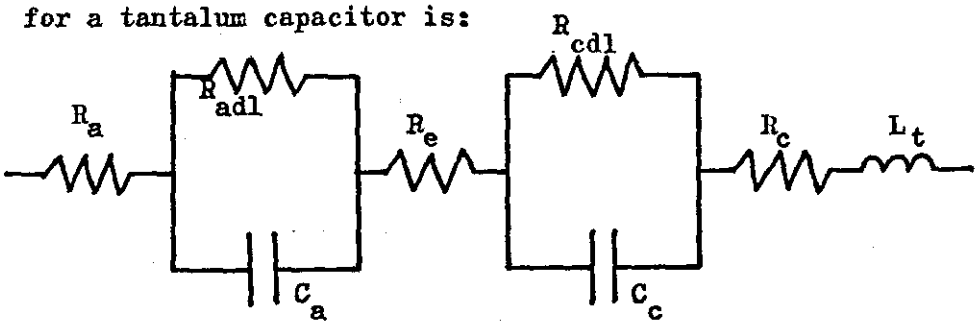

where R_a and R_c are the resistance of the tantalum of the anode and cathode respectively, R_{adl} and R_{cdl} are the resistances of the anode and cathode dielectric leakages, C_a and C_c are the capacitances of the anode and cathode, R_e is the resistance of the electrolyte and L_t is the total inductance of the circuit.

The two resistances R_a and R_c may be ignored compared to R_e, and at low frequencies L_t may also

be neglected. Furthermore the capacitance of the cathode may be neglected as it is very small relative to that of the anode. Thus the circuit simplifies to:

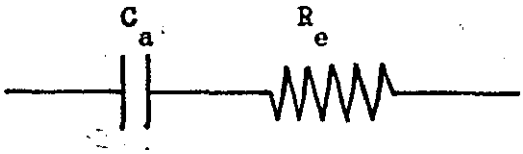

provided the contributions R_a, R_c, R_{cdl}, L_t, R_{adl}, and C_c may be ignored.

Consider this model for the anode of the capacitor in an electrolyte with a counter electrode ie Ta/Ta_2O_5/electrolyte/electrode. When a potential is applied across the cell and balanced by an AC bridge the results may be expressed in terms of the equivalent series or parallel combinations of resistance and capacitance for the cell as a whole.

The two measurements are related by the expressions:

$$R_s = R_p(1+\omega^2 C_p^2 R_p^2) \qquad 1.4.$$

$$C_s = C_p(1+1/\omega^2 C_p^2 R_p^2) \qquad 1.5.$$

where $\omega = 2\pi f$ and f is the frequency. If the impedance of the counter electrode and the electrolyte resistance can be determined separately then the contribution of the oxide film to the measured values can be calculated.

For an ideal capacitor the voltage and current would be 90^o out of phase and there would be no dissipation of power ie $R_p = \infty$, $R_s = 0$.

For real capacitors the behaviour is expressed in various ways. The mean rate of power dissipation for AC is given by $VI\cos\phi$ where ϕ is the phase angle between V and I. $\cos\phi$ is referred to as the power factor and is in general a function of the frequency:

$$\cos\phi = \omega CR \qquad 1.6$$

The deviation of ϕ from the ideal value of 90^0 is called the loss angle d, ie $d = (90^0 - \phi)$. The loss tangent tan d, is given by $\tan d = \omega C_s R_s$.

Tan d , $\cos\phi$, and d are all nearly equal for a good capacitor, because for small d

$$\tan d \simeq \sin d = \cos\phi \simeq d \text{ (radians)} \qquad 1.7.$$

The loss tangent is sometimes split into two contributions $\tan d = \tan d' + \omega CR$ where $\tan d'$ is the intrinsic loss and is frequency independent. Tan d' is usually determined from a plot of tan d versus frequency by extrapolation to zero frequency.

Although the behaviour of electrolytic capacitors is too complex to be described adequately by the simple equivalent circuit, a number of useful generalisations may be stated (Franklin, 1961):-

1. The capacitance is approximately that of the anode and cathode in series provided that the length of the electrolyte path between all regions of the anode and corresponding regions of the cathode is constant, and that the electrodes have no appreciable inductance.

2. For porous electrodes, such as those in tantalum electrolytic capacitors, there are unequal path lengths between the cathode and various parts of the dielectric, the capacitance may be less than the above value and there is a greater dependence of capacitance and power factor on the frequency of the alternating test voltage. The effect is greatest for the least conductive electrolytes. see Morley (1970), and Morley and Campbell (1973).

3. If the electrodes are appreciably inductive similar effects to that obtained for porous electrodes may be found.

4. The capacitance increases as the temperature is raised e.g. see Coursey (1937), Deeley (1938), Georgiev (1945) or Gaut (1957) and the magnitude of the change is dependent on the construction of the capacitor and, particularly at low temperatures, on the resistivity of the electrolyte.

5. The power factor is very high at low temperature owing to the high resistivity of the electrolyte, but falls when the temperature is raised because the electrolyte becomes more conductive, reaching a minimum at a temperature in the range 40 - 100^{o}C.

6. At higher temperatures the power factor is increased, probably because of increases in the dielectric losses of the oxide film.

7. As the frequency of the alternating test voltage is raised the equivalent series resistance drops to a fairly constant value which is approximately the same as the electrolyte resistance. Young (1955).

8. For most capacitors over restricted ranges the reciprocal of capacitance is linearly dependent on the logarithm of the frequency of the alternating test voltage, and the equivalent series resistance minus the electrolyte resistance is proportional to the periodic time, Young (1955). These relationships can be explained in terms of the ionic relaxation of ions moving in the oxide film occuring with such a wide range of relaxation times due to the amorphous nature of the film that an almost frequency independent tan d is produced, see Winkel and de Groot (1958) and Young (1959).

The effect of the resistance of the electrolyte in determining the final properties of the capacitor explains the choice of the highly conductive sulphuric acid electrolyte for use in tantalum capacitors. In order to give the desired standard of performance there is a need to maintain a high conductivity (low dissipation) over the temperature range $-55^{\circ}C$ to $+125^{\circ}C$.

During the early development of tantalum electrolytic capacitors two main problems were identified relating to the use of sulphuric acid

electrolyte: failure of the casing, i.e. leakage of acid; and the development of orientation sensitivity of the capacitance due to movement of the electrolyte within the capacitor. The attractive solution to these problems is the use of electrolyte contained in a gel system as the solution phase of the capacitor.

The gelling medium in common use in the Capacitor Industry at present is fumed silica, chosen for its compatibility with sulphuric acid, ease of handling, and low cost. Fumed silica has found a similar use in the Accummulator Industry for the stabilising of the sulphuric acid electrolyte in certain storage batteries e.g. Rauter (1965).

1. 4. Scope of the work.

The main aim of this work was the investigation of the effect of addition of fumed silica to sulphuric acid electrolyte on the double layer characteristics at the electrode-electrolyte interface. This aim would have most readily been achieved by measuring the impedance of the electrode-electrolyte combination. However, the oxide-metal electrode is difficult to reproduce exactly and would have produced capacitative dispersion due to the dielectric leakage, and any cracks, pores, or other surface inhomogeneity would have produced a marked effect in the de Levie sense (de Levie (1967)).

Consequently, the investigation was divided into three parts:-

1. The ionic conductance of the silica-sulphuric acid electrolyte system was to be examined using model electrodes at which dispersion would be expected to be minimum, i.e. Pt/Pt black electrodes.
   It was also hoped to examine other electrolyte systems that might offer any possible technological advantage.

2. The second part of the work was to be concerned with the properties of a tantalum/tantalum pentoxide electrode in contact with various electrolytes including gelled electrolytes.

3. Some time was also allocated to be spent at The Plessey Co. Ltd. developing ideas formulated at Loughborough.

CHAPTER 2

2. 1. The Interface.

In the previous chapter the equivalent circuit used to compare the electrical properties of the anodic part of a capacitor was derived from a very simple model of the electrical double layer at the metal-oxide/solution interface. An understanding of the theoretical background and the experimental techniques available to study the double layer are required before this simple model can be accepted and experimental investigations devised and interpreted.

The theory of the properties of the metal/solution interface has developed from the investigation of a metal in contact with a dilute solution of a simple electrolyte, and particularly from the study of the mercury-electrolyte solution interface. Mercury is of particular value in this context as it is readily available in a high state of purity, and because it is a liquid at room temperature the complications of surface roughness, and the determination of true surface areas,are not encountered. Furthermore, mercury, unlike most solid metals, does not suffer from the adsorption of oxygen and hydrogen from most aqueous solutions.

The formation of an interface will nearly always involve some redistribution of the electrical charge associated with the particles drawn from the bulk or homogeneous portion of the phase to form the interfacial region (layer). The redistribution is described in terms of the formation of the electrical double layer, a general term for the structure of the interfacial region, which may in practice consist of a number of distinct layers or regions.

Four types of redistribution may be distinguished:

1. Charge transfer across the interface.
2. Unequal adsorption of ions of opposite charge.
3. Adsorption and orientation of dipolar molecules.
4. Deformation of polarizable atoms or molecules in the unsymmetrical force field at the interface.

The thermodynamic analysis of the electrode/electrolyte interface is considerably simplified in the absence of any electrode reactions whether oxidation or reduction processes. Electrodes fulfilling this condition i.e. when under an applied potential no charges, electrons, or ions are transferred across the interface and hence electrochemical equilibrium is unattainable, were termed ideal polarized electrodes by Grahame and Whitney (1942).

The mercury/solution interface can be made such that it may be considered to be ideally polarizable, and is particularly favourable because the high over-voltage for hydrogen evolution gives a wider range of applied potentials accessible experimentally than for other electrodes.

The tendency of a liquid body to contract its surface, and, when unconstrained and in the absence of a gravitational field, to assume a spherical shape has long been recognised to be associated with the intermolecular forces at the interface between the liquid and its surroundings, usually gaseous. The tendency to contraction is described in terms of an interfacial tension γ. The interfacial region is considered to be a separate phase of characteristic composition, see fig. 2. 1, homogeneous in two directions as

Fig. 2.1 The Interface between Two Phases.

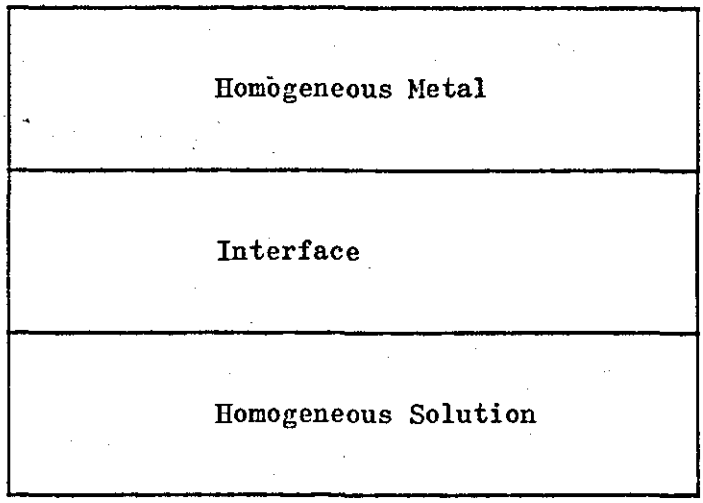

Fig. 2.2 Gibbs Model of the Interface between Two Phases.

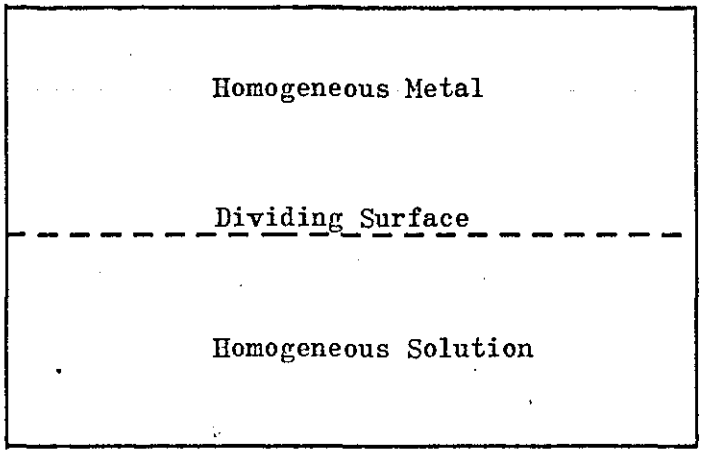

compared to the three directions of a bulk phase. For simplicity only flat interfaces will be considered. The interfacial tension of a curved interface has the same value as that of a flat interface provided the radius of curvature is not of the order of molecular dimensions.

Gibbs (1928) postulated a simple model of the interface of two phases for thermodynamic analysis. The two bulk phases were considered to be homogeneous up to a hypothetical dividing surface located within the interfacial region, see fig. 2.2 . At the dividing surface one of the components has a surface excess, Γ_1, of zero, and the other component is adsorbed and has a surface excess, Γ_2. The surface excess of the adsorbed species at the interface is related to the change in the interfacial tension, $d\gamma$, by the equation:

$$d\gamma = -RT\Gamma_2 \, d\ln a_2 \qquad 2.1.$$

where R = gas constant, T = temperature (K), a = activity$_2$. This equation was shown to be applicable to the ideally polarized electrode without loss of rigour and with much simplification by Grahame and Whitney (1942) .

Grahame (1947) reviewed the background of this treatment, Parsons and Devanathan (1953) have given a very thorough analysis, and Parsons (1954) has used a particular case of his general treatment to demonstrate the essential points in the derivation of the equation:

$$-d\gamma = q \, dE_{\pm} + \Gamma_{\pm} \cdot d\mu \qquad 2.2.$$

which relates the change in interfacial tension, $d\gamma$, to the charge, q, per unit area on the metal. The potential of the electrode

is $E_{\pm}$ with respect to a reference electrode which is reversible to either the cation (E_+) or the anion (E_-). The surface excess of adsorbed species is $\Gamma_{\pm}$, either anion (Γ_-) or cation (Γ_+), and the change in chemical potential of the other species is $d\mu$.
The equation is valid only for constant pressure, temperature and electrode composition.

Rearangement of equation 2. 2 enables the charge per unit area on the electrode to be given by:

$$q = -\left(\frac{d\gamma}{dE}\right) \qquad 2.\ 3.$$

which is the Lippmann equation.(1875).

2. 2. Experimental methods of examining the Double Layer.

From equation 2.3 it is apparent that a useful method of investigating the metal-solution interface is to determine the charge from the variation in interfacial tension with applied potential. (The potential is measured relative to that of a reversible reference electrode e.g. standard calomel electrode) There are several experimental techniques available for this purpose:

1. The capillary electrometer, see fig. 2.3, was first used by Lippmann (1875) and is an example of the capillary rise method of determining interfacial tension. Consequently, the plots of interfacial tension versus applied potential are commonly referred to as electrocapillary curves. The interfacial tension is proportional to the height of mercury required to bring the interface to a given point on the capillary.

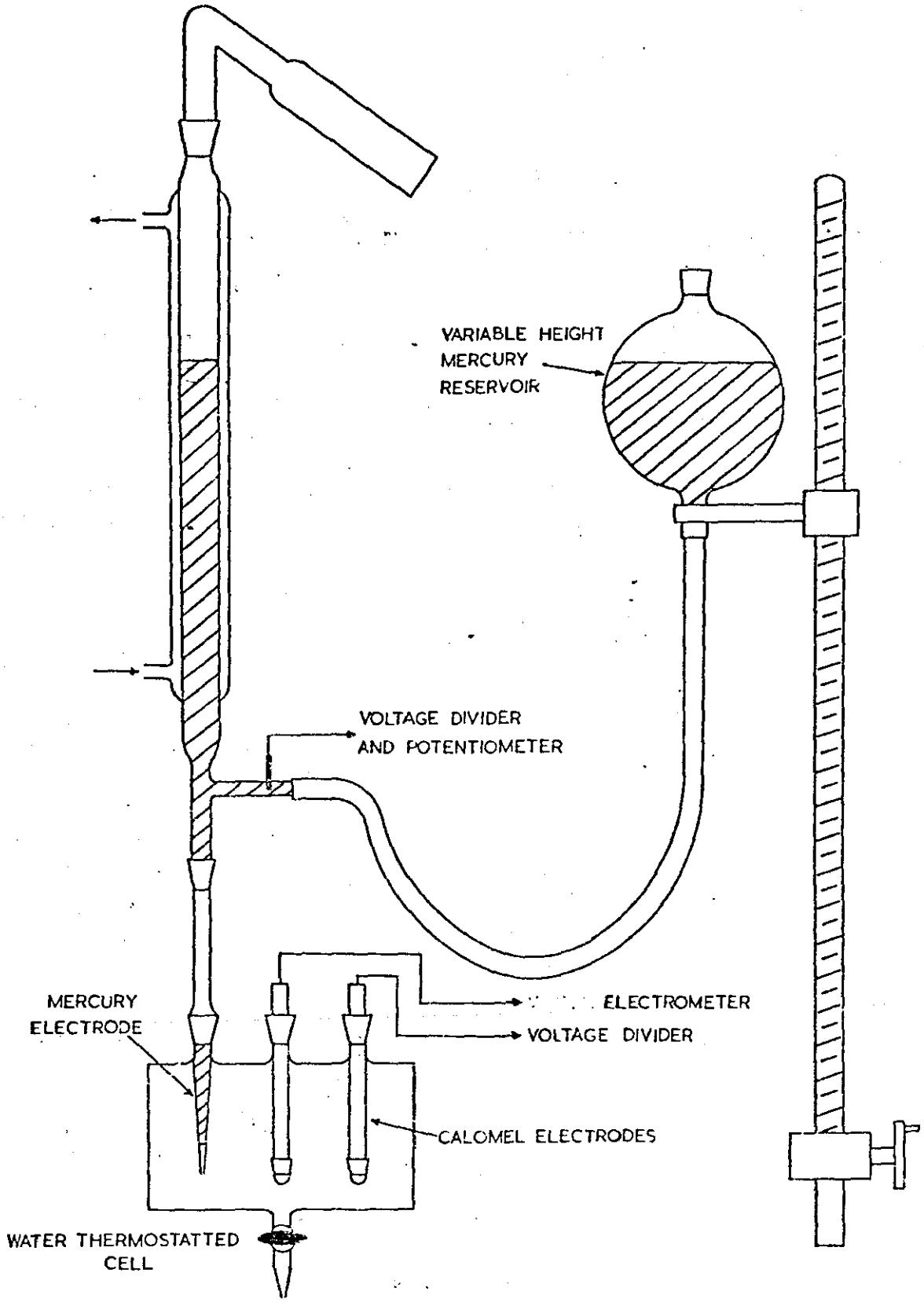

Fig. 2.3 THE CAPILLARY ELECTROMETER.

2. The dropping mercury electrode, which utilises the drop weight method of determining interfacial tension, is shown schematically in fig. 2.4. The drop weight is proportional to the interfacial tension, and the proportionality constant may be determined empirically or theoretically.

3. A method which has regained importance in recent years with the development of on-line computer techniques which both run the experiment and analyse the results is the maximum bubble pressure. In this technique the capillary is turned upwards and the pressure of mercury is slowly increased. There is a critical pressure beyond which the mercury drop on the capillary is unstable and the drop bursts. This critical pressure is linearly related to the interfacial tension, and its variation with applied potential may be measured, allowing an electrocapillary curve to be drawn.

To obtain reliable and reproducible electrocapillary curves the apparatus used must be scrupiously cleaned, the chemicals thoroughly purified, and the solutions must be deoxygenated. If reducible substances are present electrochemical reactions might take place at the interface and an electric current may flow. For this situation the interface is no longer ideally polarised and the potential is no longer an independent variable.

Fig. 2.4 The Dropping Mercury Electrode.

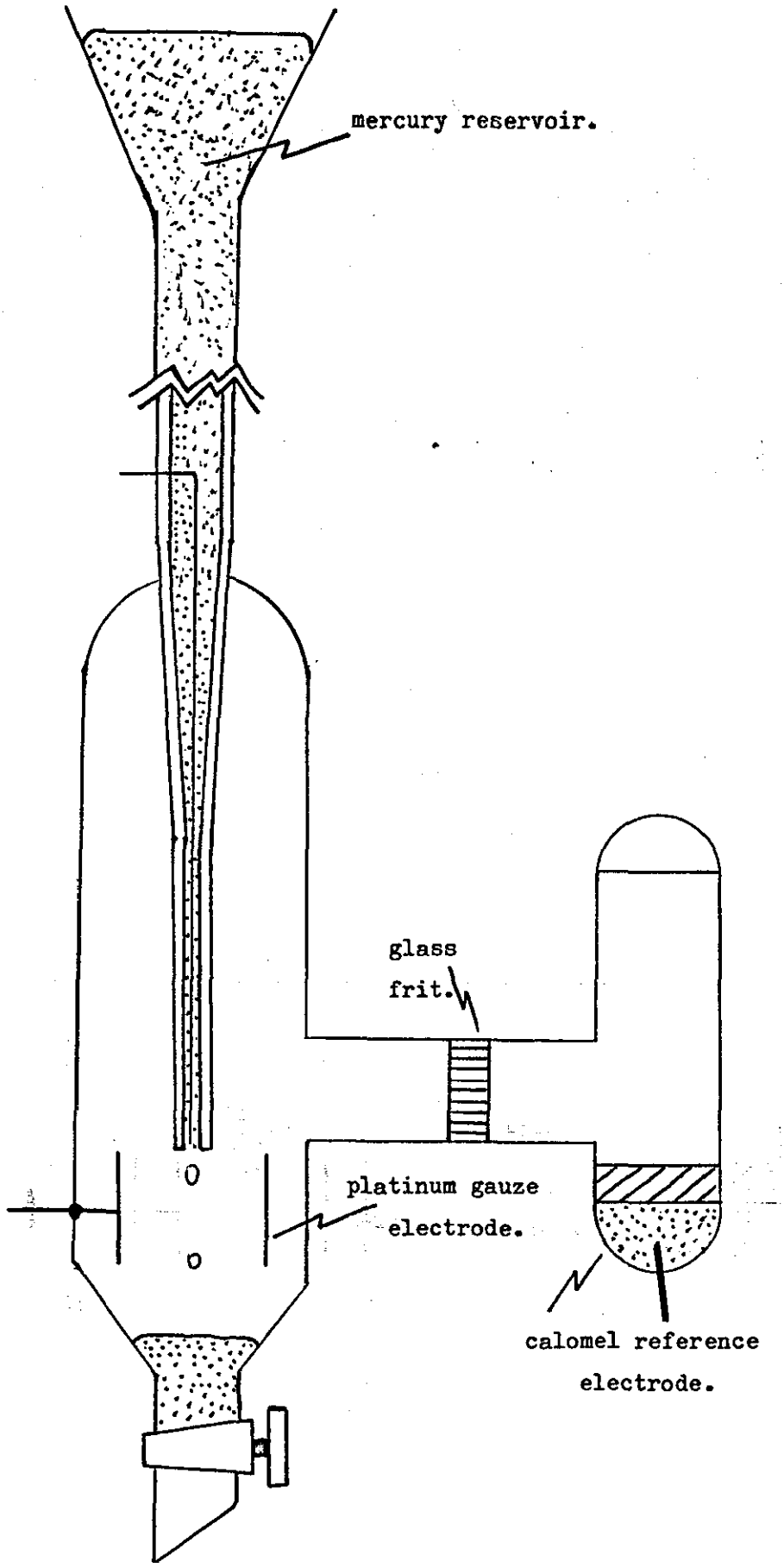

The electrocapillary curves have the general shape of a parabola. They vary markedly with the nature of the electrolyte at the more positive potentials, but often coincide at very negative potentials. The charge q has the value zero at the apex of the parabola, and the potential corresponding to this point is termed the zero charge potential or the potential of the electrocapillary maximum, E_{ecm}.

For solid metals the same data as for mercury are required, but there are no experimental methods available for measuring the absolute value of the interfacial tension between a solid metal and a solution. However, the change in interfacial tension can be obtained from the measurement of the contact angle, θ, between a gas bubble and a metal surface immersed in a solution. Moller (1908) measured the contact angle of an electrolyte with different metals and showed that it varied with the potential on the metal. Frumkin (1932, 1934) has extended this work for a wide range of metals.

Rehbinder and Wenstrom (1944) have measured the logarithmic decrement of the oscillations of a Herbert pendulum whose suspension is a sphere resting on the metal surface covered with electrolyte. The decrement is related to the interfacial tension of the metal-electrolyte system. Bockris and Parry-Jones (1953) have shown that E_{ecm} for amalgamated copper determined by this method is in agreement with E_{ecm} derived from other methods. The pendulum method provides a useful method of determining E_{ecm} for solid metals.

Another method of investigating the solid metal/solution interface is the determination of the surface charge from current measurements. The amount of electricity which must be passed into an electrode of known and constant area e.g. standing drop or solid electrode, in order to change the potential by a given amount is measured. A similar result

may be obtained from observing the rate of decay of electrode potential on open circuit provided that the rates of any electrode processes occuring are known from independent measurements.

The last and probably the most useful of the methods available for studying the electrode/solution interface is the measurement of the electrode capacity. The capacity may be obtained in three ways:-

1. by the double-differentiation of the electrocapillary curve versus potential.
2. from the slope of the charge versus potential curve obtained by current measurements.
3. by direct measurement using AC techniques.

1. The electrocapillary curves have the general shape of a parabola e.g. fig.2.5a from Grahame (1947). This implies that the second derivative of the interfacial tension with respect to the applied Potential, E, which is the differential capacity, C, would be constant if E is varied.

$$C = -\left[\frac{dq}{dE}\right] = -\left[\frac{d^2\gamma}{dE^2}\right] \qquad 2.4$$

This is found to be a very crude approximation as shown by the typical plots of C versus E shown in fig. 2. 5b. Consequently there is a deal of uncertainty over the theoretical and experimental implications of the results derived from electrocapillary curves.

Fig. 2.5a. Typical Electrocapillary Curves.

Grahame (1947)

Mercury/Various Electrolytes at 18°C

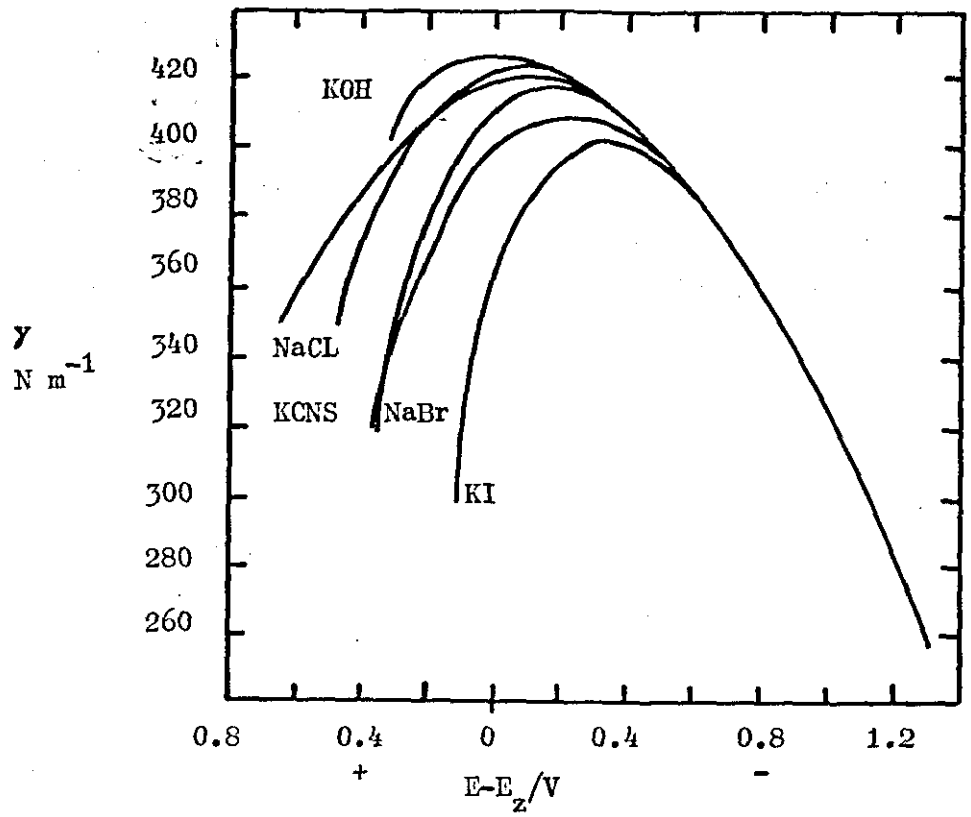

Fig. 2.5b. Typical Differential Capacity vs Potential Curve. Mercury/0.916M Sodium Fluoride.

Grahame (1954)

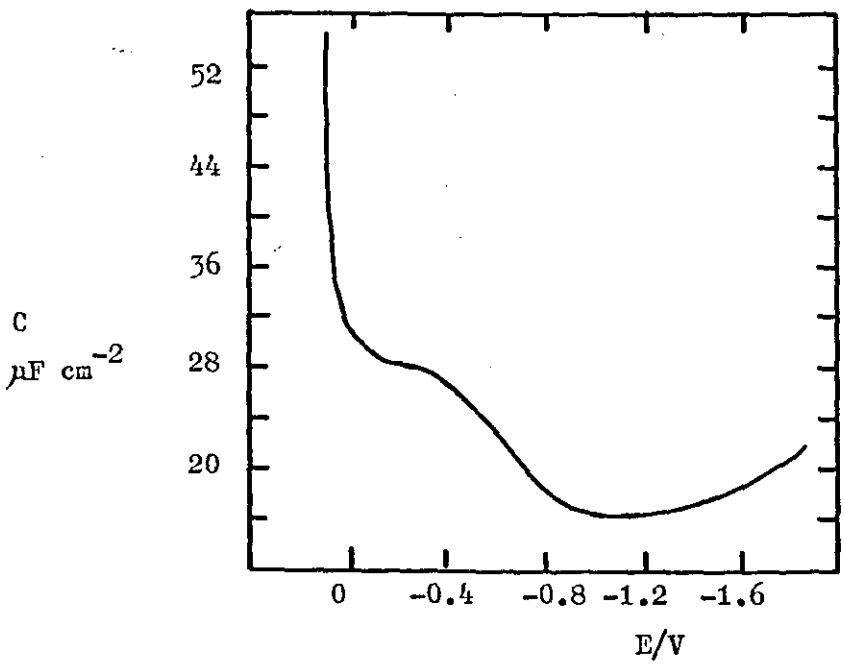

2. The results obtained from current measurements are difficult to interpret if formation of an adsorbed layer occurs, or if currents due to depolarization reactions are of the same order of magnitude as the charging current. Consequently capacities are usually determined directly using AC techniques.

3. The AC methods are the most versatile and accurate way to determine capacities, and have been widely used. Wein (1896) measured the capacity of electrodes by means of an AC bridge of similar construction to that used for measuring the electrical conductivity of solutions. The capacitative part of the cell impedance was balanced by an inductance in series with the cell.

Much of the early work is invalid due to contaminated electrodes, the first satisfactory results for a clean electrode were obtained by Proskurnin and Frumkin (1935). Graham (1941, 1949) combined the dropping mercury electrode with an AC bridge and has published a series of results for mercury in aqueous solution for which he claims an accuracy of 1% on capacities lower than 30 $\mu F\ cm^{-2}$ and a relative accuracy of 0.1%. The equipment used by Grahame with the modifications of Hills and Payne (1965, 1965) is shown schematically in fig. 2. 6. Since the auxillary electrode has a very large surface area relative to that of the droplet, it is the latter which determines the total capacity.

An alternative but less accurate method than the AC bridge method is the direct measurement of the alternating potential difference produced across the test cell by a known alternating current e.g. Borisova and Proskurnin (1936, 1940, 1947). The method was improved by

Fig. 2.6. Schematic Diagram of the Dropping Mercury Electrode and AC Bridge used for Capacity Measurements.

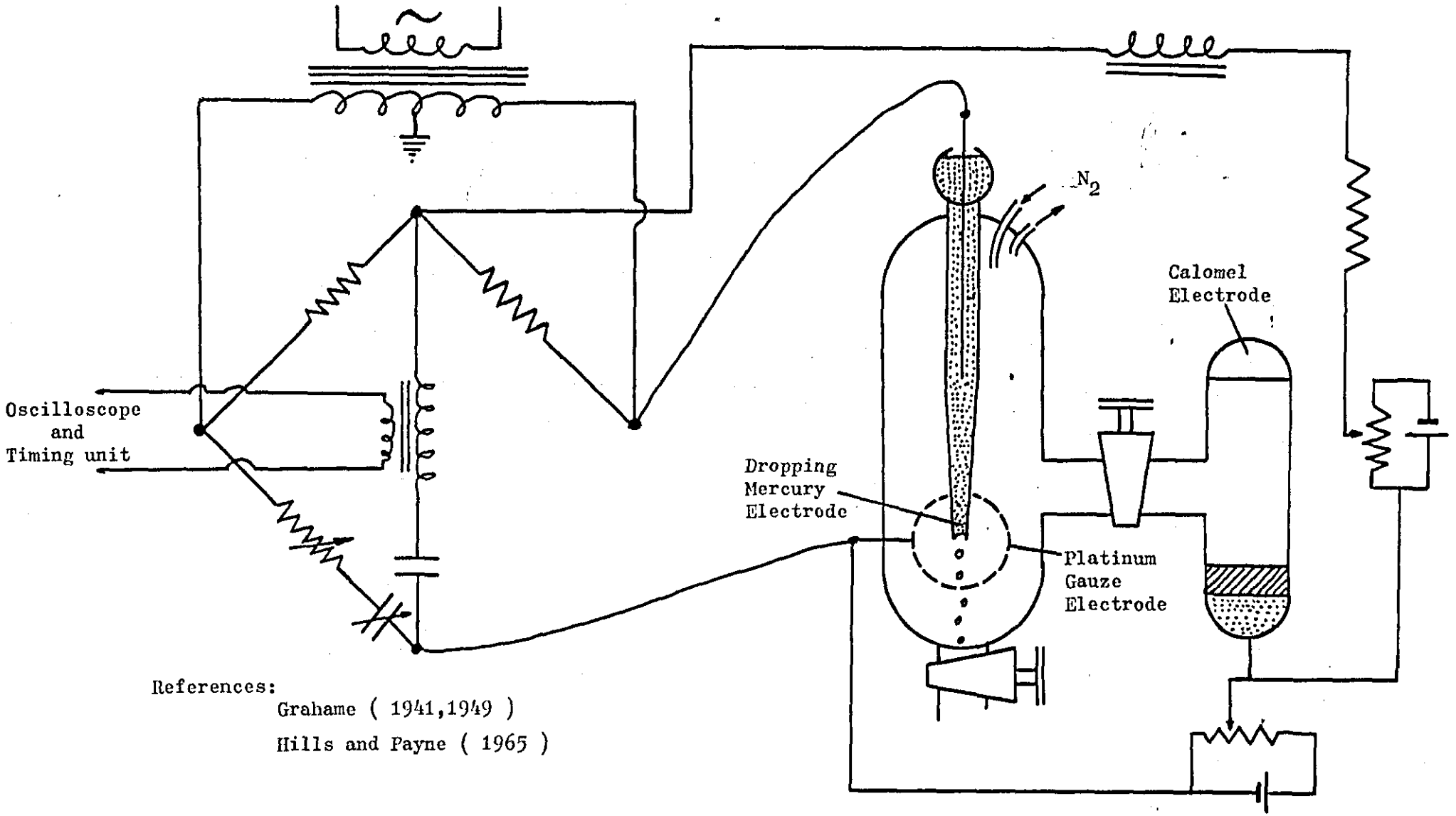

References:

Grahame (1941,1949)

Hills and Payne (1965)

Randles (1947) who made the instrument phase sensitive. This improved method provides the same information as the bridge method, but it is unlikely to be as accurate as the bridge method which is a null method. However the phase sensitive method may well gain in importance as it is readily adapted to on-line computer control.

2. 3. Theories of the Double Layer.

The results obtained from the different experimental methods of examining the interface outlined above have led to the proposal of various theories and models of the metal/solution interface.

The term "double-layer" was first used by Helmholtz (1853) to describe the array of charges at the interface of two dissimilar metals:

metal 1 +++++

metal 2 -----

Helmholtz (1879) compared the double layer of the metal 1/metal 2 interface with that of the platinum/aqueous solution interface. This model of the double layer in its simplest form of two charge layers whose thickness and distance apart are of atomic dimensions postulated by Helmholtz (1879) (and Quincke (1861)) allows the distribution of the potential and of the particles to be calculated from the classical electrostatic theory for a parallel plate capacitor. However calculations using this simple model left most of the electrocapillary curve unexplained.

The simple model was improved by Gouy (1910, 1917) who pointed out that the electrostatic interaction between the field and charges on the ions is counteracted by random thermal motion which would cause a degree of diffuseness on the charge on the solution side of the interface.

A similar theory was proposed independently by Chapman (1913). The calculation is very similar to the ion atmosphere theory of Debye and Huckel (1923) which is based on the same premises. Both theories use a Poisson-Boltzmann equation as their basis.

The assumptions of the Gony-Chapman model are:-

1. the volume of an ion is zero, i.e. point charges.
2. the value of the dielectric constant is independent of the ionic concentration and of the field strength in the diffuse layer, and is therefore constant.
3. the potentials appearing in the Poisson equation, which relates the potential at any point to the charge density at that point, are identical to those of the Boltzmann equations for the distribution of the ions.

The Gony-Chapman diffuse-double-layer model as it came to be known represents a substantial improvement over the Helmholtz model in that a dependence of the differential capacity on both potential and concentration is predicted. However, large discrepancies between theoretical predictions and experimental results were still found, the measured capacities were nearly always much lower than the calculated values except in very dilute solution. The variation of capacity with potential observed experimentally only agrees with the predicted values at potentials near the potential of zero charge and for very dilute solutions.

A major cause for the discrepancies was that the compact part of the interface had been overlooked. The theory was modified accordingly by Stern (1924), who combined the two previous models to give a model consisting of a monolayer of ions on the electrode

with the remaining ions in a diffuse layer according to the Gouy-Chapman model. He also accounted for the finite size of the ions by postulating that the non-adsorbed ions could not reach the electrode beyond a plane of closest approach. He assumed the same plane for both cations and anions, but indicated in a footnote that this assumption might not be valid. Thus in the Stern model there are effectively two capacitors operative in determining the total differential capacity of the interface. For convenience C_H will be used to denote the capacity due to the Helmholtz or compact layer and C_G for the capacity due to the diffuse layer which extends from the plane of closest approach to the bulk solution. Since the two regions are adjacent to each other, the two capacitors will act in series, and the total capacitance, C, will be given by:

$$\frac{1}{C} = \frac{1}{C_H} + \frac{1}{C_G}$$

This is of great importance because it shows that the smaller of the two contributions will be predominant in determining the total capacitance. Although this model was an improvement on the previous description, the conflict between experimental results and theoretical predictions remained.

Grahame (1947) used the Stern model to develop a model of the interface consisting of three layers although it is still commonly referred to as a double layer. The first region extends from the electrode to a plane passing through the centres of the adsorbed ions (anions), usually called the inner Helmholtz plane. The next layer consists of the hydrated cations at their distance of closest

approach, and the plane through their centres is known as the outer Helmholtz plane. The final layer between the outer Helmholtz plane and the bulk solution is the diffuse layer of Gouy-Chapman. Grahame also suggested that the capacity of the compact layer was only dependent on the charge on the electrode and independent of electrolyte concentration and obtained a reasonable agreement between experimental and theoretical values for mercury in sodium floride. The differences between the various models and the predicted variation of potential with distance through the interface are most readily understood by comparing fig.2. 7 - 2. 10.

Grahame's model gained considerable acceptance after his publication of a series of measurements more accurate than those of 1947 on the mercury/sodium fluoride solution interface in 1954 and 1957. The agreement between the experiment and predicted results was very good and the results are summarized in fig. 2.11. Grahame's model is the basis of the modern theory of the electrode/ solution interface. The results also demonstrate the small influence of the diffuse layer capacity on the total capacity of the interface, that it is likely that there is only a very small degree of adsorption of sodium fluoride on mercury, and that the capacity of the compact layer varies markedly with the charge on the electrode.

In the theory of Gouy-Chapman-Stern the effect of the solvent has been neglected. One might expect to find a layer of solvent molecules attached to the electrode surface in a fixed orientation and probably several other layers with an orientation intermediate between that of the first layer and the bulk. This idea is analgous to the situation

Fig. 2.7 Helmholtz Model of the Double Layer.

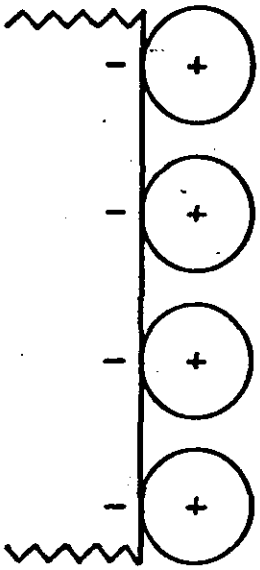

Variation of Potential with Distance through the Interface predicted by the Helmholtz Model.

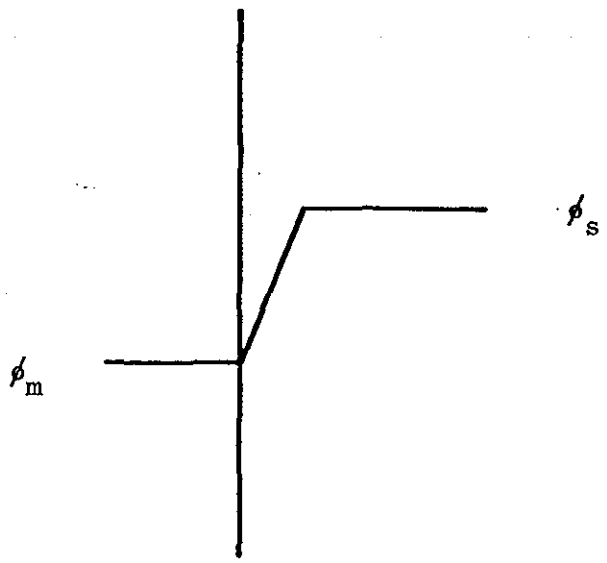

Fig. 2.8 Gouy - Chapman Model of the Double Layer.

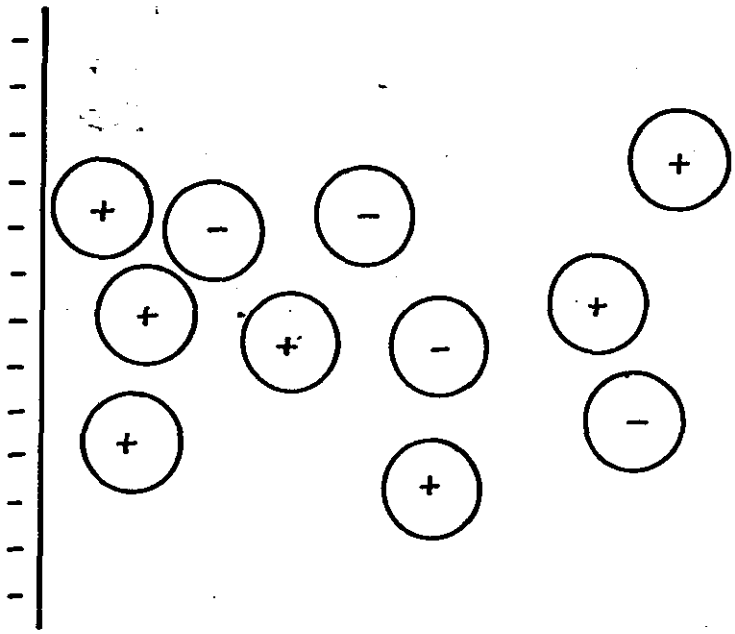

Variation of Potential with Distance through the Interface predicted by the Gouy - Chapman Model.

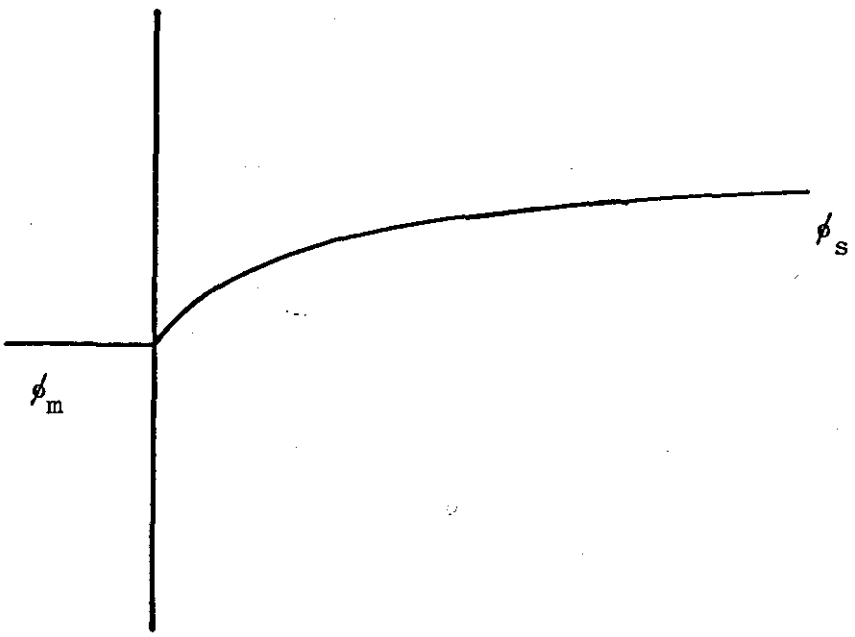

Fig. 2.9 Stern Model of the Double Layer.

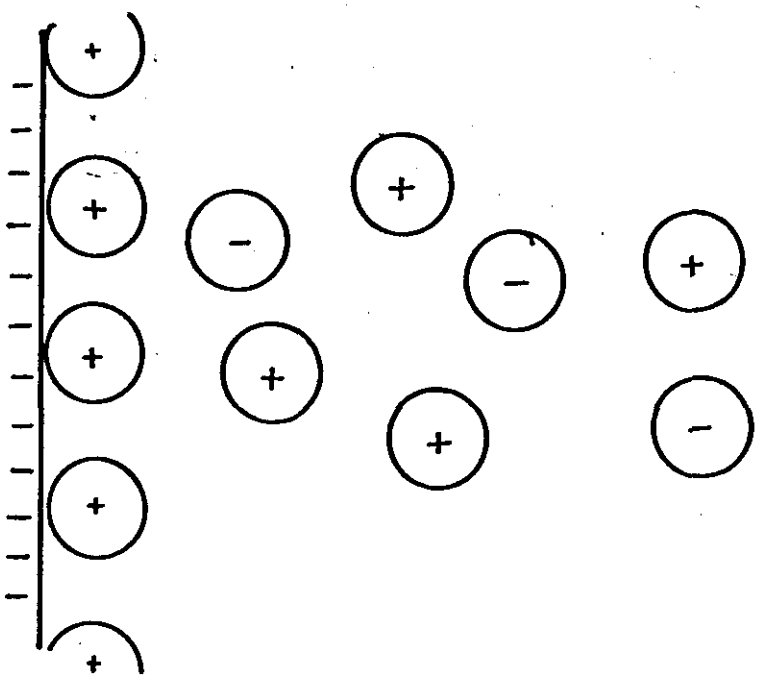

Variation of Potential with Distance through the Interface predicted by the Stern Model.

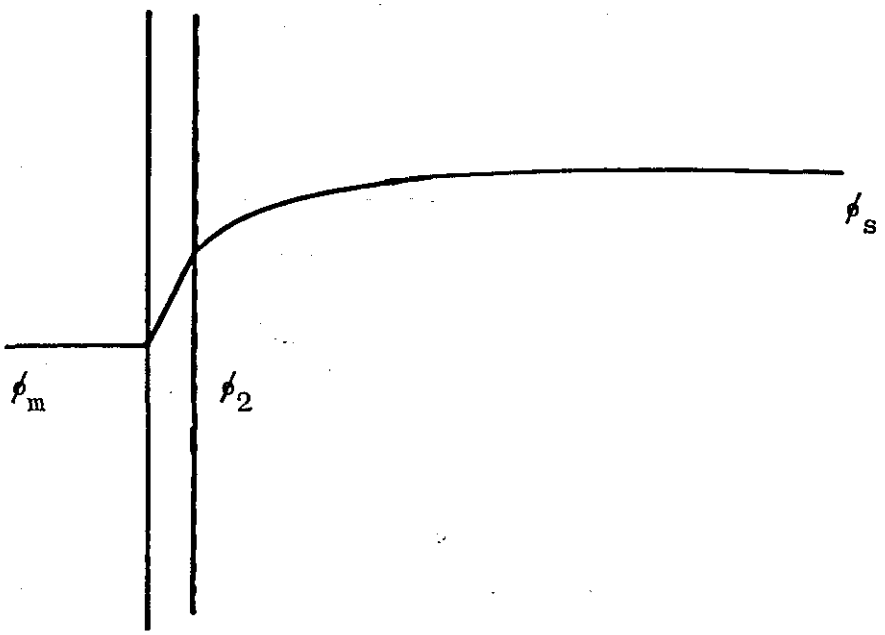

Fig. 2.10 Grahame Model of the Double Layer.

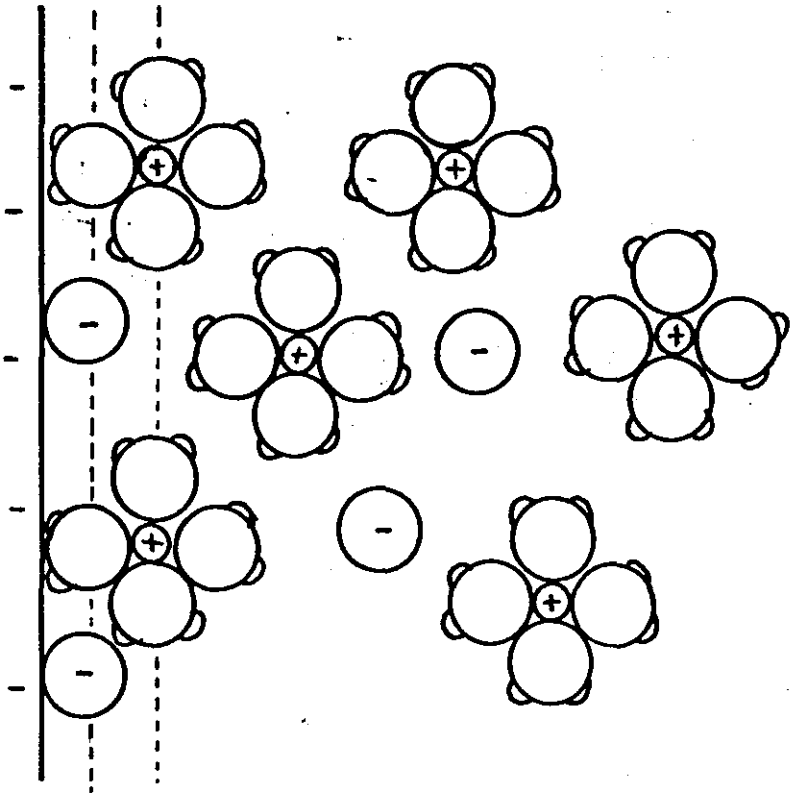

Variation of Potential with Distance through the Interface predicted by the Grahame Model.

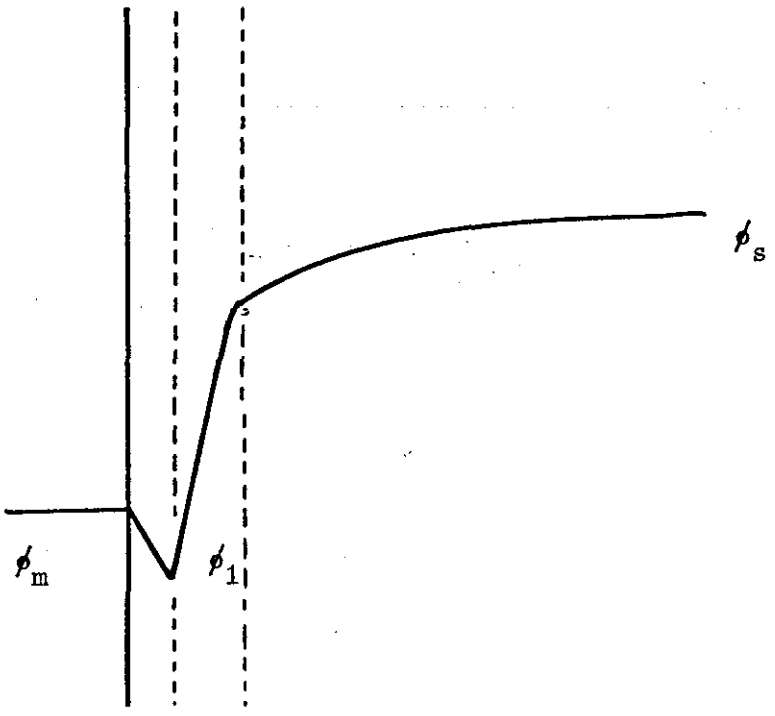

Fig. 2.11. Grahame's Experimental Differential Capacity Curves for Mercury in Aqueous Sodium Fluoride at $0^{\circ}C$ and $85^{\circ}C$.

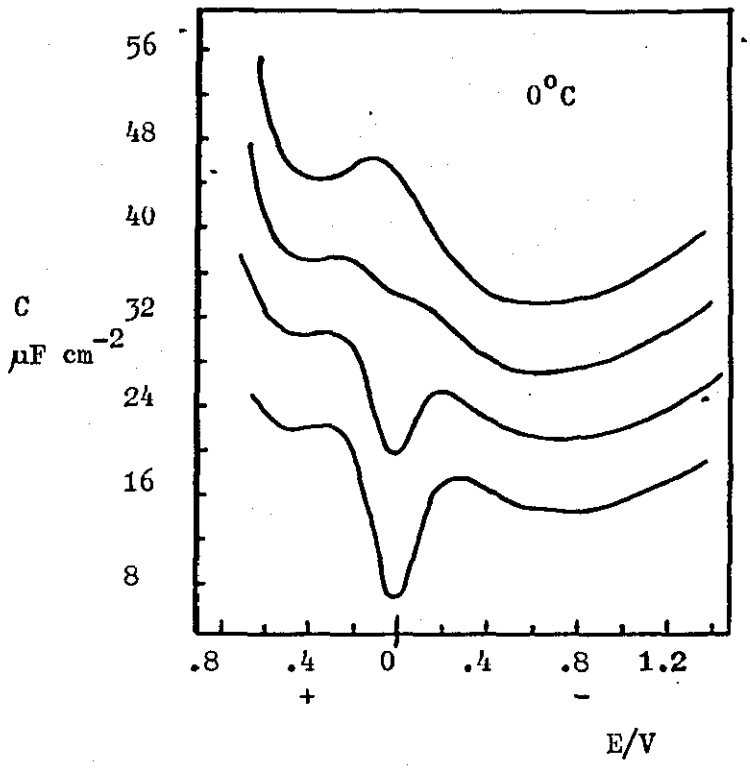

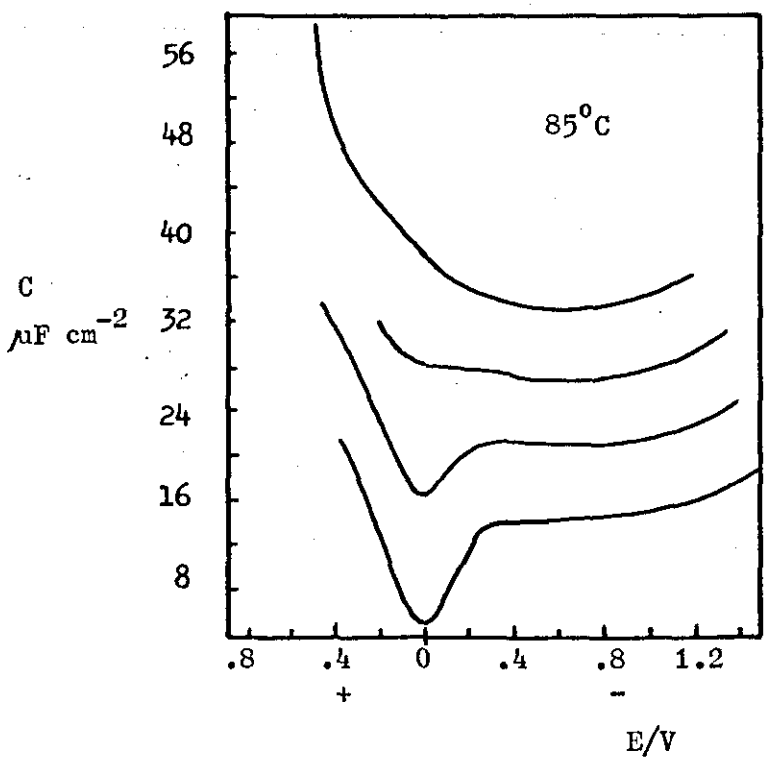

of a large central ion with primary and secondary solvation shells. Bockris, Devanathan and Muller (1963) have proposed a model of the double layer which explicitly takes into account the predominant existence of the solvent in the interphase. They suggest that in aqueous solutions the majority of the electrode is covered with an orientated layer ofwater molecules, but on certain sites, the water molecules are replaced by specifically adsorbed ions which do not carry a hydration shell. The plane passing through the centres of these specifically adsorbed ions is the inner Helmholtz plane. Next are the ions which retain their hydration shell and are placed outside the primary layer of water molecules adsorbed on the electrode surface. The plane passing through their centres is the outer Helmholtz plane. This situation is shown in fig. 2. 12.

The difference between ions in the inner and outer Helmholtz planes is of great importance because chemical work must be done to remove the hydration shell around the ion of the inner Helmholtz plane, and one or more water molecules from the electrode surfaces.

The final state is stabilized by the specific interactions between the ion and the surface. This effect is absent for the ions of the outer Helmholtz plane and the interactions are mainly electrostatic.

Much of the work on the theory of the double layer since 1963 has been concerned with the compact layer and has concentrated on the orientational behaviour of the layer of water molecules within this layer e.g. Levine, Bell, and Smith (1969) Damaskin & Frumkin (1974), Parsons (1975).

Fig. 2.12.

Bockris, Devanathan, and Muller Model of the Double Layer.

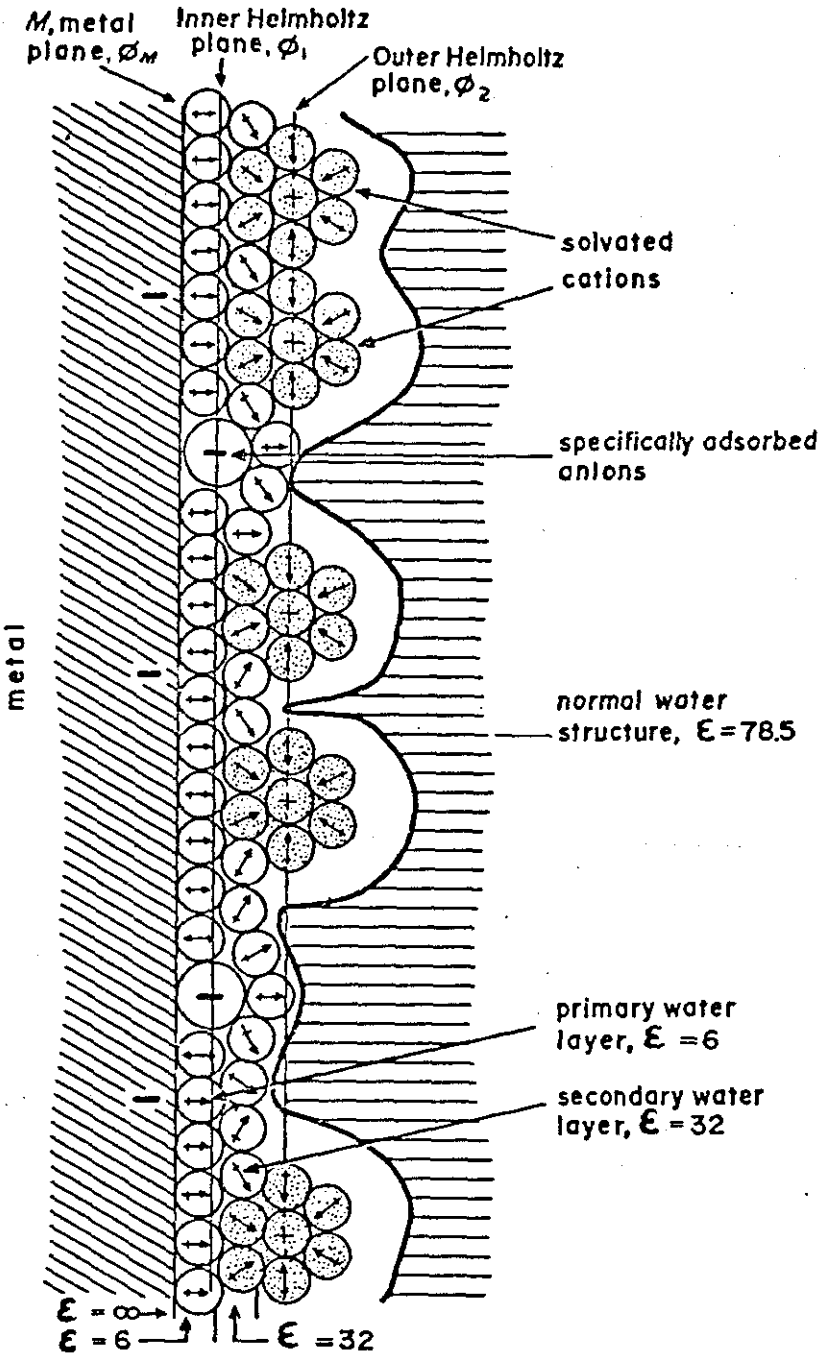

In a series of papers published over the last three years Cooper and Harrison (1975, 1977 a, b, c, 1978) have questioned this subdivision of the double layer into a concentration independent compact layer and a diffuse region and particularly with regard to the structure and properties of individual solvent molecules within the compact layer. They point out that as the experimental measurements appertain to changes in the distribution of ions in a polar solvent in the transition zone between the metal and bulk electrolyte it is surprising that the highly structured and reproducible results are attributable solely to the orientational behaviour of water molecules in the liquid phase, particularly for the more concentrated solutions. They have therefore re-examined the whole problem from first principles, particularly with regard to the assumptions involved in separating the differential capacity into two independent series contributions. They conclude that the subdivision is in fact only formal and should not be interpreted literally as is the present custom, and therefore a completely new approach is required.

They have proposed (1977b) such a new approach to the double layer in which it is treated as a single entity with no basis on the concepts of compact layer, inner or outer Helmholtz planes, or contact adsorption. The structure of the double layer is considered to arise specifically from the known differences between anions and cations in aqueous solution.

The essential points of the model are:

1. The net distributed charge $\rho(z)$ acts at a mean distance $\langle z \rangle$ from the electrode.
2. The differential capacity C is given by:

$$C = \frac{dq}{d(\Delta E)} = \frac{\varepsilon}{\langle z \rangle + q\left(\frac{d\langle z \rangle}{dq}\right) - q\left(\frac{\langle z \rangle}{\varepsilon}\right)\left(\frac{d\varepsilon}{dq}\right)} \qquad 2.5$$

where q is the surface charge density,

ΔE is the potential drop between the electrode and bulk electrolyte, and

ε is the appropriate effective permittivity of the interface (interfacial permittivity).

ε is dependent on the amount of free (orientatable) water in the interface, and is therefore determined by the extent of the interface.

$\mathcal{E}$ will have a value approaching that of the bulk electrolyte when $\langle z \rangle$ is large, for example in dilute electrolyte and low values of $|q|$, and will have a small value corresponding to very little free water in the interface when $\langle z \rangle$ is small as in the case of high concentrations of electrolyte and large values of $|q|$. The small values of $\mathcal{E}$ at high concentrations is consistent with the similarities of C-q data at high $|q|$ irrespective of concentration.

The well known ' humps ' in the C-q curves which occur at different values of q for different anions and the variable decreasing portion following the hump is explained by this model in terms of a temporary increase in $\langle z \rangle$ with q, before the ultimate continuous decrease at more positive values of q. The temporary increase in $\langle z \rangle$ is considered to arise from an ionic redistribution at the interface, caused by anions and cations entering the interface as q increases. The differences in absolute values of differential capacity are related to the fact that small anions can approach more closely to the electrode, and in greater numbers, than the larger hydrated anions coupled with the likely suggestion that anions are to be found closer to the electrode on average because of their known smaller size compared to cations. Therefore the Cooper - Harrison approach to the double layer qualitatively explains the general behaviour of the C-q curves in terms of variations in $\langle z \rangle$ determined by the different effective sizes of anions and cations in aqueous solution. Of particular significance is the use of the mean distance $\langle z \rangle$ of the net ion excess from the electrode which permits future incorporation of detailed statistical theories for the excess ion distributions $\sigma_{\pm}(z)$ at the interface, and this may well be instrumental in producing an approach to the double layer capable of explaining all the experimental results.

The models of the double layer discussed have been for the case where the point of zero charge potential, E_{ecm} is electrolyte concentration independent, which in terms of the Gouy-Chapman-Stern model is explained in terms of the absence of specific adsorption at the electrode. However, there are many electrode/electrolyte systems where E_{ecm} is markedly dependent on concentration, and the dependence is discussed in terms of specific adsorption of either ionic or neutral species.

For predominantly anion adsorption the E_{ecm} moves to more negative potentials with increase in concentration, and to positive potentials for predominantly cation adsorption. For the case where both cation and anion adsorption occurs the direction of shift of E_{ecm} may be reversed with change in electrolyte concentration.

The adsorption of neutral species and some bulky organic ions gives rise to two peaks in the C vs E curve as shown in fig. 2.13 . The two peaks correspond to the two regions of the coverage vs E curve given in fig. 2.14 .

This aspect of the double layer will not be discussed further as there were no adsorption peaks on the C vs E curves for tantalum in the electrolytes examined, neither was the point of zero charge potential identified.

2.4. Double Layer Capacity of the Tantalum Electrode.

From section 2.2 it is clear that the experimental problems encountered when trying to examine the metal-solution interface mean that the results for solid metal electrodes must, for the most part, be considered to be less reliable than those for mercury. The measurement of the double layer capacity using AC techniques coupled with the measurement of faradaic current vs potential appears to be the most useful method of

Fig. 2.13. Typical Differential Capacity vs Potential Curve for the Case of Adsorption of a Neutral Species.

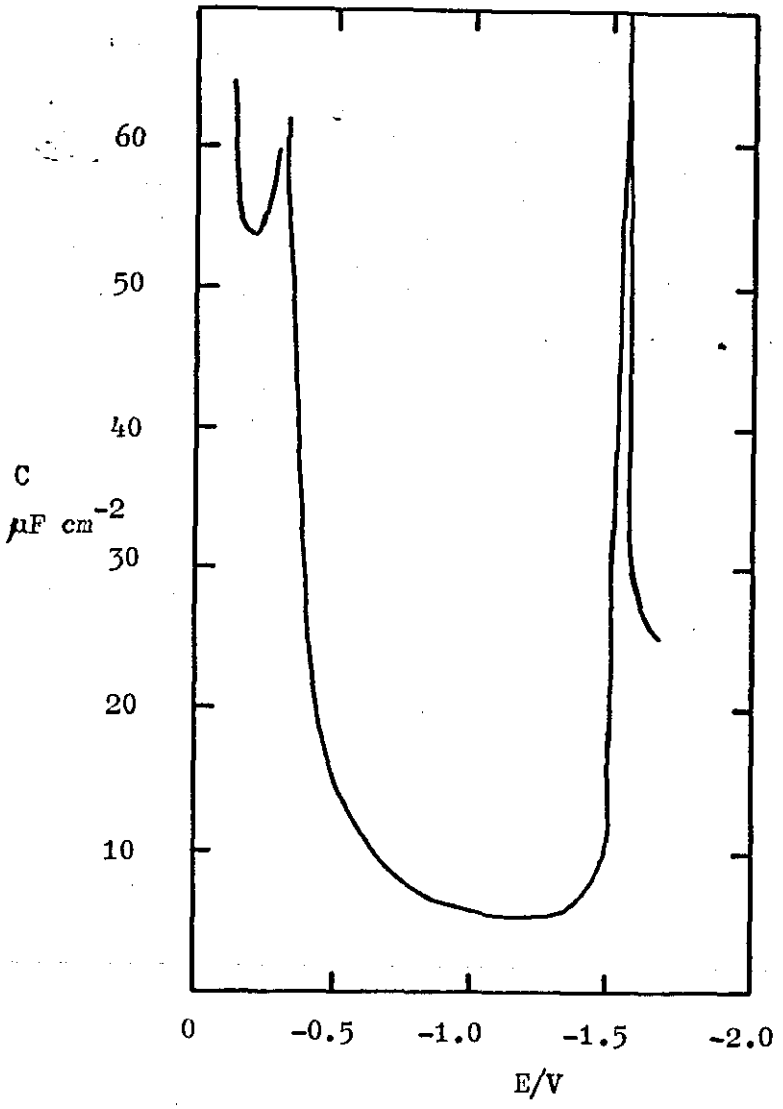

Fig. 2.14. Coverage vs Potential Curve for the Situation Shown in Fig. 2.13.

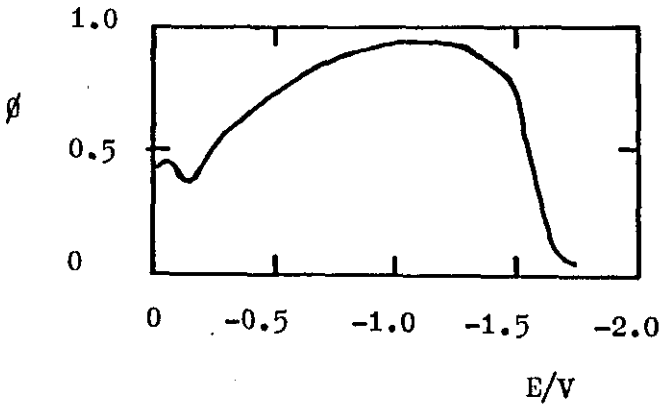

studying the solid metal-solution interface.

A review of the large number of capacity measurements reported for solid metals is outside the scope of this thesis. It is sufficient to refer to some of the many partial reviews of the double layer that include some mention of the results on solid metals, see for example Parsons (1954), Delahay (1965) Frumkin (1955, 1960, 1963), and Hampson (1972, 1973).

In general the results on solid metals may be summarised as follows:-

1. The polarizable region available with solid metals often has a very limited potential range compared to that for mercury because of the high exchange currents for the hydrogen evolution reaction and the high affinity of the metals for oxygen.
2. The various crystal faces of the metal may have quite marked differences in their properties, and this is mirrored by the differing values of the capacity minimum.
3. For metal-electrolyte systems where specific adsorption effects or faradaic effects are absent, the minimum in the capacity vs potential plot, which may become more pronounced for dilute solutions, may be assigned with confidence as occurring at the potential of zero charge (E_{ecm}) .
4. For systems with specific adsorption, the effect of frequency on the capacity permits an estimation of the adsorption to be made.

In section 1.1 it was mentioned that tantalum is invariably covered with a thin protective layer of oxide (Ta_2O_5) for all pH's in aqueous solution. Therefore the behaviour of tantalum will depend essentially on the behaviour of the oxide towards the solutions considered. Depending on whether or not this layer is of good quality i.e. compact, impervious, continuous and thermodynamically stable or unstable in the surrounding medium, tantalum will behave as either an uncorrodible or a corrodible metal.

The measurement of the double layer capacity of a clean tantalum electrode surface in aqueous solution has therefore been considered to be impossible because of the protective oxide film, see Udupa and Venkatesan (1974). Brodd and Hackermann (1957) and also McMullen and Hackermann (1959) have reported a low value of capacity for the tantalum electrode of $\sim 9\ \mu F\ cm^{-2}$ in 0.5M Na_2SO_4 solution. Similarly, Isaacs and Leach (1962-3) found a value of $\sim 15\ \mu F\ cm^{-2}$ for tantalum in various carbonate solutions.

The reversible potential for the reaction:-

$$Ta_2O_5 + 10\ H^+ + 10\ e^- \rightleftharpoons 2\ Ta + 5\ H_2O$$

is well established to be inaccessible directly on account of the protective power of the oxide in screening the metal from aqueous solutions, at least in the absence of complexing agents, Pourbaix (1966) .

The potential vs pH (Pourbaix diagram) shown in fig. 2.15 implies that tantalum pentoxide can be reduced to metallic tantalum However, it does not seem possible to bring about this reduction by electrolytic means starting directly from the oxide, Pourbaix (1966) . Bouhard (1907) has stated that it is possible to deposit tantalum on a carbon or platinum cathode by electrolysis

Fig. 2.15 Potential vs pH Equilibrium Diagram for the Tantalum - Water System at 25°C. (Pourbaix Diagram.)

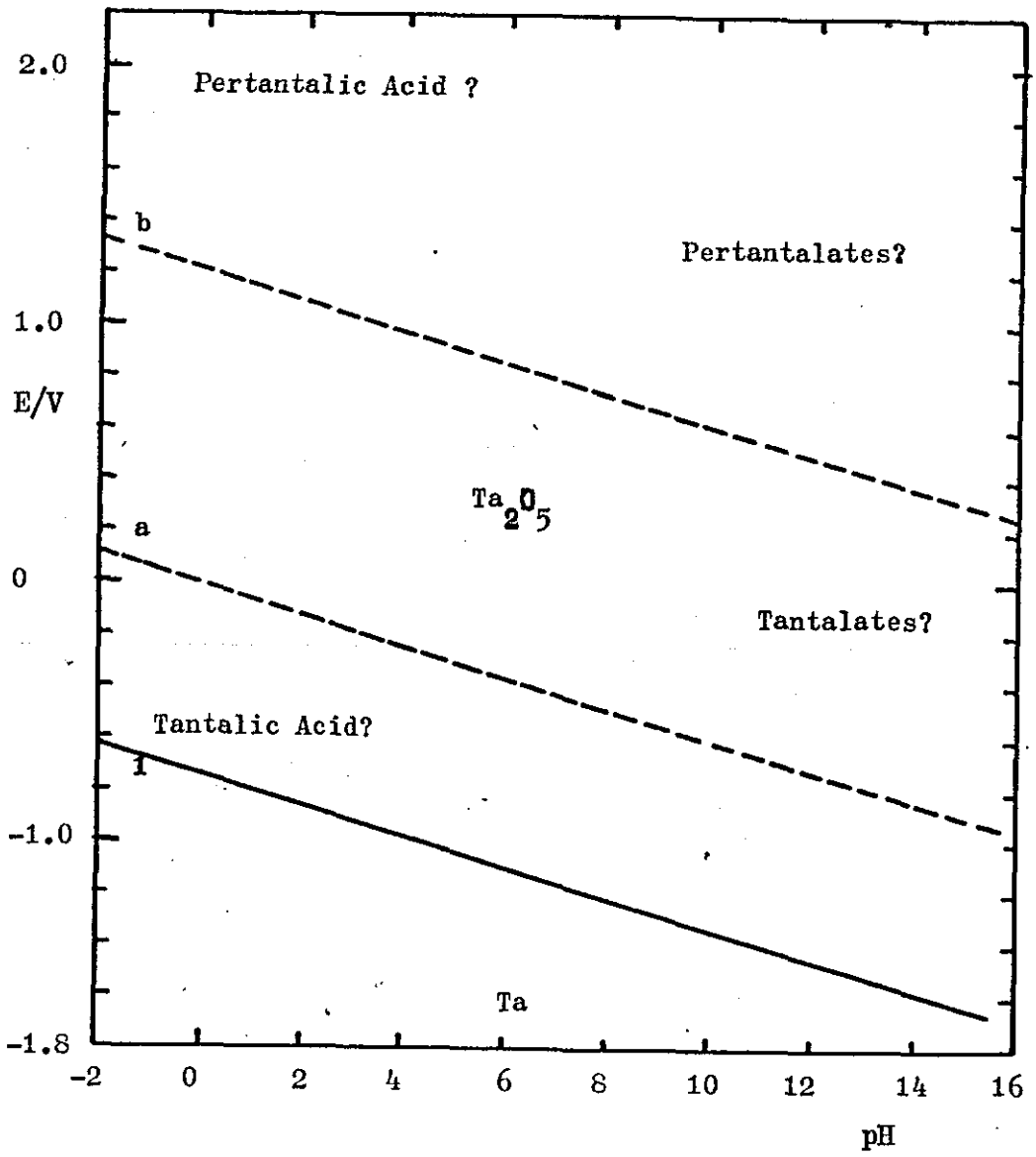

of an oxalic solution of tantalic acid acidified with 3% hydrochloric or sulphuric acid.

It should be noted that due to the lack of thermodynamic data, tantalic acid and pertantalic acid (solids) and tantalates and pertantalates (dissolved) were marked by Pourbaix purely as a guide and have no experimental foundation.

Tantalum can give rise to numerous complexes, eg fluorinated and oxyfluorinated complexes, tartaric and oxalic complexes, and complexes with hydrogen peroxide and polyhydric alcohols, Charlot (1957), Cotten and Wilkinson (1966).

2.5. Properties of Tantalum Oxide Films.

The final section of this chapter is devoted to the various properties of tantalum oxide films which contribute to the leakage across it, and which therefore determine R_{adl}.

When a piece of tantalum is made the anode of an electrochemical cell during anodization, the applied current either sets up an electrostatic field, or increases the electrostatic field already present in the oxide film that is almost invariably present on the metal. The electrostatic field causes continued growth of the oxide film provided that the electrolyte in the cell does not dissolve the oxide.

The growth of the oxide proceeds by pulling either tantalum or oxygen ions through the film, and is therefore described in terms of ionic conductivity, complicated by the presence of two interfaces, Ta/Ta_2O_5 and Ta_2O_5/solution, at which transfer processes must occur.

A diagrammatic plot of current vs potential for a tantalum electrode on which a very thin oxide film has already been formed is shown in fig. 2.16, Young (1961). The current during anodic polarization is small and irreproducible until the range of potentials is reached at which the ionic current starts to predominate over the leakage current. The ionic current then rises very rapidly with increasing potential. The leakage current due to flaws in the oxide film is defined as the number of microamps per microfarad volt after the voltage has been applied for a certain time, usually 3 minutes. Typical values of the leakage current lie in the range 0.01 to 0.1 $\mu A\ \mu F^{-1} V^{-1}$. The anodic leakage usually causes oxygen evolution once the potential has reached values where this process becomes thermodynamically possible.

In theory, an ionic current flows at all potentials above the reversible potential of the oxide electrode, but in practice it is negligible in comparison with the leakage current at low potentials. Once the electrostatic field is large enough for an appreciable ionic current to pass, the behaviour becomes time dependent due to the increase in thickness of the oxide film.

Anodization may be carried out by one of two simple experimental methods :-

1. at constant ionic current.
2. at constant voltage.

1. Films produced by anodization at constant current are the best characterised for scientific purposes because a complete description of the films is given by stating the current density, final potential, solution, temperature, metal purity, and mode of surface preparation. During anodization at constant current, each new layer of oxide of thickness dD requires an additional potential dV to

Fig. 2.16 Current vs Potential for Tantalum/Tantalum Pentoxide Electrode.

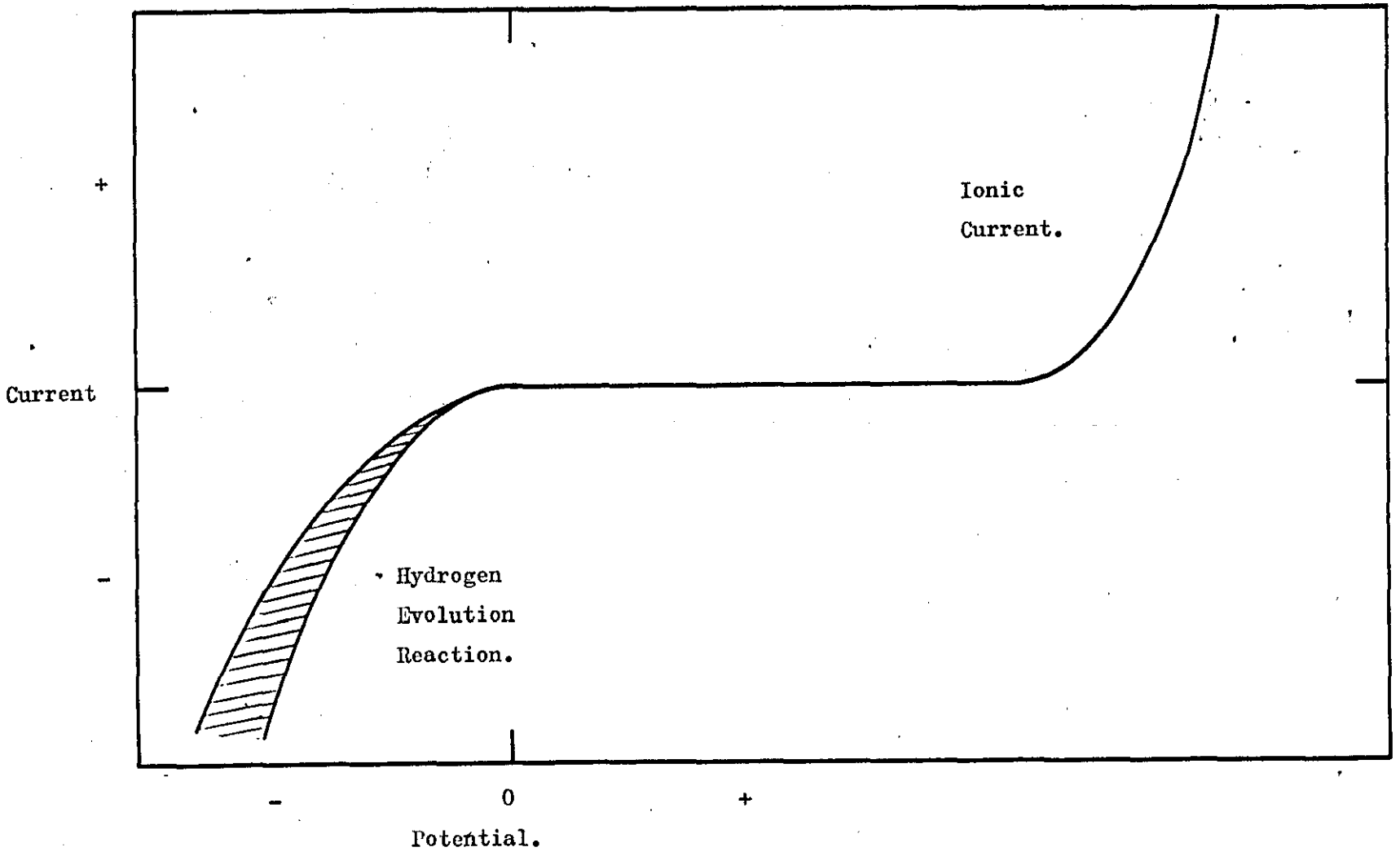

be added across the film to maintain the field (and hence the current) in the oxide constant. dV/dD is known as the differential field strength and is given the symbol E_d . If the existing potential fall in the film is not changed during further growth, E_d is the actual field strength in the new layer being formed. Typically E_d does not vary with increasing thickness for anodization at constant ionic current density. The relation between rate of increase of potential and the current density is derived as follows :- the rate of increase of thickness dD/dt is given by :

$$dD/dt = iM/zF\rho \qquad 2.6$$

where D is the thickness of the film, t is the time, i is the ionic current density, z is the number of Faradays (F) required to form the molecular weight of oxide, M, of density ρ .

If E_d is constant, then :

$$E_d = dV/dD$$

$$dV/dt = E_d . dD/dt = iE_dM/zF\rho \qquad 2.7$$

For practical purposes E_d varies slowly with i , being less than 10% for a 10 fold change in i , so dV/dt is roughly proportional to i . For tantalum at room temperature dV/dt is about 3 Vs^{-1} for a current density of $\sim$ 10 mA cm^{-2} .

2. During anodization at constant potential the increase in the film thickness causes a continuous decrease in the field strength and therefore in the current. As the current falls the rate of decrease of field falls and consequently the rate of decrease of the current also falls. Therefore after a certain time the rate of growth of oxide is sufficiently small that for most practical purposes the film thickness may be considered to have reached a limiting value. There is no

such value in a mathematical sense, hence the preference of the constant current method for scientific work.

For crystalline solids the ionic conduction occurs through the movement of lattice defects. The defects may be vacant positively or negatively charged sites, or interstitial anions or cations.

The ionic conductivity in anodic oxide films is usually considered in terms of the movement of interstitial metal ions moving through the interstices of a network of immobile metal and oxygen ions. The ions are assumed to be equivalently placed in terms of ease of movement, but this is only a first approximation as the oxides are amorphous. The applied field is assumed to reduce the potential energy required for movement from one site to another. The observed current is the difference between the forward current due to ions moving with the field, and the backward current due to ions moving against the field. The usual situation found for the high resistance oxide film is that to obtain a measurable current the field strength that must be applied is so large that the backward current is negligible compared to the forward current. Hence the growth of the oxide film may be considered in terms of the forward current only, which because of the high field strength involved will be due to high field conduction processes. The high field conduction processes of importance in the oxide films are complicated because of the amorphous nature of the films which have a different structure at different temperatures and under different field strengths. At constant potential the thickness is proportional to the logarithm of the time, and the current is an exponential function of the electric field strength. Vermilyea (1954)

has shown that the tantalum ion with the normal valency for the ionic charge on the ion is the moving entity under high fields. The mechanism is thought to involve single ion jumps between equilibrium positions of the ionic structure, Vermilyea (1957) , but there is also some evidence that there may be a relaxation of the film structure with change in temperature, field strength, or film history which is supported by the dependence of the rate of dissolution of Ta_2O_5 in HF on the formation field and temperature, Vermilyea (1957).

Other anodic processes such as oxygen evolution are almost entirely inhibited, even though there may be a potential difference of some hundreds of volts across the film, provided that the tantalum surface is smooth (scratch free), not contaminated by other metals, and free from inclusions.

The formation of the film is normally limited by a breakdown which occurs when a certain range of thickness is reached, or alternatively, when a certain potential is reached. Breakdown is characterised by scintillation, oxygen evolution, and field recrystallization. Tantalum pentoxide is particularly resistant to breakdown, presumably because the field required for ionic conduction is very much less than that required for avalanche breakdown.

As the voltage rises during formation at constant current the first sign of breakdown is the appearance of short bursts of gas at different sites over the surface. Scintillation then occurs, often the discharge travels over the surface leaving a trail of thick grey oxide. This form of breakdown is thought to be due to flaws in the material rather than due to the properties of the homogeneous material. The conduction of electrolyte in

such imperfections causes the production of heat and leads to the formation of localised hot spots which fail.

The amorphous oxide Ta_2O_5 does not recrystallize until temperatures of several hundred degrees centigrade are reached. However, crystalline oxide may be caused to appear in anodic films by holding them under a voltage at temperatures of less than 100°C, Vermilyea (1955, 1957). The process is not strictly a recrystallization since it is believed that the crystalline oxide is formed "de novo" and mechanically displaces the amorphous oxide film. The term field induced recrystallization seems established and the process is an important mode of failure of the formation process in the manufacture of tantalum capacitors.

During formation at constant voltage the current falls with time, see fig. 2.17 , until a limit is reached which corresponds to nearly all leakage current. The onset of recrystallization is accompanied by an increase in current which is required to grow the crystalline oxide.
As recrystallization goes to completion the current decreases once more. The process depends on the metal, the surface preparation prior to anodization, the temperature, the field strength, and the nature of the solution. Jackson (1973) has shown that the rate of radial growth of crystalline areas may be controlled by the selection and modification of the electrolyte composition. The number of nuclei formed after a given period under standard conditions depends on the batch of metal, but it is unclear which impurities are responsible.

The onset of recrystallization on strongly adherent films formed by anodization of tantalum which has been chemically cleaned (polished) followed by leaching in

Fig. 2.17 Current vs Time for Formation of Tantalum Pentoxide at Constant Voltage.

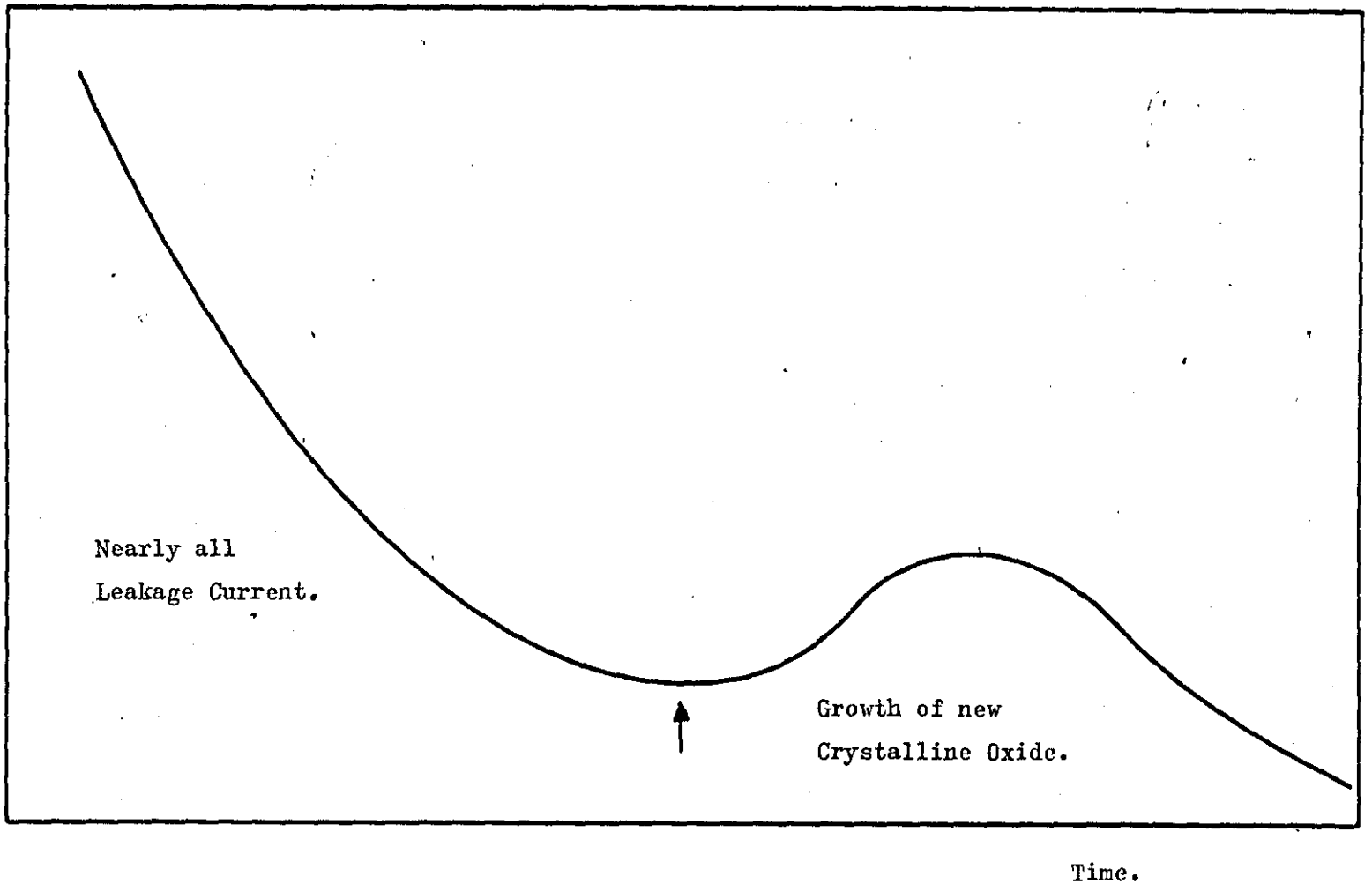

boiling water, is seen under magnification as a number of small rounded areas of a different colour, or as small raised areas with cracks radiating outwards. Anodic oxide films on tantalum normally appear flat and structureless, even under the electron microscope.

For poorly adherent films the nuclei lift the film off the surface, terminating the process.

The optimum conditions for producing field recrystallization with sulphuric acid electrolyte are 0.2% acid at 85°C with a constant current density of ~ 0.1 $mAcm^{-2}$ until a formation voltage of 120V is reached, which is held for a further 60 minutes, Vermilyea (1955). It appears that recrystallization is at least delayed although not completely inhibited if concentrations of greater than 40% sulphuric acid are used.

One of the easiest ways to investigate the effect of gelled electrolytes on the various properties of the oxide films outlined above is to anodize tantalum in both gelled and non-gelled electrolytes and then measure and compare the properties of the two samples of oxide produced. Because of the problems encountered with the anodization and reproducibility of the porous electrodes used in capacitors eg. determination of the surface area, this comparison is most easily made using foil specimens.

CHAPTER 3.

3.1. Gels.

The "gelled" electrolyte used in the tantalum electrolytic capacitors consists of 5%(wt/vol)i.e.3.7%(wt/wt)fumed silica dispersed in a 40% by weight sulphuric acid solution. An important point to note is that the volume fraction of the silica in this gel when well dispersed is only 0.022 This ratio of silica : sulphuric acid was chosen empirically as that producing sufficient thickening of the acid to prevent leakage and orientation sensitivity of the capacitor and yet still be easily dispensed during capacitor assembly. Generally, the addition of silica to the electrolyte had little effect on the overall properties of the capacitors. There is an occasional problem with the $-55^{\circ}C$ impedance and The Plessey Company Ltd have noted certain anomalies in the conductivity of gel systems.

The "gelled" electrolyte seems to be thixotropic - a small amount of stirring or agitation changes the gel from a fairly rigid state (the container housing the gel may be inverted without effect) to an easily flowing liquid which reverts to the original state on standing.

However, the term "gel" is difficult to define,see D. Jordon Lloyd (1926), because it has been used to describe systems as diverse as the transparent homogeneous mass (- a typical gel) obtained by the neutralisation of a concentrated solution of sodium silicate solution,to the hard , transparent,glass-like substance formed on drying the previous substance.

The mineral agate is also included in the category of a gel as it is likely that it originated naturally from a silicic acid gel. Furthermore, the original dry substances such as gelatin which form "gels" if they are permitted to swell by absorbtion of fluids are included.

For that reason it is useful for this work to use the definition of a gel given by Hermans (1949) as a system characterised by the following conditions:

a. a coherent colloid disperse system of at least two components.

b. as exhibiting mechanical properties characteristic of the solid state.

c. both the dispersed and the dispersion media extend continuously throughout the whole system.

Criterion b. will be taken to refer to the fact that on mechanical deformation such as a shearing tension, whether or not the system exhibits a yield value, and consequently whether it shows the phenomenon of strain.

Two fundamental conditions must be fulfilled in order for a gel to be formed from a colloidal solution:

1. a solid state substance shall separate from the solution in a finely dispersed colloidal state.

2. the separated solid particles shall neither be deposited under gravity, nor remain in colloidal suspension as freely moving kinetic units, but be joined together to form a continuous framework (or network) throughout the mass of the solution.

There are four different possibilities concerning the nature of the gel network which are shown diagrammatically in fig. 3.1 for spherical particles, rod like particles, and linear macro-molecules with either crystalline junctions or chemical cross-linking respectively.

Fig. 3. 1. Four Types of Gel Structure.

(a) spherical particles. (b) rod like particles.

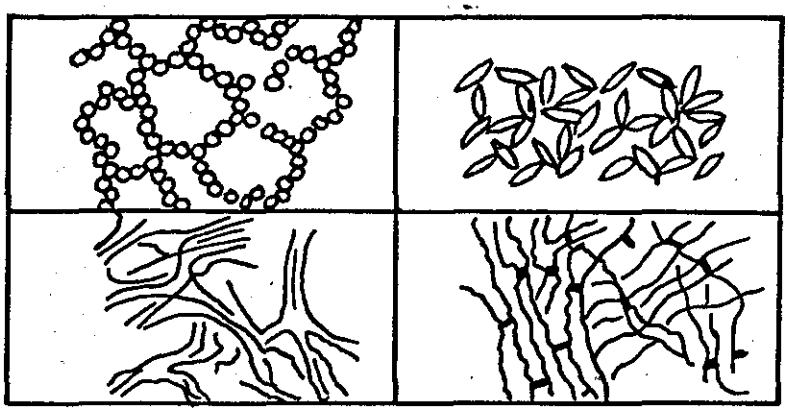

(c) linear macro-molecules with crystalline junctions (d) linear macro-molecules with chemical cross-linking.

Table 3. 1. Packing Type, Co-ordination Number and Associated Void Volume.

Packing Type.	Co-ordination.	Void Volume %
hexagonal close packed.	12	26
cubic close packed.	12	26
face centred cubic.	12	26
body centred cubic.	12	32
simple cubic	12	48
least dense packing	3	94.4 *

References.

Atkins. (1978)

*Heesch & Laves. (1933).

An outline of the wide variety of gel structures has been presented by Hermans (1949), Duclaux (1953) and Weiser (1950). The gel structure that is likely for the silica/electrolyte systems is that of approximately spherical particles adhering to each other in an approximately linear arrangement. It should be noted that the spherical structure particles may be single silica particles or aggregates of silica particles. There is also the possibility that short chains made up of single silica particles may be cross-linked to form the gel network or be the link between the spherical aggregates.

Manegold (1941) has considered the volume fraction of the space occupied by a continuous network. For spherical particles various regular packings are possible with a variation in co-ordination number of each particle of between 3 and 12. The most dense packing gives a co-ordination number of 12 and a volume fraction of 0.74 (i.e. the void volume is 0.26)and for the least dense packing condition a co-ordination number of 3 and a volume fraction of only 0.056,see Heesch & Laves (1933). A list of packing types and the corresponding void volumes is given in Table 3. 1.

For any system capable of gel-formation there will be a limit of dilution beyond which gel-formation becomes impossible. However, there is no sharp limit between gel-formation and the formation of a flocculate or precipitate. In many cases it may be difficult to differentiate between a gel and a liquid as the solution maintains its fluid character. Very sensitive measurements are necessary to demonstrate that the solution has a definite yield value, but the junctions between individual particles are easily broken.

Before discussing further the properties of the gelled electrolyte it is useful to consider the properties of the fumed silica and the sulphuric acid separately.

3. 2. Sulphuric Acid.

Sulphuric acid is probably better characterised than most compounds in respect of its physical properties in both its pure state and for its aqueous solutions.

The conductivity of aqueous solutions of sulphuric acid for concentrations between 0.5 and 99% by weight of acid over a wide range of temperatures has been well established to an accuracy of $\pm$ 0.0005 S cm^{-1} or better, see Roughton (1951), Campbell et al (1953a), Darling (1964), and Gerzberg et al (1969).

A maximum in the conductance is observed at an acid concentration of between 25% and 40% (4.99M) for all the temperatures investigated. The maximum occurs at higher concentrations as the temperature is increased, see fig. 3. 2.

For aqueous solution, dissociation of the acid gives :

$$H_2SO_4 + H_2O \underset{\leftarrow}{\overset{K1}{\rightleftharpoons}} H_3O^+ + HSO_4^- \quad ; \quad HSO_4^- + H_2O \underset{\leftarrow}{\overset{K_2}{\rightleftharpoons}} H_3O^+ + SO_4^{2-}$$

The ratio of HSO_4^- to SO_4^{2-} is approximately 2 : 1 for 5 Molar acid at 25°C. The ratios for a range of acid molarities and three temperatures determined by Raman spectroscopy, Hamer (1959), are given in table 3. 2 and shown in Fig. 3. 3 as a function of stoichiometric molarity.

The primary contribution to the abnormally high conductivity of such solutions comes from the large excess of hydrogen ions H_3O^+. A reasonable explanation of this phenomenon has been found by Bernal and Fowler (1939) in terms of a proton jump mechanism by which a proton passes from one water molecule to a favourably orientated neighbouring one, but in doing so leaves these molecules unfavourably orientated for another jump. The proton jump mechanism can be

Fig. 3.2.

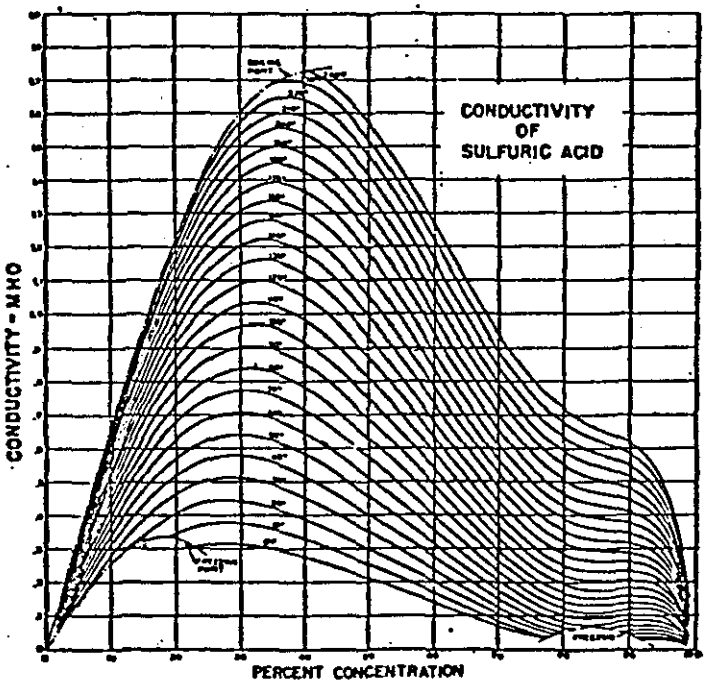

Constant temperature curves of conductivity vs. percent concentration (5.0% to 90%)

Reference Darling (1964).

TABLE 3.2 CONSTITUTION OF AQUEOUS SOLUTIONS OF H_2SO_4
(Mole liter^{-1})

0°C.				25°C.				50°C.			
M	$[SO_4^{2-}]$	$[HSO_4^-]$	$[H_2SO_4]$	M	$[SO_4^{2-}]$	$[HSO_4^-]$	$[H_2SO_4]$	M	$[SO_4^{2-}]$	$[HSO_4^-]$	$[H_2SO_4]$
18.89	0.0			18.62	0.0			18.37	0.0		
				18.11	0.0	4	15				
16.49	0.0	11	5.4	16.24	0.0	10	6	16.00	0.0	10	5.5
15.42	0.0	13	2.2	15.18	0.0	12	2.8	14.95	0.0	12	2.9
14.15	0.3	14	0.1	13.94	0.3	13.6		13.74	0.20	12.3	1.2
11.00	1.6	9.4		10.85	1.1	9.7		10.70	0.6	10.1	
7.93	2.1	5.8		7.82	1.8	6.0		7.71	1.3	6.4	
6.08	2.2	3.9		5.99	1.8	4.2		5.91	1.3	4.6	
4.03	1.7	2.3		3.97	1.3	2.7_0		3.91	0.8	3.1	
				2.95	0.9_7	1.9_8					
1.486	0.70	0.79		1.47	0.4_4	1.0_3		1.453	0.30	1.15	
				0.98	0.2_7	0.7_1		0.967	0.17	0.79	
0.496	0.24	0.26		0.492	0.1_{45}	0.3_5					
				0.332	0.08_9	0.2_4		0.328	0.07	0.26	
				0.204	0.05_6	0.15					
				0.101	0.03_2	0.06_9					
				0.050	0.01_7	0.03_3					

reference Hamer (Editor), 1959

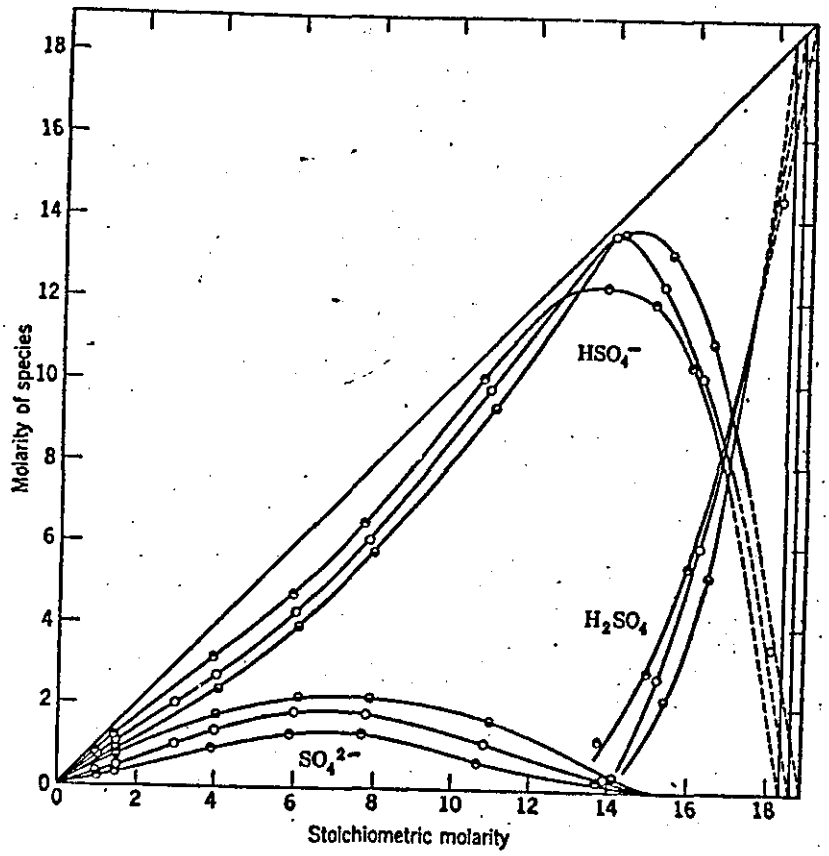

Fig. 3.3 Concentrations of three molecular species vs. stoichiometric molarity of H_2SO_4. ⊖, 0°C.; ○, 25°C.; ⊖, 50°C.

represented diagrammatically after Glasstone, Laidler and Eyring (1941) as follows:

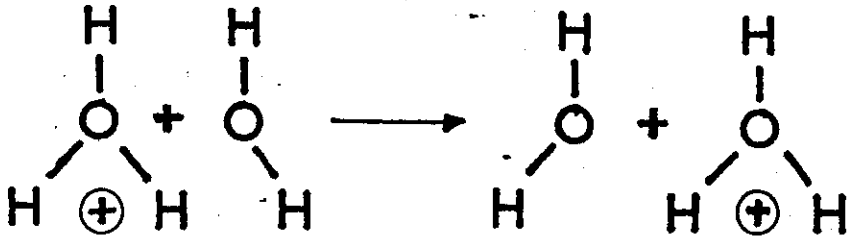

A similar proton transfer process accounts for the high mobility of the aqueous hydroxide ion, which is second only to that of the hydrogen ion:

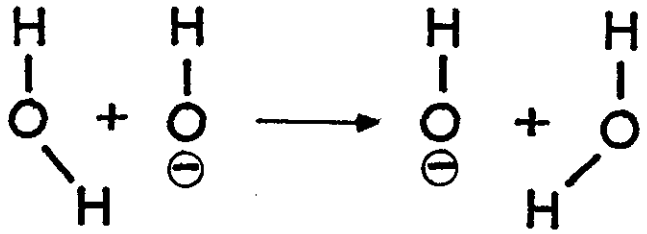

At any one time only a relatively few protons need jump to produce the observed conductivity. The rest of the hydrogen ions will be incorporated in the normal water structure, i.e. associated with a water molecule and moving in the normal manner. Robinson and Stokes (1970) have suggested the water molecules with associated hydrogen ions are moving at about the same speed as hydrated lithium ions from thermodynamic considerations.

The hydrated lithium ion and hydrogen ion are of very similar size and involve about the same number of water molecules. There is also a remarkable similarity between the activity coefficients of lithium chloride, bromide, iodide, and perchlorate, and those of the corresponding acids.

3. 3. Potassium Chloride.

The other electrolyte used extensively during this work was potassium chloride. In addition to its function in the calibration of conductance cells, gels were prepared using potassium chloride solutions of concentrations less than 1Molar.

There were several reasons for this choice:

1. Potassium chloride in aqueous solution belongs to the class of simple 1 : 1 non-associated electrolytes i.e. a simple cation and anion, possibly solvated,but with no experimental evidence for co-valent molecules of solute or any lasting association of oppositely charged ions.

2. Potassium chloride is readily obtained in a high state of purity and may be used to make up solutions of accurately known concentration directly after oven-drying at 200°C to remove any absorbed water.

Therefore potassium chloride solutions have been universally used in some of the most accurate conductivity measurements undertaken in the search for a satisfactory theory of electrolytic conductivity, e.g. Gordon et al (1940, 1942, 1945), Shedlovsky (1932, 1934), Jones and collaborators (in 1930's).

It was hoped that the conductance measurements on gels in potassium chloride would complement those from gels in acid because it is a simple electrolyte, gelling should be encouraged as there is not the dehydration of the silica surface, and it is a much more pleasant system to handle from a practical viewpoint.

3. 4. Silica.

The fumed silica (silicon dioxide) used in this work is manufactured by the process of flame hydrolysis. Silicon tetrachloride vapour is hydrolysed in a flame of oxygen and hydrogen:

$$2H_2 + O_2 \longrightarrow 2H_2O \qquad 3.\ 1.$$

$$SiCl_4 + H_2O \xrightarrow{1800^{\circ}C} SiO_2 + 4HCl. \qquad 3.\ 2.$$

In the combustion process silicon tetrachloride burns to produce molten, primary spherical particles with diameters in the range 7 → 14 nm and of final surface area between 400 and 200 $m^2 g^{-1}$. While still semi-molten these primary spherical particles collide and fuse with one another irreversibly to form branched, three dimensional chain-like secondary groupings termed aggregates. As the aggregates cool to below the fusion temperature of silica, 1710°C, a further but reversible agglomeration occurs. Further agglomeration also takes place during the collection and bagging processes.

The residual hydrogen chloride adsorbed on the silica surface is reduced to less than 200 ppm by calcination. The resultant amorphous silica is a high purity, fluffy, white powder, with a bulk density of 0.032 g cm^{-3}, the true density of the silica being 2.20 g cm^{-3} (Cabot Carbon Ltd.).

The amorphous nature of the fumed silica is shown by the absence of lines in the X-ray diffraction and electron diffraction patterns e.g. Radczewski and Richter (1941). The amorphous nature is also the reason for the silica particles tending towards a spherical shape. The silica manufacturers, Cabot Carbon Ltd, state that the particles are non-porous.

Silica in this amorphous form is soluble in water to about 0.01% expressed in terms of SiO_2. The soluble form of silica is the monomeric $Si(OH)_4$, but the state of hydration in water is unknown. $Si(OH)_4$ polymerises rapidly if the concentration exceeds a few hundredths of a per cent. The solubility of amorphous silica has been described by Iler (1955), reviewed by Wittman (1961) and again by Iler (1973).

Carman (1940) was probably the first to postulate a structure for a single silica particle in an aqueous system, as shown in fig. 3. 4. He suggested that the particle could be considered as having two parts:

1. an interior composed of anhydrous, amorphous, three dimensional network of SiO_4 tetrahedra conforming in composition to SiO_2 by the linking of every oxygen atom to two silicon atoms.

2. a surface region in which the silicon atoms are co-ordination deficient, and will strive to achieve the favoured tetrahedral co-ordination. In aqueous systems or when moisture is present this will be accomplished by the formation of OH^- groups on the surface. He visualised that two hydrogen ions are held equally by the two negatively charged oxygen ions, giving effectively OH^- groups on the surface.

Two types of surface hydroxyl groups may be distinguished by Infra red spectroscopy as shown in fig. 3. 5:

1. isolated OH^- groups, which are attached to surface silicon atoms surrounded by siloxane groupings (Si-O-Si). These OH^-groups are of hydrophilic character and characterised by an IR absorbance peak at 3750 cm^{-1}.

Figure 3. 4

Particle of colloidal silica

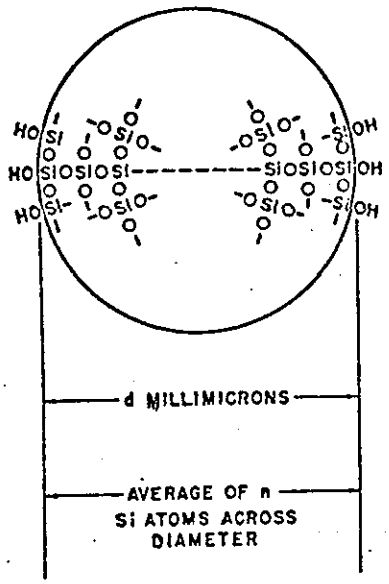

interior of anhydrous amorphous Si O_2,

surface of silanol groups.

Figure 3. 5 Infra red spectra of silica .

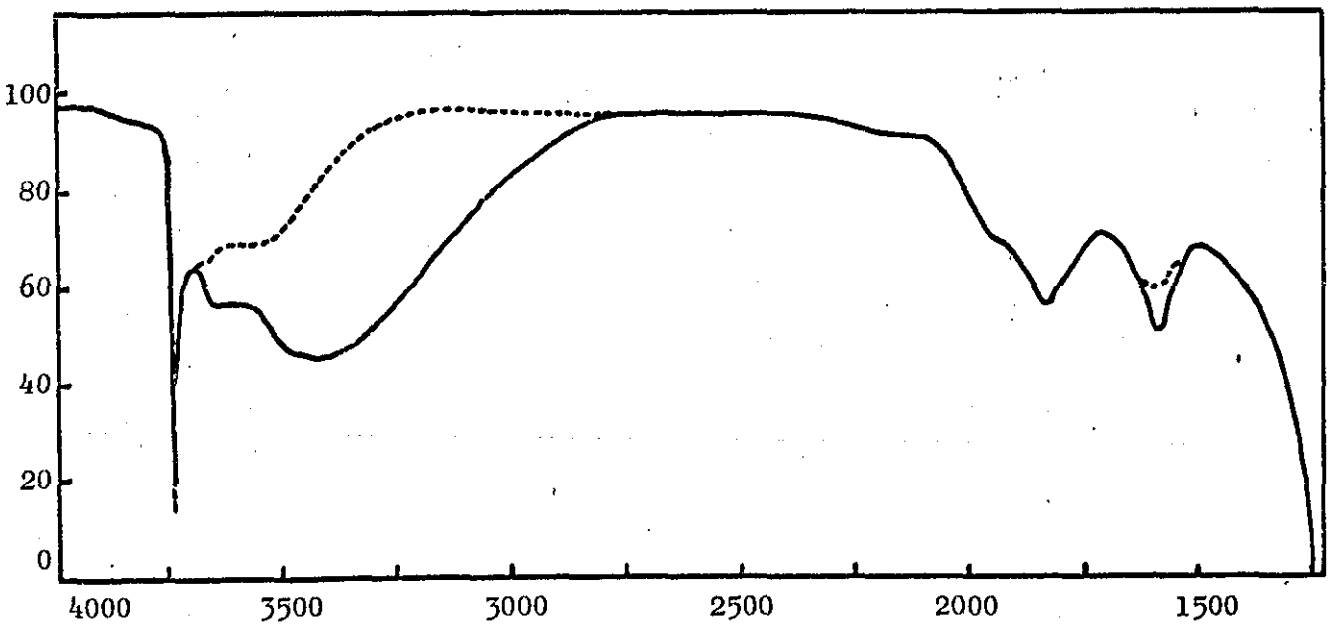

2. hydrogen-bonded OH^- groups, a result of OH^- groups on neighbouring silicon atoms. These groups are also hydrophilic and characterised by a broad absorbance peak between 3,700 and 3,500 cm^{-1}.

A third surface grouping may be identified as siloxane groups, Si - O - Si, which are responsible for the hydrophobic character of the silica surface. This picture of the silica surface is summarised in fig. 3. 6.

The surface of pure silica in water adsorbs OH^- ions (or loses H^+ ions) and becomes negatively charged in alkaline suspension. However, there is no evidence for the converse of loss of OH^- in acid solution with the formation of a positively charged surface. The surface does not adsorb acid as it does base. Therefore, at any pH below about 3, the isoelectric point of silica, the particles are in the isoelectric condition and do not move when a potential is applied across the solution as in electrophoresis.

The gelling mechanism of colloidal silica has only become better understood during the last twenty years with the development of methods of preparing colloidal silica sols of a uniform and known size on a commercial scale. The first method was described by Bechkold and Snyder (1951) and many other methods and refinements in controlling particle size, degree of aggregation and purity have been developed subsequently covering the whole colloidal size range.

The basic step in gel formation is the collision of two silica particles with sufficient contact time for bonding to occur. It is to be understood that the silica particles could be single, part of a short three-dimensional chain, or part of a larger aggregate of particles.

Fig. 3. 6 Summary of the structure of a silica particle surface.

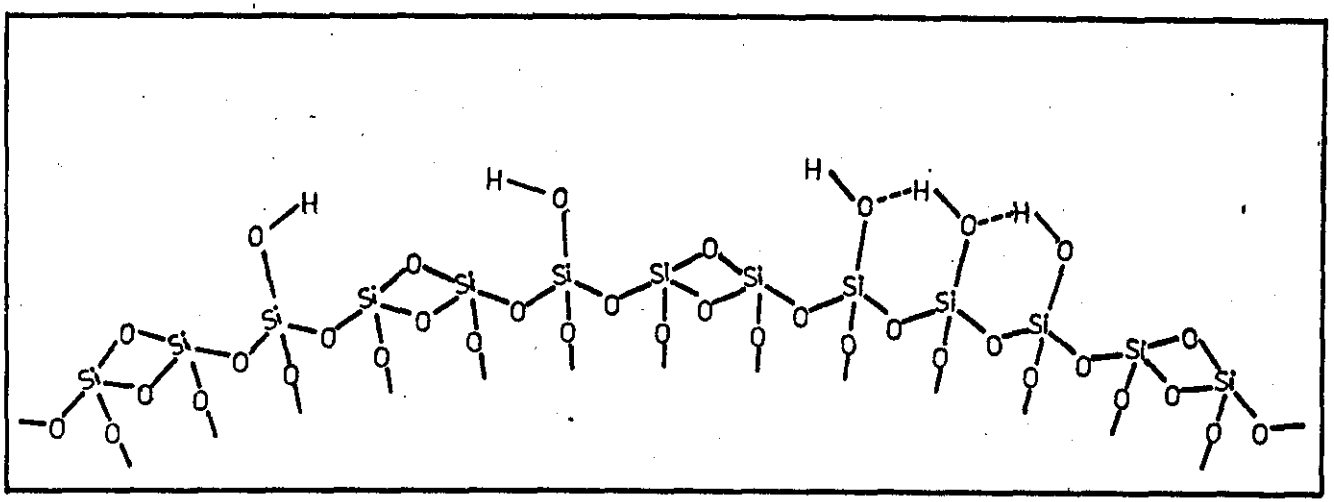

Two types of interparticle bonding may be identified:-

1. Hydrogen bonding, 2. Siloxane bonding.

It is likely that the first bonding in all gel formation is hydrogen bonding between the isolated surface OH^- groups of the two particles or more particles, see fig. 3. 7. This bonding is reversible, the network may be temporarily destroyed by changing the pH or mechanical agitation.

In basic media the hydrogen bonded particles may become irreversibly bonded by a siloxane link under the catalytic action of OH^- with the elimination of water, see fig. 3. 8. Under these conditions it has been shown by Alexander (1957) that silica may be deposited around the point of contact, the Si - O - Si link, particularly for pH > 5. This is because the solubility of silica from a thermodynamic viewpoint is greater when the radius of curvature of the surface of the particles is small and positive, compared to where the radius of curvature of the surface is negative and small such as at the point of contact. Therefore silica dissolves from the two particles and is deposited at the point of contact to minimise the negative radius of curvature, see fig. 3.9.

In acidic media there may be sufficient OH^- to catalyse some interparticle siloxane bond formation, but the solubility of silica at low pH and the concentration of OH^- are too small to permit any coalescence at the point of contact. Therefore gelling is reversible in acid media. Iler (1952) has shown that traces of F^- ion in the silica in acid media of pH < 1.5 with the formation of HF may also catalyse gelling.

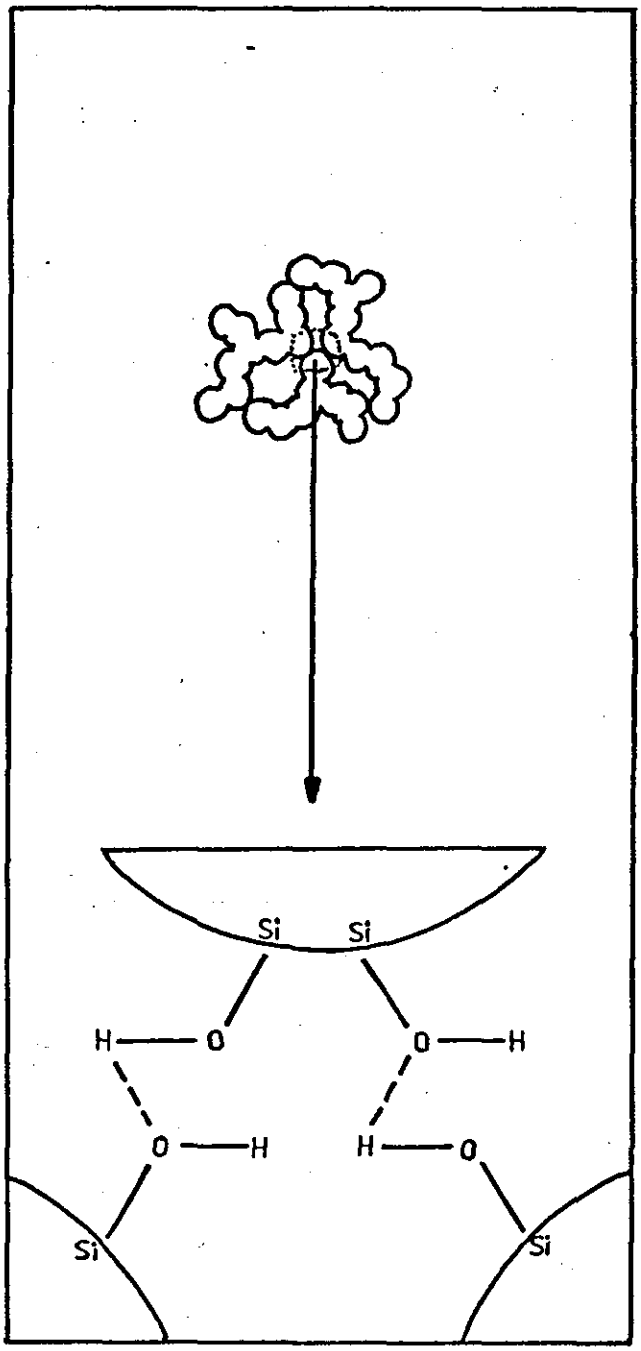

Fig. 3. 7.

Hydrogen bonding between two silica particles.

Fig. 3. 8. Formation of a siloxane link between two silica particles.

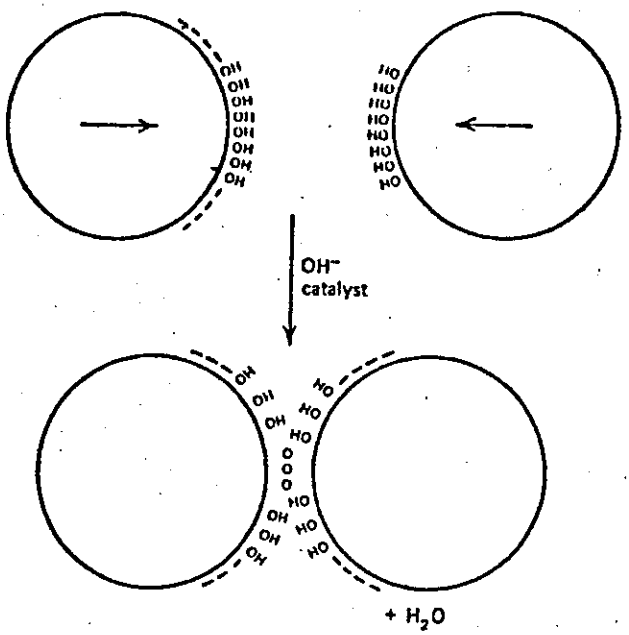

Fig. 3. 9. Deposition of silica at the point of contact of two silica particles.

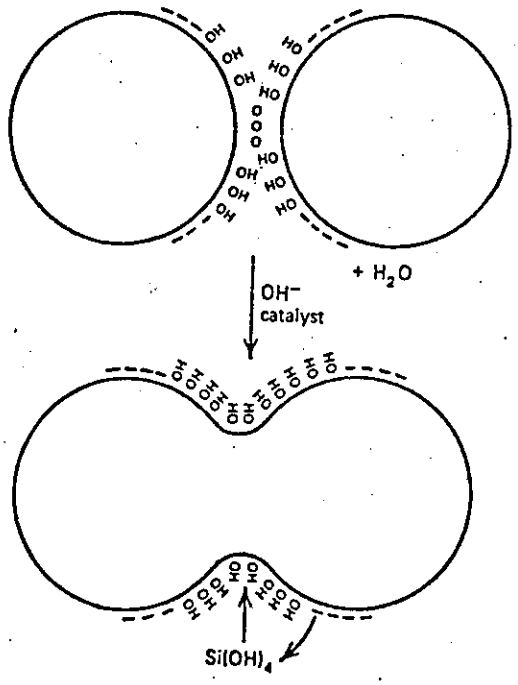

However, in any hydrogen bonding liquid the solvent molecules will be in competition with the isolated hydroxyl groups for hydrogen bonding, see fig. 3. 10, resulting in partial or total solvation of silica aggregates and a reduction in the formation of network structure, effectively means a greater concentration of silica is required to form a gel.

The other determining factor governing network formation is the degree of dispersion of the silica. A balance has to be achieved between under-dispersion which leaves relatively large agglomerates with a small amount of cross-linking between them, and over-dispersion with the result that the agglomerates are broken into such small, widely separated fragments, that they are statistically unlikely to collide and hence unlikely to form networks.

The overall behaviour of silica may be summarised as in fig. 3.11.

The rate of gelling reaches a minimum at pH 2→3, and a maximum at a pH = 5. In the range pH < 1.5 the gelling is catalysed by HF, Iler (1952), in the range pH = 3→5 the rate increases in proportion to the concentration of OH^-. Above pH = 6 the rate decreases due to there being fewer collisions between particles as a consequence of the increased surface charge. Above pH = 10.5 silica dissolves quite rapidly. The rate of gelling as a function of pH is shown schematically in fig. 3. 12 reproduced from Iler (1973).

The rate of gelling is also dependent on the concentration of silica and the particle size. The two factors are inter-related as the rate of gelling appears to be proportional to the total surface area of silica surface present. As the surface area is inversely proportional to the diameter of the particles, suspensions with the same concentration to particle-diameter ratio gel at about the same rate, Iler (1973).

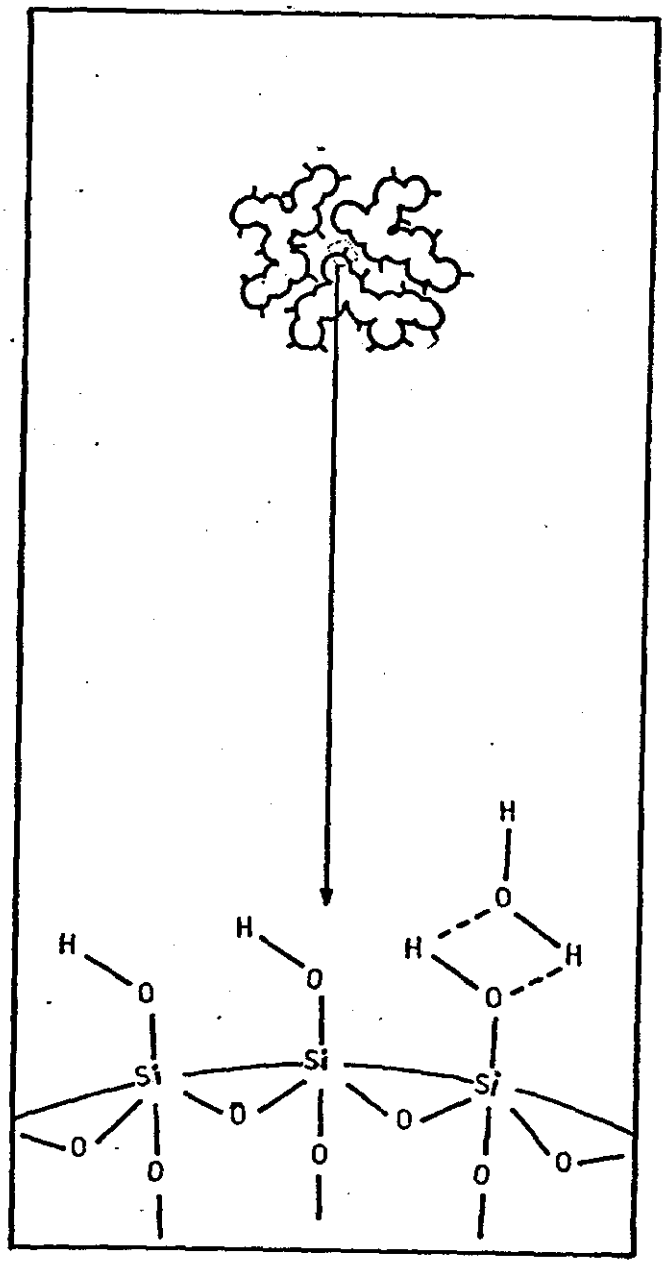

Fig. 3.10.
Solvation of isolated hydroxyl groups
on a silica surface.

Fig. 3.11. Summary of overall behaviour of silica.

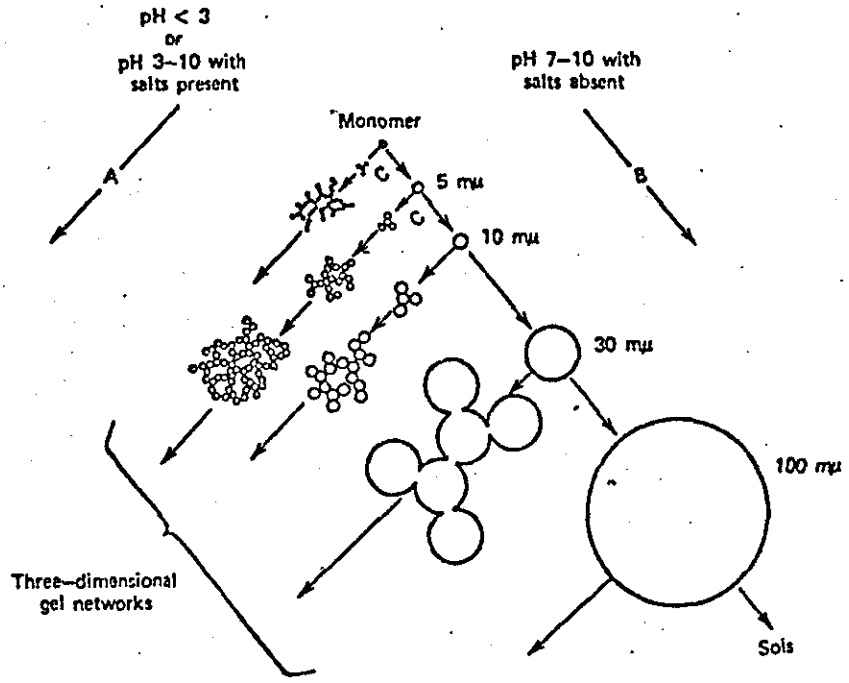

Polymerization behavior of silica. In basic solution (B) particles in sol grow in size with decrease in numbers; in acid solution (A) or in presence of flocculating salts, particles aggregate into three-dimensional networks and form gels.

Fig. 3.12. Rate of gelling of silica-water system as a function of pH.

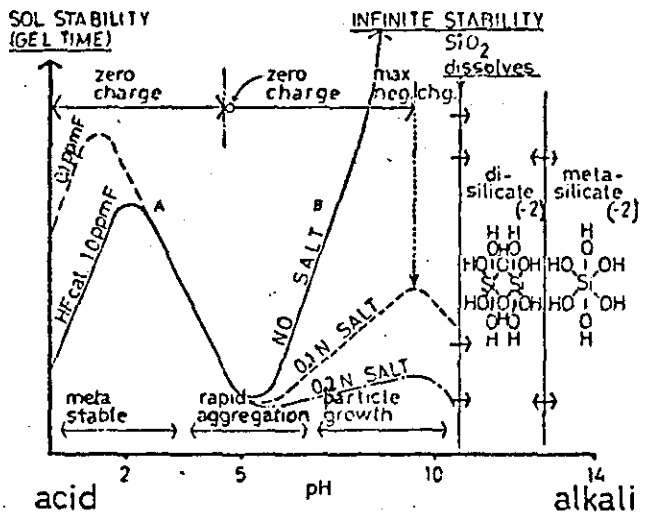

3. 5. Ionic Conductivity.

The ionic conduction through an electrolyte occurs by ion migration to the oppositely charged electrodes when an electric field is applied. Electrolytes approximately obey Ohm's Law, but because of their susceptibility to electrolysis, conductivity measurements are usually made using alternating current circuits.

The resistance, R, of a sample of material is proportional to the length, l, of the sample, and inversely proportional to the cross-sectional area, A:

$$R = \rho \frac{l}{A} \quad \text{or} \quad \rho = R. \frac{A}{l} \qquad 3.3.$$

where ρ = a proportionality constant called the resistivity of the material, and is defined as the resistance of a sample 1 m long and of 1 m^2 cross-sectional area, therefore the units of ρ are ohm m. (Ω m).

Conductance, "G", is defined as the reciprocal of the measured resistance and conductivity, K , as the reciprocal of the resistivity. i.e.

$$G = 1/R \text{ units S, previously } \Omega^{-1} \text{ (ohm}^{-1}\text{)} \qquad 3.4.$$

$$K = 1/\rho = \frac{1}{R} \cdot \frac{l}{A}$$

The units of conductivity are Sm^{-1}, where S is the Siemens. Prior to S.I. units, the common unit for conductivity was $\Omega^{-1}\ cm^{-1}$.

The conductivity of the electrolyte may be defined as the conductance of a sample 1 m long and of 1 m^2 cross-sectional area.

A conductance cell has fixed electrodes, so the ratio l/A is a constant, the cell constant, K_{cell} , and is a characteristic of the cell i.e.

$$K = \frac{1}{R} \cdot K_{cell} = G. K_{cell} \quad Sm^{-1} \qquad 3.6.$$

The conductance cells are calibrated by determining the conductance of a standard solution, the conductivity of which is very accurately known under closely defined conditions, usually a solution of potassium chloride at 25°C. The solutions are prepared by a weight/weight method. The term "demal" was introduced by Parker & Parker (1924) in an early definition of a standard solution and has been retained by Jones and Bradshaw (1933) as a useful term to describe their standard composition. They define a 1 Demal solution (1D) as a weight in vacuo of potassium chloride in 1000 g of solution.

Jones and Bradshaw (1933) determined the conductivity in international ohm^{-1} cm^{-1} of three carefully defined solutions of potassium chloride at three temperatures and these values are generally accepted for use in determining the K_{cell} of conductance cells. A table showing the composition and conductivity of the solutions is given in table 3.3.

The requirements for precise measurement of electrolytic conductivity are accurate temperature control, avoidance of electrode polarization, and accurate electrical measurement.

The majority of aqueous electrolytes have a temperature coefficient of conductivity of about 2% per degree at 25°C, but that of the H^+ ion is about 1.4% per degree. Therefore, temperature control of better than $\pm$ 0.005° is required for an accuracy of 0.01% in the conductivity. Usually the standard solution of potassium chloride used to determine the cell constant has a similar temperature coefficient to that of the solution to be studied. Therefore, provided the temperature is constant, the exact temperature is not required to the same accuracy as a constant

Table 3.3.

Conductivities of Standard Potassium Chloride Solutions.

Concentration	g KCl/1000g solution (in vacuo)	K Scm^{-1}		
		0^{o}	18^{o}	25^{o}
1 D	71.1352	0.06517_6	0.09783_8	0.11134_2
0.1D	7.41913	0.007137_9	0.011166_7	0.012856_0
0.01D	0.745263	0.0007736_4	0.0012205_2	0.0014087

Jones and Bradshaw (1933).

error of a few hundredths of a degree will largely be compensated for by the corresponding change in the conductivity of the standard.

Accurate temperature control is most readily achieved using water as the thermostatting medium because of its specific heat capacity, low viscosity which facilitates stirring, and its slow evaporation to dissipate surplus heat.

However, Jones and Josephs (1928) inferred from AC theory that the presence of a conducting medium near to a conductivity cell would cause an error in the measurement of resistance due to the following causes:

1. the capacitance introduced by an earthed conducting liquid in the thermostat would be expected by geometrical considerations to be greater than the capacitance introduced by the metal plate.

2. the walls of the glass cell may act as a dielectric in a condenser, permitting AC current to flow in the water outside the cell. This extra parallel path for current referred to as a capacitance bypath, consisting of two condensers and a resistance, must decrease the measured resistance.

3. the AC current in the cell will induce eddy currents in the water outside the cell and will increase the apparent resistance in accordance with the well known behaviour of a short-circuited transformer. The eddy currents tend to counteract the error due to the capacitance by-path.

These sources of error may be functions of frequency, resistance of the cell electrolyte, the conductivity of the thermostatting water, the cell geometry, the thickness and electrical properties of the glass, and the proximity of measuring leads. Jones and Josephs (1928) showed that these errors amounted to between 0.1 and 0.51% for water. Therefore oil must be used for its excellent insulating properties. The disadvantages with respect to stirring, specific heat capacity, and loss of the cooling effect due to evaporation must be remedied in the construction of the thermostat or tolerated where this is impracticable.

The use of direct current methods is only satisfactory when one of the electrodes is truly reversible to one of the ions in solution and the other electrode is truly reversible to the ion of opposite charge. For most systems errors due to electrolysis of the electrolyte and electrode polarization are encountered when direct current methods are used. Polarization errors may be minimised in two ways: by the use of audio frequency alternating current for the conductivity measurements; and by the electrodeposition of a heavy deposit of platinum black on smooth platinum electrodes, first suggested by Kohlrausch (1897) and developed by Jones and Bollinger (1935). However, platinum black may catalyse unwanted reactions, or may adsorb appreciable quantities of solute from dilute solutions. The latter may be controlled by repeated filling and emptying of the cell until a constant conductivity is obtained, the former by using a much lighter deposit of platinum black.

The design of high precision AC conductance bridges was studied by Shedlovsky (1930) and by G. Jones and colleagues during the 1930's and the principles they listed for good bridge design are the basis of

those in use today, see Haque & Foord. (1971).

The simple Wheatstone bridge circuit used for DC measurements , see fig. 3. 13, is adapted for use with AC potentials by the substitution of the battery with a sinusoidal alternating potential from an oscillator, and the galvanometer by an AC null detector, see fig. 3. 14. The balance condition determined by the null detector is when the potentials at A and B are of equal amplitude and are exactly in phase. At this point the impedances (the AC analoque of resistance) are related by the equation :

$$\frac{s_1}{s_2} = \frac{s_3}{s_4} \qquad 3.\ 7.$$

The ideal bridge is constructed with all the arms equal, a requirement which can only be met once the properties of the electrolyte are known. Consequently commercial bridges designed to measure over a wide range of conductivities have ratio arms R_3 and R_4 equal (usually 1000 Ω) and of as identical construction as possible and with a negligible inductance at audio frequencies. The variable capacitor C_2 in parallel with R_2 is necessary to obtain a sharp balance point because the cell impedance is rarely purely resistive.

Thus the use of an AC method greatly complicates the electrical technique, and furthermore the frequency is introduced as another possible variable governing the measured conductivity.

If the electrode effects have not been eliminated by platinisation they will become apparent when the conductivity is measured at various frequencies and the values differ. Usually three values of frequency between 100 & 5,000 Hz are sufficient. In this situation the theory of electrode processes must be applied in order to calculate the "true" conductivity of the electrolyte.

Fig. 3. 13. Wheatstone bridge circuit for DC conductance measurements.

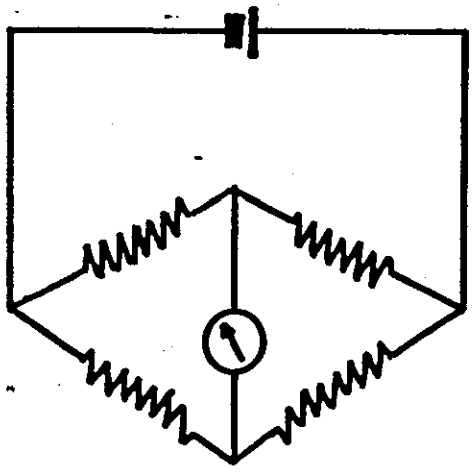

Fig. 3. 14. Bridge circuit for AC conductance measurements.

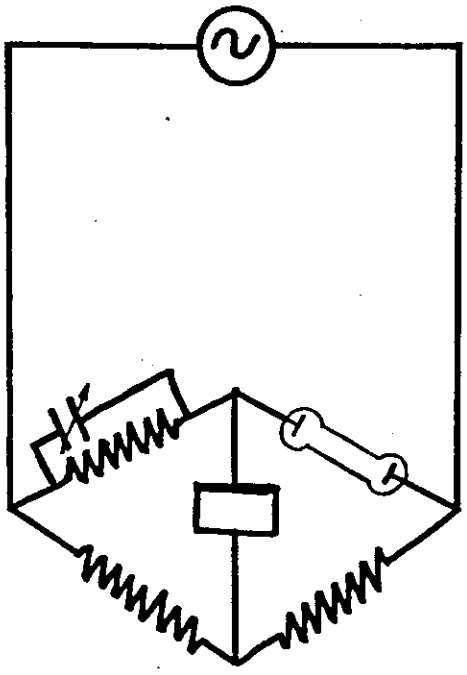

The conductance cell may be represented by the equivalent circuit shown in fig. 3.15 originally proposed by Feates, Ives, and Pryor (1956) with the addition of a "Warburg impedance" .

R_1 in this circuit represents the true ohmic resistance of the electrolyte, the quantity which is required. R_1 is normally independent of frequency at audio frequencies because the Debye-Falkenhagen effect does not become appreciable until radio frequencies are attained. The Debye-Falkenhagen effect is associated with the relaxation of ionic atmospheres. The ions of opposite charge which surround a central ion moving under the influence of an applied field tend to be left behind, but after a short time, the relaxation time, thermal agitation restores the normal symmetry of the distribution. The effect of high frequencies with a period of oscillation similar to that of the relaxation time is to prevent the ion atmosphere relaxing to its symmetrical distribution, so the hinderance to the central ion is diminished and abnormally high conductivities are observed. It should be noted that the electrophoretic effect, the tendency of moving ions to drag solvent molecules with them, remains fully operative.

Capacity C_1, in series with R_1, is the capacity of the double layer at the electrode/electrolyte interfaces and is also independent of frequency. The current through the electrolyte crosses the interface by virtue of this capacity, and at model electrodes (no polarization) crosses without discharge or formation of ions. For electrodes where polarization occurs and there is a reaction at the electrode, the situation may be represented as a faradaic leakage in parallel with the double layer. The faradaic leakage was shown by Grahame (1955) and Randles (1947) to consist in general

Fig. 3.15 Equivalent Circuit of a Conductance Cell.

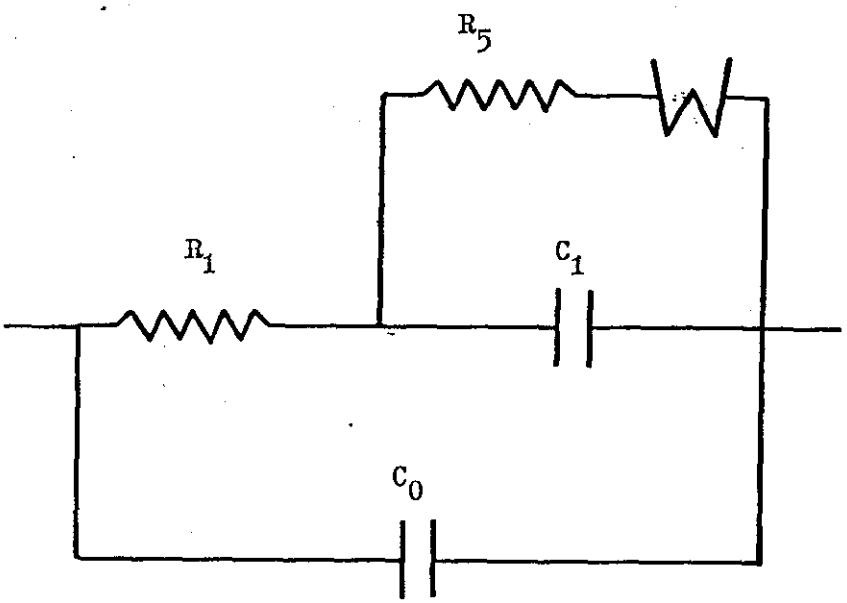

R_1 = true Ohmic Resistance of the Electrolyte.

C_1 = Capacity of the Double Layer.

R_5 = pure Resistance
-W- = Warburg Impedance
} = Faradaic Leakage.

C_0 = Capacity due to Cell, Cell Leads etc. and is usually negligible for a well designed Cell.

of two parts, a pure resistance, R_5, which is independent of frequency, and a Warburg impedance at the electrode, $-W-$, which may be represented by a resistance and capacitance in series the impedance of both being the same at any one frequency, but both impedances varying inversely with $\omega^{1/2}$. The two parts act together as

$$-W- = k(1 - j)/\sqrt{\omega} \qquad 3.8.$$

where k = constant of dimensions resistance.time$^{-1/2}$ and

$$j = \sqrt{-1}$$

If the impedance of the cell arm, with the omission of C_o, is Z cell, the solution of the balance conditions is:

$$\frac{Z_1}{Z_2} = \frac{Z\text{cell}}{Z_2} = \frac{Z_3}{Z_4} \qquad 3.9.$$

and for the case where $Z_3 = Z_4$

$$\frac{Z\text{cell}}{Z_2} = 1 \qquad 3.10.$$

$$\therefore \quad Z\text{cell} = Z_2 \qquad 3.11.$$

For a capacitor and resistor in parallel the reciprocal of the impedances add and therefore the impedance of arm 2 is given by

$$Z_2 = \frac{1}{R_2} + j\omega C \qquad 3.12.$$

Assuming capacitance errors in the cell have been eliminated or are small enough to allow C_o to be neglected, then denoting the impedance of the cell arm, with the omission of C_o, by $Z\text{cell}'$, solving the balance conditions gives:

$$\text{real part of } \frac{1}{Z\text{cell}'} = \frac{1}{R_2} \qquad 3.13.$$

The special cases of interest are:-

1. If C_1 is very large such that its impedance is small compared to that of the Faradaic leakage, as is very nearly the case for heavily blacked platinum electrodes, then $R_1 = R_2$ at all frequencies.

2. If R_5 is infinite so the electrodes are ideally polarized, which is difficult to achieve in aqueous solutions due to the depolarizing effect of dissolved oxygen, then :

$$R_1 + (\omega^2 C_1^2 R_1)^{-1} = R_2 \qquad 3.14.$$

3. If the Warburg impedance is negligible compared to R_5 and in most instances as $R_1 \gg R_5$, then the situation approximates to :

$$R_1 + R_5/(1 + \omega^2 C_1^2 R_5^2) = R_2. \qquad 3.15.$$

This equation is found to correspond to the behaviour of grey platinised electrodes, and for bright platinum electrodes in aqueous solutions.

It has been found in practice (Steel and Stokes, 1958) that although this equation is not easily adapted for extrapolation to infinite frequency, the value obtained by solving the equation for three frequencies agrees well with that obtained from a linear extrapolation of R_2 versus ω^{-1}.

4. When -W- is large compared to R_5 but small compared R_1 solutions are found of the type:

$$R_1 + k/\sqrt{\omega} = R_2 \qquad 3.16.$$

e. g. Silver electrodes in silver nitrate solution.
Jones and Christian (1935).

5. There are also cases reported where the behaviour is midway between 3 and 4 shown by marked curvature of the R_2 versus $\omega^{-1/2}$ curves e.g. Jones and Christian (1935) for silver electrodes in potassium chloride solution, and Brody and Fuoss (1956) have reported several examples where R_2 is quadratic in $k/\sqrt{\omega}$.

Therefore when first examining a particular electrolyte with a new conductance cell the frequency dependence of the conductivity should be determined, preferably by making a series of measurements in the frequency range 200 to 5,000 Hz.

With reference to the equations 3. 5 and 3. 6 given previously and relating to conductivity, cell constant, area of cross-section and separation of the electrodes of the conductance cell, it may be deduced that for highly conducting solutions the cell length must be large compared to the diameter of the flat circular electrodes, and that the cell constant must be high to permit accurate measurement on the bridge. Conversely, for solutions of low conductivity the cross-sectional area of the electrodes must be large compared to their separation and the cell constant must be small. Typical cell designs for measurement of solutions of high, moderate, and low conductivity are shown in fig. 3.16.

For dilute solutions, a dilution cell after the design of Shedlovsky (1930) with the modifications of Daggett, Blair and Kraus (1951) may be used to determine the effect of changing the concentration of the electrolyte on the conductivity. The method of use of such cells is described in chapter 4.

Brody & Fuoss (1956) have described designs of electrode assemblies for use as dip electrodes in containers of any size. Care must be taken

(a)

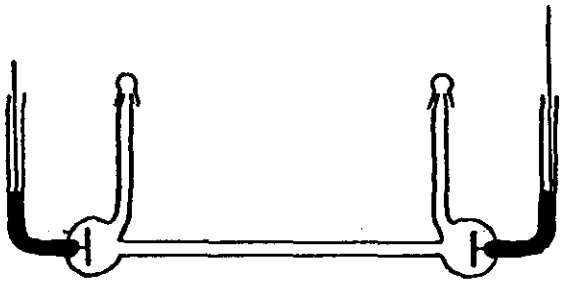

(b)

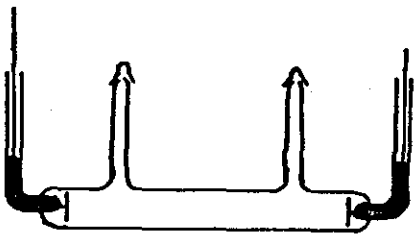

(c)

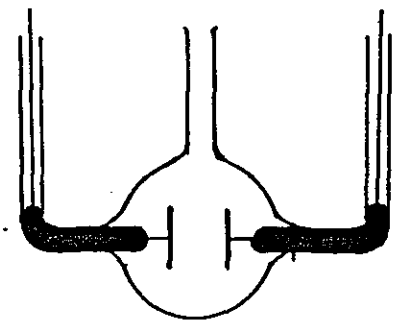

Fig. 3. 16 Typical conductance cell designs

(a) high, (b) medium (c) low, conductivity.

in use of such dip electrodes as any distortion of the electrodes will alter the separation and hence alter the cell constant. Also the cell constant is determined to some extent by the container affecting the available conducting paths.

For absolute measurements conventional conductance cells are to be preferred,but dip cells are of particular advantage for measuring the conductivities of a large number of similar solutions quickly for comparatitive purposes e.g. as a quality control measurement.

The standard solutions of potassium chloride specified by Jones and Bradshaw (1933) for use in the calibration of conductance cells have accurately known conductivities at 0^{o}, 18^{o}, and $25^{o}C$. The calibration of cells for use at other temperatures poses a serious problem. Some workers have used an equation to calculate the conductivity of potassium chloride at the desired temperature and calibrated the cell assuming that value of conductivity. e.g. Darling (1964) who used the equation:

$$K_s = 0.065430 + 0.0017319T + 0.000004617T^2 \qquad 3.17.$$

where K_s is the specific conductivity of potassium chloride at temperature T, the solution temperature in ^{o}C. It is not immediately clear where the equation is derived from as there is no mention of it in the reference quoted : Jones and Prendergast (1937). However a least squares polynomial fit on the conductivity of 1N potassium chloride at 0^{o}, 18^{o}, 20^{o} and $25^{o}C$ given by Jones & Prendergast (1937) results in the equation of Darling (1964), but is only valid for 1N potassium chloride in the region close to the temperature range 0^{o} to $25^{o}C$.

The vast majority of workers e.g. Roughton (1951), Campbell and Kartzmark (1952) have considered that the effect of temperature on the

dimensions of the cells constructed from pyrex glass and platinum electrodes to be negligible, and therefore the change in cell constant will be insignificant and have used the value determined at 25°C. Robinson and Stokes (1970) have shown that the correction varies with cell geometry and considered the effects of temperature on two extreme types of cell design, cells (a) and (c) of fig. 3. 16. They show that if the expansion coefficients of the glass and electrodes are equal, which is approximately the case for soda glass and platinum, the correction is the same for both cells, but if pyrex glass is used differences may arise.

For most purposes in this work the interest was of a comparative nature i.e. the effect of gel addition on the conductivity of the electrolyte compared to that of the electrolyte alone at a constant temperature. Consequently a knowledge of the exact cell constant was not essential provided that it remained the same throughout the measurements. This condition was easy to verify by checking the conductance of a standard solution and noting if the value had changed from the previous determination.

3. 6. Ionic Conductivity of Silica/Sulphuric Acid gels.

Having discussed the separate properties of sulphuric acid, potassium chloride, silica, the likely structures of gels produced from them and the measurement of ionic conductivity, consider now the ionic conductivity of such gels.

There is very little work in the literature on the effect of gel structure on the motion of ions in an electric field. The volume of related work in analytical chemistry on gel chromotography and gel electrophoresis is not relevant to the current problem because of the

large volume fraction of solids used and the nature of the solid. The system under investigation has a volume fraction of solids of less than 0.023 for the gels used on the production lines.

Similarly the work on ion exchange resins and membranes, see for instance the review by Spiegler (1953), or Helfferich (1962), concerns solid particles that have an appreciable conductivity, whereas fumed silica is an excellent insulator.

There is a brief comment in the second volume of Colloid Science ed. Kruyt (1949) referring to gels which states "as a rule the electrical conductivity and dielectric constant are what they should be expected to be for a mixture of two phases of given composition" but no references are given.

A recent paper by Orkina and Aguf (1975) on the structural-rheological properties of a gel-like electrolyte appears to be the only paper directly related to this work, and reports on the conductivity of a closely allied system: aerosils A-175 or A-300 in sulphuric acid electrolyte, as a function of temperature and silica concentration. Their conductivity results are reproduced in fig. 3. 17. The measurements were made using an AC bridge circuit and a cell with smooth platinum electrodes of cell constant 16.6 cm^{-1}. The frequency dispersion of the measured conductance was observed over the range 500 - 20,000 Hz and the value of conductivity obtained by extrapolation to infinite frequency was taken as the true value (after Robinson & Stokes (1970)).

The decrease in conductivity observed on addition of silica to the sulphuric acid is between 0.05 and 0.10 S cm^{-1}, i.e. less than 10% decrease.

Fig. 3. 17. Conductivity of Aerosil-sulphuric acid gels as a function of temperature.

Orkina and Aguf (1975)

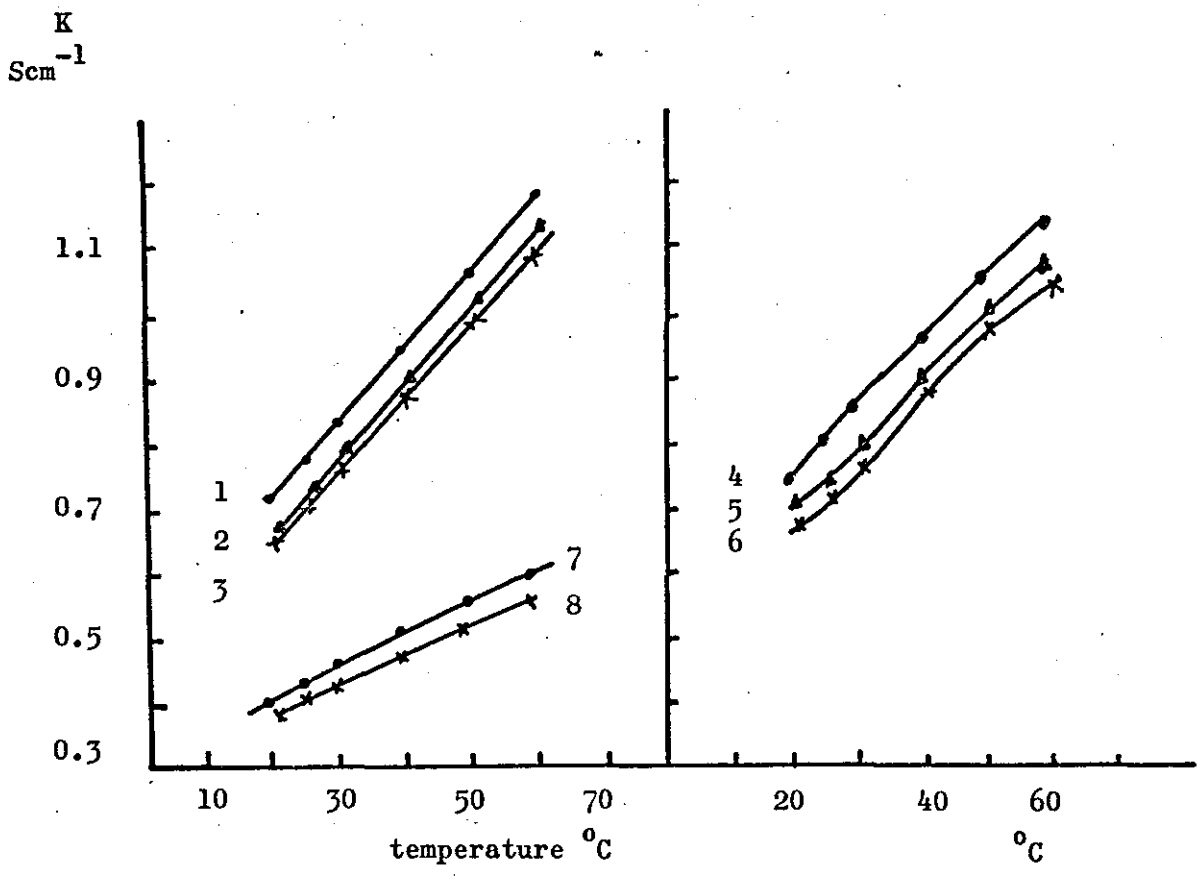

1. H_2SO_4 d = 1.28 g cm^{-3}
2. " " + 4-5% SiO_2
3. " " + 6-7% SiO_2
4. H_2SO_4 d = 1.17 g cm^{-3}
5. " " + 5-6% SiO_2
6. " " + 7% SiO_2
7. H_2SO_4 d = 1.07 g cm^{-3}
8. " " + 7-8% SiO_2

They state that such a small effect can be explained by the "estafette" * mechanism of electrical conductivity, due mainly to the migration of H^+ ions. They also suggest the increase in resistance is probably connected with the lengthening of the chain of hydroxyl ions along which the protons are displaced. They also state that the conductivity did not change during the course of the formation of the structure of the gel which they suggest took place over a period of 1 – 2 days.

One of the aims of this work on conductance measurements was to find a method of predicting the conductivity of a gel from a knowledge of its percentage composition of silica and the conductivity of the free electrolyte.

The starting point for such a description is to make the assumption that the silica, regardless of the way it is dispersed in the gel, makes no contribution to the total conductivity of the gel i.e. the silica is an inert insulator and that the only conduction pathway is via the acid electrolyte between the silica. The conductivity of the gel, K_g, will therefore be lower than that of the bulk acid, K_a, as a result of the loss in conducting volume occupied by the silica. K_g may be calculated by multiplying the conductivity of the bulk acid by the volume fraction of acid, ϕ_a, in the gel.

$$K_g = K_a . \phi_a = K_a (1 - \phi_s) \qquad 3.18.$$

ϕ_s = vol fraction silica and is related to ϕ_a by

$$\phi_a + \phi_s = 1 \qquad 3.19.$$

* I have been unable to find any reference to the estafette mechanism of conductivity and have written to the authors with a request for details, but have not received a reply.

Therefore a plot of conductivity versus volume fraction of silica should be a straight line of gradient - Ka, intercept Ka. However, this description is obviously much oversimplified and there are many possible effects which may influence the conductivity of the gel. In no order of importance or probability of occurance some possible effects are:

1. surface conduction along the short silica chains, or around the discrete silica particles and aggregates, or along the 3D gel network. This effect is likely to be swamped at the higher acid concentrations because of the high conductivity of the protons in the bulk acid, but may become significant at lower acid concentrations.

2. sorption by the silica of ions and solvent molecules from the electrolyte. Absorption is presumably small as the manufacturers claim the silica is non-porous (Cabot Carbon Ltd). Adsorption is almost certainly present because of the hydrophilic nature of the surface. Iler (1955) states that there is at least a monolayer of bound water on the silica surface, see also (Mysels 1959) and Graham (1947). The effect of adsorption on the conductivity of the gel is difficult to assess, but it is most likely to be seen as causing an increase in surface conductivity at low concentrations of acid.

3. minute traces of impurities such as F^- or aluminium may influence the conductivity because of the great effect they may have on gel formation. Iler (1952).

4. finally, there may be a reduction in the conductivity of the gel because the ions will have to travel around the silica regardless of the form in which it is present in the gel, and will therefore have a longer path compared to that in the bulk acid.

Of the various possibilities the latter is the most likely to cause a measurable effect, and fortunately may be incorporated into the conductivity relatively easily in one of two ways:

1. by the introduction of a tortuosity factor derived from a formation resistivity factor.
2. by application of the obstruction effect of dielectric theory to conductivity.

1. The study of liquid flow through porous media has been continuing for many years because of the vital part played by fluid flow phenomena in the extraction of petroleum from sedimentary rocks. The employment of electrical resistivity measurements to help analyse the rock formation penetrated by the drilling bit and give an estimation of the nature of the fluids contained within the pores of permeable rocks, led to the suggestion by Archie (1942) that a dimensionless parameter, F, the formation resistivity factor, could be determined by measuring the resistivity, ρ , of the rock saturated with a conducting electrolyte and dividing this resistivity by that of the electrolyte, ρ_e. F may be shown to be independent of the resistivity of the saturating electrolyte provided the rock matrix does not contain electrolytically conducting material and that the resistivity of the electrolyte is high enough to obviate surface conductivity effects. In the terminology of conductivity experiments, F is the cell constant of a porous medium and is a parameter reflecting the influence of pore geometry on electrolytic conduction

through the pore system (Wyllie & Spangler, (1952)). Wyllie (1950), Wyllie and Rose (1950), and by implication Thornton (1949), have suggested that the measurement of F leads directly to an evaluation of tortuosity, T, a term first coined by Rose and Bruce (1949).

The tortuosity is defined as:

$$T = (L_e / L)^2 \qquad 3.20.$$

where L_e is the average path length through the porous medium and L is the apparent path length:

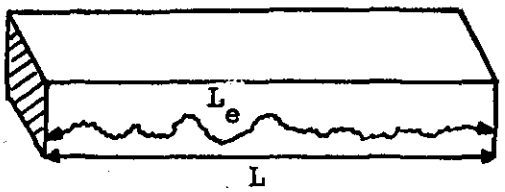

The pore space may be considered as a single channel of involved shape but constant cross-sectional area, ϕ A, where A. is the cross-sectional area normal to the path and ϕ is the void volume. Therefore the resistance of a homogeneous porous medium saturated with electrolyte may be considered to be the resistance of a volume of liquid of length L_e and area ϕ A, and will be equal to $\frac{\rho_c L_e}{\phi A}$.

However, the resistance of a volume of fluid of the same external dimensions as the saturated porous medium measured with the same relative orientation of electrodes is $\rho_c \cdot \frac{L}{A}$.

Therefore formation resistivity factor F is equal to:

$$F = \frac{\frac{\rho_c L_e}{\phi A}}{\rho_c \frac{L}{A}} \qquad 3.21.$$

which simplifies to:

$$F = \frac{\left(\frac{L_e}{L}\right)\frac{1}{\phi}}{} \qquad 3.22.$$

$$F = \frac{T^{1/2}}{\phi} \qquad 3.22.$$

Tortuosity is only capable of analytical expression for a straight tube where $L_e = L$ and hence T = unity. Fricke (1931) has considered the conductivity of systems of randomly dispersed particles. From his equations an expression for the formation resistivity factor, F, of non-conducting particles in a system of porosity, ϕ, is given by:

$$F = \left[(x + 1) - \phi\right]/xy \qquad 3.23.$$

where x is a shape factor and y is the axial ratio of particles which approximate to elipsoids. For spheres x = 2, y = 1.
Therefore $F = (3 - \phi)/2$ for spherical particles,
and using the definition of F but written in conductivity terms:

$$F = \frac{K_a}{K_g} \qquad 3.24.$$

Thus for the gel system under consideration, whether as randomly dispersed particles, short chains, or aggregates, the formation resistivity factor, F, should be independent of electrolyte concentration except when surface conductance effects are present. It should therefore be possible for example, to calculate F from the conductivity results obtained for silica in 40% acid and use the value of F obtained to predict the gel conductivities for acids of lower concentration. Deviations of the experimental values from the predicted values as the electrolyte concentration is lowered could be discussed in terms of surface conductance effects at the silica/electrolyte interface.

2. The other way of allowing for the increased path length of the ions passing round the silica in calculating the conductivity is derived from the obstruction effect of Dielectric Theory.

The addition of molecular solutes to water has the effect of increasing the viscosity. The resistance of an ion moving through the solution is also increased, but not in direct proportion to the viscosity as predicted by simple hydrodynamic considerations. The explanation is that the increased viscosity and the increased resistance experienced by the moving ion are two parallel effects of a common cause - the obstructive effect of the added solute, rather than a related cause and effect. In viscous flow the solute ions or molecules cause a distortion of the stream lines introducing a rotational quantity into the previously irrotational flow. The effect on conductivity and diffusion is an increase in the path length of the moving particles. This theory was first advanced by Wang (1954).

The situation may be visualised in terms of the simple model given in fig. 3. 18. The moving particles and solvent molecules are considered to be of negligible size compared to the particle causing the obstruction. The latter are regarded as rigid insulating spheres dispersed randomly in a continuous conducting medium.

The motion of ions can be discussed in terms of the passage of electric current through the system, and from the standard methods of electrical theory the current lines are distorted as shown in the fig. 3. 18 with a consequencial increase in resistance.

The real problem of a large number of such ellipsoids comparatively close together has been discussed by Fricke (1924, 1953), in connection with the conductance of blood.

However problems of steady current flow in conductors and lines of force in insulators are well known to be formally identical. Therefore the equations derived for the latter initially by Rayleigh (1892) and

Fig. 3. 18. Simple model of the obstruction effect.

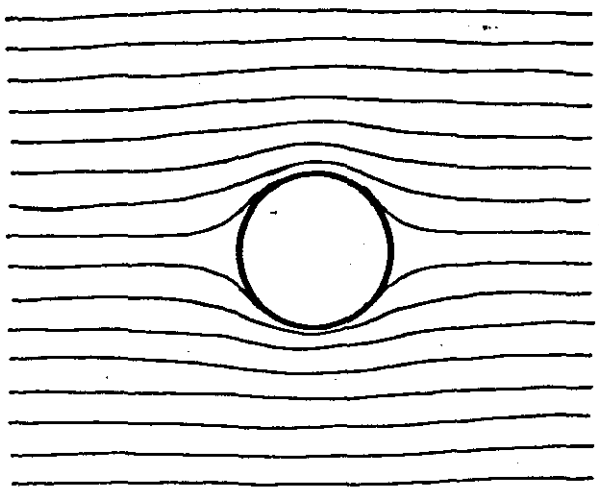

Robinson and Stokes (1970)

Table 3. 4. Equations for calculating the Dielectric obstruction effect and the corresponding equations for conductivity.

Dielectric	Conductance
1. Rayleigh (1892) $\frac{\varepsilon_m - \varepsilon_B}{\varepsilon_m + 2\varepsilon_B} = \frac{\varepsilon_s - \varepsilon_B}{\varepsilon_s + 2\varepsilon_B} \cdot \phi$	1. $\frac{K_m}{K} = \frac{1 - \phi}{1 + \phi/2} \approx 1 - 1.5\phi$
2. Bruggeman (1935) $\frac{\varepsilon_s - \varepsilon_m}{\varepsilon_s - \varepsilon_B} = (1 - \phi)\left(\frac{\varepsilon_m}{\varepsilon_B}\right)^{1/3}$	2. $\frac{K_m}{K} = (1 - \phi)^{3/2} \approx 1 - 1.5\phi$
3. Böttcher (1945) $\frac{\varepsilon_m - \varepsilon_B}{3\varepsilon_m} = \frac{\varepsilon_s - \varepsilon_B}{\varepsilon_s + 2\varepsilon_m} \cdot \phi$ ε_B = constant of medium ε_m = " " mixture ε_s = " " spheres	3. $\frac{K_m}{K} = 1 - 1.5\phi$ K = conductivity of medium K_m = " " mixture K_s = " " spheres = 0

subsequently by Bruggeman (1935), and Bottcher (1945), may be applied to the conductivity problems by simple substitution of specific conductivities for dielectric constants, see table 3. 4. It is important to note that although the mathematics are formally identical, the electrical conductivity of the spheres may take the value zero, but the dielectric constant can never be less than unity. All workers are in agreement that only the fraction of the volume occupied by the obstructions, regardless of the size of the particles, appears in the dielectric equations and the corresponding conductivity equations derived from them. For low volume fractions the equations all reduce to the same result:

$$K_m = (1 - 1.5\,\phi)\,K \qquad 3.25.$$

where K_m is the conductivity of the mixture and K is the conductivity of the dispersing medium.

Hence, the interpretation of the conductivity results would be based on the simple volume fraction approach initially, with the introduction of a correction for the increased path length of the ions moving through the gel should the simple approach be insufficient.

CHAPTER 4.

4. 1. Schering Bridge.

The capacitance of the tantalum electrode in various aqueous electrolytes was measured using a Schering polarizable impedance bridge. The bridge circuit is shown diagrammatically in fig 4.1 and was constructed from high quality components supplied by Muirhead Ltd. The detector was a Hewlett Packard Waveform Analyser model No. 302A which had the capability of both phase and resultant null detection. The potential was provided by a 6V lead-acid battery.

The Schering bridge used for this work was chosen because of the proven accuracy of the AC bridge method in the investigation of the double layer capacity. The advantage of measuring the cell impedance as a series combination is apparent when it comes to the interpretation of results. The experimental capacitance was balanced by a resistor and vice versa. This is of advantage as large, accurate, variable resistors are more readily available and cheaper than the corresponding capacitors, which allows the large pseudo-capacitances that are occasionally observed to be easily dealt with. With reference to fig 4.1, the effective series capacitance of the electrode is denoted by C_{xs}, the equivalent series loss resistance of the imperfect capacitor by R_{xs}, and the impedance, Z, of each arm by Z_1, Z_2, Z_3, and Z_4 respectively.

For zero out of balance current :

$$\frac{Z_1}{Z_3} = \frac{Z_2}{Z_4}$$

Where Z_3 is the impedance of the cell arm.

Fig. 4. 1. SCHERING BRIDGE.

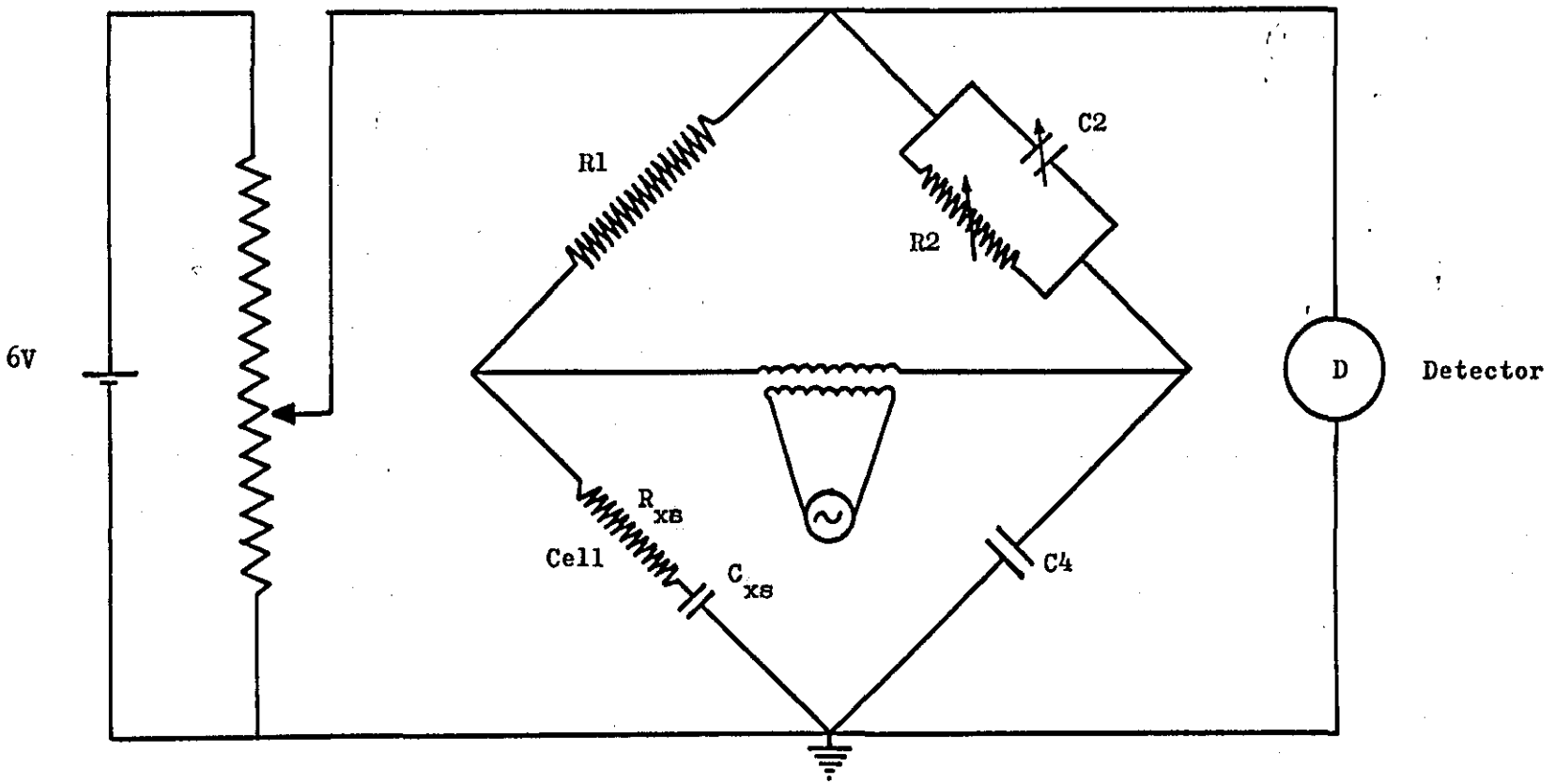

The impedances are given by:

$$Z_1 = R_1, \qquad Z_2 = \frac{R2}{1 + j\omega C_2 R_2}$$

$$Z_4 = \frac{1}{j\omega C_4}, \quad Z_3 = R_{xs} + \frac{1}{j\omega C_{xs}}$$

Solving the balance condition gives:

$$R_{xs} = \frac{R_1 C_2}{C_4}, \qquad C_{xs} = \frac{C_4 R_2}{R_1}$$

The loss angle of the cell Tan d $= \omega C_{xs} R_{xs}$

Substituting for C_{xs} and R_{xs}, Tan d, $= \omega C_2 R_2$.

In general d, which represents the defect of phase angle, ϕ, from $\pi/2$, is small, so the power factor Cos ϕ is given by :

Cos ϕ = sin d = tan d = d, as mentiontioned earlier.

Therefore it is convenient to depict the loss of C_{xs} by a series resistance because the balance point is independent of frequency. However, as R_{xs} is generally not a constant, the experimental bridge balance will be frequency dependent.

4. 2 Electrolytic Cell.

The electrolytic cell consisted of four compartments as shown in fig 4.2. The reference and working compartments were separated by a liquid seal tap in conjunction with a Luggin capillary system. A glass frit separated the working electrode compartment from that of the counter electrode. The fourth compartment, a purification limb/nitrogen circulating pump, also connected the working electrode and counter electrode compartments.

The cell was cleaned prior to use by treatment with 1:1 vol/vol concentrated nitric acid: concentrated sulphuric acid for 24 hours, washed with copious amounts of tri-distilled water, then dried in an oven at 120°C for 24 hours.

The purification limb of the cell contained activated charcoal which had been purified by refluxing for several months with 50:50 hydrochloric acid:water in a sohxlet arrangement. The charcoal was then transferred to a second still where it was refluxed with tri-distilled water. The water was changed every few days until no trace of chloride ion could be detected. The charcoal was then stored under tri-distilled water until required. For each electrolyte the charcoal in the purification arm was renewed. An amount of charcoal was decanted from the stock to a flask containing a small quantity of the chosen electrolyte. The flask was shaken and the fine material present in the

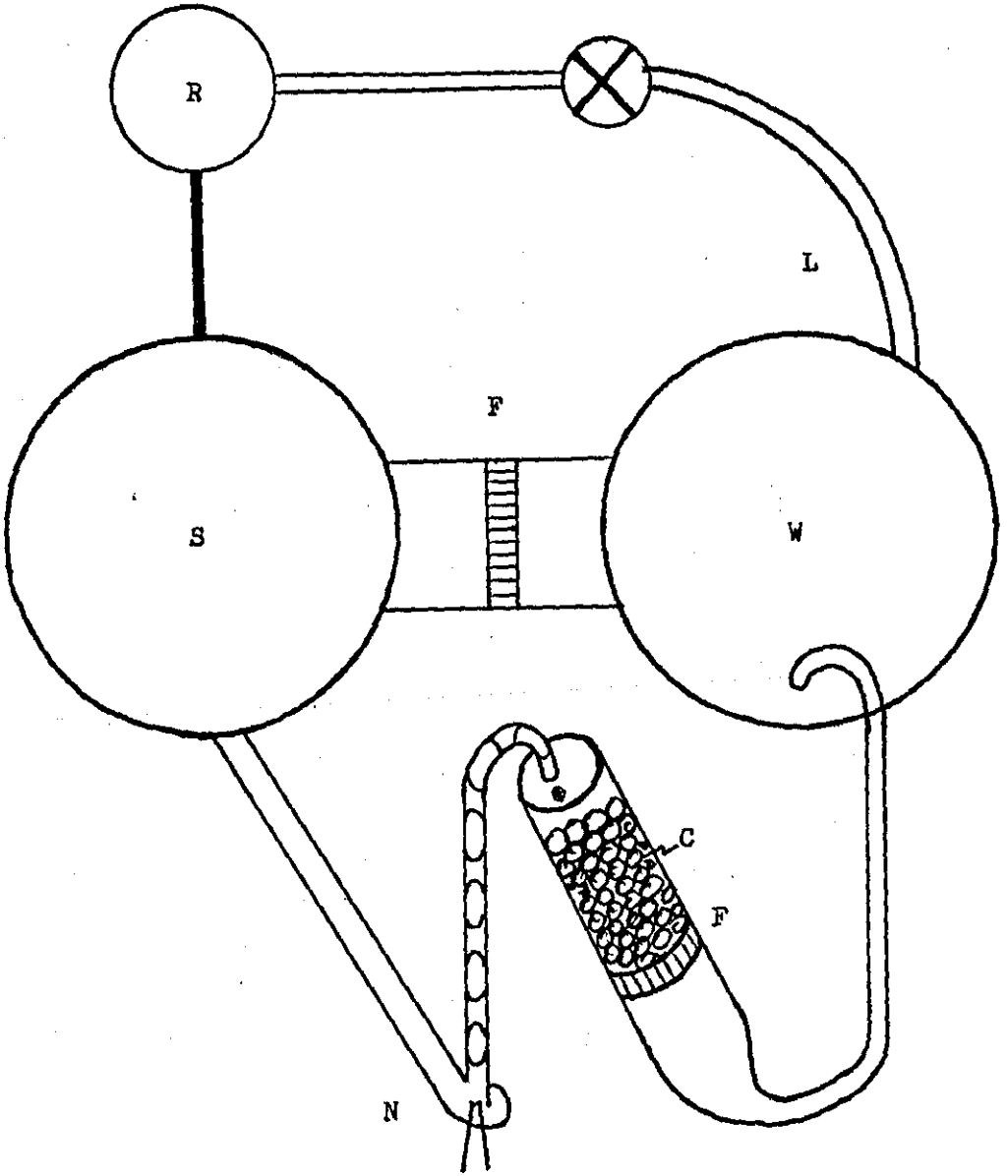

Fig. 4.2 Electrolytic Cell(schematic).

C = activated charcoal
F = glass frit
L = luggin capillary system
N = nitrogen circulating pump
R = reference electrode compartment
S = secondary electrode compartment
W = working electrode compartment

solution was decanted. This process was repeated until a solution free from fines, which might otherwise pass through or block the frits, was obtained. The fine-free charcoal was gently washed down the purification limb with electrolyte and the cell filled with electrolyte. The reference and counter electrodes were fitted and nitrogen passed through the bubbler. The electrolyte was circulated under an atmosphere of nitrogen for at least 72 hours before measurements were made.

The counter electrode was a platinum gauze electrode of large surface area and the reference electrode was a standard calomel electrode.

4. 3. Tantalum Electrode.

The tantalum electrodes under investigation were prepared from 4.5 mm diameter tantalum rod of 99·99% purity.

The first electrode consisted of a length of tantalum rod sealed in a pyrex glass support by the thermosetting plastic "Alkathene", a diagram of the electrode is shown in fig 4. 3 (a). Electrical contact was by means of a thick copper wire joined to the tantalum rod by conducting epoxy resin ("silver Araldite"). Unfortunately a problem arose when this electrode was mechanically polished. Because of the large difference in the hardness of the plastic and the tantalum, the plastic was worn away much more rapidly by the cloth covered polishing wheel.

This problem was overcome by using Araldite to mount the rod. A length of rod was placed in a well greased cardboard "pill" box and the Araldite poured in. The box was transferred to a vacuum oven and the Araldite allowed to set very slowly to ensure that any air bubbles present were removed. The Araldite mould was mechanically polished on a coarse abrasive paper until the tantalum rod was revealed. The mould was mechanically polished on successively finer abrasive papers, followed by polishing cloths with 1 μ, 0.5 μ and 0.25 μ diamond paste. The polished mould was lathed down to give a tight fit in the Pyrex support in which it was sealed with rapid-setting Araldite. In this electrode, mercury was used to provide the electrical contact between the tantalum and the copper connecting wire. See fig. 4. 3 (b).

Fig. 4. 3. (a) TANTALUM ELECTRODES Fig. 4. 3.(b)

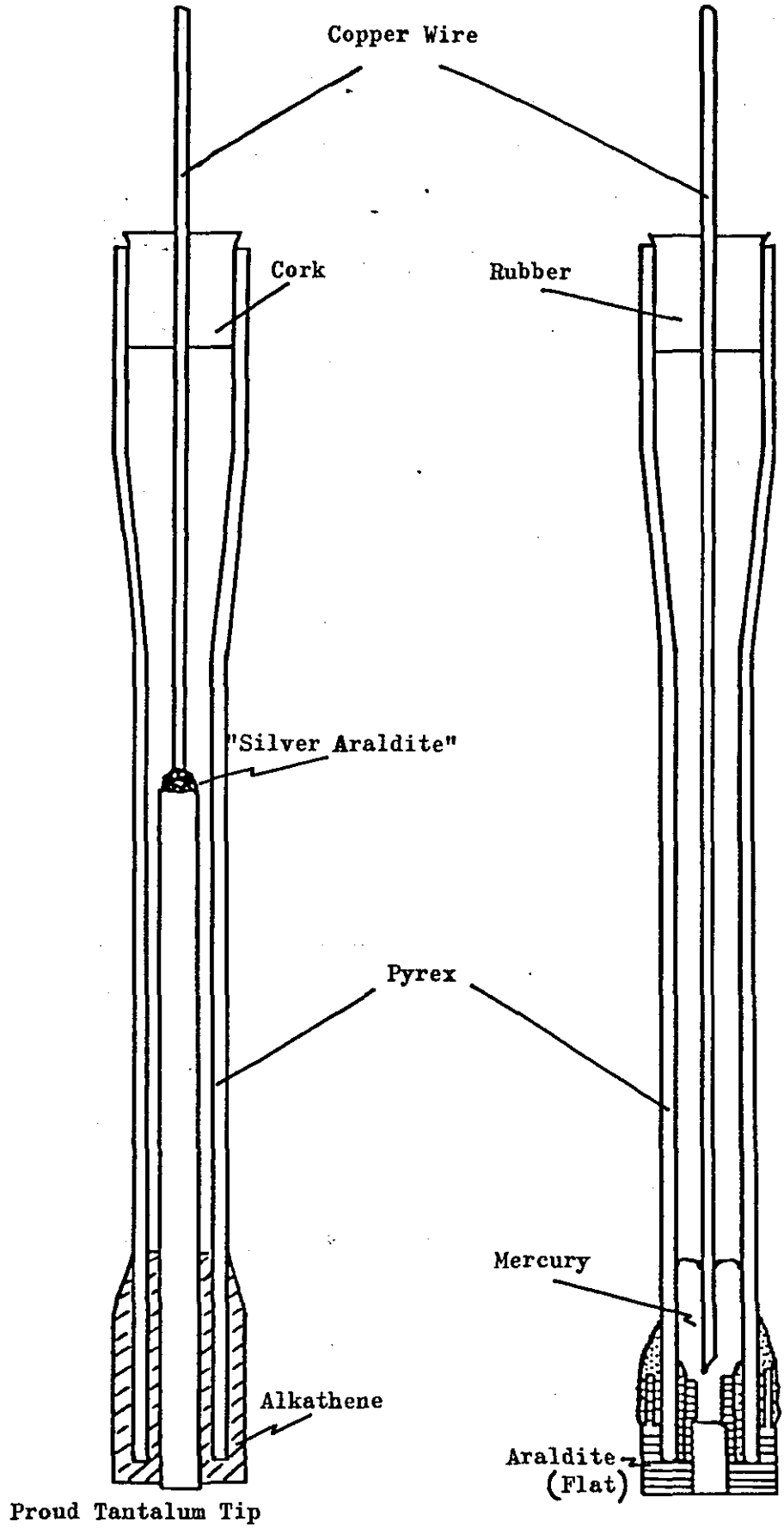

Preparation of the electrode surface was found to be critical, small differences in the treatment produced marked changes in the values of capacitance measured. The electrode was mechanically polished on abrasive paper to 600 μ grits, then on polishing cloths with 1 μ, 0.5 μ and 0.25 μ diamond paste. The electrode was cleaned with ethanol and large amounts of distilled water between each stage and after the 0.25 μ polish. The electrode was chemically cleaned using the cleaning procedure recommended by Tegart (1956): a ten second dip in a 5:2:2 mixture of 98% H_2SO_4 : 70% HNO_3 : 49% HF followed by leaching in boiling water for $\frac{1}{2}$ hour. This produced a highly reflecting, slightly rippled appearance to the flat electrode surface.

A negative potential was applied to the electrode before fitting it into the cell to discourage any oxidation which may otherwise occur due to the great affinity of oxygen for tantalum.

4.4. Experimental Measurements on the Tantalum Electrode.

The different sets of measurements made for each electrode/electrolyte combination under investigation were:

1. The polarizable range was determined by connecting a DC microammeter between capacitor C4 (see fig. 4.1) and the tantalum electrode. Starting with a negative potential applied, typically -1.0V vs SCE (standard calomel electrode), the current was noted after intervals of 2 and 5 minutes. The potential was then made more positive by an increment of 0.1V and the current again noted after 2 and 5 minutes. These measurements were repeated until the polarizable range had been identified.

2. The electrode capacitance and series loss resistance were measured as a function of:

   (a) Potential at fixed frequency.

   (b) Frequency at a fixed potential.

   (c) As a function of time at a fixed potential and frequency.

4. 5. The Anodizing of Tantalum.

The investigation of the effect of forming the oxide on tantalum by anodizing in gelled electrolytes on the properties of the oxide film was carried out at The Allen Clark Research Centre, Towcester, Northants.

The apparatus used in the laboratory for the anodization of tantalum foil in either sulphuric acid or gelled sulphuric acid electrolyte is shown schematically in fig. 4. 4 and the construction of the anodization cell is shown in more detail in fig 4. 5. The power supply constructed by the electrical workshops of the Research Centre allowed anodization to be carried out at either constant current or constant potential. The current flowing through the cell and the applied potential were measured on either a digital meter or an avometer, and one was also monitored as a function of time on a chart recorder. Temperature control was achieved by a mercury in glass contact thermometer operating via a simple relay an Isomantle, and the electrolyte was stirred by a small stirrer driven by an electric motor. Temperature control was of the order of $\pm$ 2°C for the gelled electrolytes and $\pm$ 1°C for the acid alone. The cathode was a loop of ~2.5 cm wide bright platinum foil located about half-way down the lower part of the cell and held in place by the cooling coil. A thick platinum wire welded to the foil and passing through a glass seal in the side of the cell allowed electrical contact to be made. The anode, a short length of the

Fig. 4. 4. BLOCK DIAGRAM OF ANODIZING APPARATUS.

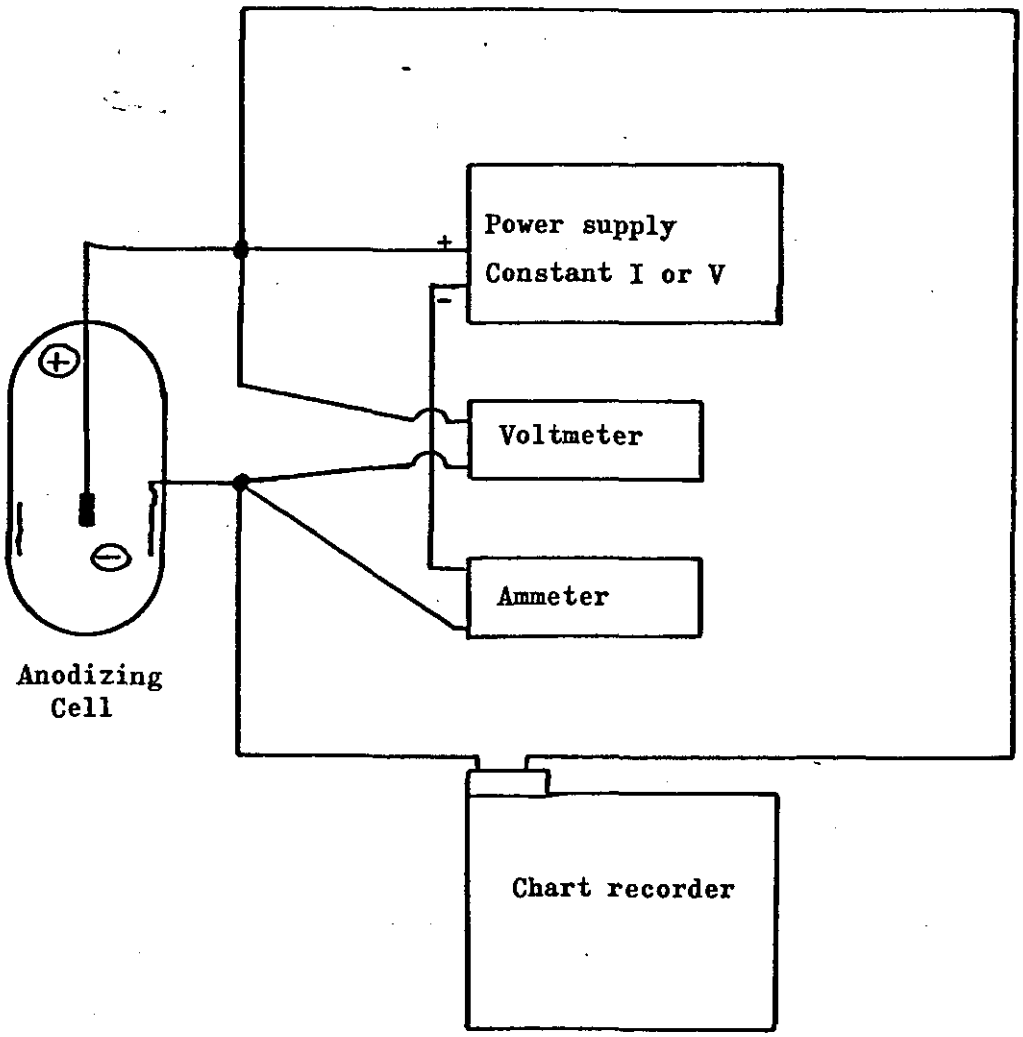

Fig. 4.5. Anodizing Cell.

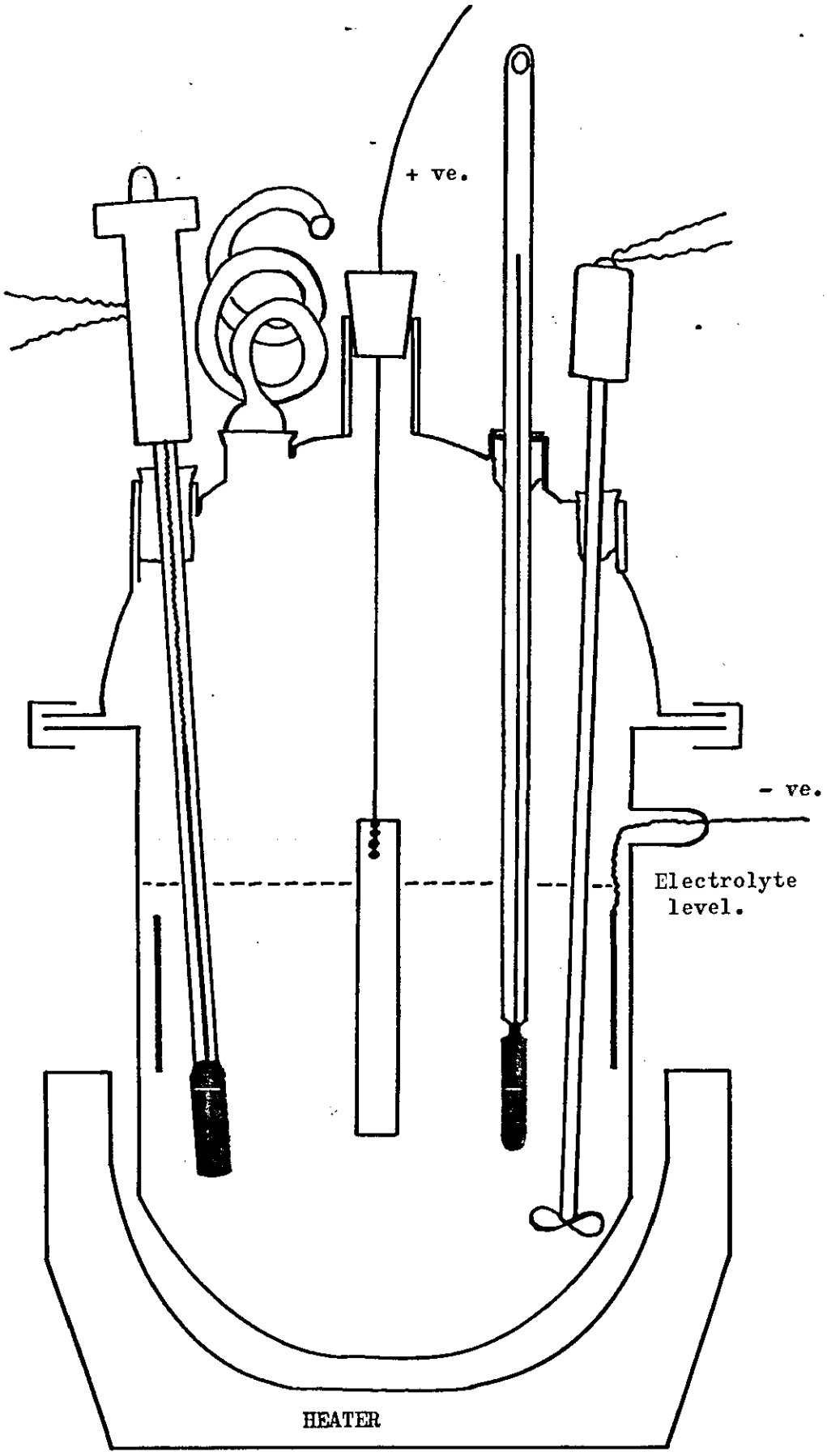

tantalum foil, was supported in the anodizing cell by one of the methods shown in fig 4. 6.

There were certain problems encountered when attempting to anodize in gelled 40% sulphuric acid electrolytes. Firstly, the thin foils proved difficult to immerse in the viscous electrolyte and a glass rod was used to stop the foils just lying on the surface of the gelled electrolyte instead of hanging vertically within it. Secondly, the voltage was found to increase slowly as expected but only until about - 10 V was reached. The voltage remained constant at this value instead of continuing to increase. The cause of this behaviour was traced to the uneven heating within the cell which created hot spots in the gel and caused it to bubble vigorously. Large lumps of gel were thrown onto the sides and lid of the anodization cell and eventually sufficient acid was present on the surfaces to create a conducting path from the anode support wire to the cathode by-passing the foil and anodization stopped."Stopping Off" the support wires with "Lacomit" reduced the likelihood of the conducting path being created and most runs proceeded without trouble. The simple expedient of wiping the lid should anodization be halted permitted anodization to be completed. The third and minor problem was that anodization in the gelled electrolyte seemed much more sensitive to traces of grease or oil on the foil surface and on occasion anodization was halted, so extra care was required during the handling of the foil after the cleaning stage not to contaminate the foil.

Fig. 4.6. Methods of Supporting Foils During Anodizing.

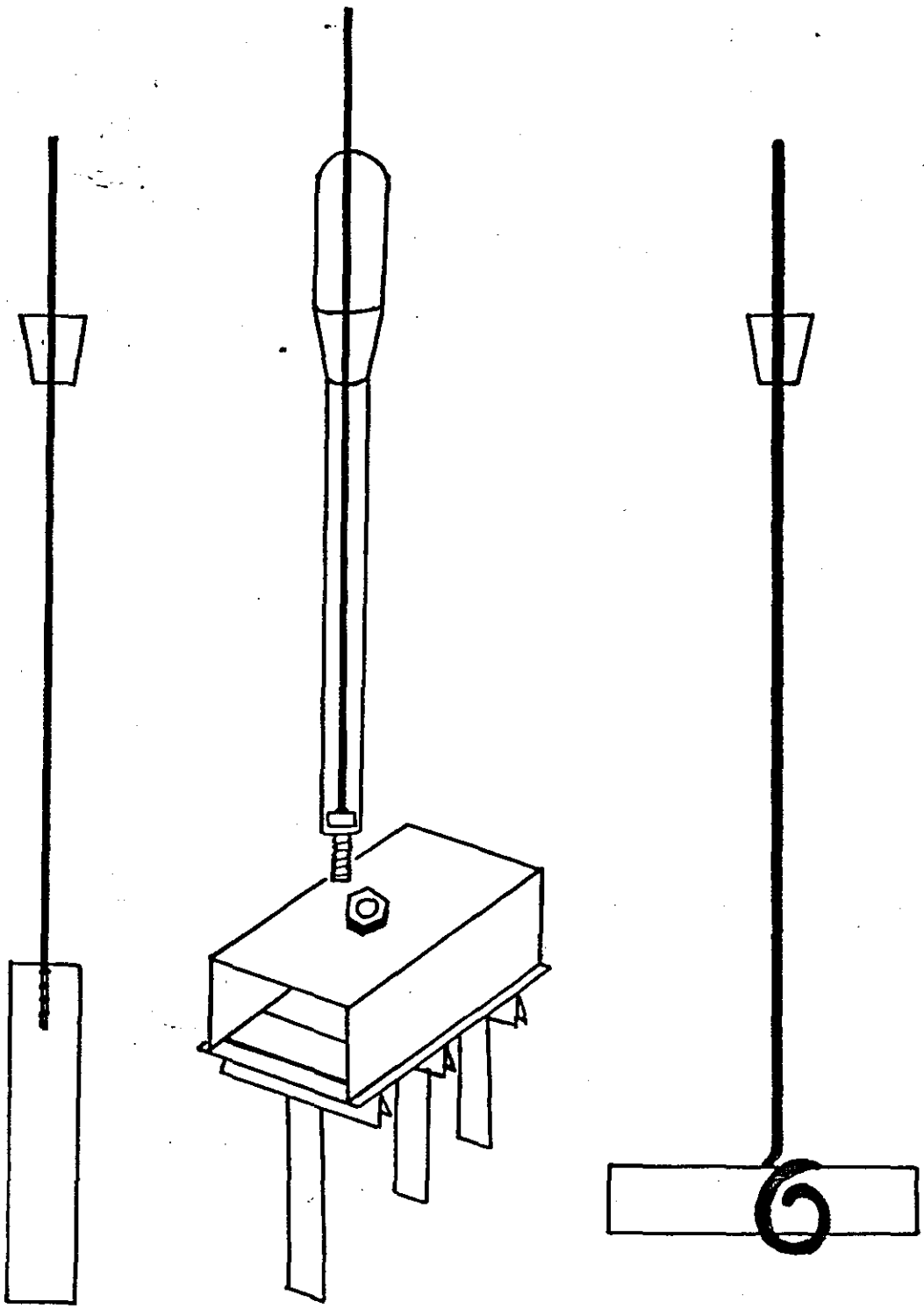

a. b. c.

4. 6. Field Recrystallization.

For the field crystallization study, thin tantalum foils (7.60 μm thick) were used. Prior to anodizing, the foils were cleaned in hot propanol for thirty minutes to remove any grease and rolling oils collected during the manufacturing process. The foils were formed to 120V at a constant current of 0.1mA cm^{-2} at 85°C and held at this potential for 60 minutes. Samples of foil were anodized in sulphuric acid, and in a series of gelled sulphuric acid electrolytes with silica contents in the range 3.7 to 7.5 per cent by weight. Gels for use in the anodization cell were prepared by the Loughborough standard method*, but a weight of silica per volume of acid was used because of the large quantity of gel required to fill the anodization cell. After anodization the foils were washed with distilled water and dried. Representative areas of foil selected from the central section of each foil were examined under both the optical and scanning electron microscopes.

The first micrographs of foils anodised in gelled sulphuric acid had a "woolly" appearance, and the use of EDAX demonstrated that silica was present on the surface. Various methods of treating the foils to remove the silica were tested including cold and hot dilute sodium hydroxide . The best and simplest method was scrubbing the foils with cotton wool under distilled water. This method was shown to remove the silica deposit very efficiently and all subsequent foils were treated in this manner after anodization.

* For details of mixing method see page 93.

4. 7. Scintillation Voltage.

The scintillation voltage of foils in various electrolytes was determined by anodizing at room temperature and at a constant current density of $2mA\,cm^{-2}$. The formation voltage was set on the power supply to 200V which was a much higher value than the potential where scintillation was expected to commence. Two foil thicknesses were used, 7.6 μm and 102 μm. The thicker foils were chemically polished for 10 seconds in the 5:2:2 ratio by volume of 98% H_2SO_4 : 70% HNO_3 : 49% HF acid bath recommended by Tegart (1956), followed by leaching in boiling water for 30 minutes.

The other foils were too thin to be treated in this way as they would have disintegrated and they were cleaned using the propanol treatment mentioned earlier.

The variation of voltage with time as anodization proceeded was monitored on a chart recorder. The onset of scintillation could be detected from the recorder trace as the smooth increase in voltage changed at this point to a series of rapid voltage fluctuations see fig 4. 7. For anodization in the acid alone the small sparks which trailed across the foil surface were easily visible giving a second method of determining the onset of scintillation. The two observations were separated by between 2 and 3V because the recorder trace picked up the breakdown which occurs at the foil/electrolyte/air interface at a potential

Fig. 4. 7. Onset of Scintillation seen from Volts versus time.

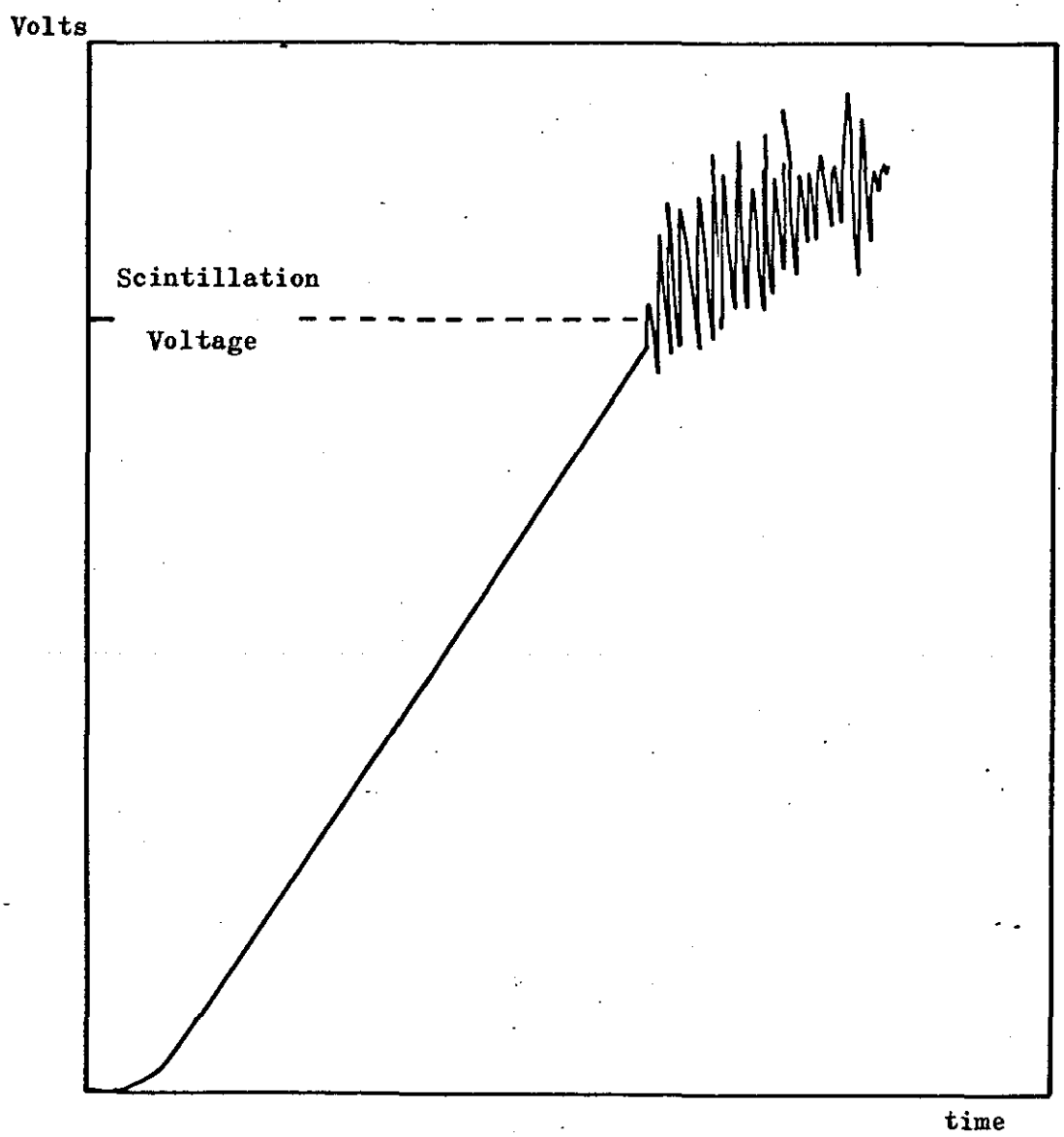

less than that of the oxide/electrolyte interface alone. For the opaque gels the measurement relied solely on the recorder trace so the correction for the breakdown at the foil electrolyte air cannot be made and consequently there is a larger error in the scintillation voltages for gels.

4.8 Electrical Properties of Oxides.

The effect of anodizing in gelled 40% sulphuric acid compared to the acid alone on the electrical properties of the oxides formed required large area specimens of foil of closely defined area. The area was defined with the aid of a " stopping off " compound (either Durafix or Lacomit) after the foils had been anodized at 85°C and a current density of 0.1 mA cm^{-2} to 120V and held at this potential for 60 minutes.

The properties compared were :

1. capacitance
2. tan d'
3. current versus potential in both the forward and reverse directions.

The measurement of capacitance and tan d' were made using an Electrolytic Capacitance Bridge model CB 154/5 manufactured by the British Physical Laboratory coupled with a waveform generator model LF141 manufactured by Servomex Ltd.

The tantalum foils were suspended midway between the two large counter electrodes of the simple cell shown in fig. 4.8 . The counter electrodes were 2.5 cm square platinum black electrodes externally

Fig. 4. 8. TEST CELL

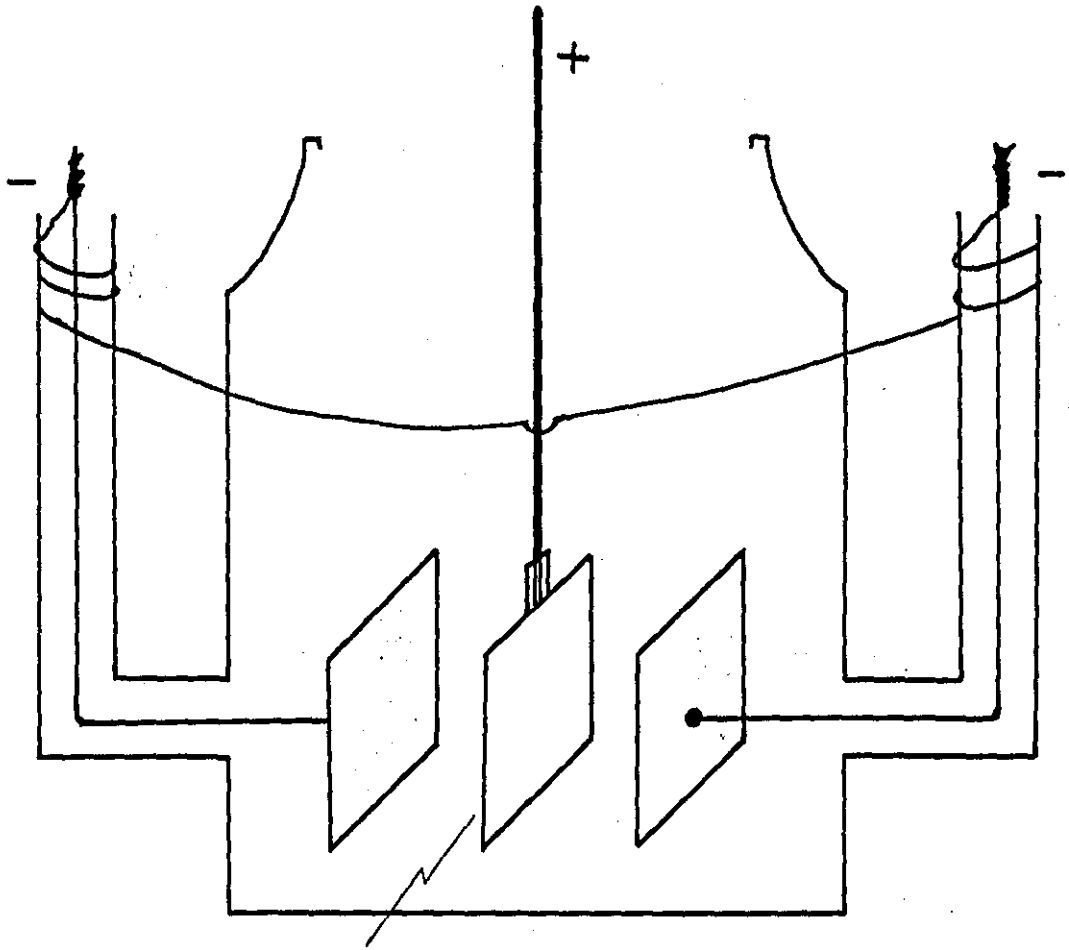

linked with platinum wire. The cell contained a boric acid-ammonia (aq.) electrolyte of resistivity ρ = 150 to 200 ohm cm. The capacitance and dissipation factor were measured at 100 mV, 500 Hz and 60V DC (half the formation voltage), and then at six other frequencies below 500 Hz.

The current-voltage curve was obtained using digital voltmeters and ammeters, the power supply used with the anodizing apparatus, and the test cell and boric acid-ammonia (aq.) electrolyte used for the capacitance and dissipation measurements. The positive branch of the curve was examined first because of the possibility of damaging the oxide film at negative potentials.

The chemical composition of the oxide films formed by anodizing tantalum foils in the gelled 40% sulphuric acid were examined using Auger electron spectroscopy and the EDAX (energy dispersive analysis of X-rays) facility of the scanning electron microscope. The main purpose of this investigation was to search for evidence of the incorporation of silica into the bulk of the oxide film and/or into the oxide surface.

4. 9. Thermostatted Tank.

The thermal coefficient, α, of conductivity for aqueous solutions is fairly high, being approximately 2% per degree near room temperature. Therefore temperature control must be better than $\pm$ 0.005°C to ensure the desired accuracy of 0.01% in the measurement of conductivity. The requirement was achieved by the construction of a thermostatted oil bath as detailed below:

an 80 l metal domestic water tank with a plate glass window fitted in the front panel to allow observation of the conductance cells, see fig 4.9, was insulated on the other three sides with ~ 2.5 cm thick expanded polystyrene and ~ 0.3 cm thick hardboard. The tank was mounted on a ~ 2.5 cm thick wooden base and the same material was used to make the lid. The lid was constructed in three sections, two sections were bolted in place and the other was used between measurements to maintain the temperature. During measurements the gaps between the plates supporting the cells were covered with sheets of asbestos and/or short lengths of wood. Three variable speed motors (50 - 500 r.p.m.) fitted with stirrer blades were mounted on three corners of the lid. The speed of the motors was controlled by a variac and two transformers. The voltage and current across the field coils (93V,0.22A) and across the brushes (25V,0.1A)

Fig. 4.9 Thermostatted Tank.

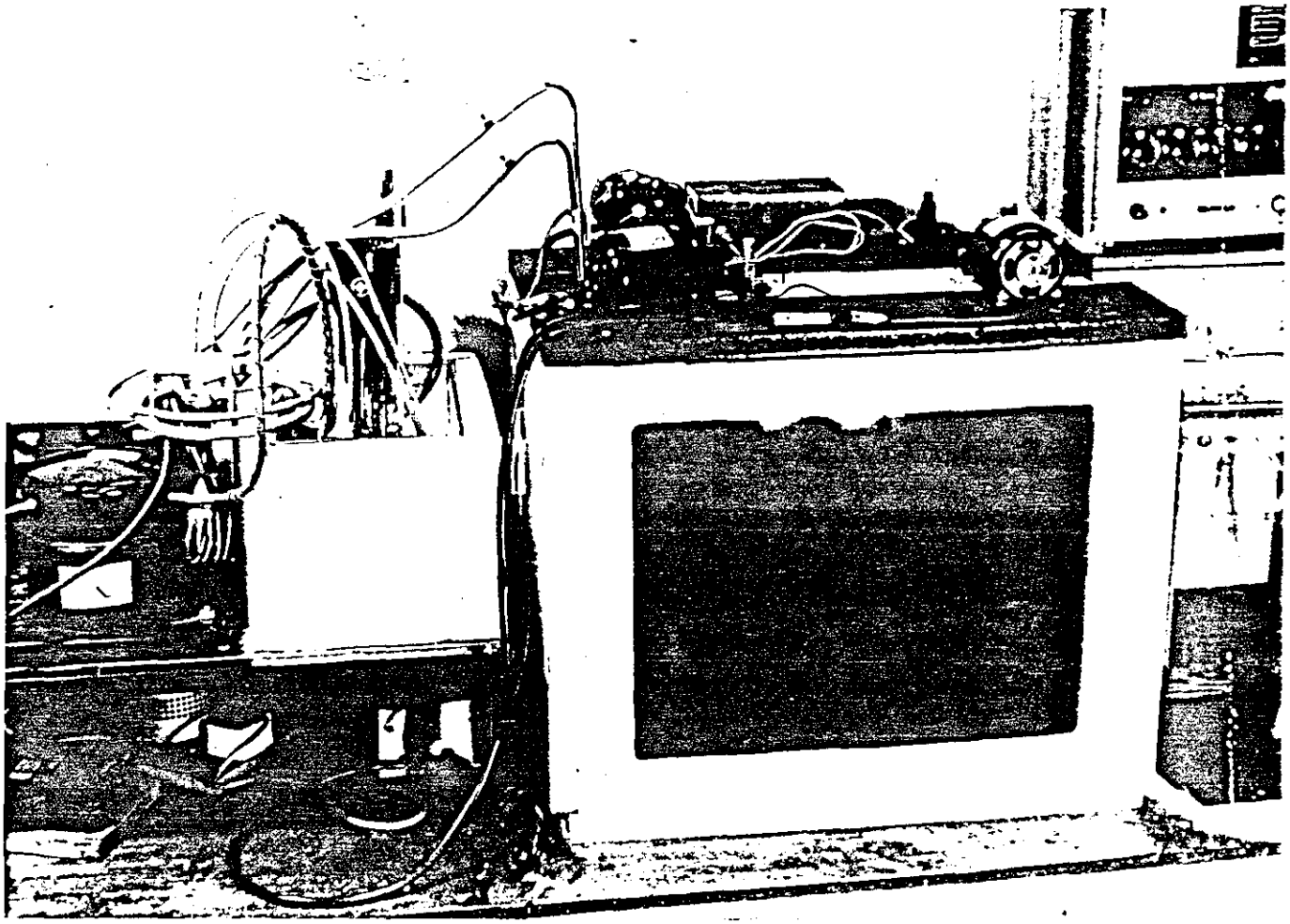

were measured. One transformer was wired across the field coils and the other across the commutators and the variac used to vary the input across the field coils to vary the motor speed. For temperatures in the region of 25°C the stirrer motors were run at minumum speed, but for higher temperatures the speed was considerably increased. At 25°C the heat generated by rapid stirring was equal to a large proportion of the total heat input required to maintain the temperature above that of the room and consequently after a few hours of operation the temperature would rise continuously. At higher temperatures the total heat input required is much larger and the contribution due to the stirrers is insufficient to affect the temperature control.

A mercury in glass contact thermometer placed in the remaining corner of the lid of the tank controlled the heaters via a relay system. The heaters, two or three light bulbs of various wattages in the range 40-100 watts could be operated in series or parallel. In addition a 150 watt bulb could be included in the circuit for rapid heating.

A cooling loop made from 5m of 0.6cm diameter copper tubing was fitted along the base of the tank and connected to the mains water supply for the operation of the tank at temperatures in the region of 25°C. For lower temperatures antifreeze solution cooled by a refrigeration unit was circulated through the coil, or the refrigeration unit was coupled directly to the tank.

Accurate temperature control is most readily achieved using water as the thermostating medium because of its specific heat capacity, its low viscosity which facilitates stirring, and its slow evaporation to dissipate surplus heat. Water is also plentiful, cheap, clean and odourless. However, as described in the introduction it may not be used in thermostats designed for conductance measurements because of its conducting properties, see Jones & Josephs (1928).

Therefore, oil with its excellent insulating properties has to be used and the disadvantages with respect to viscosity, specific heat capacity, and loss of the cooling effect due to evaporation have to be remedied in the construction of the thermostat.

The oil chosen for this purpose after consultation with the Technical Services Division of The Shell Oil Co. was Faunus Oil which had a relatively low viscosity over the temperature range 10^{o} - 120^{o}C, no unpleasant odours on heating, and was relatively transparent.

4. 10. Conductivity Measurements.

Conductivity measurements were made using a Wayne Kerr Universal Bridge for the measurement of admittance or impedance at audio frequencies. Eight decades, four for conductance and four for capacitance were operated in succession to obtain a balance. The frequency used for routine measurements is that of the internal oscillator of the bridge which is set at 1592 Hz, chosen because that frequency leads to $w = 10^4$. Conductance measurements quoted in this work were made at this frequency unless otherwise stated.

The bridge has the capability of operation with an external source and either the internal detector for the frequency range 200 Hz - 50kHz, or with an external detector for a wider frequency range.

The effect of frequency on the conductivity was measured with the aid of an oscillator designed around a Voltage Controlled Audio Oscillator Chip (range 200Hz to 20kHz) and a General Radio tuned amplifier/null detector. The waveforms of the input signal to the bridge from the oscillator and the output signal from the bridge to the detector were monitored on an Advance oscilloscope when the bridge was used in this mode to ensure distortion effects on the signal were minimal.

The earthing loops between the various components were eliminated by rewiring all the earth terminals to a mains water pipe. The thermostatted tank was also earthed to a mains water pipe as an additional assurance against capacitance by paths interfering with the measured conductivity. See Jones and Josephs (1928).

4. 11. *Conductivity Cells.*

A modified version of the conductance cell for use with sulphuric acid solutions described by Roughton (1951), was constructed from pyrex glass with two Pt/Pt-black electrodes and copper connecting wires, see fig 4. 10. The electrodes were platinum discs of 1 cm diameter welded to platinum support wires mounted in a graded glass seal. (Pt - soda glass-pyrex). The electrodes were platinum blacked to minimise errors in the conductance measurements due to polarization (see Kohlrausch 1897) using the conditions recommended by Jones and Bollinger (1935), namely in 0.025M hydrochloric acid containing 0.3% platinum chloride and 0.025% lead acetate at a current density of 10 mA cm^{-2}. The polarity of the electrodes was altered every 10 s until an even black deposit could be seen on both electrodes.

The thick copper connecting wires were silver soldered to the platinum support wires and the other ends silver soldered to female gold plated microconnectors. The screened co-axial cables from the bridge to the cell were fitted with the corresponding male microconnectors.

The lead resistances of the cell were determined by filling the cell with mercury and measuring the cell conductance. Using the value for the resistivity of mercury at $20^{o}C$ given in the International Critical tables of 0.58×10^{-5} ohm cm and the measured conductance of 24.56 m ohm^{-1} and equation 3.3 given in the introduction, the lead resistance

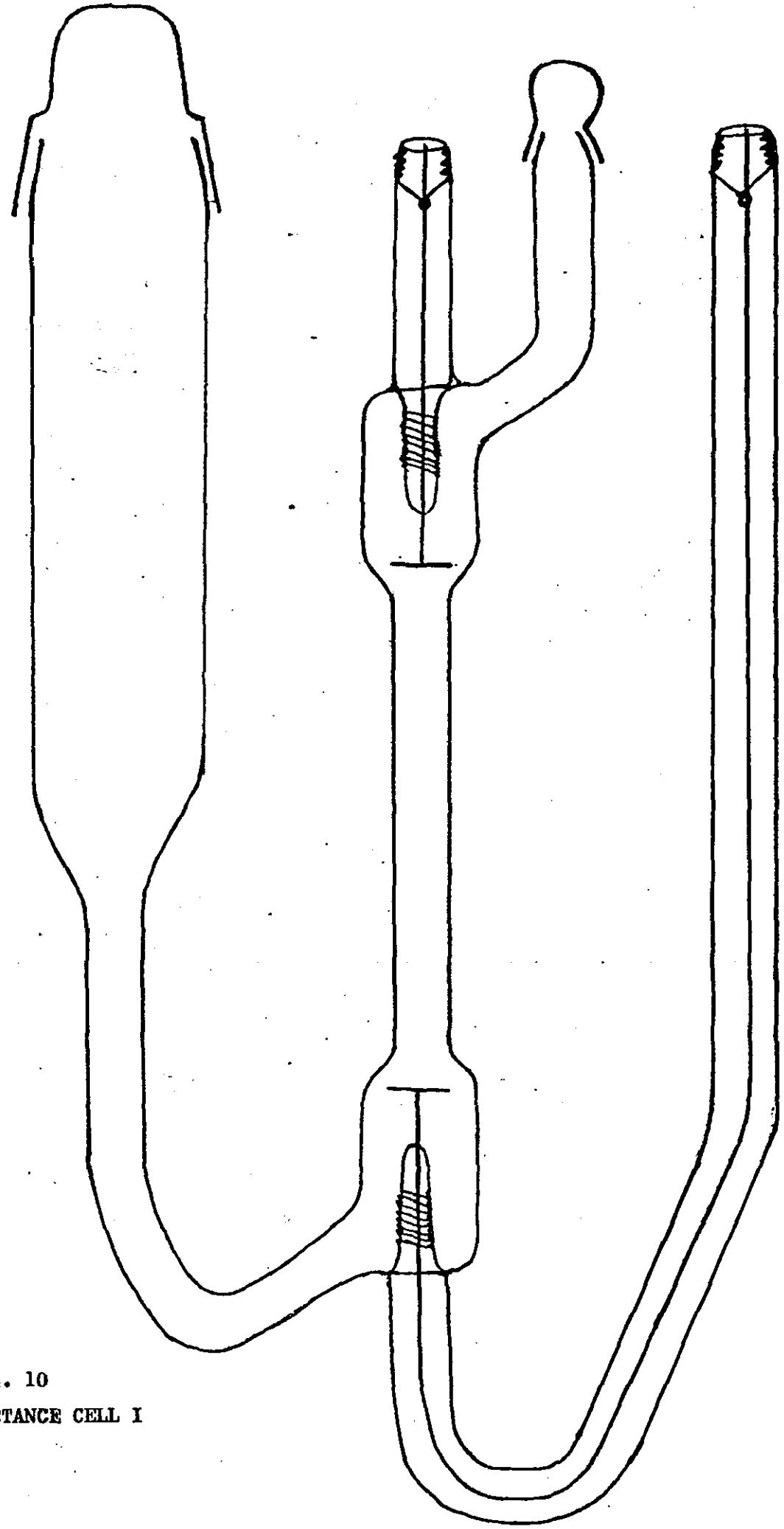

Fig. 4. 10

CONDUCTANCE CELL I

was found to be 2.88×10^{-6} S which may be ignored as it is within the error of the bridge.

The cell suffered from two disadvantages: part of the cell filling arms and the caps were above the oil level and consequently condensation occurred on these parts, causing an alteration of the concentration of cell electrolyte and hence of the measured conductance with time; secondly, cell filling and emptying of the more viscous gels was extremely difficult. The first of these problems was easily resolved by the introduction of a ground glass seal in the filling arms below the oil level. The cell was made air-tight by a long-stemmed ground glass stopper, see fig. 4.11. The cell was filled with electrolyte to within 1cm of the stopper. On immersion of the cell in the oil the air space above the electrolyte in each filling arm rapidly reached the equilibrium saturated vapour pressure at the temperature of the oil and further changes in concentration were eliminated.

The filling of the cell with the more viscous gels remained a problem and imposed a restriction on the maximum gel concentration that could be examined for each electrolyte concentration.

A second cell of a different design, see fig. 4.12, was constructed from similar materials to those used in the first cell. The narrow-bore tube separating the electrodes was in the

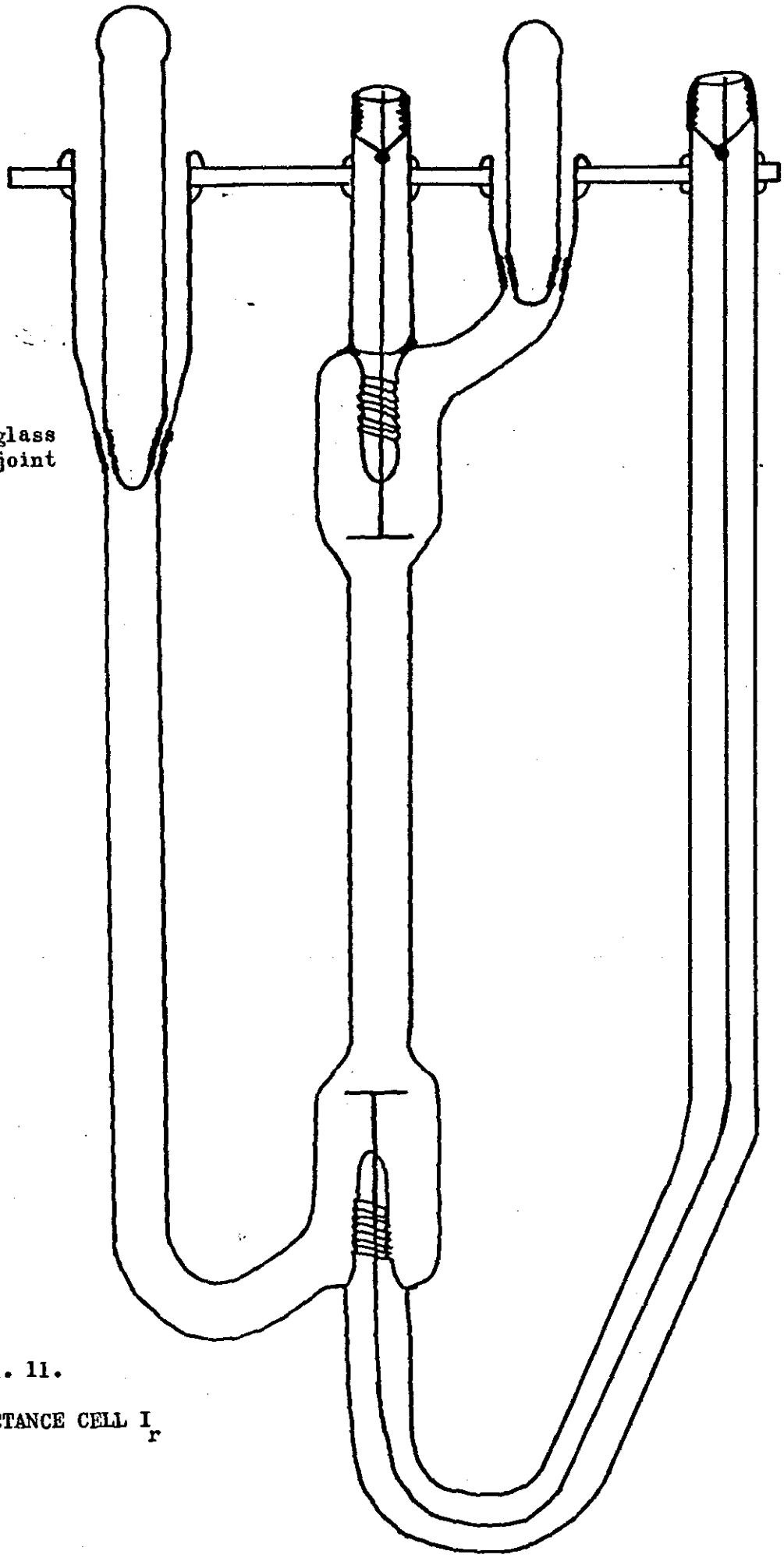

Fig. 4. 11.

CONDUCTANCE CELL I_r

Fig. 4. 12. CONDUCTANCE CELL II

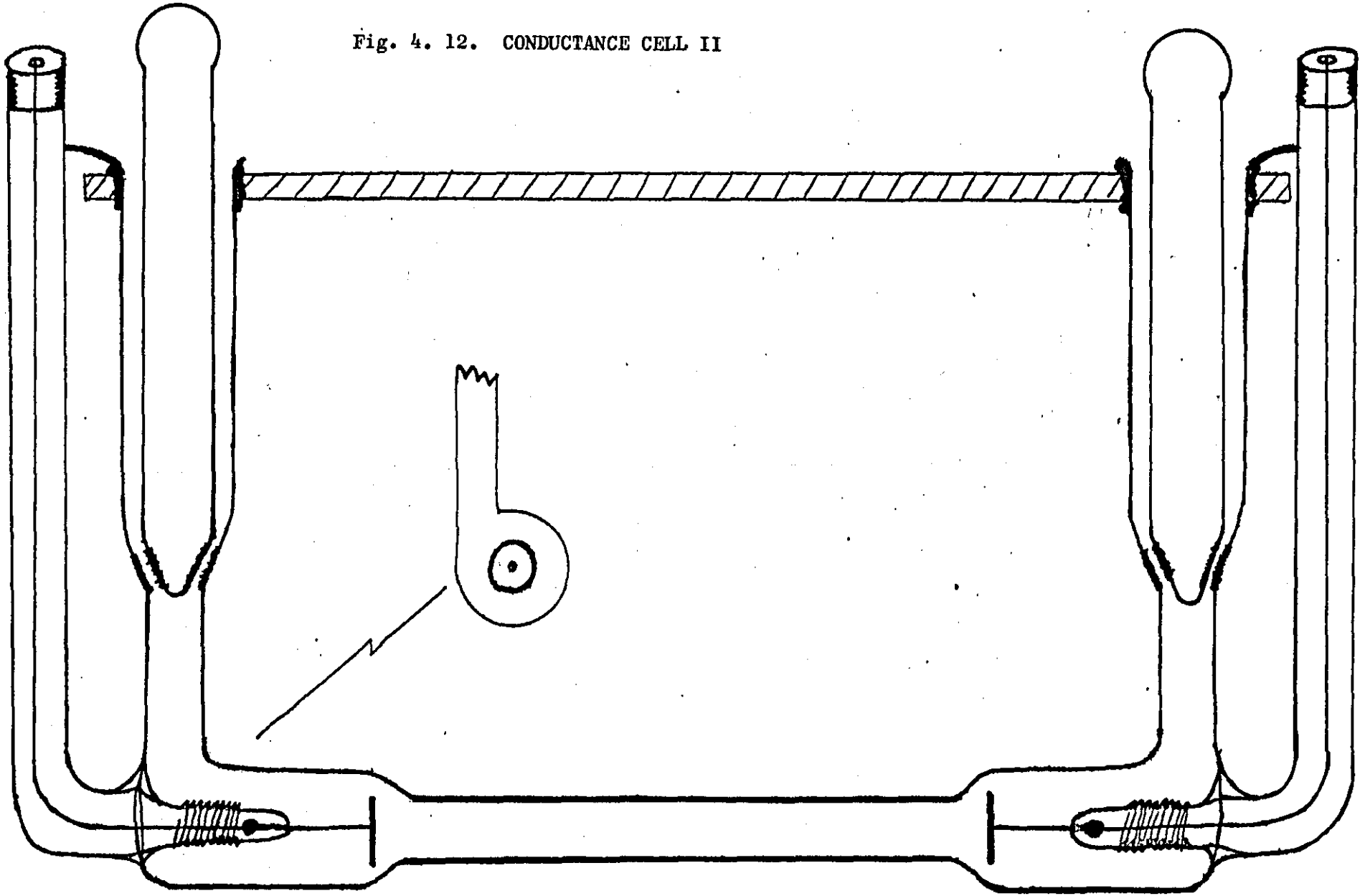

horizontal plane and the filling arms were offset from the centre of the cell to aid filling and emptying, and to create turbulence when flushing out the cell with running water. The other reasons for the choice of this design for the cell were that the cell constant was lower, that any possible temperature gradient with depth within the oil would have a minimal effect on this cell compared to the first, and that any compression effects on the gel due to gravity which might influence the gel structure and possibly the conductance would again be minimised compared to those in the first cell.

Cells I and II were attached to thick aluminium plates by the filling arms using a silicone rubber adhesive to give them some rigidity and as an aid to handling. The plates slotted into the groove between the fixed portions of the lid of the tank with the added advantage that the cell was always immersed in the oil to the same depth and that an effective air seal could be obtained helping reduce any temperature fluctuations due to changes in room temperature.

A third cell based on the dilution cell of Shedlovsky (1932) and Daggett et al (1951), see fig 4. 13 , was used for the examination of gels prepared from potassium chloride. The cell could not be used with the more highly conducting acid gels because the cell constant was only 5.00 cm^{-1}.

The method of use of the cell is as follows; a known amount of an accurately prepared gel is poured into the flask. The flask is tilted to allow the gel to enter the cell and

Fig. 4. 13. CONDUCTANCE CELL III

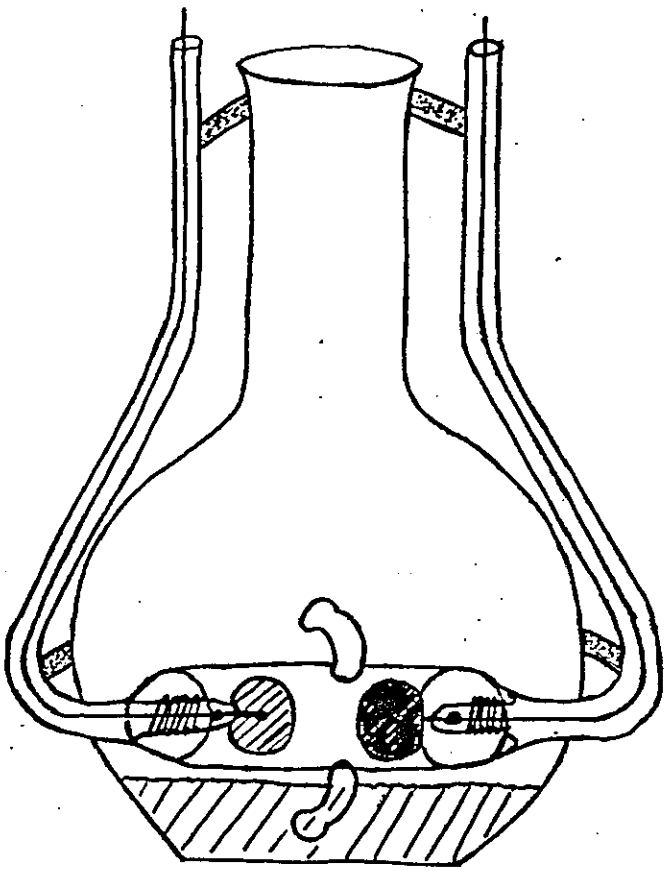

the conductance is measured. The gel is run from the cell back into the flask and a weighed amount of the potassium chloride solution used in the preparation of the gel is added to the cell from a weighing pipette, see fig. 4. 14. The gel and solution are mixed by shaking and the resultant "gel" is flushed through the cell a few times and the conductance measured. Successive additions of electrolyte to a maximum of 250 mls total volume may be made, the conductance is measured after each addition.

The fourth and last type of cell is shown in fig. 4.15 and was designed for use in the temperature cycling cabinet described below with acid solutions at $-55^{\circ}C$, and with the potassium chloride gels at room temperature for rapid comparison of different gels. The dip-part of the cell consisted of a B 56 cone drawn down to join a graded glass seal (pyrex to soda). A length of platinum rod of approximately 1.5 mm in diameter was set in the soda glass and silver soldered to the copper connecting wires which were sheathed in polythene tubing. The dip-cell was fitted into a cylindrical round bottomed tube, the two parts being always aligned in the same way by use of two marker lines to minimise variations in the cell constant due to the dissymmetry of the cell. The platinum electrodes were platinum blacked in the same way as described earlier for the other cells.

Fig. 4. 14. WEIGHING PIPETTE.

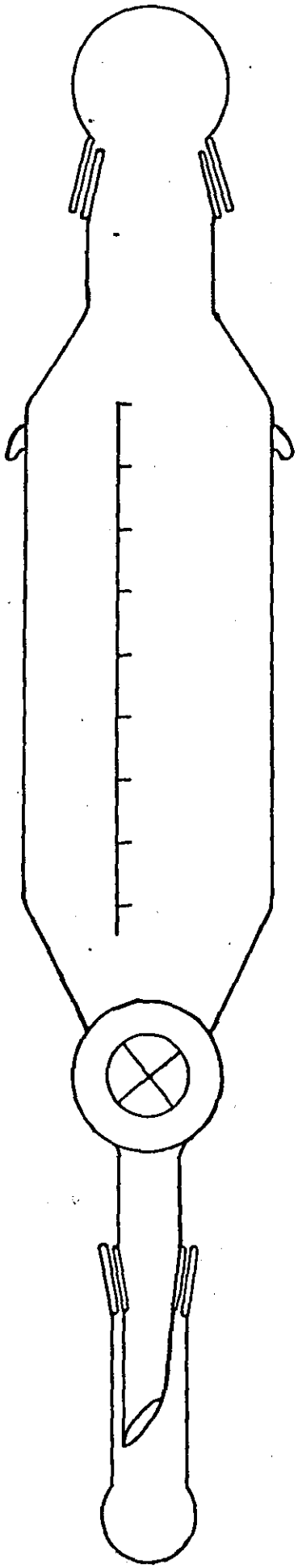

Fig. 4. 15. CONDUCTANCE CELL IV.

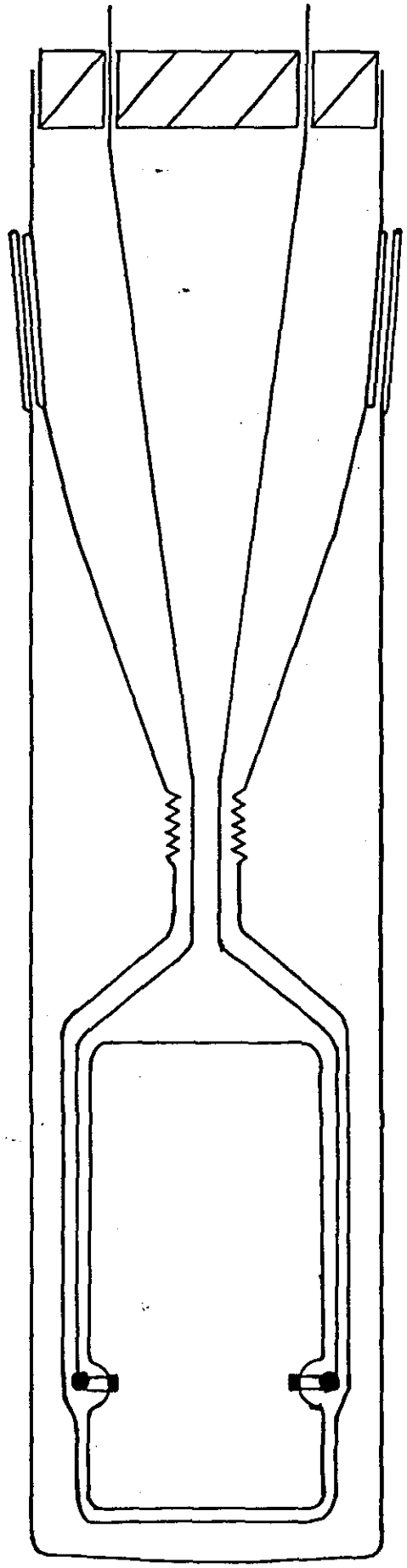

4. 12. Low Temperature Thermostatted Cabinet.

A temperature cycling cabinet commonly used for the routine testing of electrical and electronic components over the range -100° to $+ 150^{\circ}C$ controlled to $\pm 2^{\circ}C$ was taken as the starting point for the construction of an air thermostat giving accurate control to $\pm 0.01^{\circ}C$ or better for temperatures below $5^{\circ}C$ and particularly for use at $-55^{\circ}C$. The cabinet had internal dimensions of 25 x 33 x 30 cm with access via a stoppered porthole for measuring cables etc., and via a hinged lid on which a single speed fan and two 250 watt heating elements were mounted. Three major inconveniencies inherent in using the cabinet were (1) that the cell could not be viewed during the measurements, (2) that the cabinet could not be opened once the temperature was below $0^{\circ}C$ and (3) liquids could not be used as thermostating media.

The manufacturers claim of temperature control to $\pm 2^{\circ}C$ was rapidly confirmed from the observed variation in conductivity with time for a 40% sulphuric acid in cell II at $0^{\circ}C$ and at $-55^{\circ}C$ shown in figures 4.16 and 4.17 respectively. The time taken for the cell to reach thermal equilibrium was also determined from the plot of conductivity versus time shown in fig 4.18.

Various methods of improving the temperature control were investigated and their performance compared by following the change in conductance with time of 40% sulphuric acid in either cell II or cell IV.

The first attempt at improving temperature control was to lag cell II with foam rubber pipe insulation. A small reduction in the variation of conductivity with time., see fig 4.19

Fig. 4. 16. Conductance vs time, 40% H_2SO_4 in Cell II at 0°C

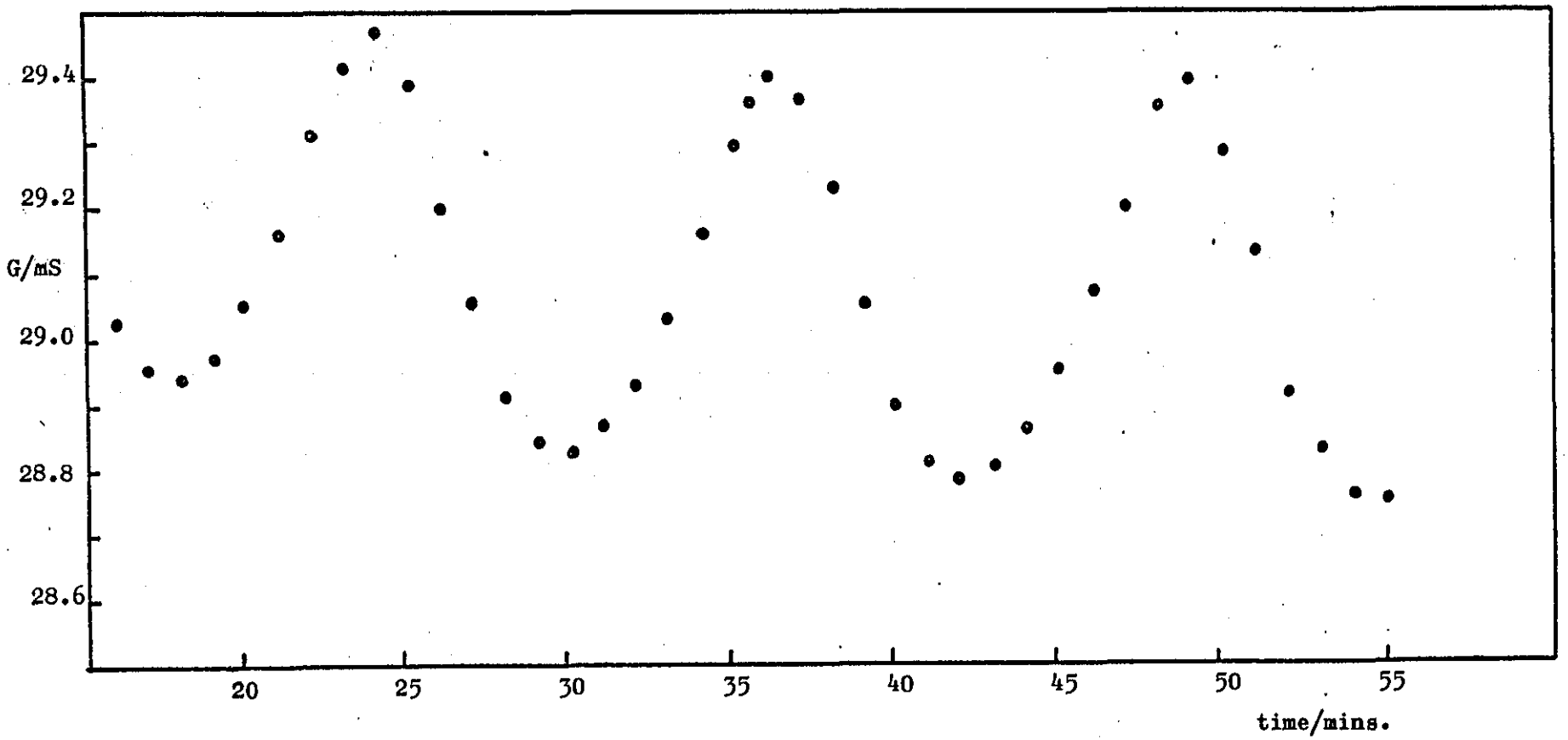

Fig. 4. 17. Conductance vs time, 40% H_2SO_4 in Cell II at -55°C

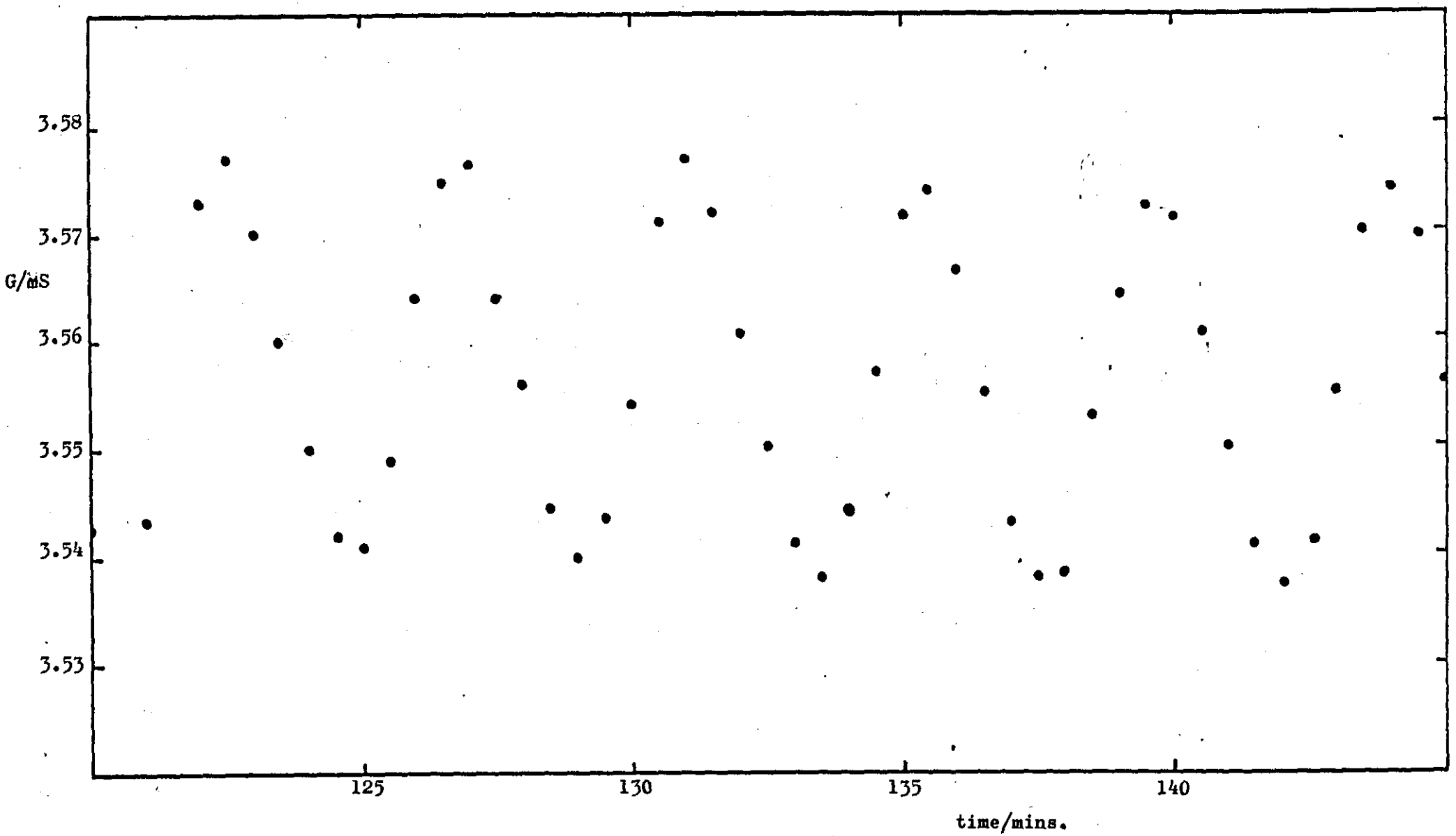

Onset of Thermal Equilibrium from

Fig. 4. 18. Conductance vs time, 40% H_2SO_4 in Cell II at - 55°C

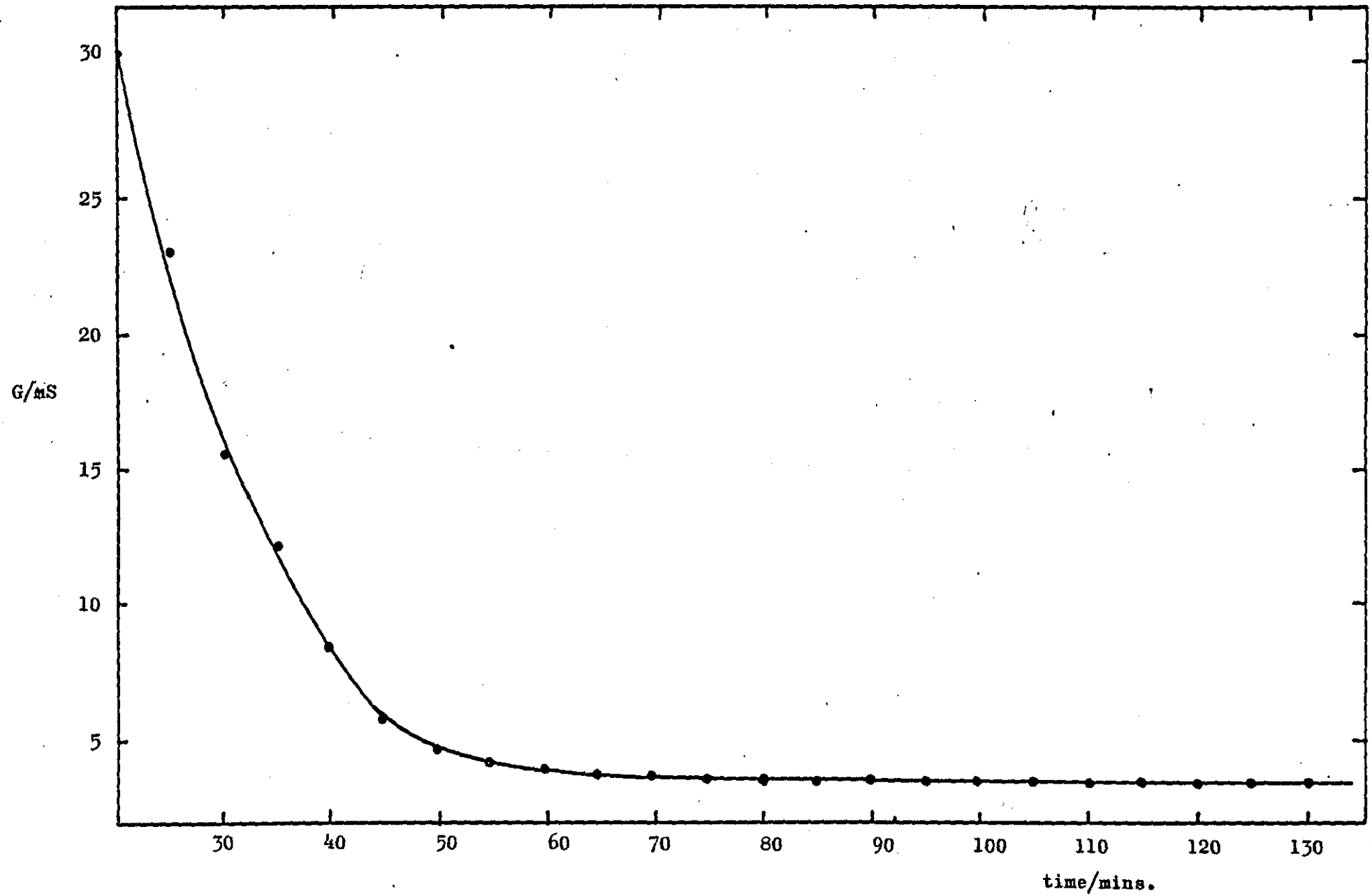

Fig. 4. 19. Conductance vs time, 40% H_2SO_4 in Cell II (lagged) at -55°C

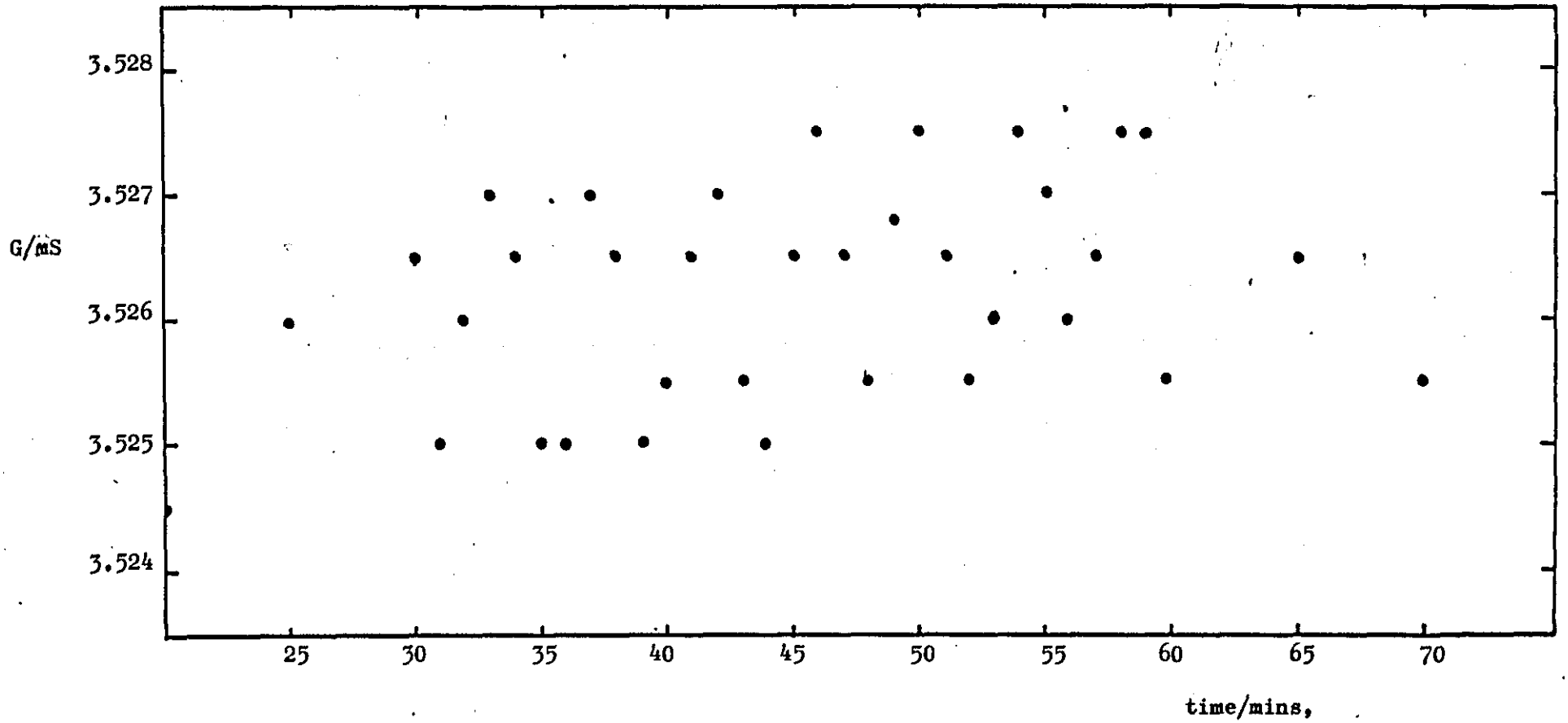

showed that the temperature control was marginally improved but the equilibration time determined from the conductivity versus time plot see fig. 4. 20, was 3 times longer than that for the unlagged cell. The average conductance was still drifting downwards with time after 5 hours. A similar result was obtained for the lagged and unlagged dip cell, cell IV.

The basic idea behind the two attempts of improving the temperature control described below was to run the cabinet cooling system continuously and balance the cooling by a secondary heating/temperature control system.

The first method was based on a hardboard/bleckboard box constructed to fit inside the cabinet. The box was lagged inside with 2.5 cm thick polystyrene. A 100 watt light bulb was used for a heater, the output was regulated by a variac and controlled by a thermocouple/relay system. The reference junction (hot) of the thermocouple was maintained at $0^{\circ}C$ by immersion in an ice/water mixture in a vacuum flask. The cold junction was taped to the narrow bore tube of the cell II which rested on polystyrene supports in the box. The cabinet temperature was set to operate at -57° to $-58^{\circ}C$. The secondary control was set to operate at $-55^{\circ}C$. The variac setting was adjusted to give the smallest change in conductivity versus time. The best combination of settings gave a very small improvement relative to that of the lagged cells, but the thermal equilibration time had increased to over 16 hours.

Onset of Thermal Equilibrium from

Fig. 4.20. Conductance vs time. 40% H_2SO_4 in Cell II (lagged) at $-55^{\circ}C$

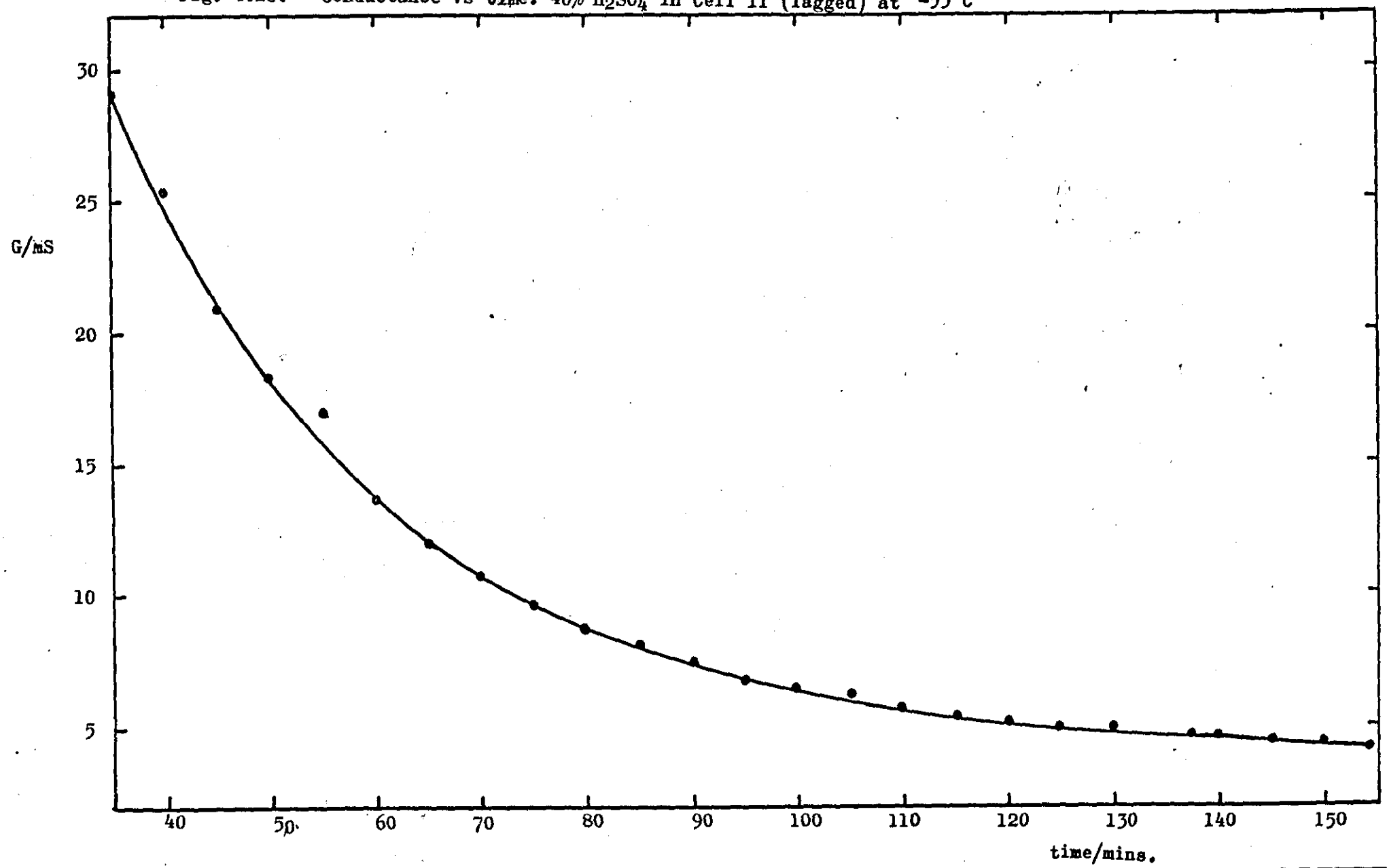

An electrically operated flap fitted in attempt to reduce this time, being left open during the cooling period then closed when the desired temperature had been reached made little, if any, difference. The probable reason for this long equilibration time was that the bulk of poorly conducting material was too great for the capacity of the cabinets cooling system to cope with. The variation in observed conductivity with time and the switching of the secondary heater and the cabinet cooler are shown in fig 4.21.

The other attempt at improving temperature control utilised a nest of light bulbs placed in one corner of the cabinet and regulated by the same thermocouple/relay system as before. A 150 watt bulb the output of which was controlled by a variac was switched on continuously once -55°C had been reached to crudely balance out the effect of the constantly running cooler. In the opposite corner from the light bulbs the cell was mounted on polystyrene blocks and partially lagged with foam rubber pipe insulation. An asbestos sheet was placed between the light bulbs and the cell to shield the cell from direct heating but air was still able to circulate freely. A 2.5 cm thick sheet of polystyrene was placed on the floor of the cabinet.

The bulb wattages and control settings were varied until the smallest change in conductance with time was found. As may be seen from fig 4.22, the variation in conductivity with time was small and equivalent to a temperature control of $\pm$ 0.002 °C

Conductance vs time, 40% H_2SO_4 in Cell II in Hardboard box at -55°C

Fig. 4. 21. Heater/Cooler switching cycles.

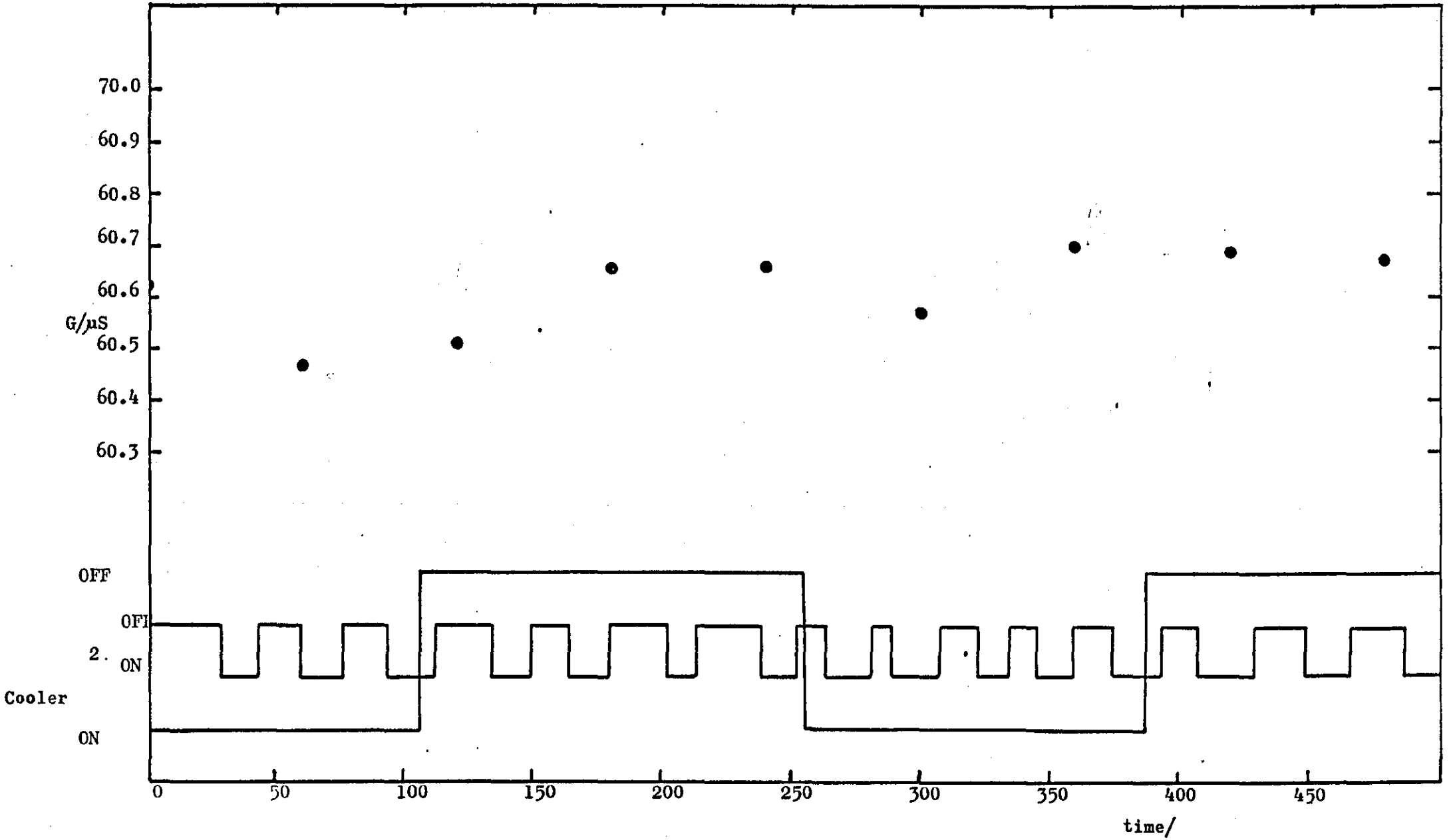

Conductance vs time, 40% H_2SO_4 in Cell II at -55°C

Fig. 4. 22. Best temperature control achieved using nest of light bulbs.

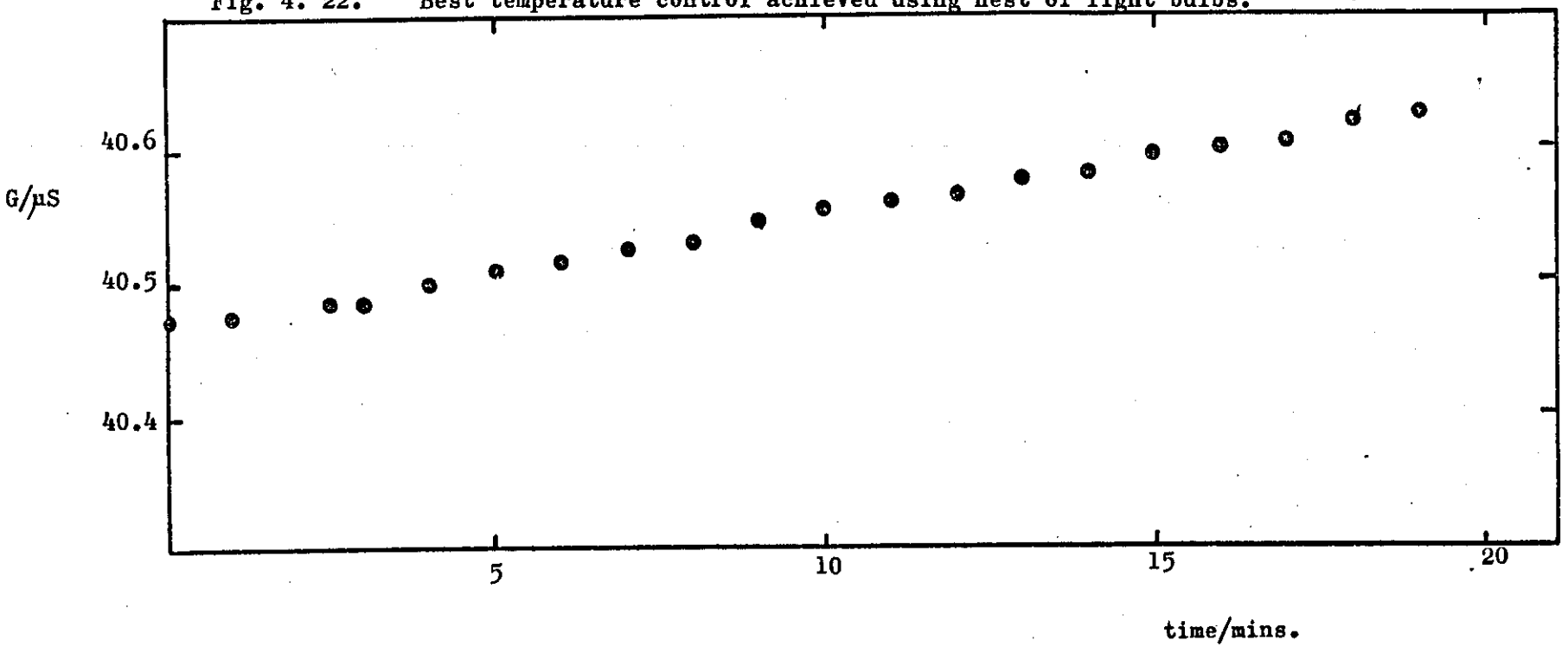

which is of the order required. However, there was a gradual and constant upward drift in temperature.

After several weeks of adjusting the bulb wattages and control settings with no further improvements, it became clear that either the amplifier in the circuit between the thermocouple and the relay was drifting due to heating effects within the circuit or that the cooling system became less efficient with time. In view of the limited time available for this work it was reluctantly decided to abandon further attempts at making conductance measurements at - 55°C.

Had more time been available a cryostat based on cooling by liquid nitrogen would have been constructed with a purpose built temperature regulating system.

4. 13, Gel Preparation.

Superficially the preparation of gels from silica and sulphuric acid was simple. The desired amount of silica was slowly added to a solution of sulphuric acid whilst stirring with a glass rod. The resultant mixture was then mechanically stirred using a single bladed stirrer for 10 minutes at 100 r.p.m. to give a smooth gel of even consistency. However, the initial conductance measurements showed marked differences between nominally similar gels. A close examination of the method of gel preparation revealed that there were small variations in consistency. These variations were first noticed during the transfer of gel from the beaker in which it was prepared to the conductance cell. The gel from the centre of the beaker flowed easily into the cell but that around the edges and base of the beaker was more viscous, although the gel had been stirred immediately before transfer. Various mixing procedures were compared, commencing with the single bladed stirrer mentioned above but in a tightly-fitting vessel, then stirrers of 2, 3 and more blades, and finally a stirrer designed to scrape the walls of the vessel and cause increased turbulence, all for a designated time at 100 r.p.m. A diagram of the various stirrers is given in fig. 4. 23.

The effect of an ultrasonic probe on the mechanically stirred gels was examined, and finally the operation of a plunger in a parallel sided vessel, see fig. 4. 24., a set number of times was tested. The procedure adopted as standard for the reasons

Fig. 4. 23 GEL STIRRERS.

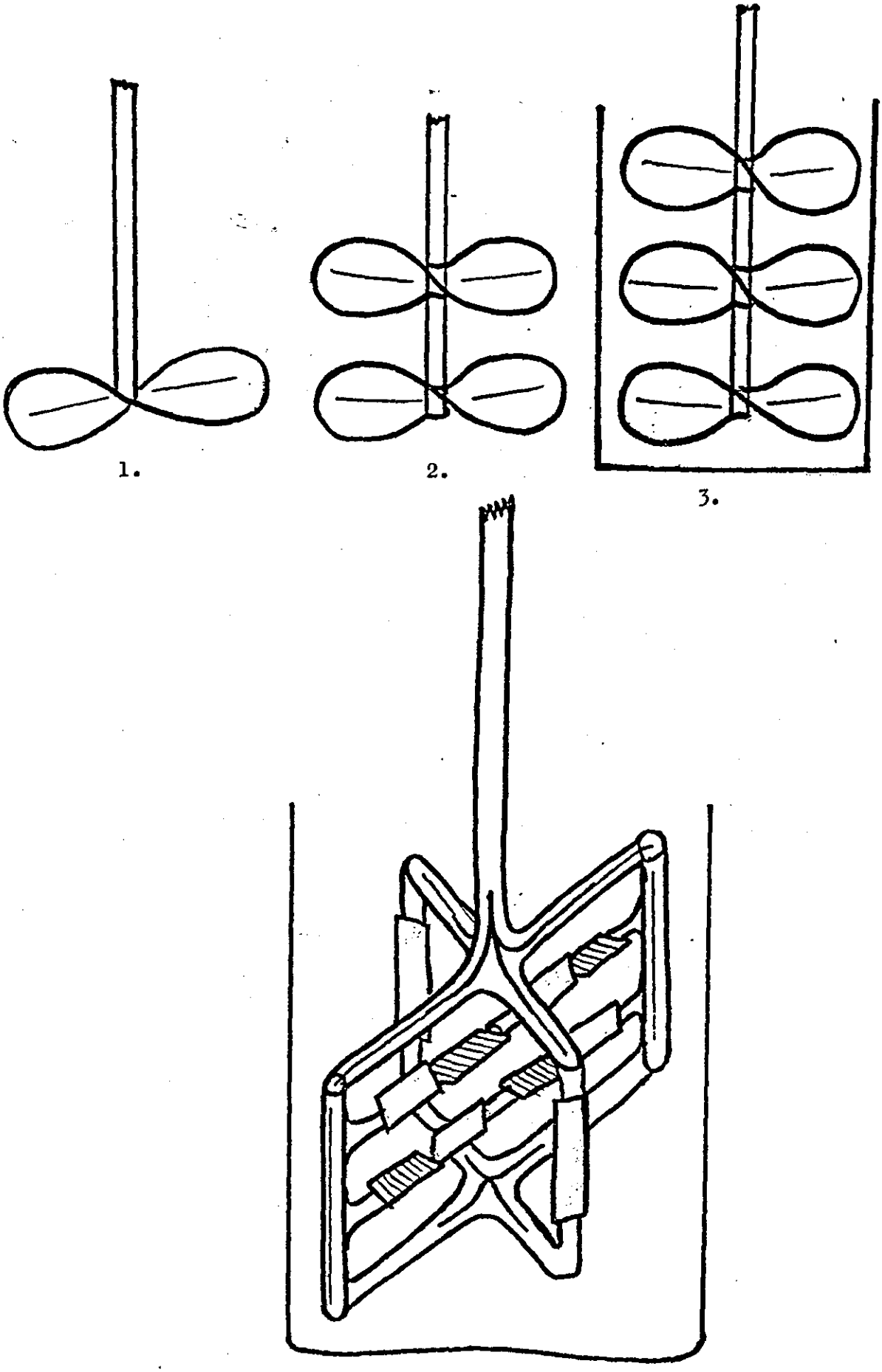

1. 2. 3. 4.

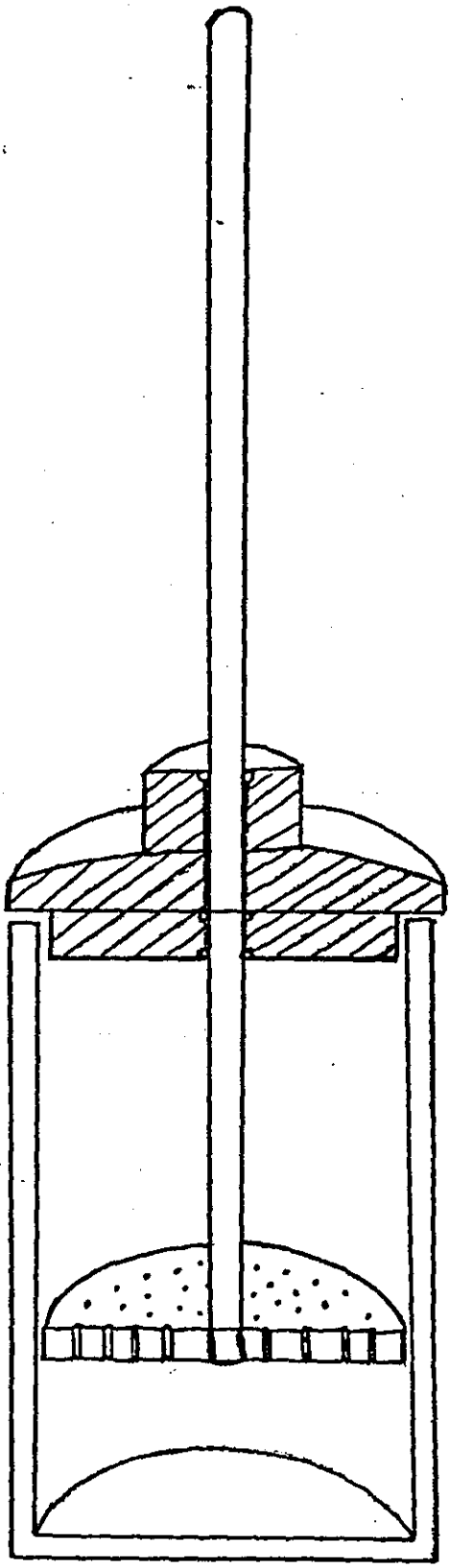

Fig. 4. 24. Plunger mixer used for Loughborough Standard Mixing Method.

detailed in Chapter 5, page109 was as follows:

The sulphuric acid electrolyte was transfered from a stock bottle to the straight-sided cylindrical vessel and weighed on a top pan balance to ± 0.005 gm. An amount of silica was weighed using a weighing boat on the same balance and slowly added to the acid whilst stirring with a glass rod. When all the silica had been added the mixture was stirred a few more times before the plunger was fitted and a set number of plunges made. The gels of low viscosity were poured directly into the conductance cell but those of higher viscosity were transferred a small amount at a time, to the filling arm of the cell and eased into the cell with a glass rod. In the latter cases the conductance was monitored for a much longer period to ensure that the gel had fully recovered from any stress sustained during filling which might have affected the gel structure and/or the conductance of the gel.

Normally a conductance cell is filled and emptied several times with each electrolyte before a measurement is made to ensure that effects such as adsorption at the electrodes and trace amounts of water left in the cell do not alter the electrolyte concentration and hence the conductance. For the case of the gels this was clearly impracticable. In order to achieve a standard condition the cell was flushed out several times with the electrolyte solution used to prepare the gel and the cell turned upside down and allowed to drain for a couple of minutes. The cell was shaken gently during this period to

ensure that the drops of electrolyte which tended to stick between the electrodes and the graded seal were removed. The gel was then transferred to the cell which was stoppered and placed in the thermostatted tank. The time taken for 40% sulphuric acid solution to reach a constant value of conductance in cell I or II at 25°C was approximately 20 mins. All gels were monitored for a minimum of 1 hour to ensure a constant value of conductance had been achieved although in the vast majority of cases the conductance ceased to change after 20 mins. At regular intervals gels or electrolyte solutions were left in the cells overnight, over a weekend, or occasionally for a longer period and the conductance monitored as a check on the temperature control of the tank and the stability of the gels.

4. 14. Density Measurements.

The density of electrolytes used to prepare the gels and that of the silica was measured using a standard density bottle of nominal volume 25 mls at 20°C.

Temperature control was by means of a common type of laboratory water bath capable of controlling temperature to ± 0.1°C.

The density bottles were filled with the electrolyte to be examined, brought to temperature and the excess electrolyte carefully removed by soaking up with a filter paper. The bottle was removed from the water bath, carefully dried and weighed. Each electrolyte density was determined several times and the mean value used in the calculations.

The density of silica was determined using the standard method for a solid using a liquid in which it does not react chemically or dissolve. It should be noted that when the liquid was being added to the silica already in the weighing bottle the addition was done in several stages and the bottle was shaken vigourously between each addition to ensure that any trapped air was released.

4. 15. Production Testing of the effect of Gels on Capacitor Properties.

The aim of the time spent during this work at the Tantalum Capacitor division of The Plessey Co. Ltd. was the investigation of the effects of the gel dispersion and gel concentration on the properties of production capacitors. The capacitors were assembled on The Plessey Co. Ltd's production line using standard capacitor components by the usual machine operators, the only difference being that the gels used were prepared by the author.

The effect of gel dispersion was examined by the comparison of the effect of two different mixing methods used to prepare the gels on the capacitance, loss angle, and leakage current of capacitors. 100 capacitors were assembled, fifty containing gels prepared using a single bladed stirrer at 100 rpm for 10 minutes in a large beaker, and the remainder containing gels prepared by the standard method devised for conductance measurements detailed earlier.

A further batch of capacitors was assembled. Ten capacitors for each gel concentration, covering 0, 5, 6, 7 & 8% wt/vol silica.

The Test procedure used to evaluate the performance of the capacitors was based on that specified in British Standard BS 9073, F003 and F004. The capacitance, loss angle, and leakage current were measured at 25°C (room temperature) on a BPL Electrolytic Capacitance Bridge and batches of capacitors subjected to one or more of a series of conditions, then retested.

Capacitors were subjected to an endurance test lasting 1000 hours. The full working voltage of 50V was applied and the temperature was 85°C. The capacitors were allowed to recover under normal laboratory conditions for 1¼ hours before the final measurements.

Other capacitors were subjected to a total of 10 temperatures cycles of -55°C to +125°C. The two extreme

temperatures were held for 0.5 hour at each point in the cycle. The capacitance, loss angle, and leakage current were measured at room temperature before the cycling started, after 5 cycles and after 10 cycles. The impedance at two frequencies, 50 Hz and 100 kHz, was measured at $-55^{\circ}C$ and the capacitance, loss angle and leakage current were also determined at $+125^{\circ}C$.

After the temperature cycling, the capacitors were subjected to a vibration test at 2000 Hz giving a movement of 0.75 mm which is equivalent to an acceleration of $\sim 98\ ms^{-2}$. The capacitors were vibrated for 15 hours in a vertical position followed by 15 hours in a horizontal position. The final values of capacitance, loss angle, and leakage current were then measured.

4. 16. Materials.

Conductivity water: tri-distilled from deionised stock in a quartz still and stored in Pyrex stoppered flasks which had been used solely for this purpose for many years. The conductivity of the water at 25°C was less than 1 x 10^{-6} Sm^{-1}.

Sulphuric acid : A.R. Grade (S.G. 1.84) manufactured by Fisons Ltd. and used without further purification.

Potassium chloride A.R. supplied by Fisons Ltd. A stock was stored in an oven at 200°C and transferred to a vacuum dessicator to cool immediately before use.

Potassium nitrate A.R., sodium sulphate A.R., potassium hydroxide A.R., sodium perchlorate A.R., and perchloric acid A.R. supplied by Fisons Ltd. and used without further purification.

Oxalic acid and potassium oxalate : Analytical Grade supplied by B.D.H. Chemicals Ltd. and used without further purification.

Fumed Silica : DT075 Grade, supplied by Ciba-Geigy Ltd. A poor quality fumed silica with a large particle size distribution and low purity commonly used as a filler in the Adhesives Industry.
M5 and EH5 Grades, supplied by Cabot Carbon Ltd. High quality grades of fumed silica with closely defined particle sizes and surface areas. These grades have a widespread use in industry and are of sufficient purity to be used in Foodstuffs.

Grade	Average Agglomerate Diameter (μm)	Surface Area $m^2 g^{-1}$	Density gcm^{-3}	pH
M5	12	200 ± 20	2.2	4
EH5	7	390 ± 40	2.2	4

Tantalum rod supplied by Metals Research Ltd, 99.99% purity.
Tantalum foil supplied by Johnson Matthey Chemicals Ltd.

Cell	I	I_r	II	III	IV
$K_{cell}(cm^{-1})$	26.23	26.228	15.54	5.00	2.18

CHAPTER 5.

5.1. Schering Bridge.

Before making any measurements on the tantalum electrode and at regular intervals during the course of this work the accuracy and working of the Schering bridge were checked using a simple cell analogue consisting of a 400 or 500 ohm resistor in series with a 1.0 μF capacitor. The resistance and capacitance of the series combination were measured over the frequency range 200 — 1,500 Hz. The typical results given in table 5.1. show the bridge to be quite sensitive. The slight displacement of values is due to the small deviation of the value of the capacitor from 1.0 μF and the problem at low multiples of 50 Hz where the harmonics tend to interfere with beat frequency detection. The bridge is most accurate at a frequency of 1 kHz. The investigation of the tantalum electrode may be conveniently divided into two sections:

1. studies using solutions containing simple inorganic ions.
2. oxalate solutions.

For brevity it is to be understood that all the electrode capacities given unless stated otherwise refer to that of the tantalum electrode measured at room temperature (23^{o}C) at a given potential with respect to a standard calomel reference electrode(SCE) at a frequency of 1 kHz in the solution stated.

Table 5.1. Resistance and Capacitance Measurements on a Cell Analogue to check the accuracy and working of the Schering Bridge.

Analogue : 400Ω 1μF

Frequency. Hz	R_2 Ω	C_2 μF
206	1041	518
310	1017	447
410	1011	425
506	1009	415
600	1008	410
710	1004	406
799	1002	405
900	1000	404
1000	998	403
1100	996	402
1200	994	402
1300	991	402
1400	989	400
1500	986	400

ie at 1000 Hz the capacitance is 0.998 μF and the resistance is 403Ω calculated using the equations given on page 68.

5.2. Tantalum Electrode in Solutions containing Simple Inorganic Ions.

The polarization curve given in fig. 5.1 is a typical result for tantalum in 1.0 M KCl, and shows that there is a well defined polarizable region between ± 1.0V . The current flow and gas evolution at the two extremes of this region interfere with the measurement of the electrode capacity.

Successive dilution of the 1.0 M KCl electrolyte down to 0.01 M caused little alteration of the polarization curve.

Typical electrode capacitance curves for tantalum in 1.0 M KCl, 0.1 M KCl, and 0.01 M KCl are given in fig. 5.2. The remarkable feature of these curves is the low value of the electrode capacitance which lie in the range below $9\mu F\ cm^{-2}$. This is a similar result to those obtained by Brodd and Hackerman (1957), and McMullen and Hackerman (1959), for tantalum in 0.5 M Na_2SO_4 solutions. The capacitance remained relatively constant as the electrode was driven more positive, but fell markedly at -0.1V in 1.0 M KCl. This fall in capacitance is interpreted in terms of oxide film thickening at the more positive potentials. The fall in capacitance was not observed for the more dilute solutions. However, there was a considerable time dependence of the capacitance observed in this region. The approximately exponential time decay of the capacitance is shown in fig. 5.3 and indicates a first order thickening of the oxide layer present on the tantalum, presumably by high field ion conduction processes. The fall of electrode capacitance in 1.0 M KCl at -0.1V is in accord with an increase in film thickness determined from the parallel plate capacitor formula (see equation 1.1).

Fig. 5.1. Current vs Potential for Tantalum in 1.0M Potassium Chloride.

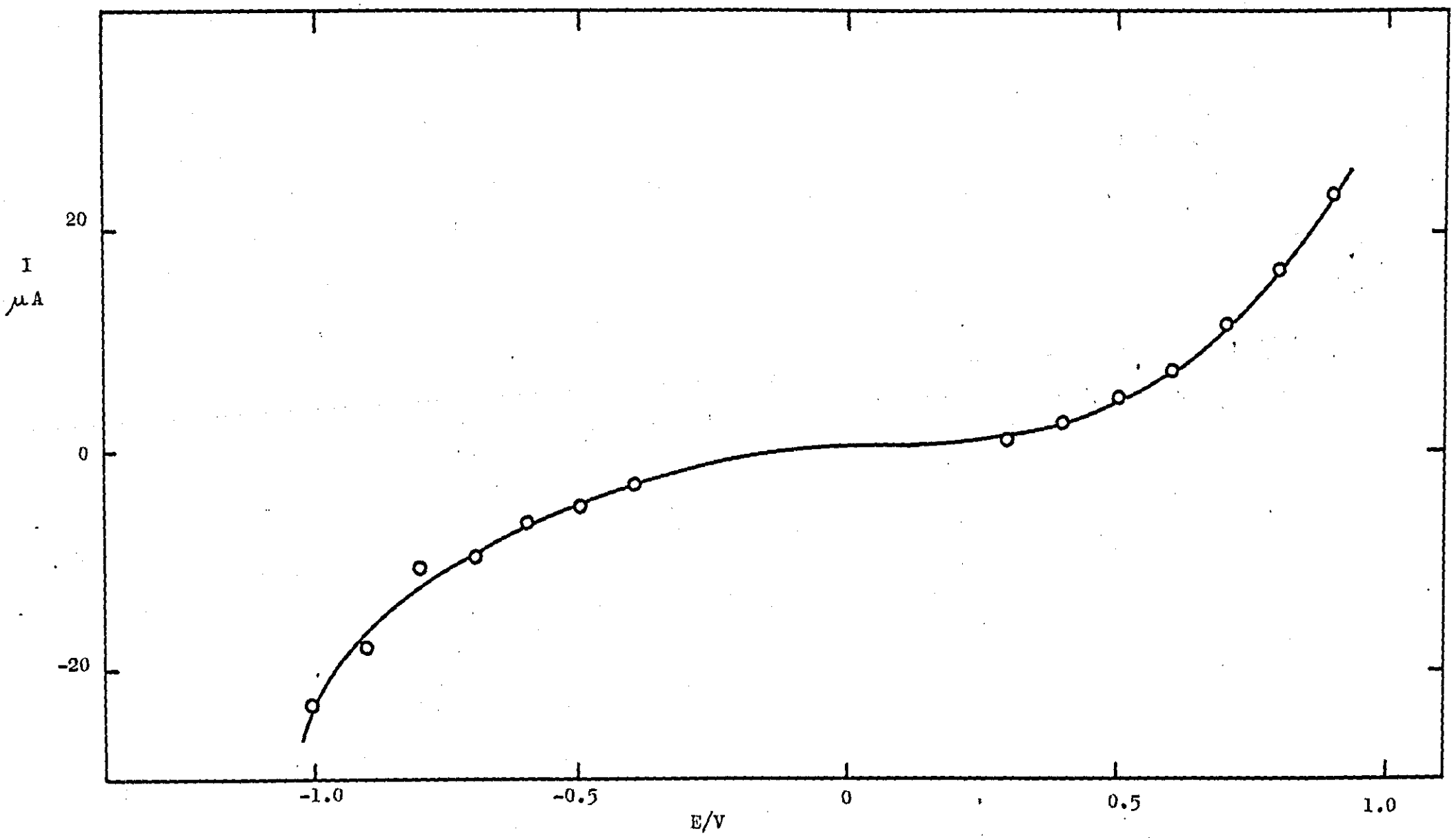

Fig. 5.2. Capacitance vs Potential
for Tantalum in
a. 1.0M, b. 0.1M, c. 0.01M Potassium Chloride

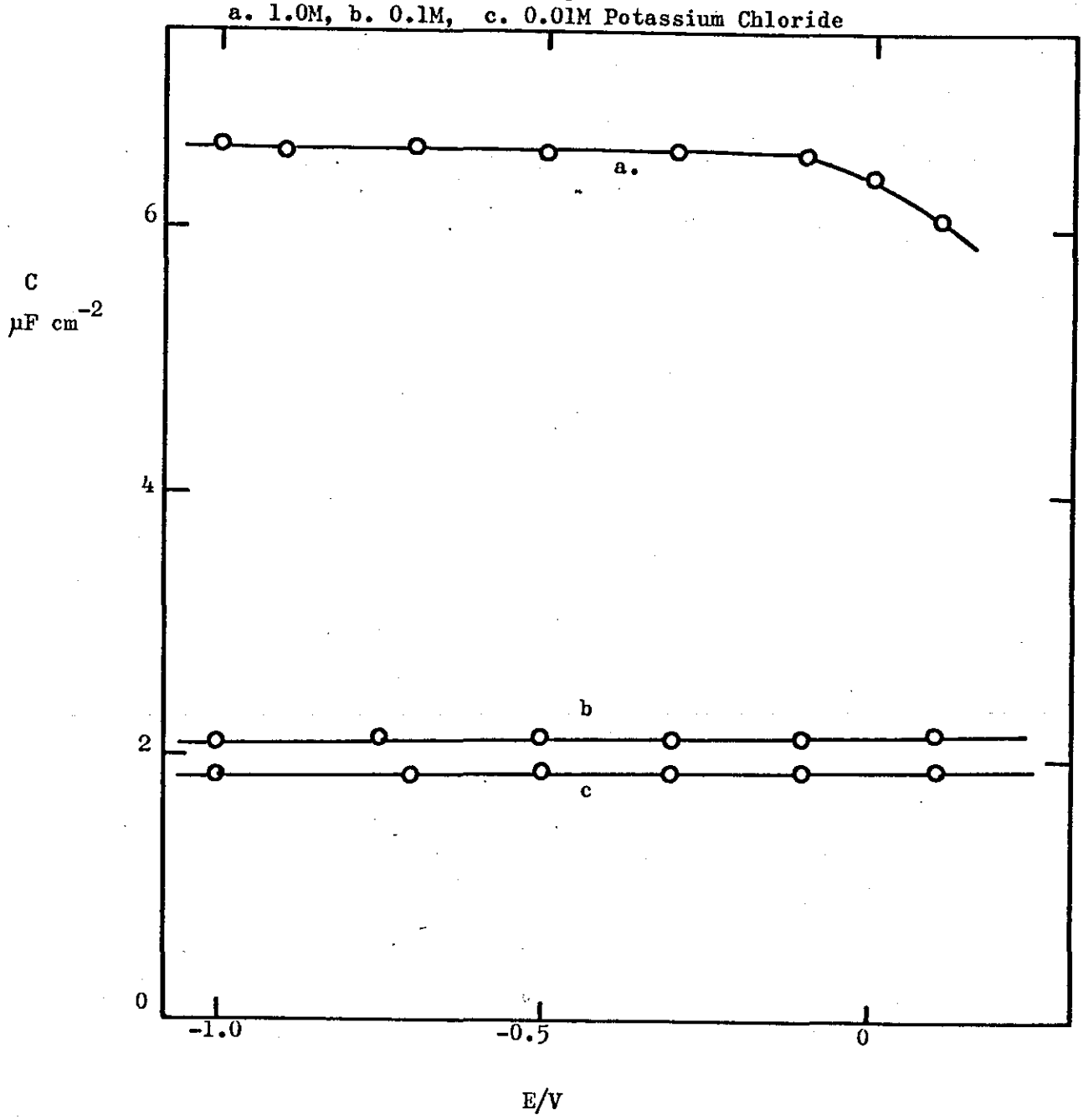

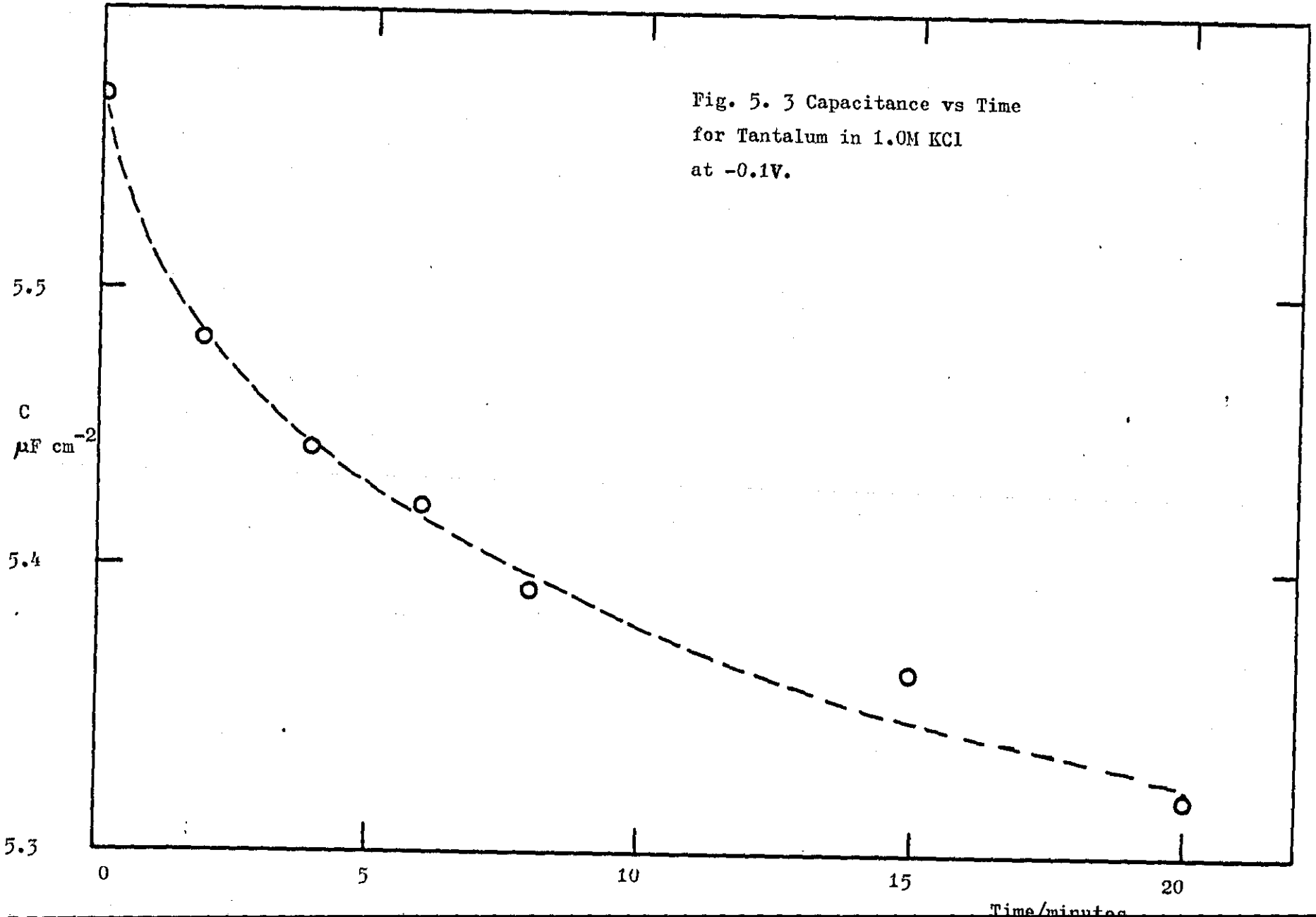

Fig. 5. 3 Capacitance vs Time
for Tantalum in 1.0M KCl
at -0.1V.

The electrode capacitance of tantalum in 1.0 M $NaClO_4$, 1.0 M $HClO_4$, and 1.0 M KOH was virtually constant over the polarizable potential range as shown in figs. 5.4, 5.5, and 5.6 respectively. The capacities were again remarkably low, lying in the range between 3 and 5 $\mu F\ cm^{-2}$.

From these results of electrode capacitance versus potential we are forced to conclude, as did earlier workers Brodd and Hackerman (1957), McMullen and Hackerman (1959), and Isaac and Leach (1962-3), that for tantalum in contact with these electrolytes at all potentials within the experimentally polarizable region, the electrode surface is covered with a thin oxide layer of high stability and protective power.

5.3. Tantalum Electrode in Oxalate Solutions.

The polarization curve for tantalum in 0.5M $(COOH)_2$ is shown in fig 5.7. The polarizable range is -1.3 to -0.2V which is considerably shifted from that observed for solutions of simple inorganic ions, see fig. 5.1. The electrode capacitance versus potential curve for tantalum in 0.5 M $(COOH)_2$ is shown in fig. 5.8, and it is immediately obvious that the magnitude of the capacitance is considerably increased to a value of $30\ \mu F\ cm^{-2}$ in the polarizable region compared to a value of less than $9\ \mu F\ cm^{-2}$ for the solutions of simple inorganic ions. The high capacitance values and shift in the polarizable region are indicative that for the oxalic acid solution, the true metal surface free from an oxide film is accessible for study.

The effect of reducing the concentration of oxalic acid to 0.04 M and then to 0.0135 M on the capacitance curves is also shown on fig. 5.8. The curves lie below that for 0.5 M $(COOH)_2$, but are still much higher

Fig. 5.4 Capacitance vs Potential for Tantalum in 1.0M Sodium Perchlorate.

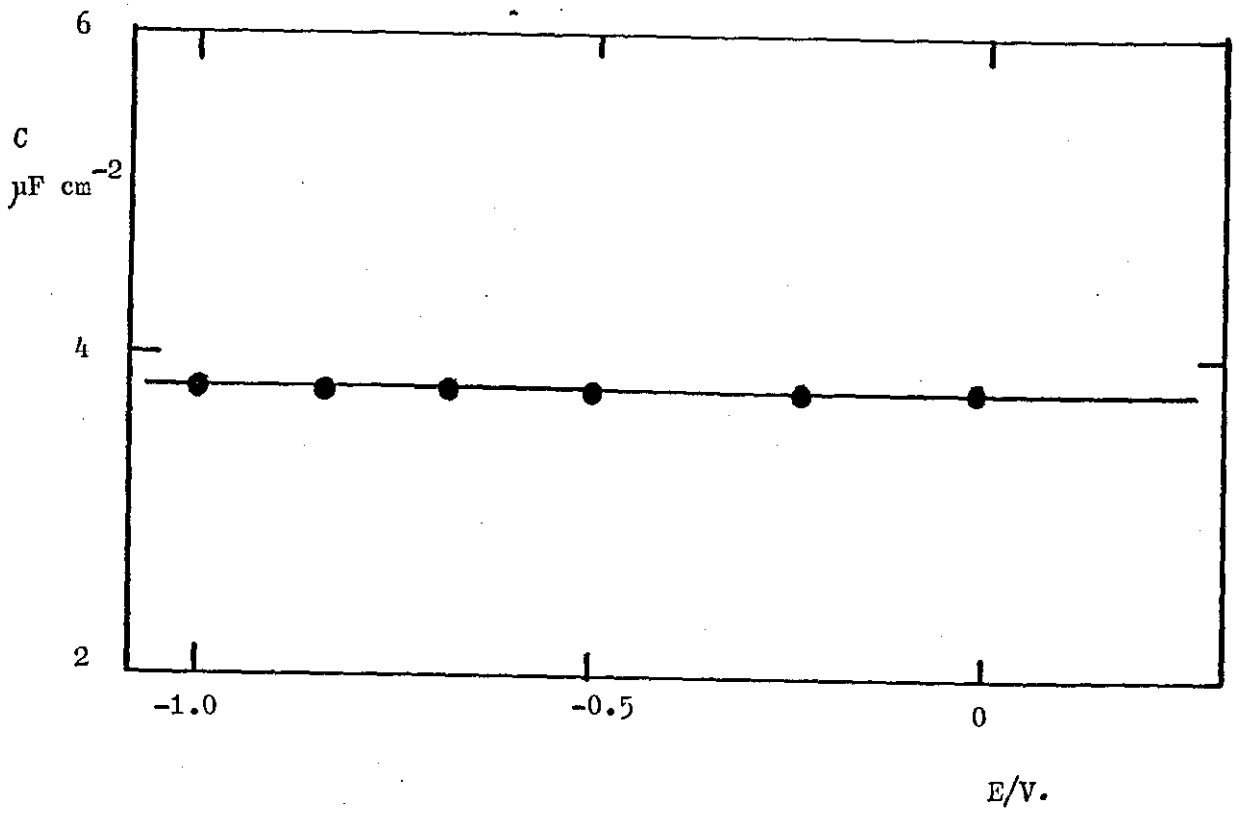

Fig. 5.5 Capacitance vs Potential for Tantalum in 1.0M Perchloric Acid.

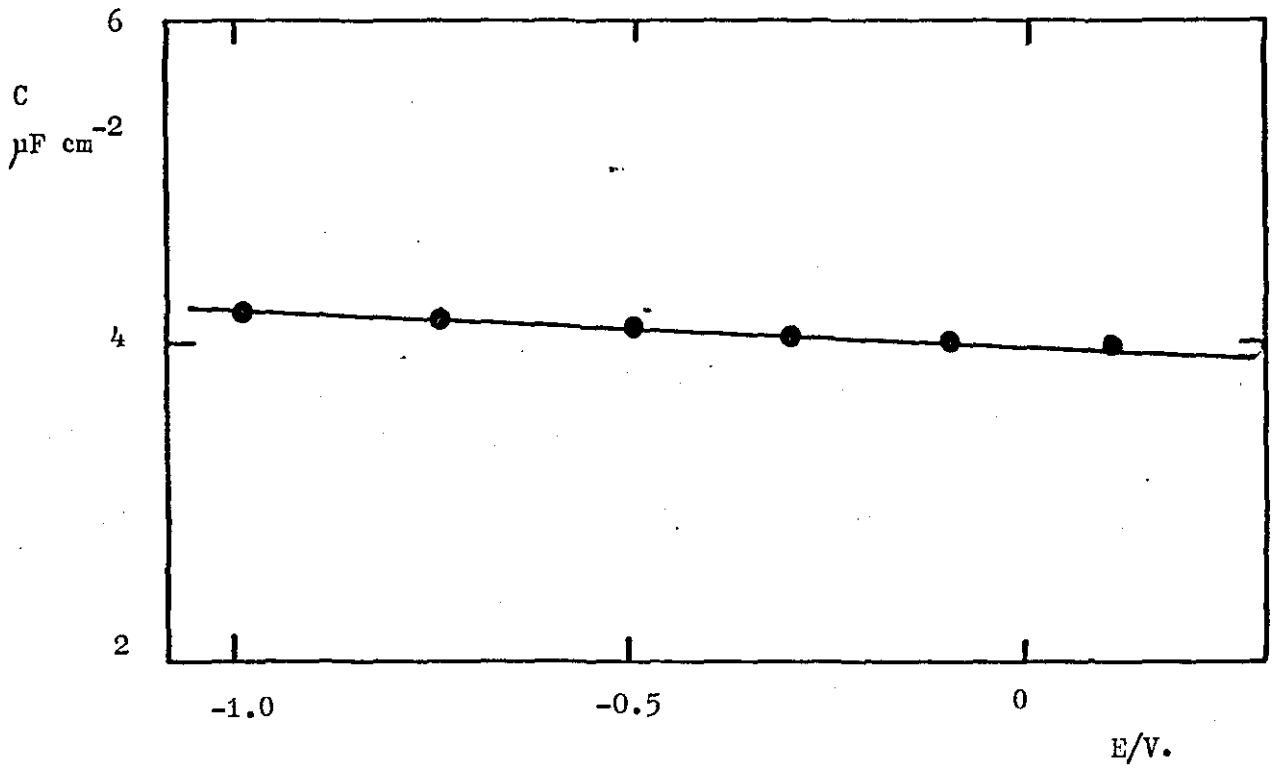

Fig. 5.6 Capacitance vs Potential for Tantalum in 1.0M Potassium Hydroxide.

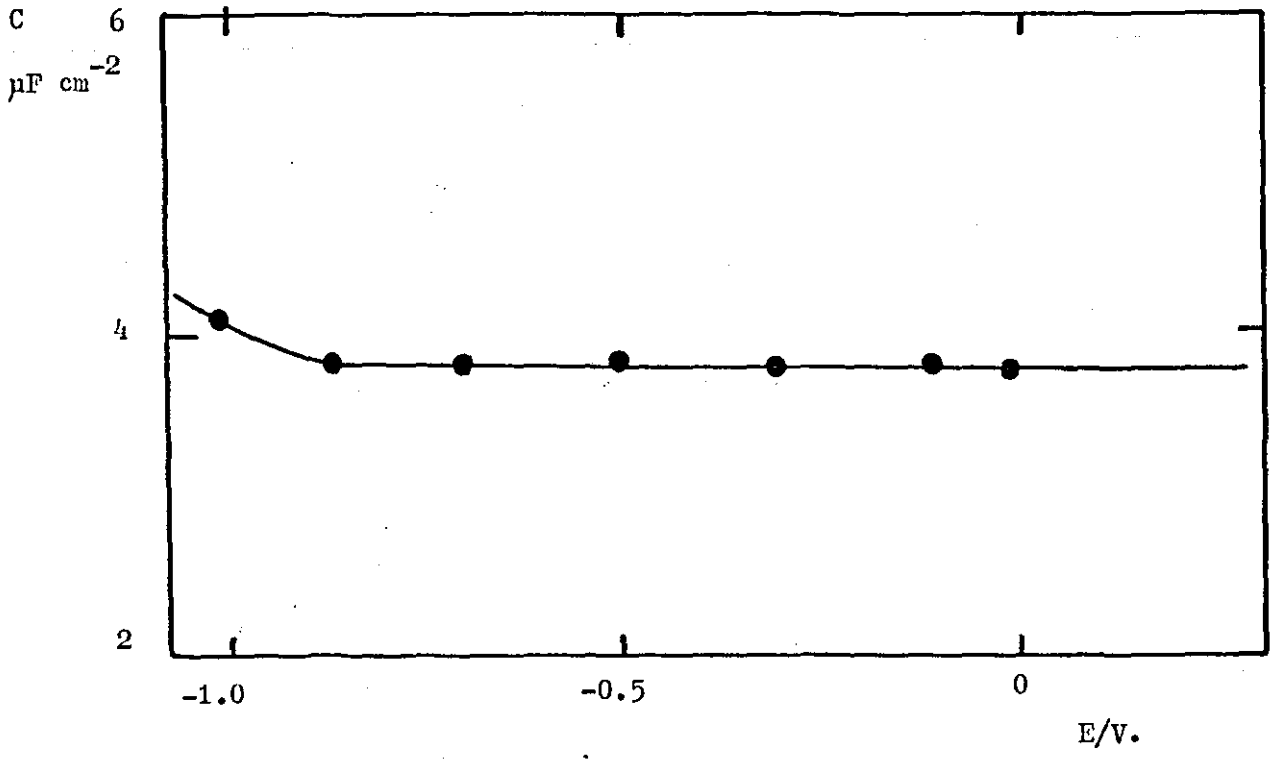

Fig. 5.7. Current vs Potential for Tantalum in 0.5M Oxalic Acid.

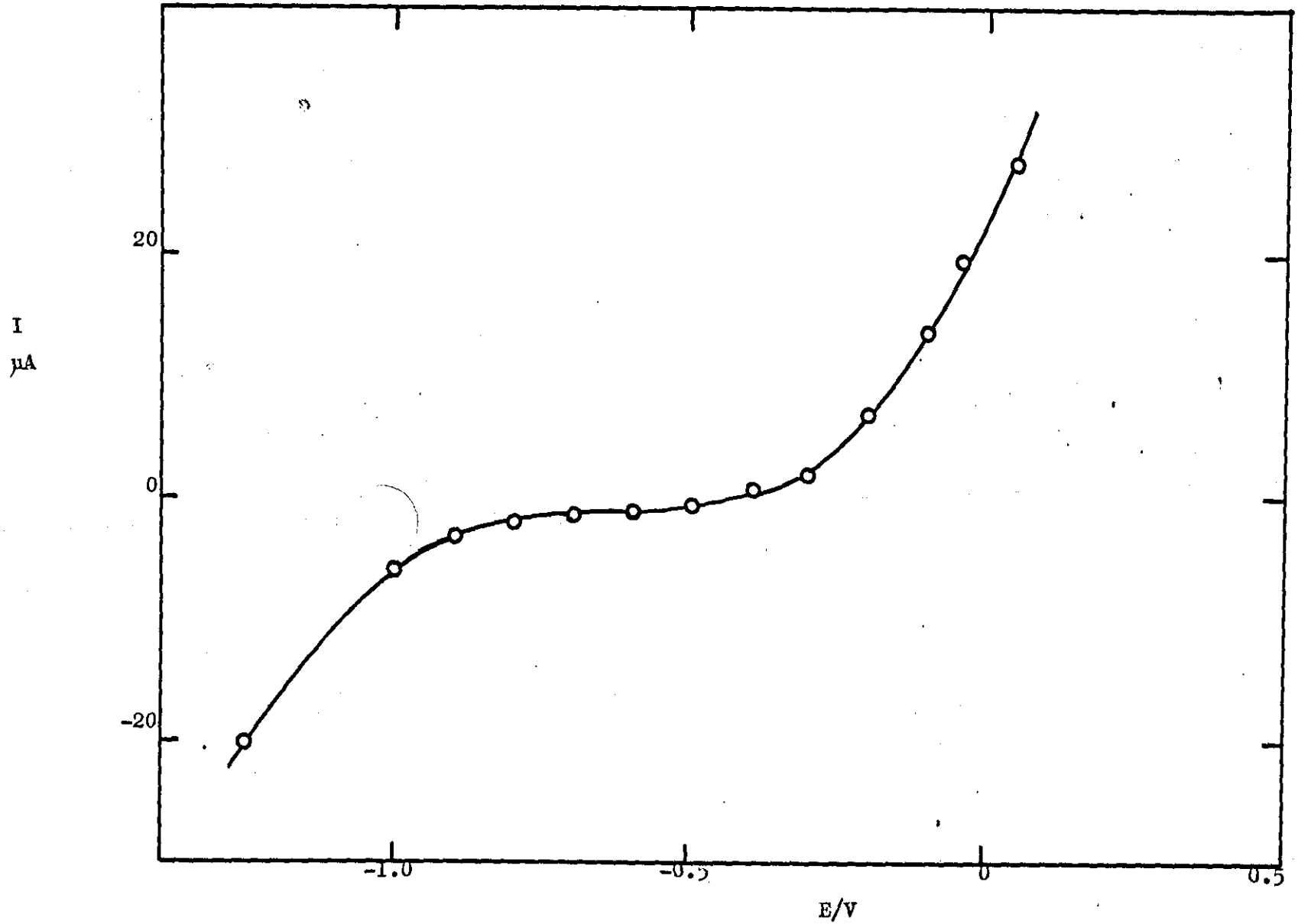

Fig. 5.8. Capacitance vs Potential for Tantalum in Oxalic Acid.

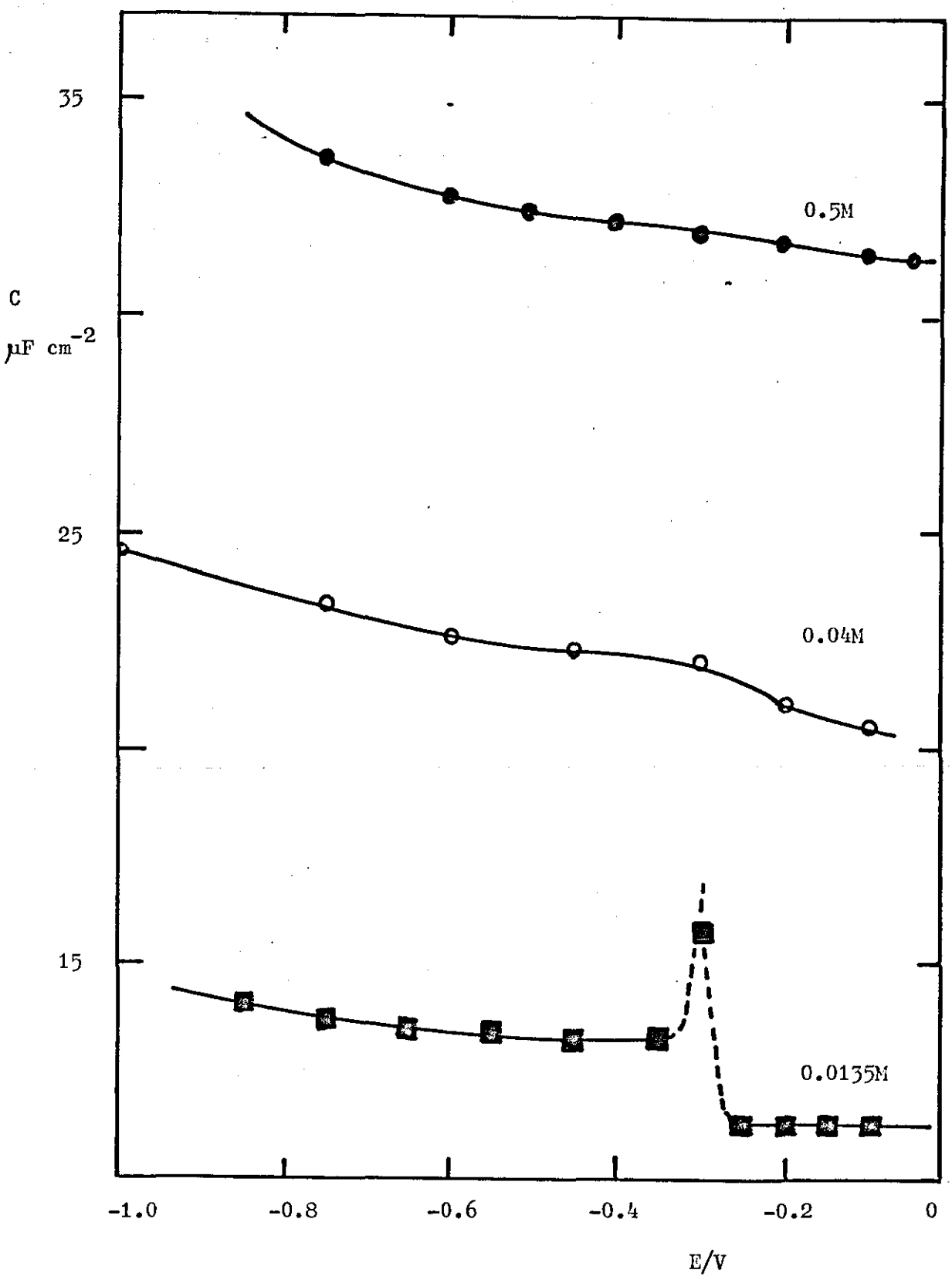

than those for solutions of simple inorganic ions.

At a higher pH oxalate solution (0.5 M $(COOK)_2$) a similar high electrode capacity is observed as shown in fig. 5.9, again indicative of an exposed interface. The negligible effect of pH on the capacitance confirms that oxalate is an effective complexant.

At potentials more positive than -0.3 V the capacitance falls, which is considered to be due to the formation of an oxide film and its subsequent growth, and implies that -0.3 V is the limit of potential at which the oxide film is forced off the surface.

For the most negative potentials investigated the retrieval of the double layer capacitance is obscured by the pseudo-capacitance due to the hydrogen evolution reaction.

A further observation of importance concerning the oxalate solutions is seen from the time dependence of capacity at a series of potentials which are given in fig. 5.10, compared to that for 1.0 M KCl solution shown in fig. 5.3.

The capacities at potentials in the range -09 V to-0.3 V reach constant value quite rapidly, which is in agreement with an equilibration process between the tantalum and the solution followed by a prolonged equilibrium.

The erratic changes in capacitance observed at a potential of -1.0V are due to the hydrogen evolution reaction. At potentials more positive than -0.3V the capacitances are low and fall exponentially with time. This indicates the formation of an oxide layer and mirrors the curve obtained for 1.0 M KCl (fig.5.3) where oxide formation is also thought to be occurring.

Fig. 5. 9 Capacitance vs Potential for Tantalum in 0.5M Potassium Oxalate.

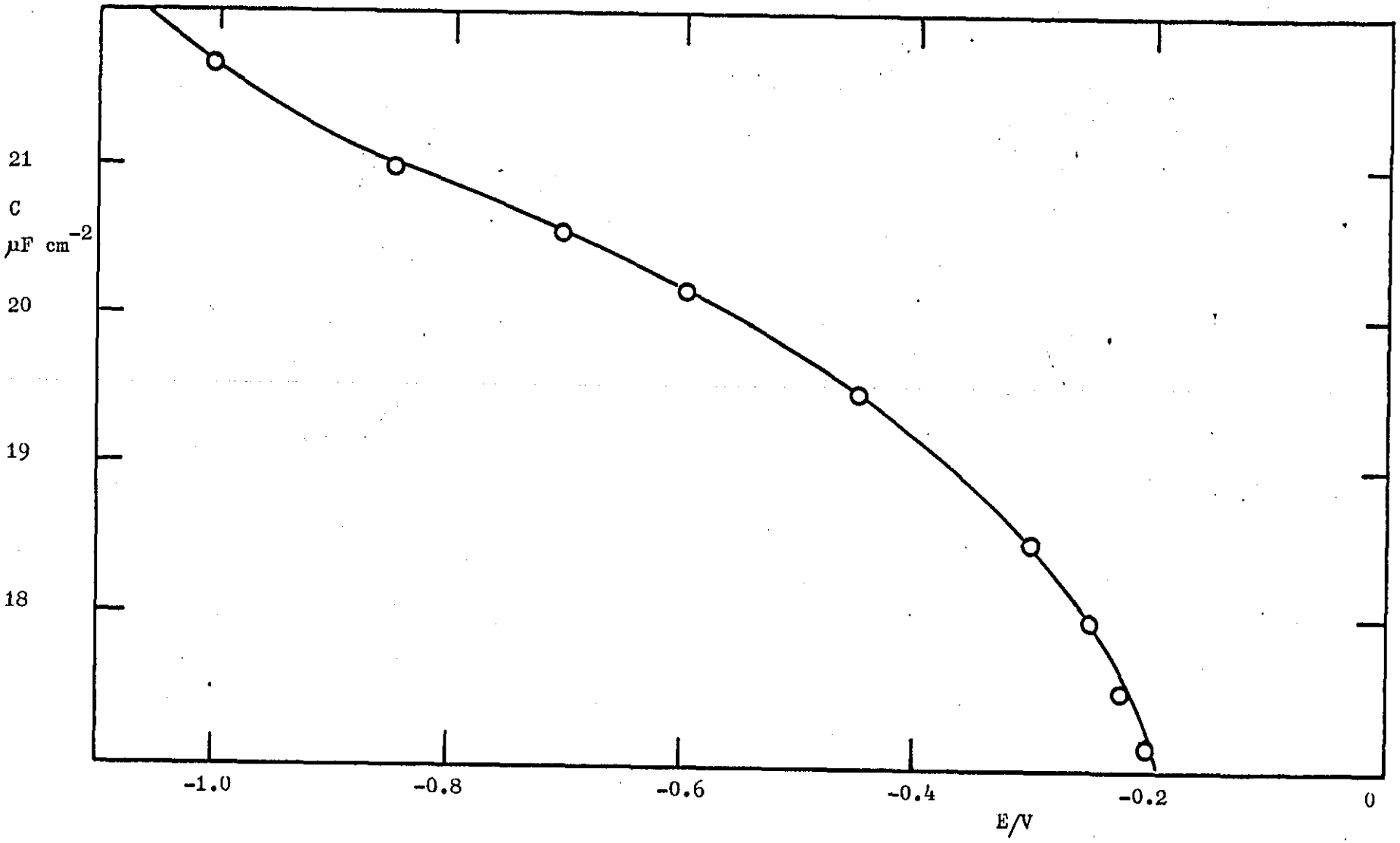

Fig. 5.10. Time dependence of Capacitance for Tantalum at different Potentials in 0.5M Potassium Oxalate.

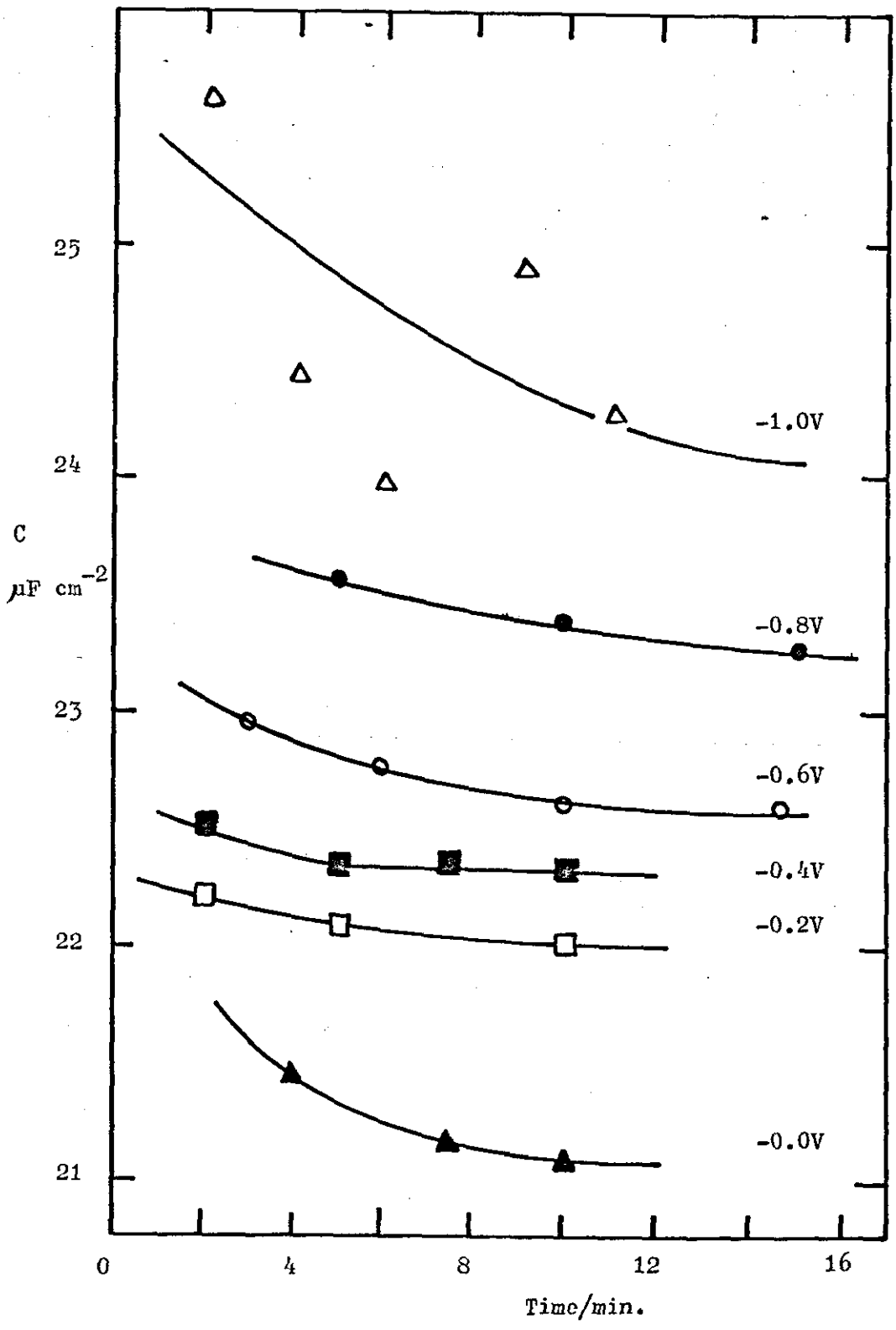

The shape of the capacitance versus potential curves did not change with concentration of electrolyte. We might have expected to identify the point of zero charge as the potential of the diffuse layer minimum. This is clearly not possible and indicates that the point of zero charge lies outside the experimental region.

5.4. The Influence of Sulphuric Acid and Gelled Sulphuric Acid on the Field Recrystallization of Tantalum Pentoxide Films.

During the setting up of the anodizing apparatus, the effect of current density on the degree of field recrystallization of the tantalum pentoxide films on 7.6μm thick tantalum foils was determined. Foils were anodized (formed) in 0.2% H_2SO_4 at 85°C using a constant current of either 0.1, 0.88, or 2.0 mA cm^{-2} to 120V, the formation voltage, which was held for a further 60 minutes. Samples taken from the central portions of foils which had been anodized at one of the three current densities were examined under both optical and scanning electron microscopes. Micrographs of these foils are reproduced in fig. 5.11 and demonstrate that field crystallization has proceeded to the greatest extent for a current density of 0.1 mA cm^{-2}, and successively decreases with increasing current density. This is in accord with the findings of Vermilyea (1955) that the optimum conditions required to produce field recrystallization of tantalum pentoxide in sulphuric acid electrolyte are a current density of 0.1 mA cm^{-2}, a formation voltage of 120V held for 60 minutes on reaching voltage in 0.2% H_2SO_4 at 85°C.

A series of tantalum foils were anodized under these conditions with the addition of M5 silica to 0.2% H_2SO_4 to give gelled electrolytes of 0, 3.7, 5.0 and 6.0% silica by weight. The scanning electron

Fig. 5.11. The Effect of Current Density on Field Recrystallization.

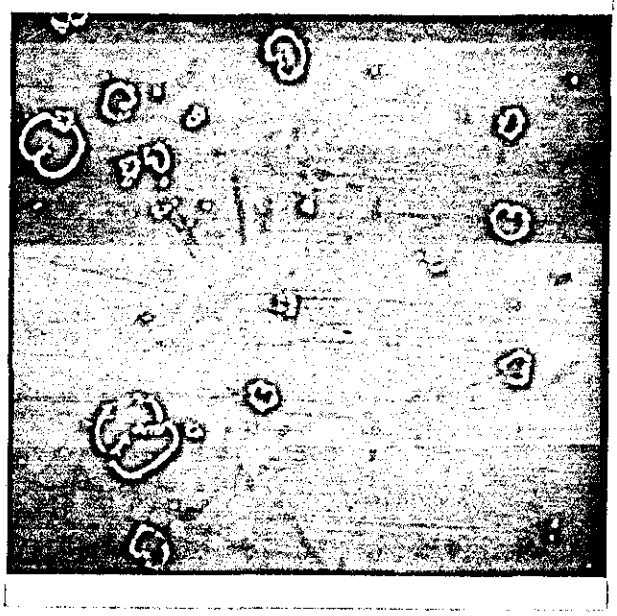

0.2% H_2SO_4

0.1 mA cm^{-2}

x200

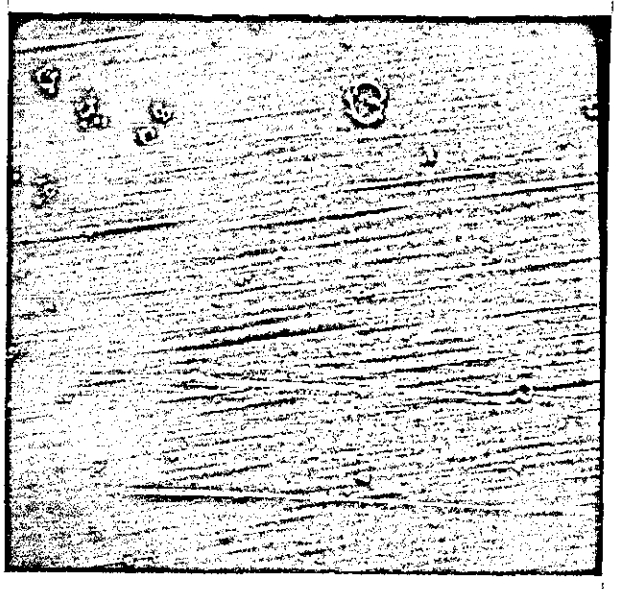

0.2% H_2SO_4

0.88 mA cm^{-2}

x200

0.2% H_2SO_4

2.0 mA cm^{-2}

x200

micrographs obtained from these foils are given in fig. 5.12 and clearly show that a significant reduction in the amount of field recrystallization with the gelled electrolytes. There is some indication that the addition of 3.7% silica caused the maximum inhibition of field recrystallization, but as the number of samples analysed was small this result must be regarded as only tentative.

In chapter 4 it was reported that the first micrographs of foils which had been anodized in gels had a woolly texture which was assumed to be a silica layer covering the oxide film and was found to be easily removed by scrubbing the foil gently with cotton wool under distilled water. Micrographs showing the silica covered surface, a silica free surface, and one with a brush stroke through the silica revealing the oxide layer beneath complete with a crystallite are given in fig. 5.13.

Field recrystallization is known to be much reduced when tantalum is anodized in 40% H_2SO_4 compared to 0.2% H_2SO_4 (e.g. Vermilyea (1955)), but as silica addition had been shown to inhibit field crystallization with the 0.2% H_2SO_4 it was considered worthwhile to investigate whether this also applied when silica was added to 40% H_2SO_4. Addition of 3.7% silica was chosen because that had produced the maximum inhibition in 0.2% H_2SO_4.

The micrographs given in fig. 5.14 demonstrate that the amount of field crystallization is further reduced in 40% H_2SO_4 on addition of silica.

Fig. 5.12. The Reduction in Field Recrystallization when Tantalum is Anodized in Gelled 0.2% Sulphuric Acid.

0.2% H_2SO_4

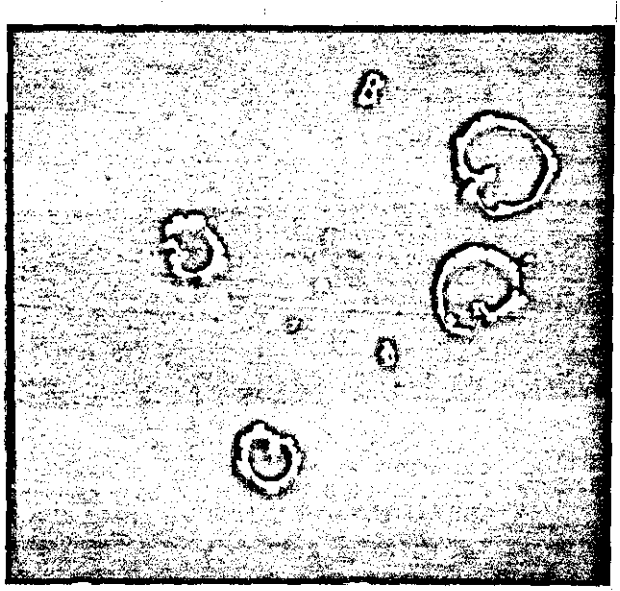

x500

3.7% M5 Silica/0.2% H_2SO_4

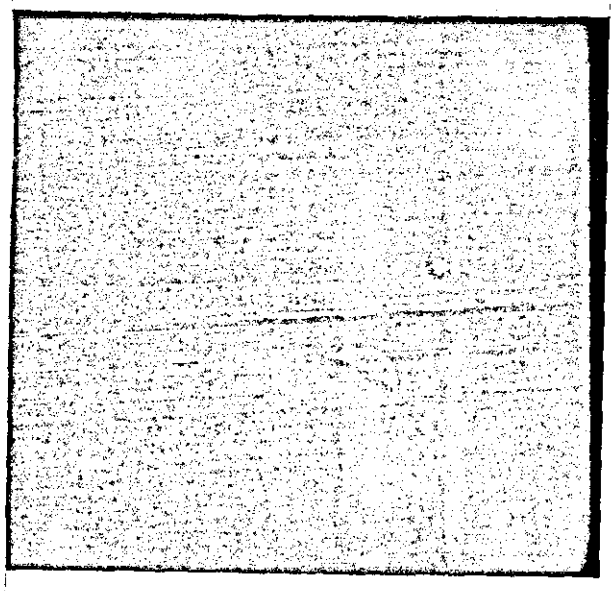

x500

5% M5 Silica/0.2% H_2SO_4

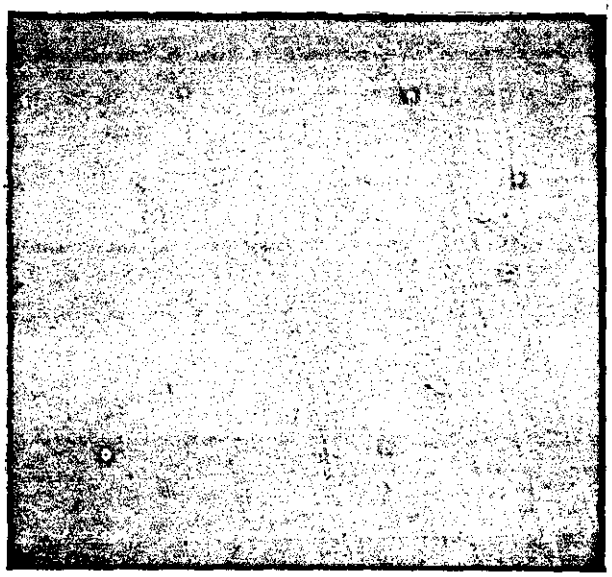

6% M5 Silica/0.2% H_2SO_4

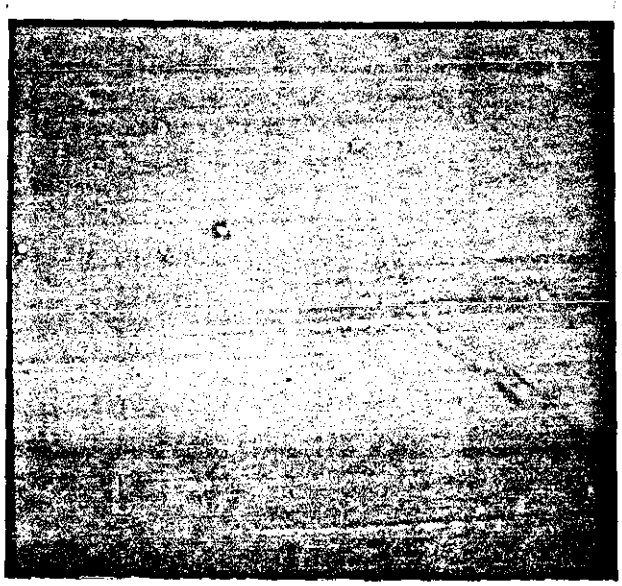

Fig. 5.13. Tantalum Pentoxide Films covered with Silica, Free of Silica, and partially covered with Silica revealing a Crystallite.

Silica free Ta_2O_5

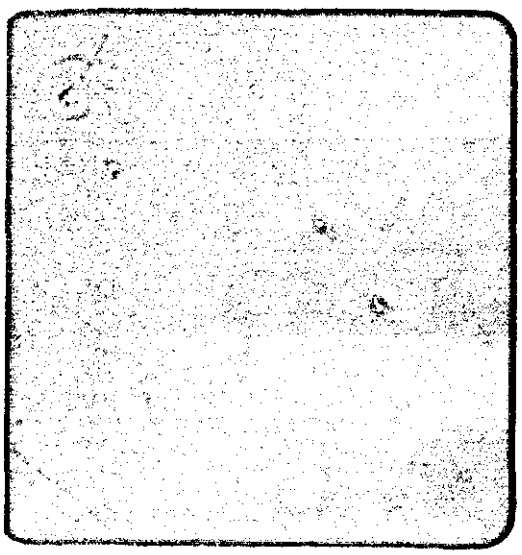

x5K

Partially covered Ta_2O_5

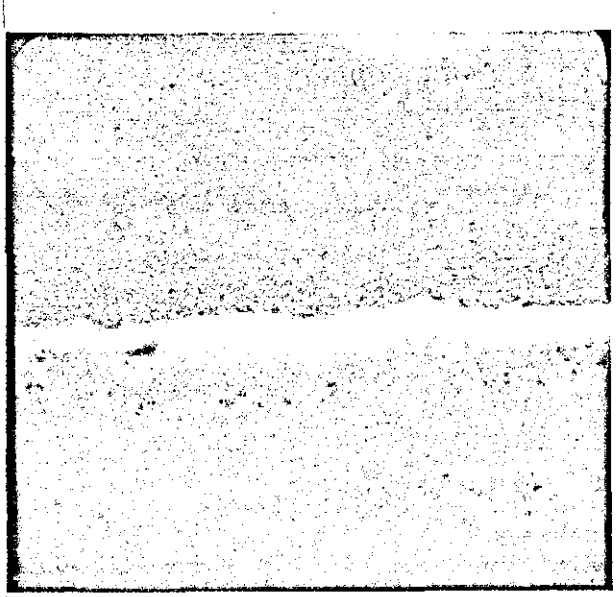

x200

Silica covered Ta_2O_5

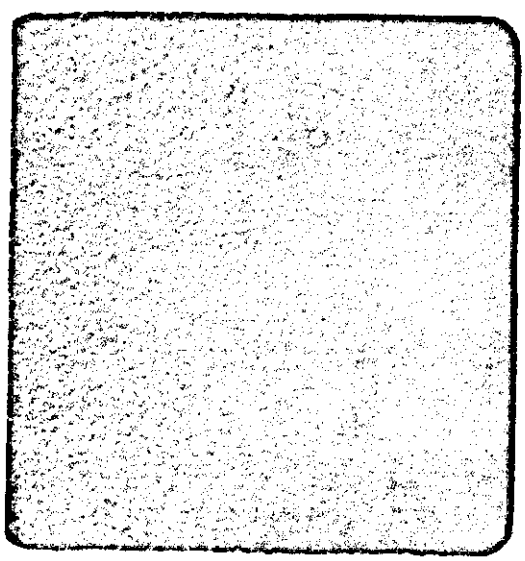

x5K

Partially covered Ta_2O_5 (higher magnification)

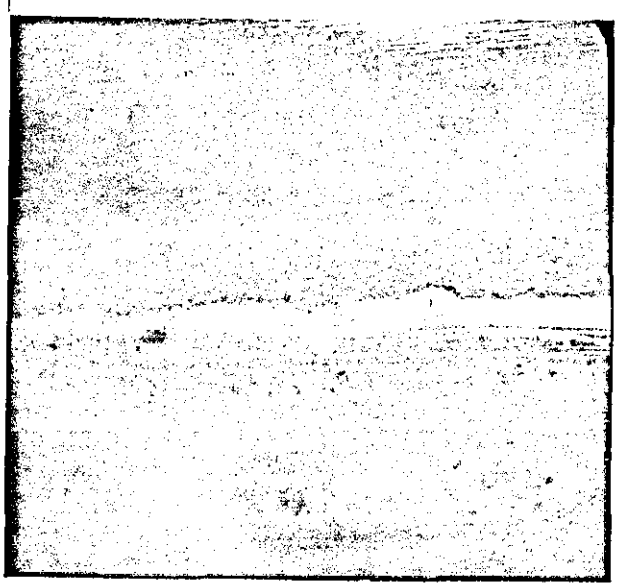

x5K

Fig. 5.14. The Further Reduction in Field Recrystallization when Tantalum is Anodized in 40% Sulphuric Acid.

40% H_2SO_4

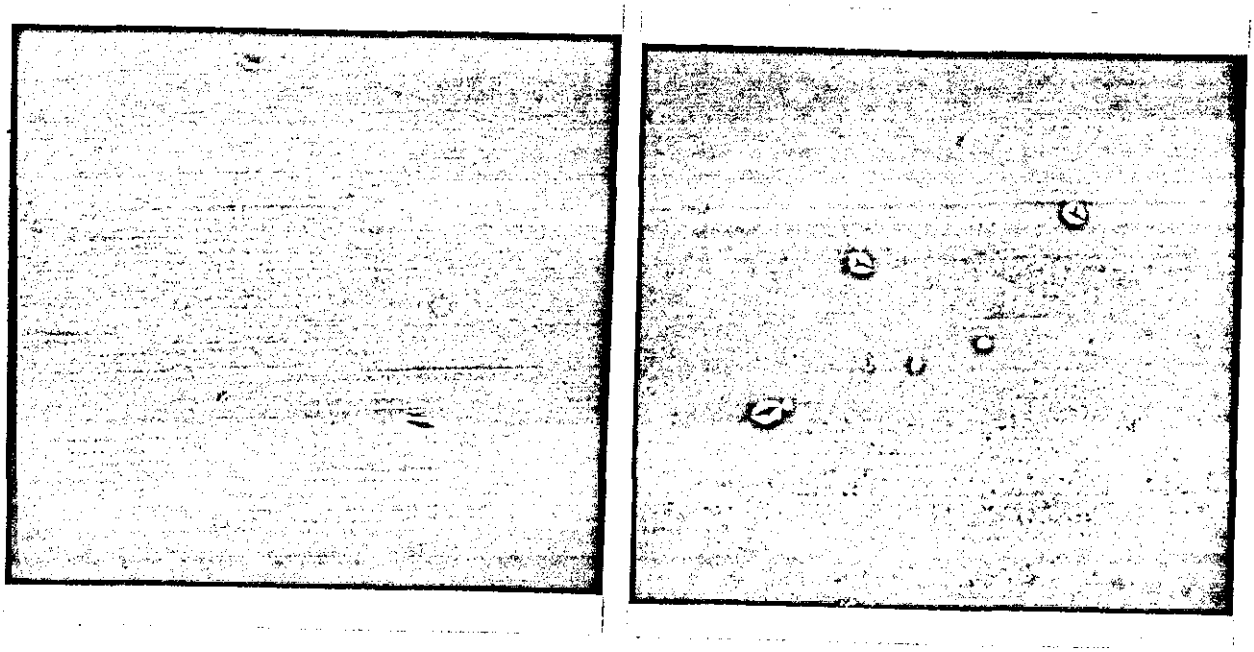

x200 x2K

3.7% M5 Silica/40% H_2SO_4

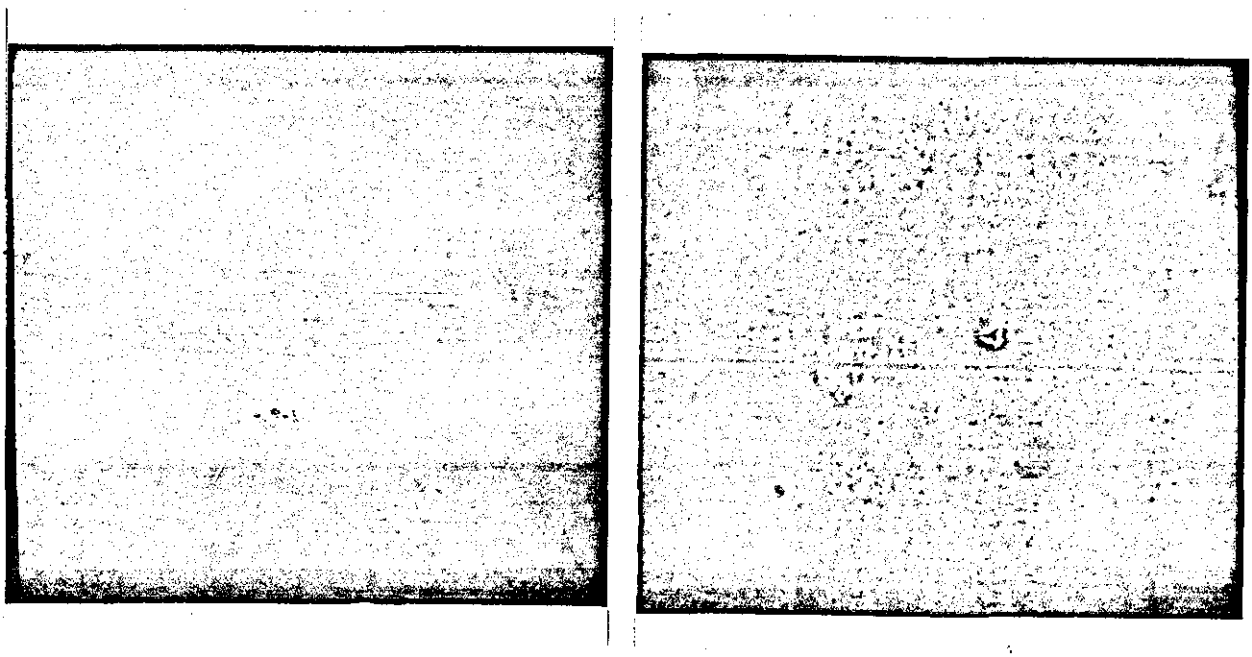

x200 x2K

There is no obvious explanation of the inhibition of field crystallization by silica during the anodizing process. There are several other substances which when added in very small percentages to either the forming electrolyte or incorporated in the electrolyte within a capacitor substantially inhibit field crystallization, see Jackson (1973), but there is no obvious common factor.

5.5. Scintillation Voltage of Tantalum Pentoxide Films.

The scintillation voltage was measured at 25°C for samples of foil which were anodized at 2.0 mA cm^{-2} in 40% H_2SO_4 containing 0, 3.7, 5, and 6% M5 silica. A small increase in the scintillation voltage was observed for foils anodized in 3.7% M5 silica/40% H_2SO_4 compared to those anodized in the 40% H_2SO_4 alone, the value rising from 110 $\pm$ 1V to 123 $\pm$ 2V. A very similar value was obtained for foils anodized at the other gel concentrations, and in view of the experimental errors it can only be concluded that a small amount of silica increases the voltage corresponding to the onset of scintillation by about 12%, but further additions of silica have little effect.

The scintillation voltage was also measured as a function of temperature for foils anodized in 40% H_2SO_4 or 3.7% M5 silica/ 40% H_2SO_4. The results given in Table 5.2 show a small increase in scintillation voltage with temperature for both sets of foils, the values for foils anodized in 3.7% M5 silica/40% H_2SO_4 all lying above those for the foils anodized in 40% H_2SO_4.

This behaviour is of great industrial importance as the scintillation breakdown process can be a limiting factor governing

Table 5.2. Scintillation Voltage at Various Temperatures for Tantalum anodized in 40% Sulphuric Acid or in 3.7% M5 Silica/40% Sulphuric Acid.

$T^{o}C$	S.V. (Acid)	S.V. (Gel)
25	110	128
40	115	132
60	118	139
85	120	-

the operating range of temperatures available to the capacitors.

5.6. Examination of Tantalum Pentoxide Films for Incorporation of Silica.

The chemical composition of the oxide films formed on foils anodized in 3.7% M5 silica/40% H_2SO_4 was examined using EDAX and Auger Spectroscopy for evidence of the incorporation of silica. The unscrubbed foils gave a positive response for silica with EDAX presumably due to the surface film of silica, but there was no response from scrubbed foils. There was no evidence of silica in the oxide of the scrubbed films detected by Auger spectroscopy.

5.7. Electrical properties of Tantalum Pentoxide Films.

The comparison of the electrical properties of large area specimens of foil which had been anodized in either gelled 3.7% M5 silica/ 40% sulphuric acid or in the acid alone also indicated that there was very little difference between the two oxide films within the limits of accuracy of the measurements. The results are given in the order in which they were made.

The initial capacity and tan d measured after 5 minutes at 60V DC, with an AC signal of 100 mV, 500 Hz were 0.091μF cm^{-2} and 9.0% respectively for the foils anodized in acid alone compared to 0.091μF cm^{-2} and 10% for the foils anodized in the gel.

The current as a function of applied potential was very similar for both films, virtually no current could be measured over the potential range -1.0V to + 100V. Each potential was held for about 1 minute and on increasing the potential by an increment of 10V an instantaneous current of ~ 5μA was observed which decreased to zero in under 5 secs.

Tan d as a function of frequency for the two foils is shown fig 5.15 and they are also very similar. There is possibly a slightly larger dissipation for the foil anodized in the gelled electrolyte, but the difference is of little significance in terms of the properties of a capacitor.

5.8. Thermostatted Tank.

The tank was shown to be controlling the temperature to better than $\pm$ 0.002°C at -25.00°C, there being no visible change detectable in the mercury level of a Beckman thermometer or in the conductivity of a sample of 40% sulphuric acid solution in Cell I.

5.9. Effect of Frequency on Conductivity.

As described in chapter 3, it is necessary to determine the effect of frequency on the conductivity of a solution in order to demonstrate whether or not any problems due to electrode polarization have been successfully overcome by the platinum blacking of the electrodes.

The conductivity of 40% H_2SO_4 and 6% M5 silica/40%H_2SO_4 in both cell I and II was measured at twenty frequencies in the available range of 200 Hz to 13 kHz. The signal applied to the cells outside of this range was shown by the oscilloscope to be too noisy for accurate measurements to be made. Within the errors of the bridge the conductivities of the acid and gelled acid were found to be independent of frequency when measured in either cell. This is the desired result and indicates that there were no polarization problems with the two conductance cells with sulphuric acid electrolytes.

5.10. Initial Conductivity Measurements on Gelled Electrolytes.

An initial study of the effect of silica addition on the conductivity of 40% sulphuric acid was performed on gels prepared by the Tantalum Capacitor Division of The Plessey Co. Ltd. from their production stocks.

Fig.5.15. Tan d vs Frequency for a Tantalum Pentoxide Film formed

a/ by anodizing Tantalum in 40% Sulphuric Acid.

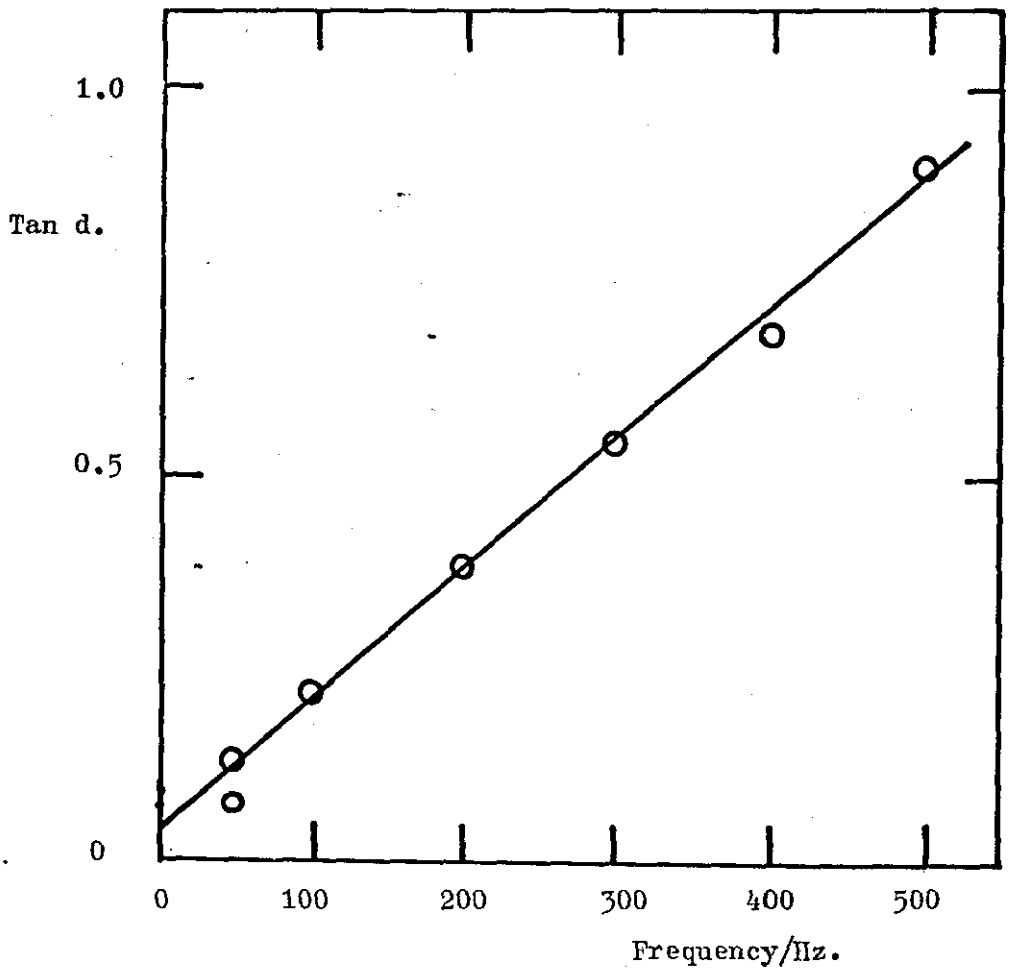

b/ by anodizing Tantalum in 3.7% M5 Silica/40% Sulphuric Acid.

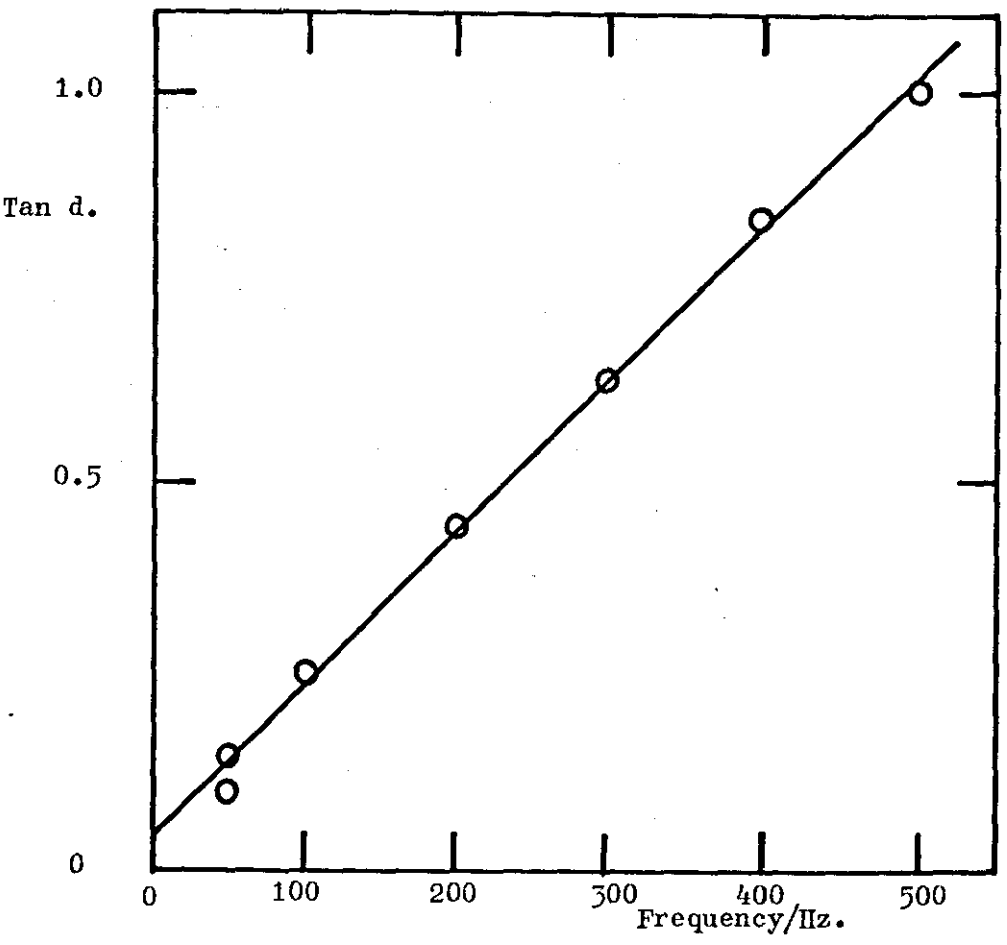

The range of gel concentrations investigated was 0 - 8% by weight silica using cell I at 25°C. The conductivity decreased non-linearly with increasing silica content, see fig. 5.16, and a difference in the conductivity was noted between two 6.5% gels, one prepared with DT075 silica, the other prepared from M5 silica. The acid and the gels had been prepared by a volume/volume and a weight/volume method respectively, the gels being stirred by a single stirrer blade at ~100 r.p.m for 10 minutes.

A more carefully controlled study on gels prepared from DT075 silica/40% sulphuric acid by a weight/weight method followed by stirring with a single bladed stirrer at ~100 r.p.m for 10 minutes resulted in a very similar curve for conductivity vs wt % silica, see fig. 5.17, as that for the initial study.

A visual comparison of the gels prepared from DT075 and M5 grade silica indicated that there was considerably less variation in consistency in the gel prepared from M5 silica. This is not surprising because the M5 silica has a much more closely defined and controlled specification compared to DT075 silica (see chapter 4). Further study was confined to gels prepared from M5 silica or EH5 silica, a silica of similar quality to M5 but having a larger surface area and smaller agglomerate size.

5.11. Dispersion of Silica to form Gelled Electrolytes.

Some difficulty had been experienced in the preparation of gels which gave a reproducible conductivity, quite a significant spread in the conductivity for a series of gels containing 6% silica was observed.

Fig. 5.16. Conductivity vs wt % Silica, DT075 silica/40% H_2SO_4 in Cell I at 25°C.

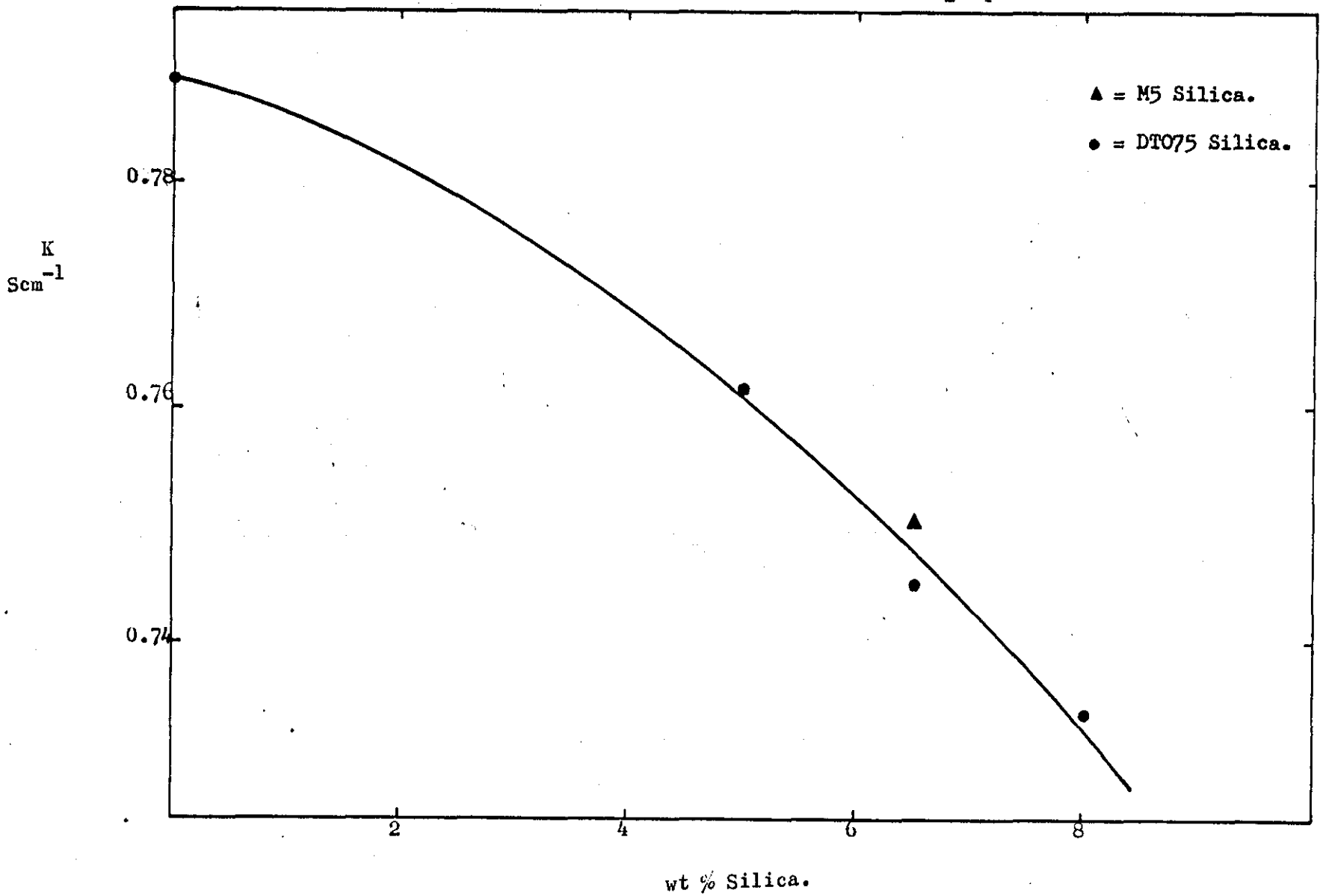

Fig. 5.17 Conductivity vs wt % Silica, DT075 silica/40% H_2SO_4 in Cell I at 25°C

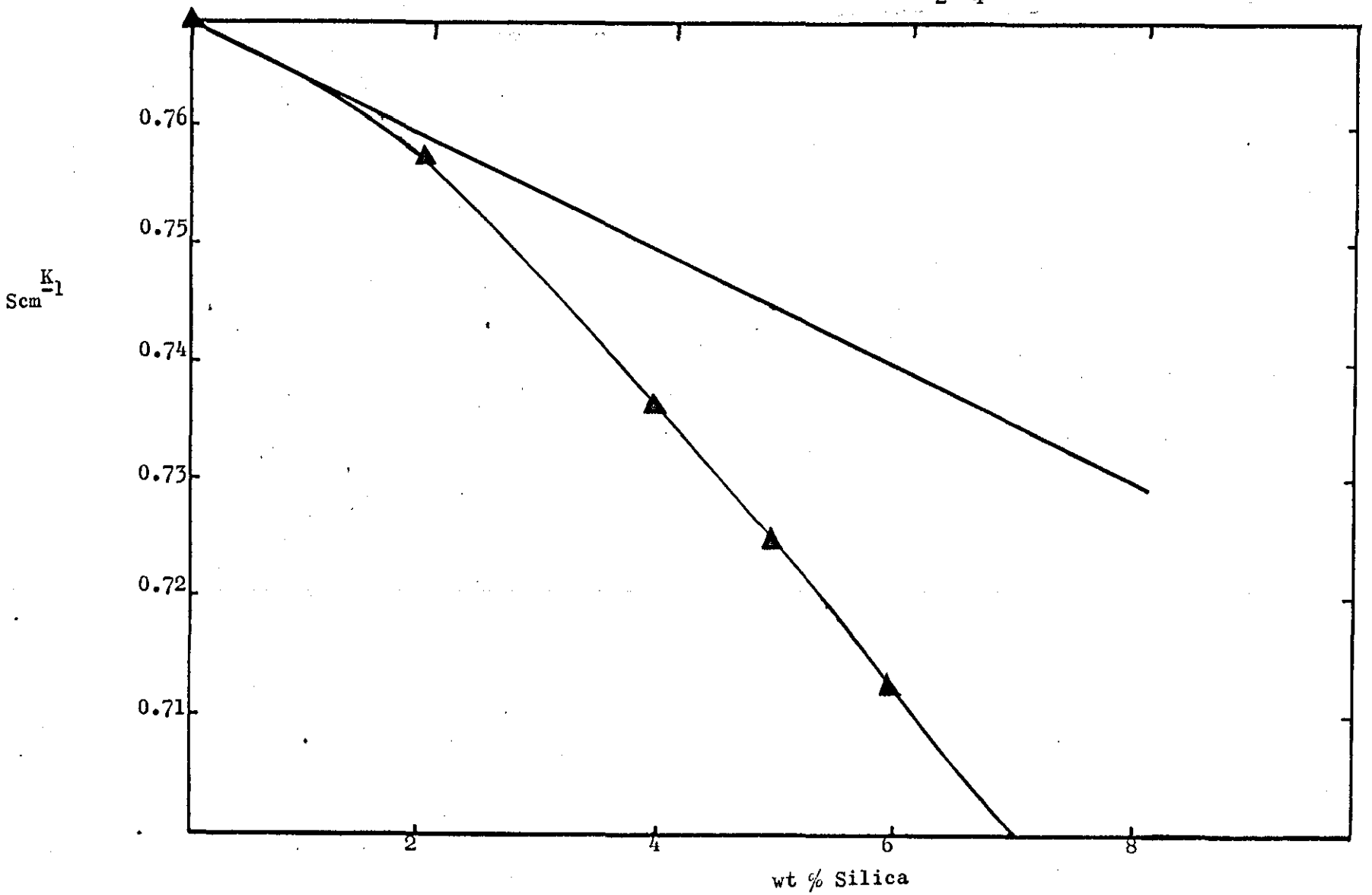

As mentioned earlier this irreproducibility was traced to variations in the consistency of the gels, more specifically to the degree of dispersion of the silica in the electrolyte,and variation of the degree of dispersion of the silica in the electrolyte,and variation of the degree of dispersion through the gel. Conductivity measurements using the dilution cell III on gels prepared from silica and potassium chloride described later also indicated that variations in the amount of mixing affected the conductivity of the gel.

A series of mixing procedures were compared to find a method of producing gels which gave the smallest spread in conductivity for a given concentration. The criterion aimed for was a mixing procedure which produced gels with conductances which differed by less than 1 unit on the last decade of the bridge. Such a difference is equivalent to $\pm$ 0.00016 Scm^{-1} for a 6% gel in 40% sulphuric acid in a conductance cell of cell constant K_{cell} = 15.54 cm^{-1}. The conductivity of samples of 40% sulphuric acid taken from a stock bottle and measured in cell I or cell II invariably lie within this specification.

It is appreciated that such a criterion may not have produced the optimum or maximum network structure for a stable gel of a particular concentration,and further,that it will not of necessity produce the same measure of the maximum network structure for other concentrations or other electrolytes.

There is some experimental evidence which indicates that the chosen method of gel preparation produces a maximum gel structure. The operation of the plunger in its tightly-fitting vessel eventually

produced gels of an even consistency throughout to the eye and of a reproducible conductivity after ~ 200 plunges. As the number of plunges was increased towards this value for successive gels the conductivity decreased, reached a stationary value over a small range of plunges, then started to rise, and the spread of conductivities also increased. A similar trend in the conductivity was observed for gels prepared using the best stirrer (number 4 on fig. 4.23), but the overall spread in conductivity was also higher, see table 5.3.

The variation of conductivity with amount of mixing may be interpreted in terms of the structure of the gels as follows:

The situation before the plunger is operated is that the silica is roughly dispersed in the acid by the stirring with a glass rod. As the first few plunges are made the macroscopic "lumps" of silica are being broken up and becoming more evenly distributed within the acid, and therefore the likelihood of gel network formation is increasing. The increase in network may lead to a greater resistance to the flow of ions due to structuring of the acid electrolyte adjacent to the network hindering the "proton jump" mechanism, ad/absorption of electrolyte as the silica is wetted, and an increase in the overall path length of the moving ions as they are forced round the silica, resulting in a fall in the measured conductance.

Once maximum network formation has been achieved a small degree of further mixing has little effect on the gel and the conductance remains constant. When the extra mixing causes irreversible network breakdown i.e. when the fragments become sufficiently small and widely separated that it is statistically unlikely for thermal motion to allow them to reform, the factors listed above as hindering ion flow other than sorption of electrolyte will decrease and consequently the conductivity will increase. This behaviour is shown pictorially in fig. 5.18.

Table 5.3. The Effect of Gel Preparation on the Conductivity of 6% M5 Silica/40% Sulphuric Acid in Cell II at 25°C.

G mS	K Scm^{-1}	Mixing
49.05	0.7510	10 mins.
47.20	0.7226	10 mins. *
46.36	0.7100	20 mins.
46.45	0.7111	20 mins
46.615	0.7137	100 plunges
46.35	0.7096	100 "
46.45	0.7111	100 "
46.42	0.7107	150 "
46.43	0.7108_5	200 "
46.43	0.7108_5	250 "
46.43	0.7108_5	250 "

* at 100 rpm using stirrer number 4 of Fig. 4.23.

Fig. 5.18 Pictorial Description of the Effect of Mixing on the amount of Network Structure and Conductivity of a Gel.

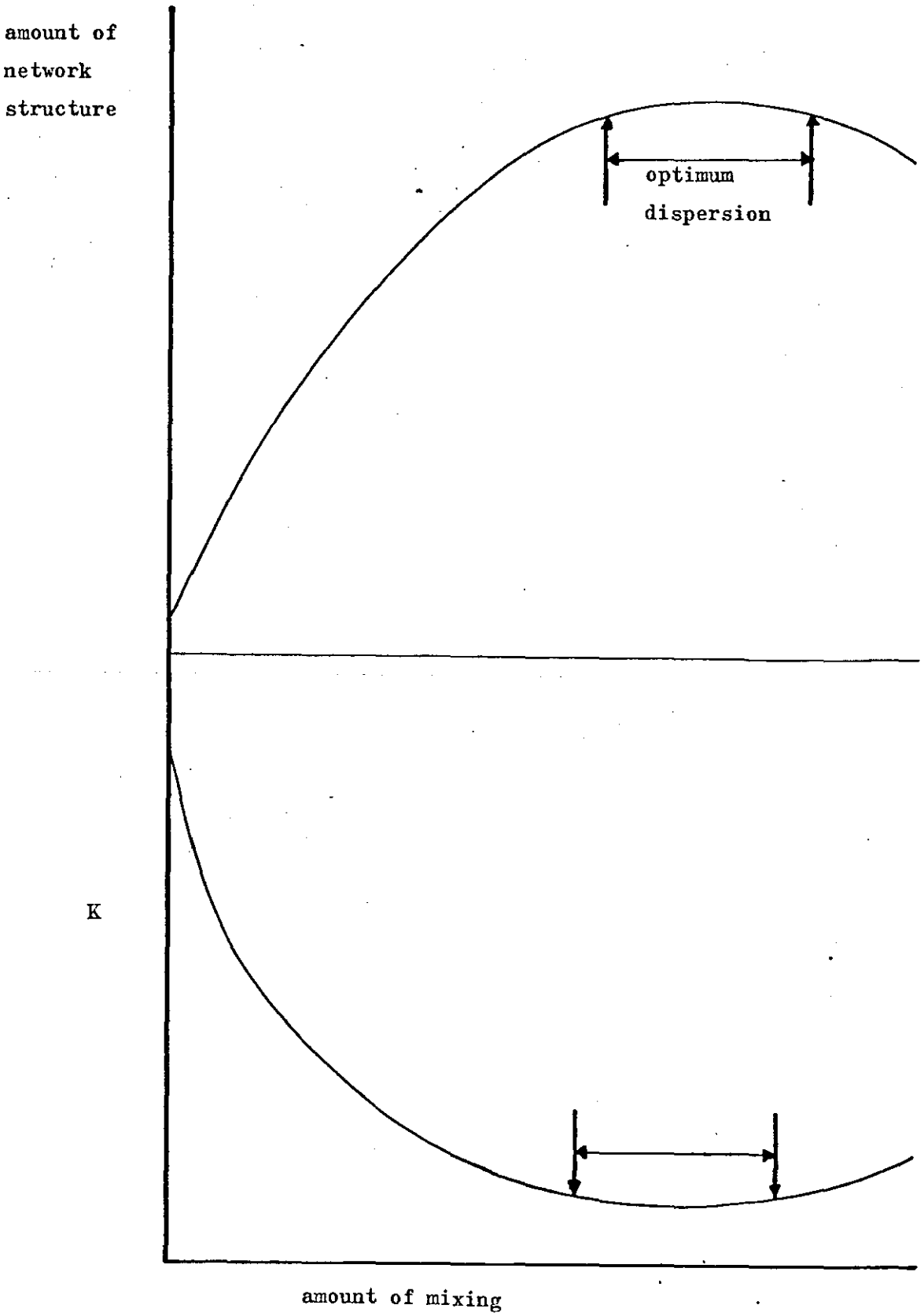

However, it must be noted that in this description of the effect of mixing on gel formation and the influence of the network structure on the conductivity, the assumption has been made that a gel system,and not a very viscous dispersion,is being examined. In the absence of rheological data on the system to demonstrate that the criteria used to define a gel are satisfied, the only other evidence that can be offered to support the argument is from visual observations and reported data on closely allied systems.

A vessel containing 6% M5 silica in 40% sulphuric acid may be upturned without detectable movement of the gel within a few hours of preparation. A small amount of agitation or stirring transforms the gel to a free-flowing liquid which will rapidly revert to a gel on standing. Such a gel was prepared and transferred to a measuring cylinder which was stoppered and left to stand. The gel was examined at regular intervals over 18 months for any signs of sedimentation, syneresis, or general loss of stability. A minute trace of liquid could be seen on top of the gel on a very few occasions. There were no other signs of change and at the end of this period the cylinder was upturned without any sign of movement of the gel.

The silica manufacturers, Cabot Carbon Ltd, report that the viscosity and thixotropic stability for a gel consisting of well dispersed silica of sufficient concentration will be quite stable for many months or years. They also give a plot of apparent viscosity versus pH for 5% M5 silica in water, the pH being adjusted with 1.0 M NaOH and 1.0 HCl solutions. Their results are reproduced in fig. 5.19 and show a maximum apparent viscosity at a pH of ~ 6.5.

Fig. 5.19 Apparent Viscosity vs pH for 5% M5 Silica in Water.

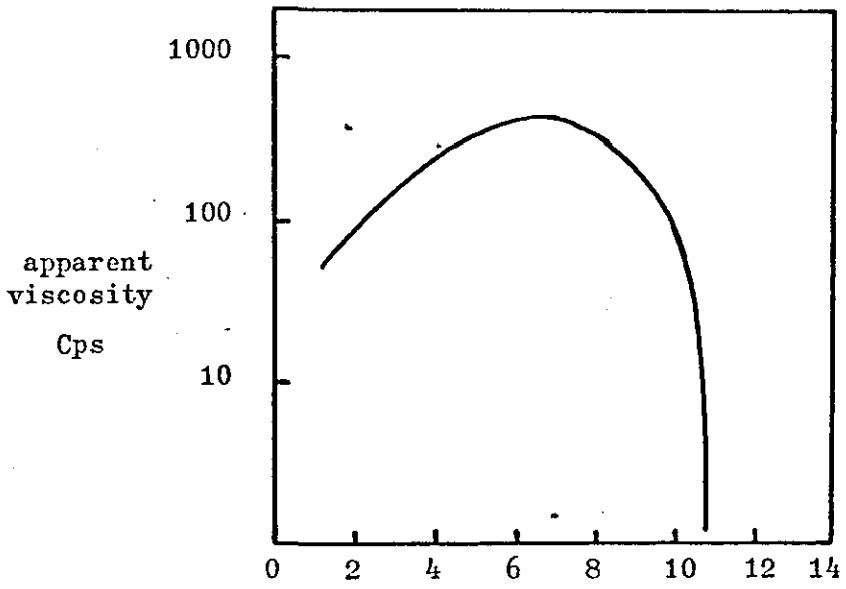

Fig. 5.20a Kinetic Deformation Curves for the aerosil/Sulphuric Acid System. 5% Silica/H_2SO_4 ρ = 1.280 g cm^{-3}.

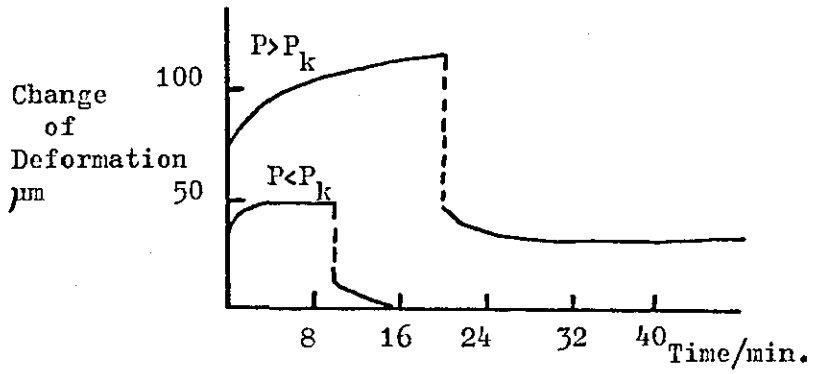

Fig. 5.20b Limiting Sheer Stress vs Time for the Aerosil/Sulphuric Acid System. 5% Silica/H_2SO_4 ρ = 1.280 g cm^{-3}.

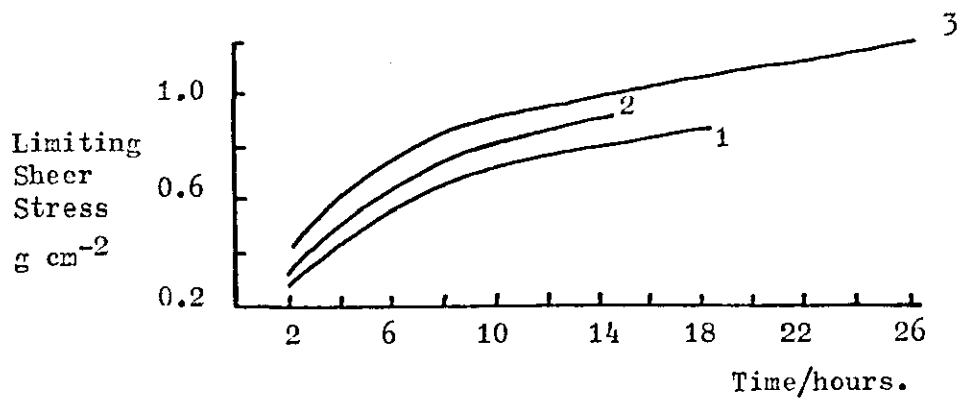

1,2, and 3 refer to the order of results, with mechanical dispersion between each measurement.

From experience in handling the silica-sulphuric acid gels, the pH of which will be below 1.5, a curve which decreased as the pH increased would have been expected because the gels become much less viscous as the acid concentration is reduced for a similar percentage of silica.

The rheological study of the aerosil-sulphuric acid system by Orkina and Aguf (1975) clearly shows the elastic properties of the gels. The curves of deformation versus time under a constant load are reproduced in fig. 5.20 (a) for two cases:

1. Shear stress (P) $>$ static yield point (P_k).
2. the reverse situation, $P_k > P$.

They also refer to a decrease in elasticity of the gels as the concentration of sulphuric acid is reduced for the same concentration of silica. This supports the view that the curve of apparent viscosity versus pH given in fig. 5.19 should change slope in the region below pH = 1.5.

The curve of limiting shear stress versus time, fig. 5.20 (b), shows the effect of successive redispersion of the silica, but unfortunately the method of dispersion is not given. The results imply that the method of dispersion being used was not as effective as that used in this work. However, the possibility that the standard method may have only produced an optimisation of the gel network for a particular size range of short chains or agglomerates of silica must not be ignored. A small change in the method such as varying the diameter of the holes in the plunger to produce more or less agitation during mixing may have produced an alteration in the size of the chains or aggregates which may have subsequently lead to another, but reproducible, gel structure.

The effect of dispersion on the degree of network formation and the rheological properties of silica-sulphuric acid gels is obviously worthy of further investigation. This aspect would have been examined at Loughborough had the financial resources been available to purchase rheological apparatus capable of withstanding attack by 40% sulphuric acid.

5.12. Conductivity of M5 Silica/40% H_2SO_4 Gels prepared by the Standard Method.

Having established the mixing technique for a 6% M5 silica/40% sulphuric acid gel, the effect of addition of silica on the ionic conductivity of 40% sulphuric acid was re-examined. A significant difference was observed in the conductivity behaviour of the gels compared to that of the previous measurements. A good linear plot of conductivity versus weight per cent silica was obtained for gels prepared from both M5 and EH5 silica in 40% sulphuric acid, as shown in figs. 5.21. and 5.22 respectively. This linear behaviour is expected from the simple volume fraction approach where the only contribution to the total conductivity is from the acid. The resultant loss in conductivity relative to that of the bulk electrolyte is given by equation 3.18:

$$K_g = K_a \phi_a = K_a (1-\phi_s).$$

Use of this equation to give a prediction of the gel conductivities gave a line $\sim 3\%$ above the experimental points. Although this approach is very much oversimplified it was expected to be more accurate than that for such low volume fractions of solid and high H^+ ion concentration. The effect of the increased tortuosity of the path length should be minimal and the values of surface conductivity commonly measured, e.g. by Kittaka and Morimoto (1976), are insignificant relative to the conductivity of the acid. Therefore the effect of gelling the acid electrolyte leads

NB. On the figures lines predicted by equation 3.18 are denoted by SVF., and the lines predicted by equation 3.25 are denoted by OBST.

Fig. 5. 21 Conductivity vs wt % Silica,
M5 Silica/40% H_2SO_4 in Cell II at 25°C

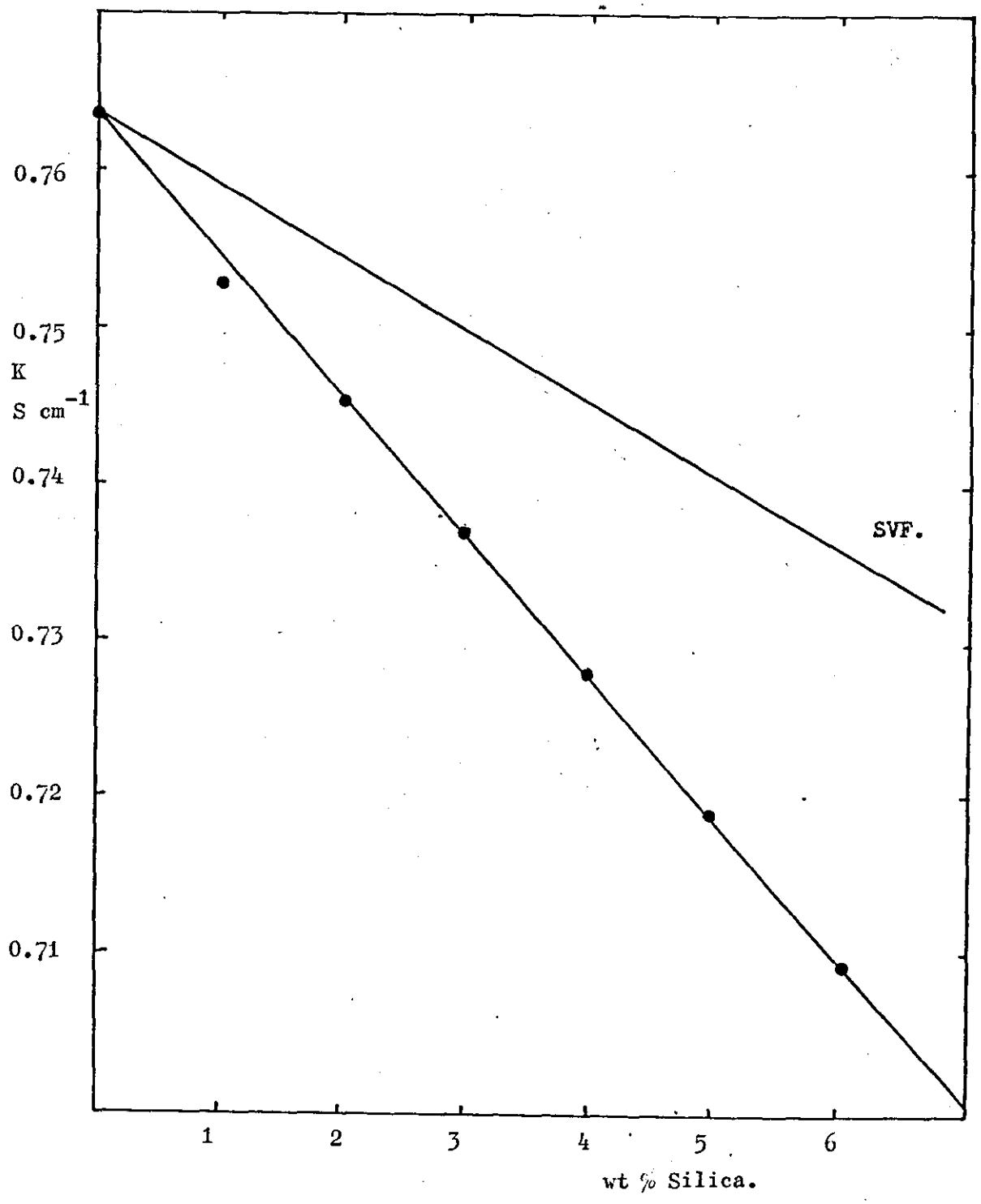

Fig. 5.22.

Conductivity vs wt % Silica,

EH5 silica/40% H_2SO_4 in cell II at 25°C.

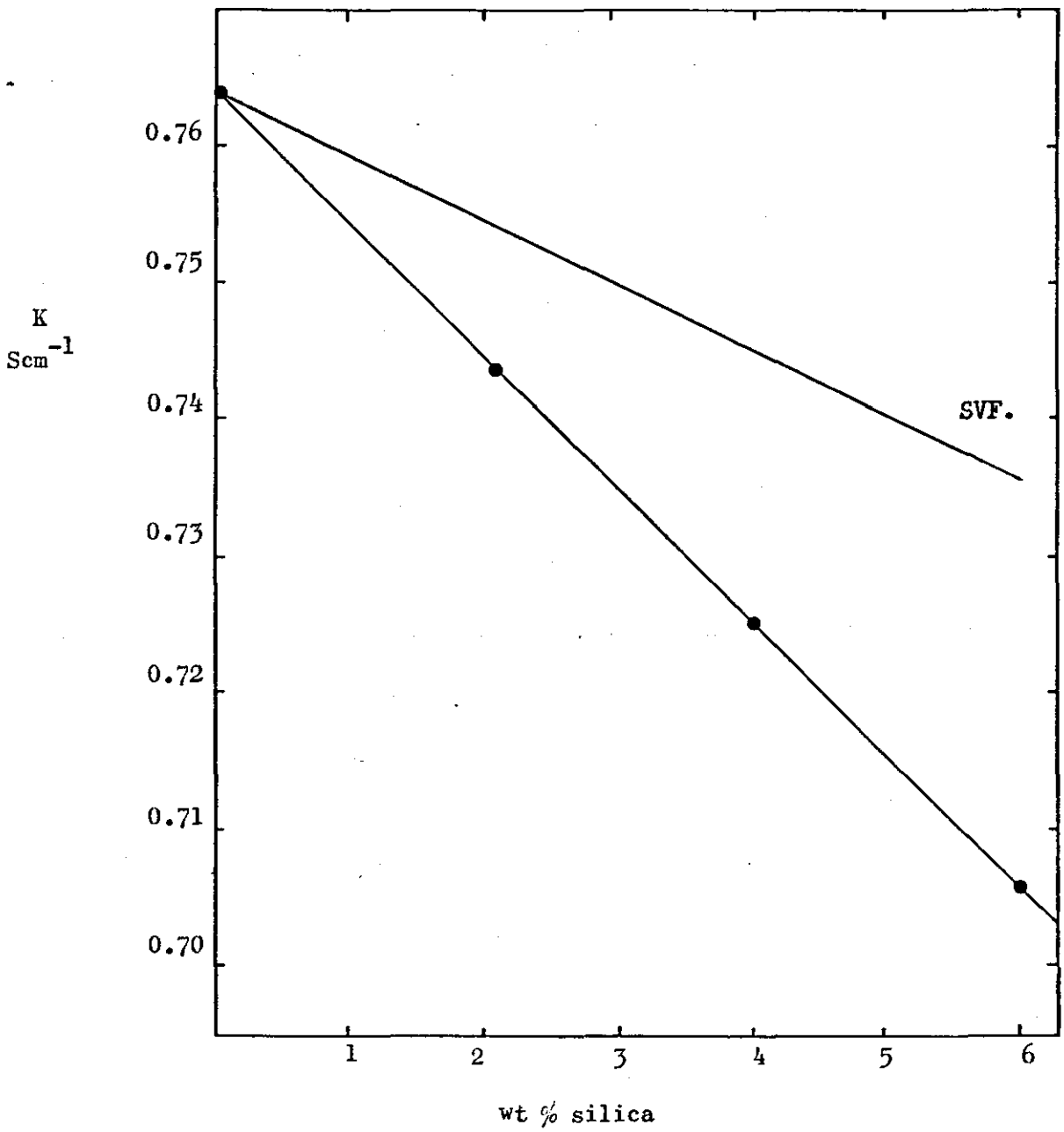

to a greater reduction in the conductivity than that expected from a simple viewpoint, and the more complex equations allowing for tortuosity or obstruction were applied.

The application of the simplified expression for the conductivity of gels derived for a low volume of solid causing the obstruction

$$K_g = (1 - 1.5\phi_s) K_a \qquad (3.25)$$

produced a line lying between the experimental and simple volume fraction lines as shown in fig. 5.23.

The more exact equations given earlier in table 3.4 produced the other lines shown in fig. 5.23, but none gave a satisfactory prediction of the gel conductivities.

Thus the theoretical approaches examined were unable to predict the effect of addition of silica on the conductivity of 40% sulphuric acid.

Although the experimental conductivities were reproducible, the experimental problems encountered in the preparation of gels and filling the conductance cells indicated that greater confidence in the results would be gained if acids of lower concentration was used. The lower acid viscosity should lead to gels of lower viscosity, and therefore dispersion of the silica would be easier and the cell filling problem eased, allowing an extension of the range of silica concentrations that could be examined.

5.13. Conductivity of Gels prepared from Sulphuric Acid of Lower Concentrations.

Linear plots of conductivity versus weight percent silica were obtained for 1.0 D, 0.1 D, and 0.01 D acid gels as shown in figs. 5.24, 5.25, and 5.26 respectively, with a similar negative deviation from the simple

Fig. 5. 23 Theoretical Predictions of the Conductivity of M5 Silica/40% H_2SO_4 Gels at 25°C.
1,2, and 3 from equations given in Table 3.4.
4, from the Simple Volume Fraction Approach Equation 3.18. (SVF.)
5, from the equation of Robinson and Stokes (1970).

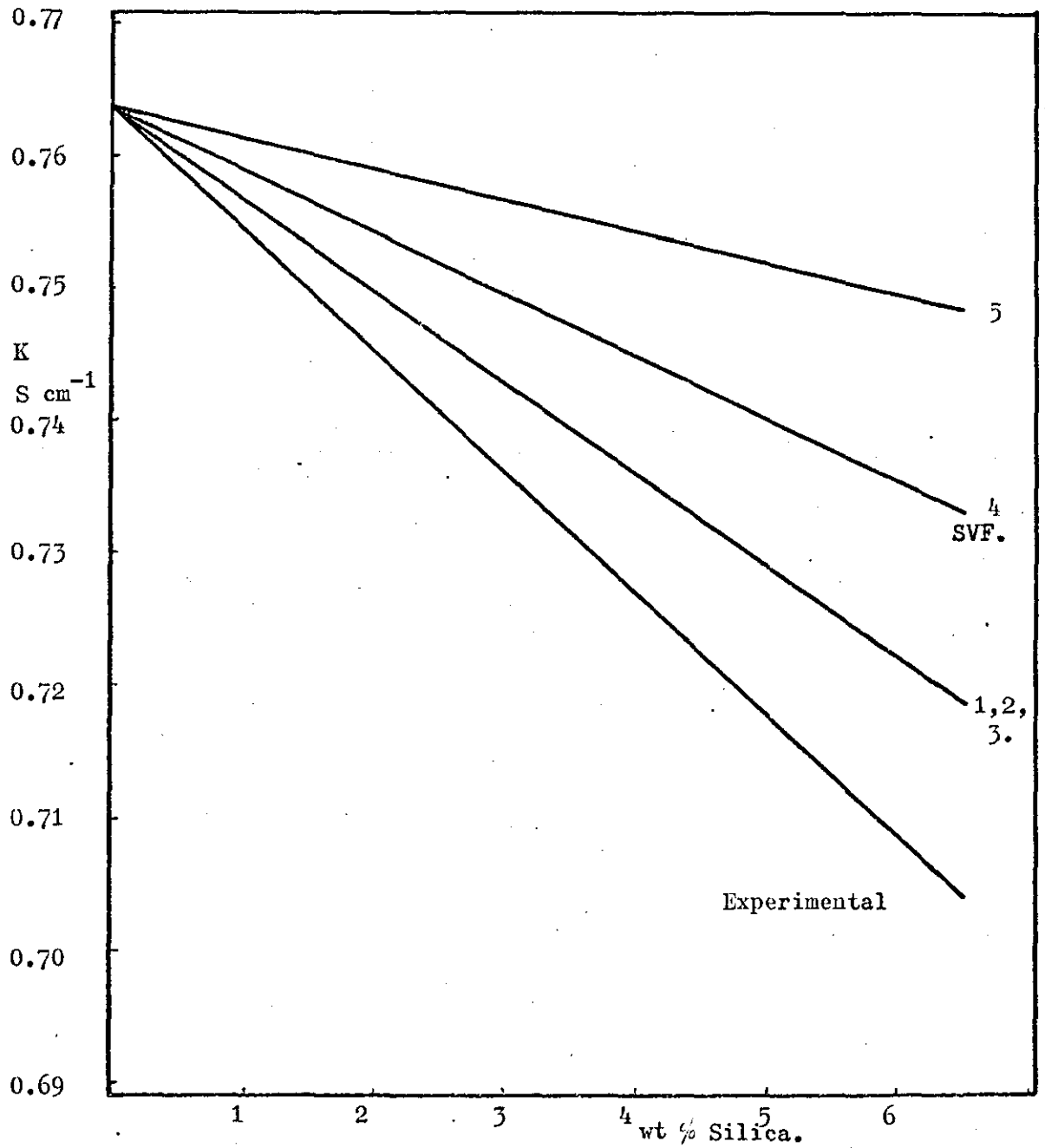

Fig. 5.24. Conductivity vs wt % silica,
M5 silica/1.0D H_2SO_4 in Cell II at 25°C

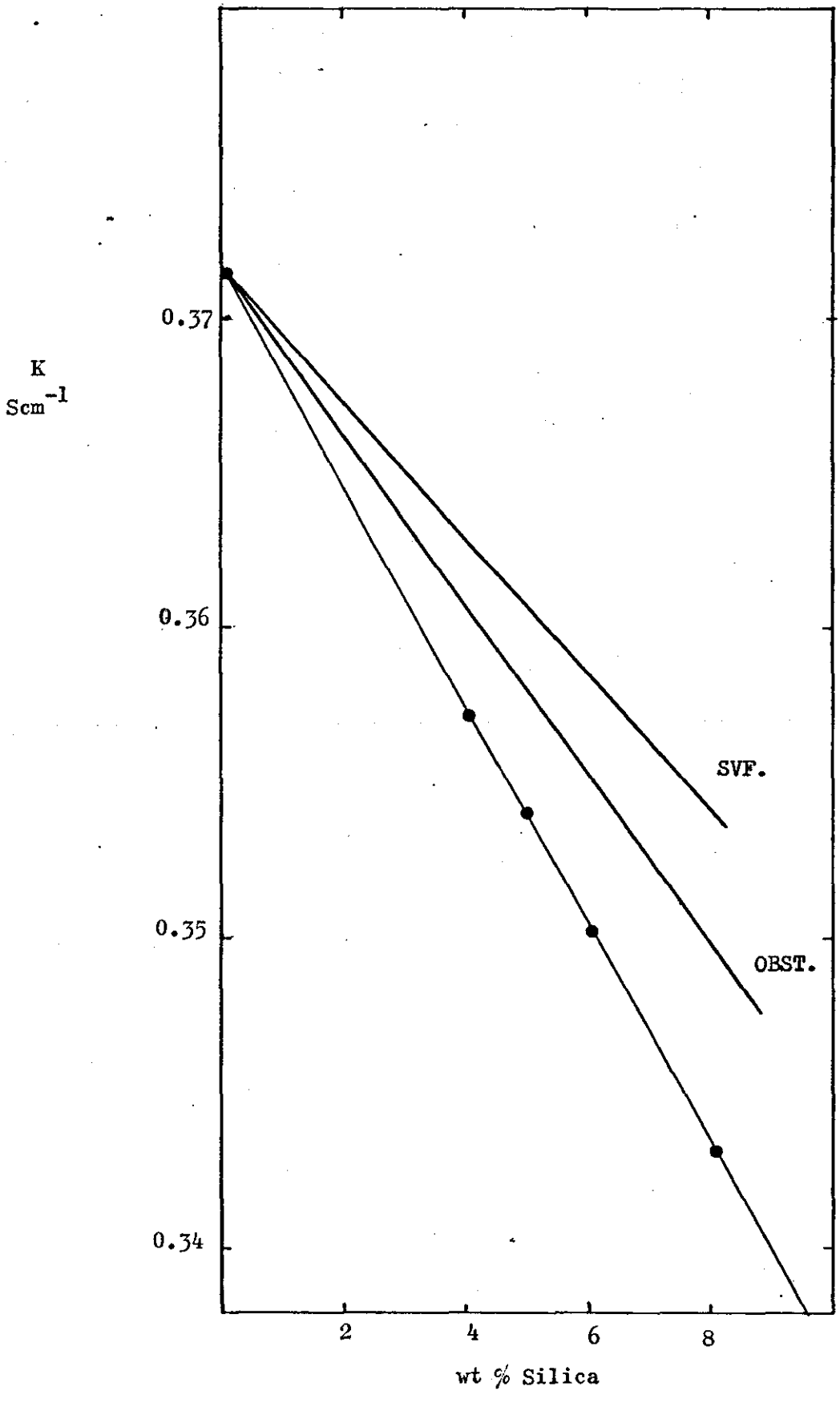

Fig. 5.25 Conductivity vs wt. % silica
M5 silica/0.1D H_2SO_4 in Cell II at 25°C

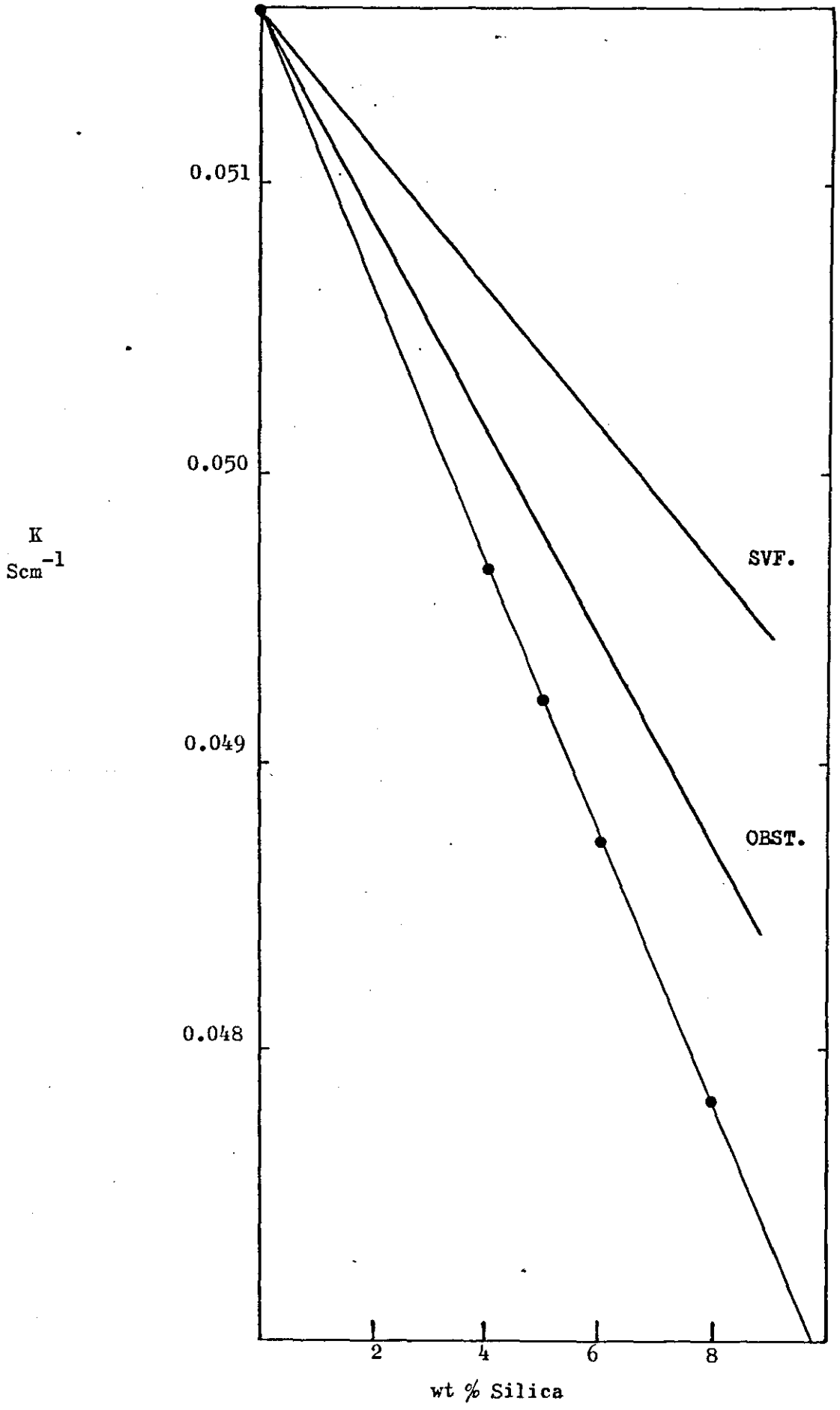

Fig. 5.26. Conductivity vs wt % silica
M5 silica/0.01D H_2SO_4 in Cell II at 25°C

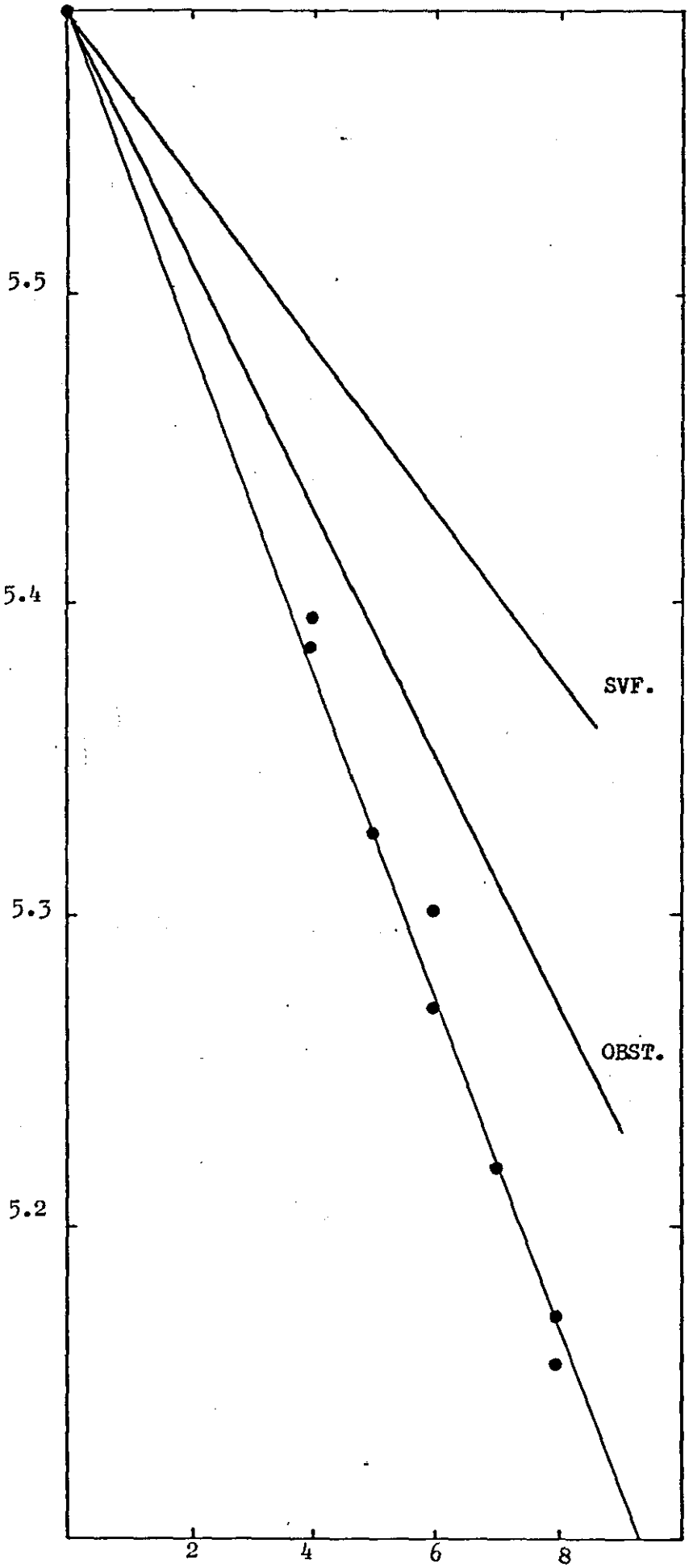

volume fraction theory line as before. However the behaviour observed for 0.001 D acid gels was completely different, the conductivity increased linearly from the value for the bulk acid as the silica content increased as shown in fig. 5.27. This last result is not totally unexpected in that for such a low acid concentration the possibility of surface conductivity along the silica agglomerates, short chains, or network structure becoming the major contributor to the overall conductivity of the gel is increasing.

The problem of the negative deviation from the simple volume fraction theory line remained and confidence increased in the conclusion that the gel structure has some significant effect on conductivity. In order to make a comparison of the experimental results a simple normalization of the conductivity was attempted. The bulk conductivity for each acid concentration was considered to be 100% conductivity, the gel conductivities were then expressed as a percentage of the bulk acid value, and plotted as a function of weight per cent silica as before. A consequence of this normalization was that if the gel structure was producing an effect of the same magnitude at each acid concentration, then all the lines would be of the same gradient, i.e. all the lines would be superimposed. As shown in fig. 5.28 this was not found to be the case.

It was realised during the calculation of normalized conductivities that for a given gel concentration in terms of weight per cent silica but different strengths of acid, the volume fraction was dependent on the density of the acid used. Thus wt % and volume fraction are directly proportional at one acid concentration, but it is invalid to compare gels of the same wt. % but different acid concentration.

Fig. 5.27 Conductivity vs wt. % Silica,
M5 silica/0.001D H_2SO_4 in Cell II at 25°C

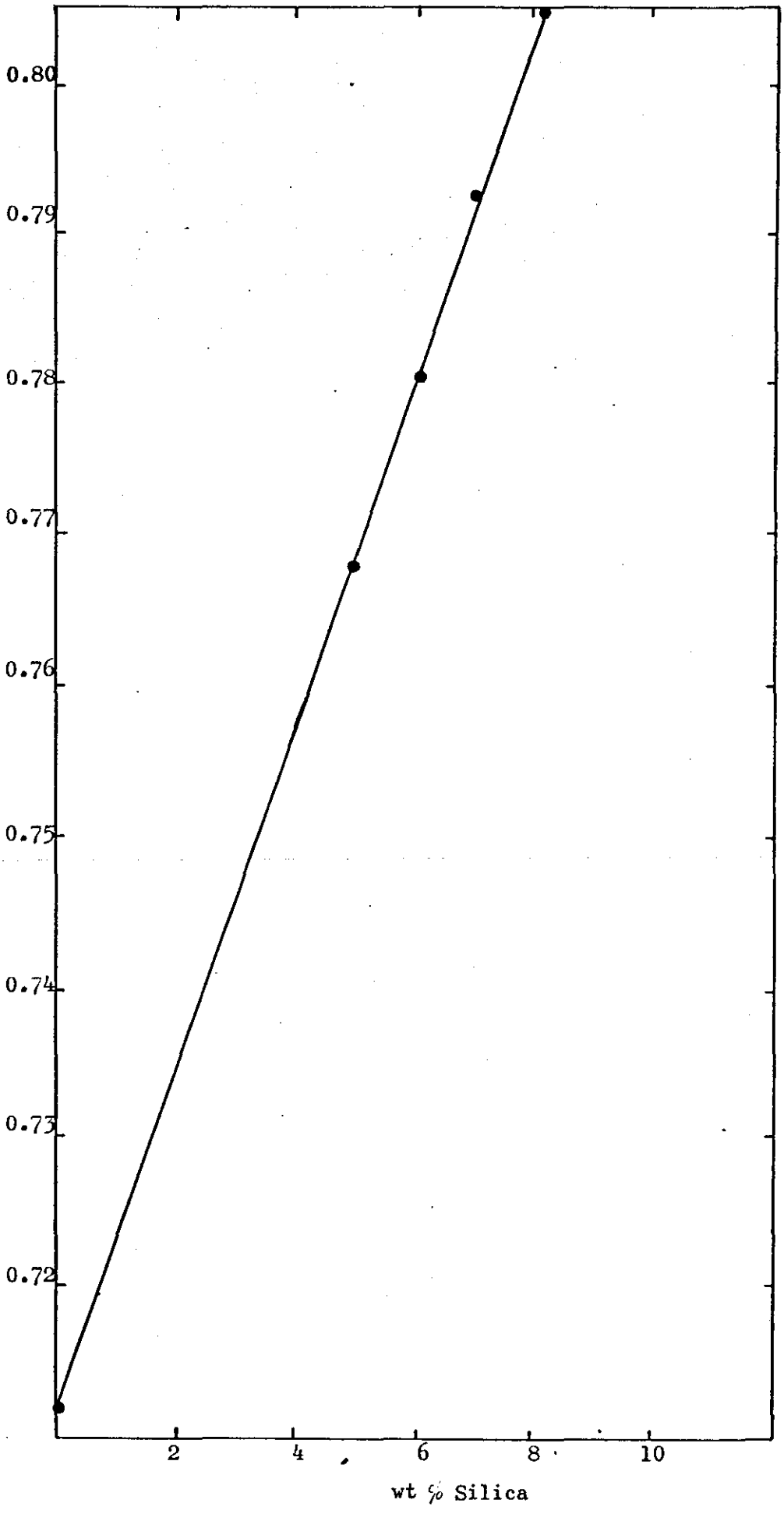

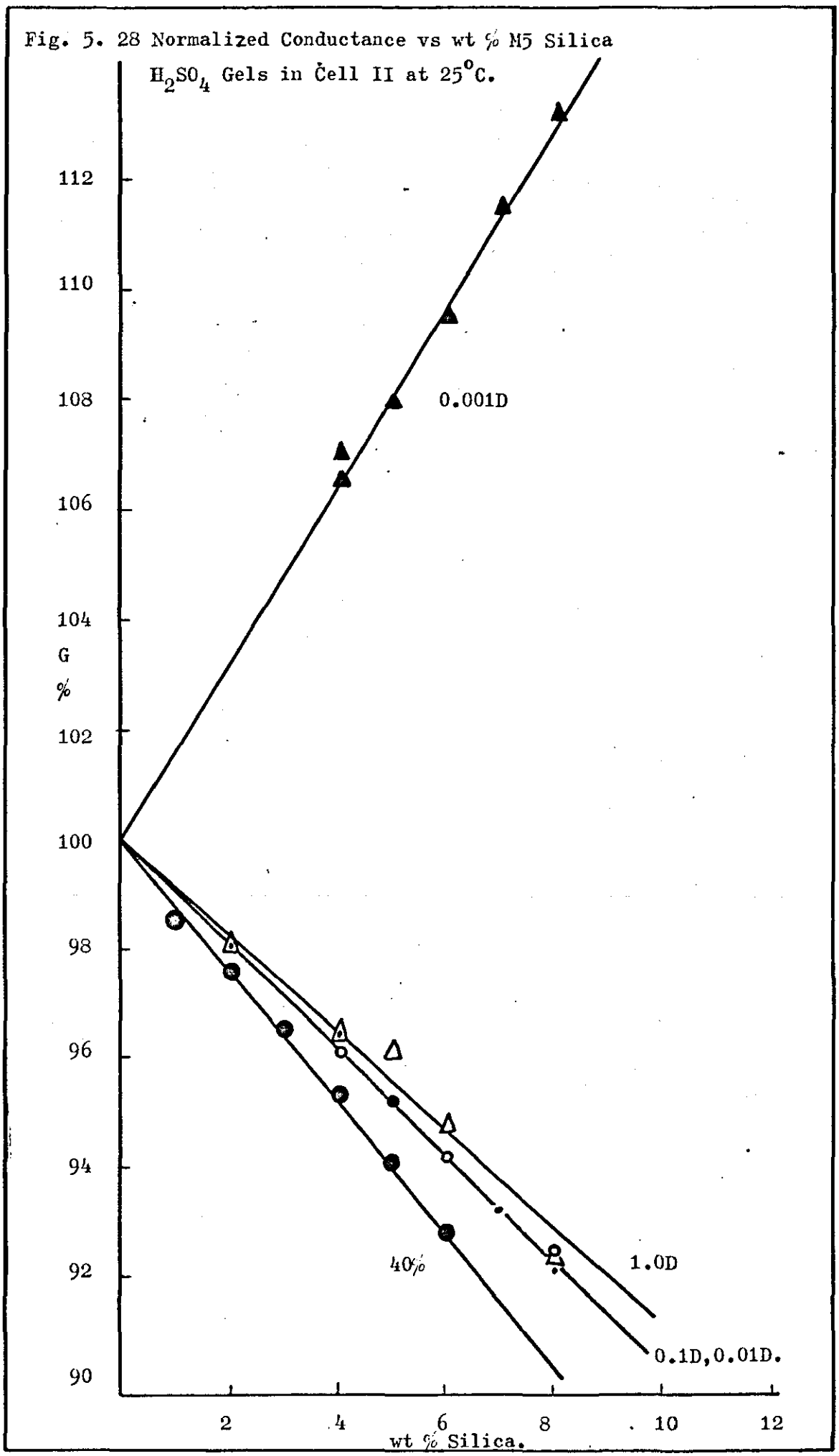
Fig. 5. 28 Normalized Conductance vs wt % M5 Silica
H_2SO_4 Gels in Cell II at 25°C.
112
110
108
106
104
G
%
102
100
98
96
94
92
90
0.001D
40%
1.0D
0.1D,0.01D.
2
4
6
8
10
12
wt % Silica.

The volume fraction of silica should be used for this purpose as the acid density is included in its evaluation.

The other terms in the expression are constant for a specified wt. % of silica. Using the relation:

mass = density x volume

ϕ_s can be expressed as :

$$\phi_s = (1 - \phi_a) = 1 - \frac{W_a/\rho_a}{W_a/\rho_a + W_s/\rho_s} \qquad 5.1.$$

Where ϕ_s = volume fraction of silica in the gel

ϕ_a = volume fraction of acid in the gel

W_a = weight of acid used to prepare the gel

W_s = weight of silica used to prepare the gel

ρ_a = density of acid used to prepare the gel

ρ_s = density of silica used to prepare the gel

Rearranging equation 5.1. to separate ϕ_a gives :

$$\phi_a = \frac{W_a/\rho_a}{W_a/\rho_a + W_s/\rho_s}$$

or

$$\frac{1}{\phi_a} = \frac{W_a/\rho_a + W_s/\rho_s}{W_a/\rho_a}$$

$$\frac{1}{\phi_a} = \frac{1 + W_s/\rho_s}{W_a/\rho_a}$$

which may be written as :

$$\frac{1}{\phi_a} = 1 + S\rho_a \qquad 5.2.$$

where $S = W_s/W_a\rho_s$. S is a constant for a given wt. % of silica in a gel.

Therefore, for a particular concentration of silica, a plot of $1/\phi_a$ versus ρ_a gives a slope of gradient S and intercept 1. Such a plot for a 6% gel is given fig. 5.29. The change in volume fraction of the silica caused by the change in acid density for a 6% gel in a. 1.0 % H_2SO_4 and b. 45% H_2SO_4 is:

$$\phi_s = (0.0376 - 0.0283) = -0.0093.$$

This must be compared to the change in volume fraction of silica of 0.03 for a change of 0% to 6% silica at one acid concentration. The difference between using wt. % and volume fraction for the normalized plots of fig. 5.28 is insufficient to explain the variation in slope as the acid concentration is decreased.

The other interesting feature of the normalized plots is that the order of the lines of decreasing gradient does not follow the order of increasingly dilute acid concentrations, a further indication that gel structure has a definite effect on the conductivity of acid electrolytes.

5.14. Density Measurements.

In the calculation of the volume fraction of silica in the gels, the only parameter which had not been determined experimentally in this laboratory was the density of the silica. The weights of acid and silica W_a and W_s were those used in preparing the gel and the acid density had been determined. Although the density of the silica is a constant, any error in the value of 2.2 given by the Manufacturers would affect the volume fraction significantly and hence the predicted conductivities.

Fig. 5.29. $1/\phi_a$ vs ϱ_a for a 6% M5 Silica/40% Sulphuric Acid Gel at 25°C.

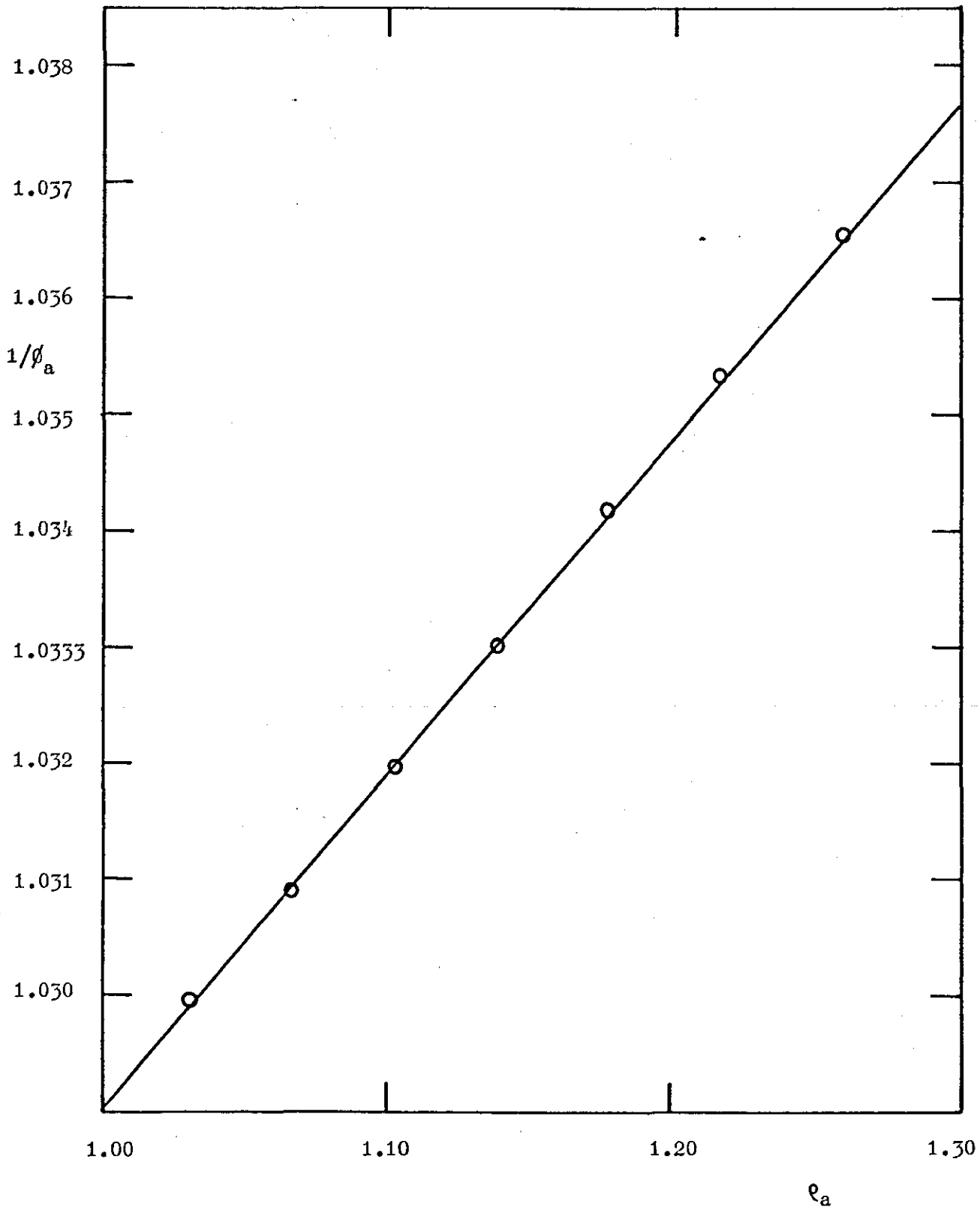

A determination of the density of silica using the method for an inert solid in a liquid in which it does not dissolve produced some very interesting results. The density of silica for a specific acid concentration and weight of silica was constant, but varied depending on the weight of silica for a given acid concentration, or varied with the acid concentration for a given weight of silica. The results are summarised in Table 5.4.

However, for methanol the density of silica was found to be 2.20 regardless of the weight of silica used. There were several possible explanations of this behaviour, the most likely being that the silica in the acid was retaining trapped air, but the air was being expelled during the methanol measurements. Attempts at removing any trapped air by subjecting the gel to ultrasonics had no effect on the spread of results in acid media.

Another possibility for the variation in the density of the silica in the acid was that the dispersion and/or size of the silica aggregates varied with acid concentration, or alternatively as the acid concentration decreased the degree of wetting of the silica aggregates altered.

The results of the density measurements provided the clue to a method of predicting gel conductivities which is described in section 5.17.

5.15. Conductivity of Gels prepared from Sulphuric Acid at other Temperatures.

The results of the conductivity measurements at 25°C on the sulphuric acid gels and the potassium chloride gels described later seemed consistent,

Table 5.4

Density of Silica Determined by Measurements in Several Liquids.

Liquid	Amount of Silica	Average Silica Density(calculated)
40% H_2SO_4	4%	1.810
40% H_2SO_4	2%	1.795
2% H_2SO_4	4%	1.590
40% H_2SO_4	* 0.5 g	1.756
Methanol	* 0.5 g	2.199

* NB. 0.5 g of silica in density bottle followed by sufficient liquid to fill bottle.

the experimental plots of the conductivity versus weight percent silica lying below the various predicted lines, apart from the 0.001D H_2SO_4 and 0.01D KCl gels where surface conductivity was predominant and the sign of the gradient of the lines had changed. It was therefore decided to investigate the behaviour of the two types of gels at other temperatures, namely 50°C, 5°C and -55°C, chosen because the working temperature range of the capacitors required in industry is 125 to -55°C. 50°C and 5°C were the limits of temperature available with the oil bath.

The thermostatted tank was shown to be operating at 50.00°C with a temperature control of $\pm$ 0.002°C or better within the cell indicated by a sample of 40% H_2SO_4 in conductance cell II, there being no detectable change in conductivity with time after the 30 minute equilibration time.

A range of acid gels were examined using cell I_r and cell II, and the pattern of conductivity results observed mirrored those obtained at 25°C. Linear plots of measured conductance versus weight per cent silica lying below the predicted line were obtained for gels prepared from 40% (~5D), 1.0D, 0.1D and 0.01D sulphuric acid/EH5 silica as shown in figs.5.30, 5.31, 5.32 and 5.33 respectively.

The 0.001D H_2SO_4/EH5 silica gels gave conductances which increased with increasing silica-content as shown in fig. 5.34, which is considered to be due to surface conductance at the silica/solution interface. Note the use of measured conductances (G) instead of conductivity (K) to avoid the uncertainty involved in determining cell constants at 50°C as outlined in Chapter 3.

The overall stability of the gels at 50°C was not so good. There was a tendency for the conductances to fall very slowly with time after

Fig. 5.30 Conductance vs wt % Silica,
EH5 Silica/40% H_2SO_4 in Cell 11 at 50°C

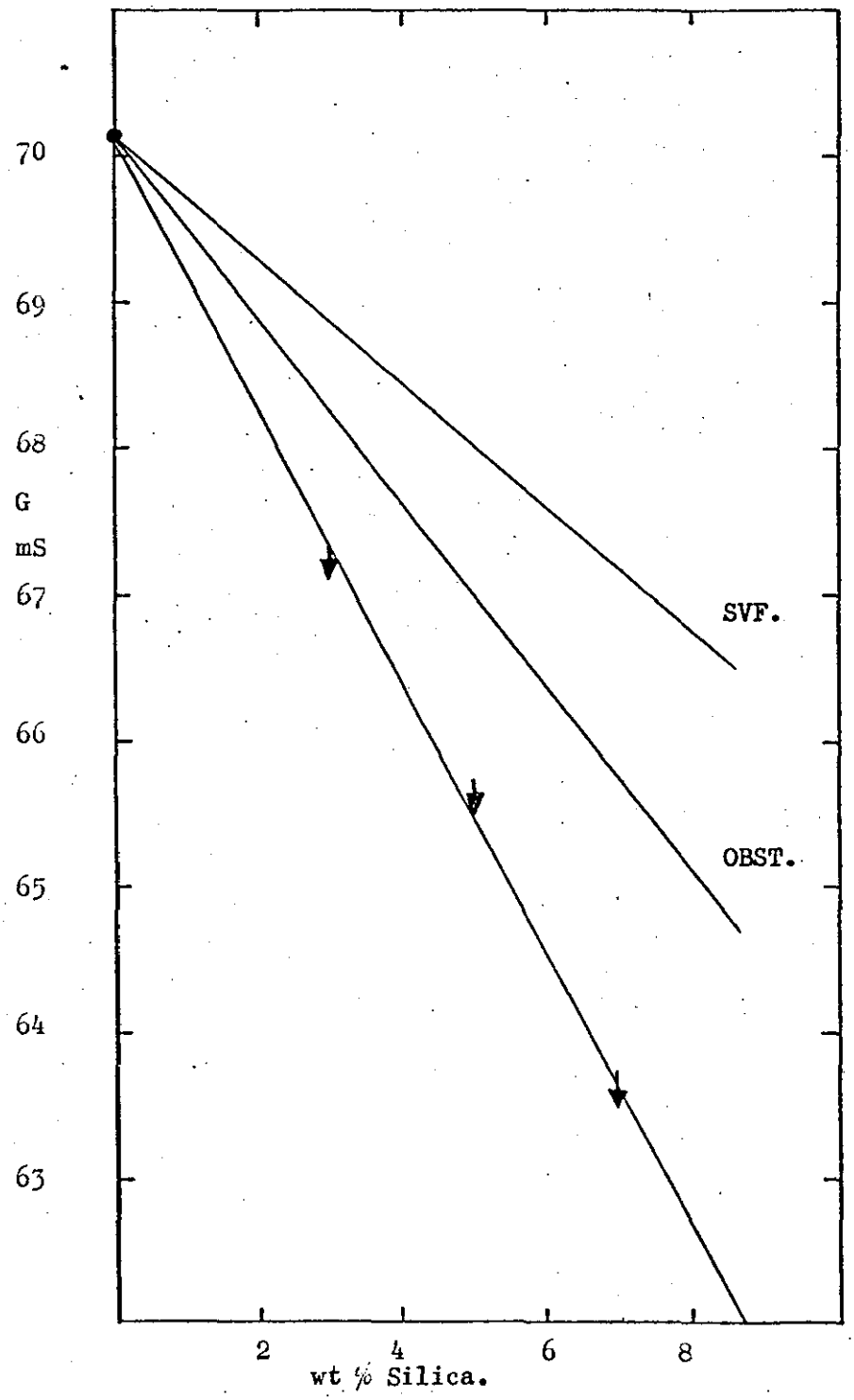

Fig. 5.31 Conductance v's wt % Silica,
EH5 Silica/1.0D H_2SO_4 in Cell II at 50°C.

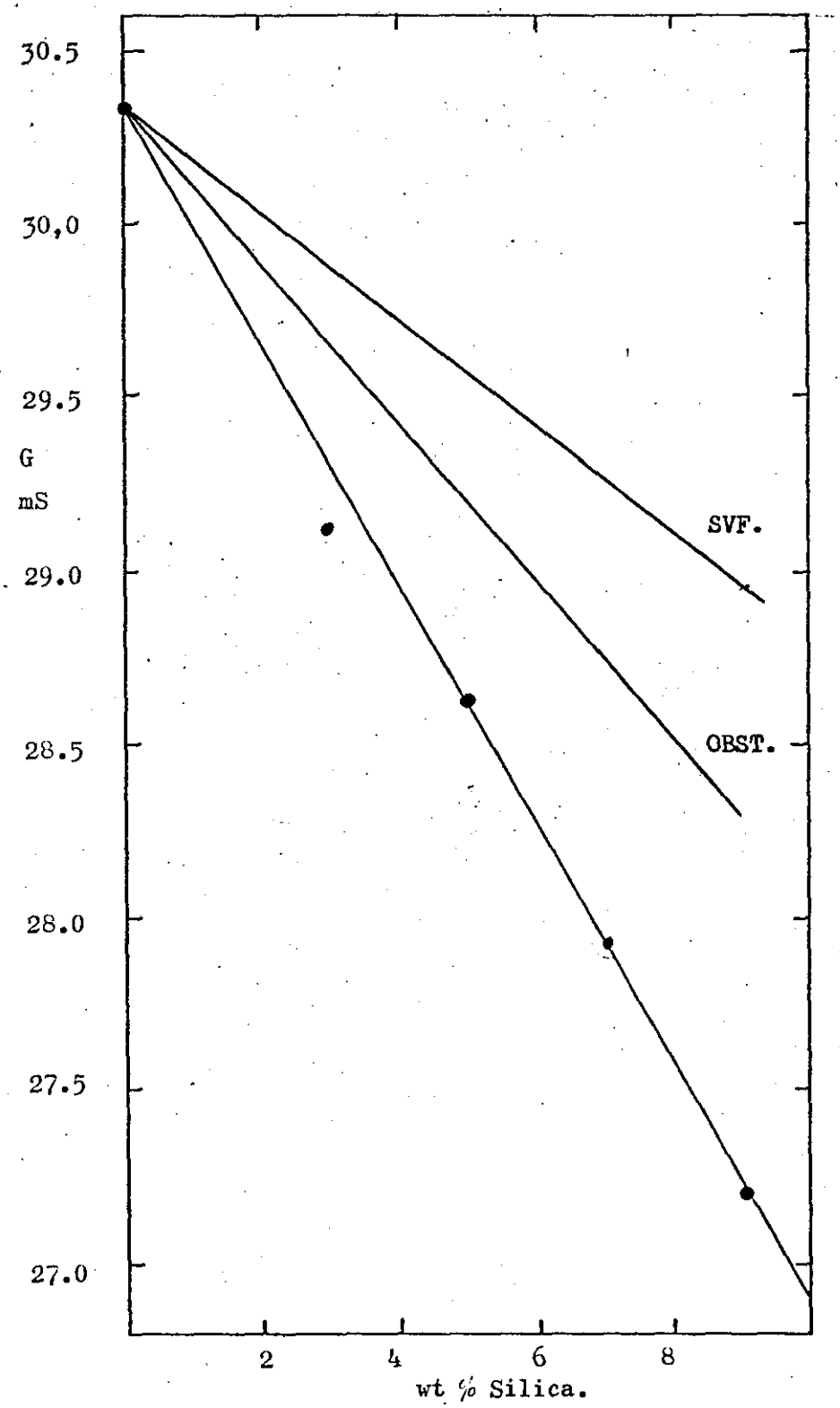

Fig. 5.32a Conductance vs wt% Silica,
EH5 Silica/0.1D H_2SO_4 in Cell II at 50°C.

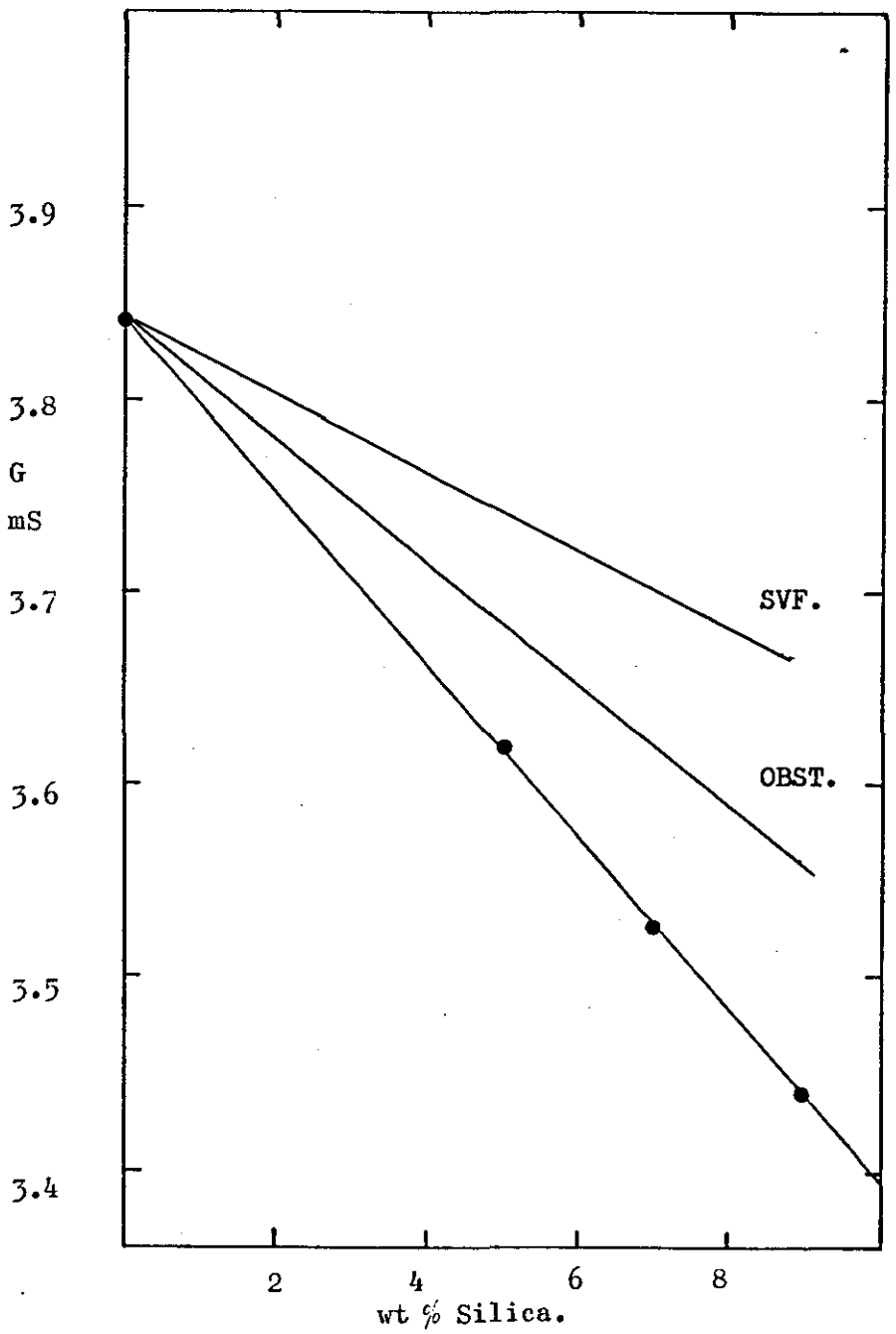

Fig. 5.32b Conductance vs wt % Silica,

EH5 Silica/0.1D H_2SO_4 in Cell I_r at 50°C.

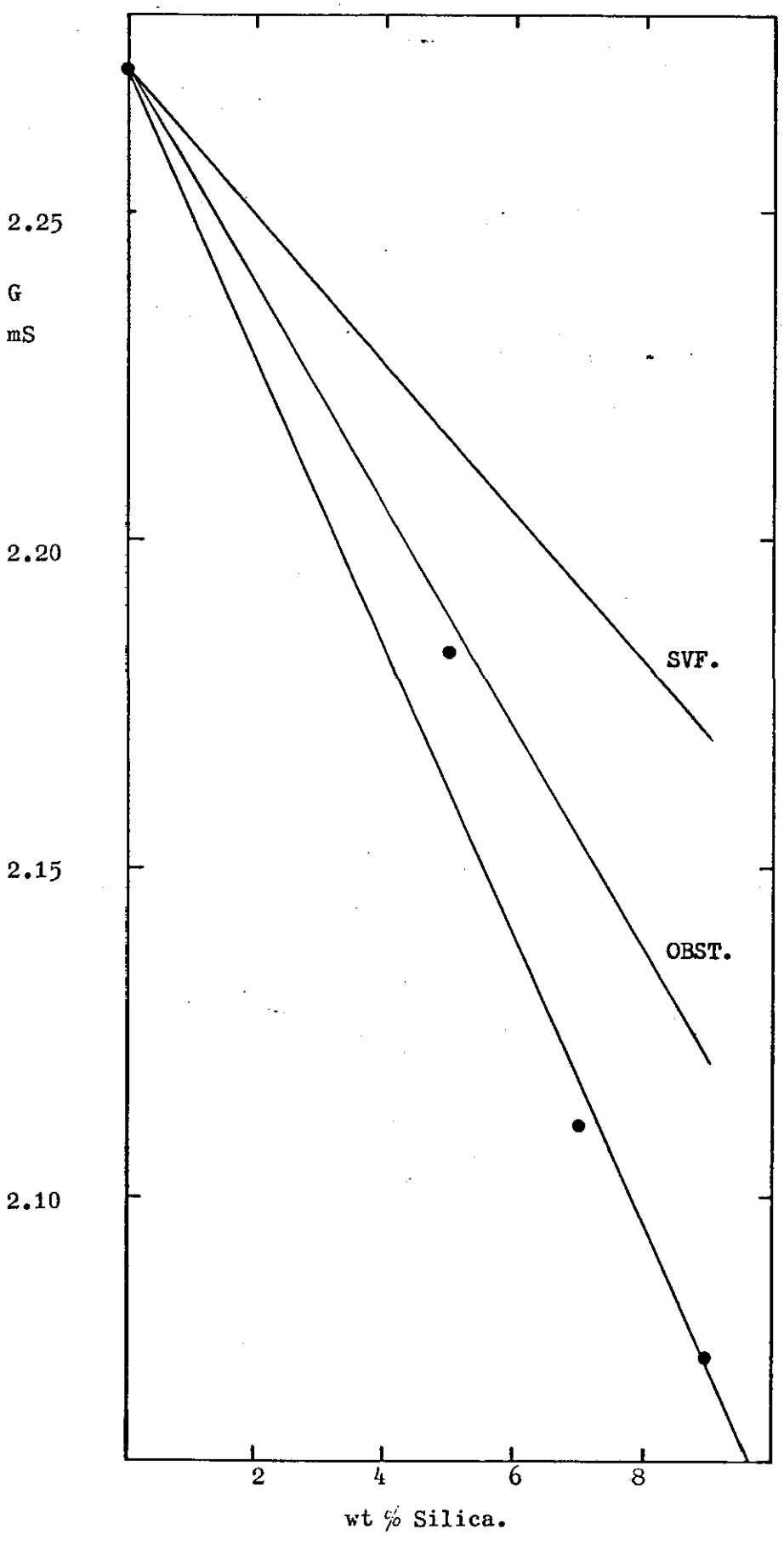

Fig. 5. 33a Conductance vs wt % Silica,
EH5 Silica/0.01D H_2SO_4 in Cell II at 50°C.

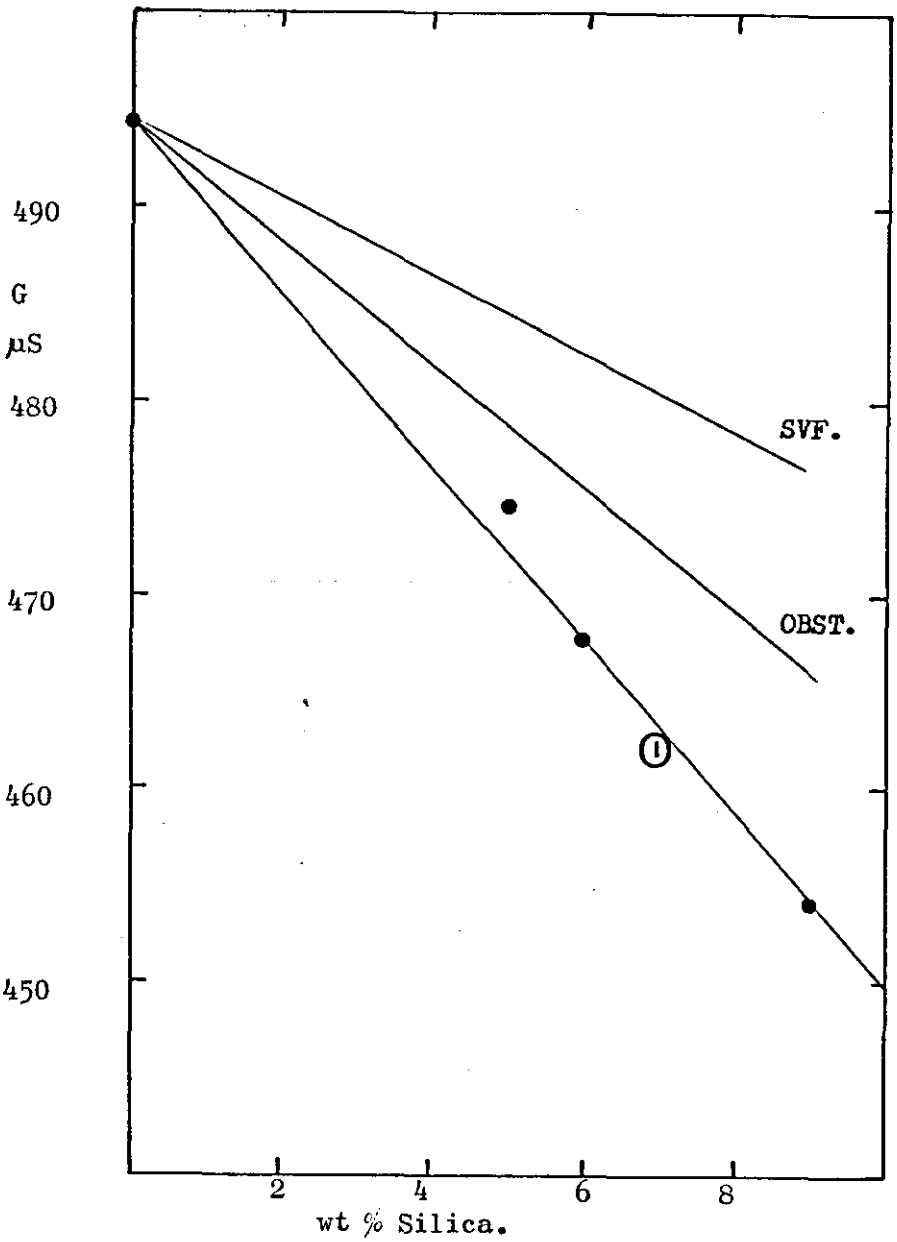

Fig 5.33b Conductance vs wt % Silica,
EH5 Silica/0.01D H_2SO_4 in Cell I_r at 50°C.

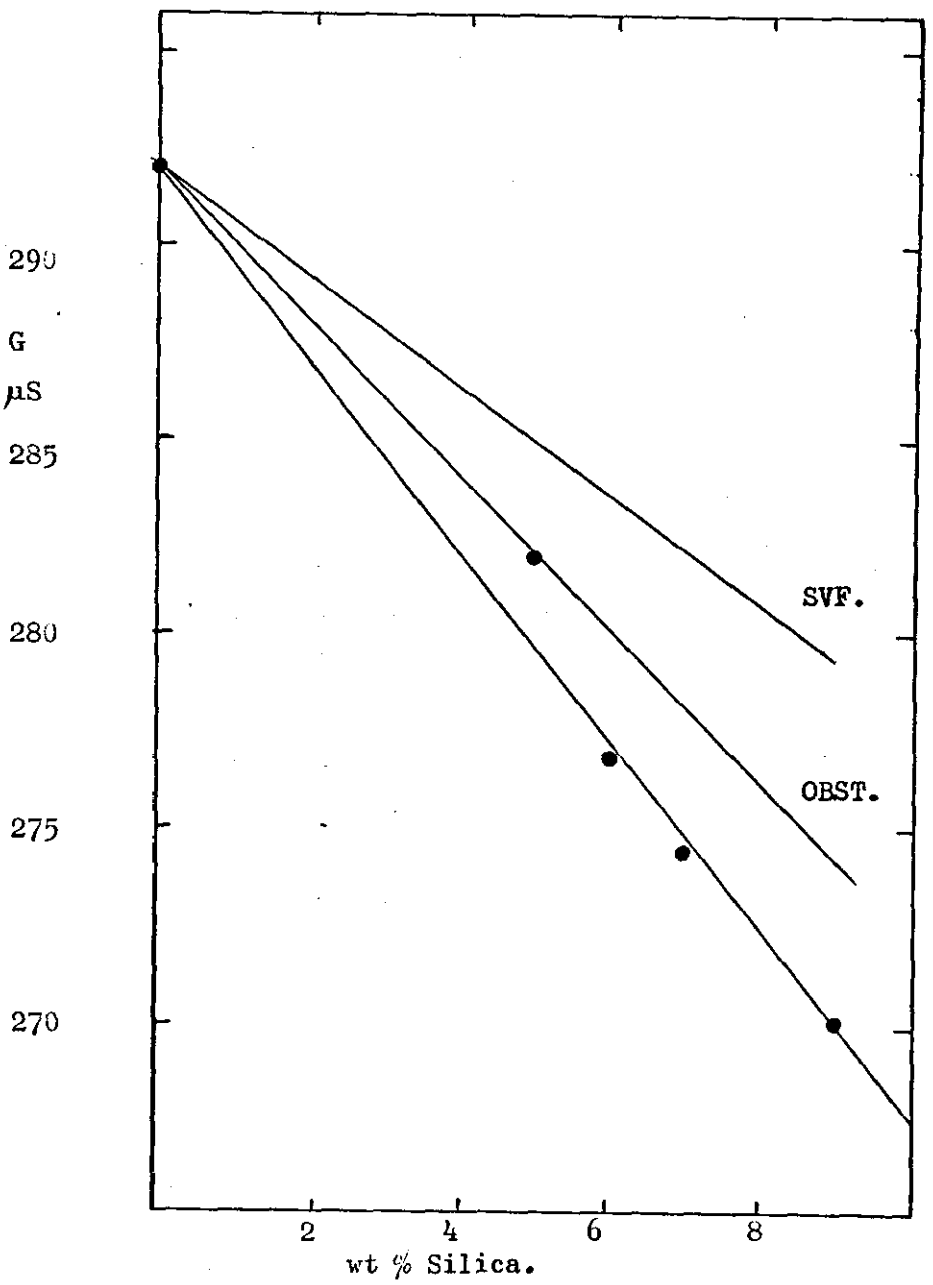

Fig. 5.34a Conductance vs wt % Silica,

EH5 Silica/0.001D H_2SO_4 in Cell II at 50°C.

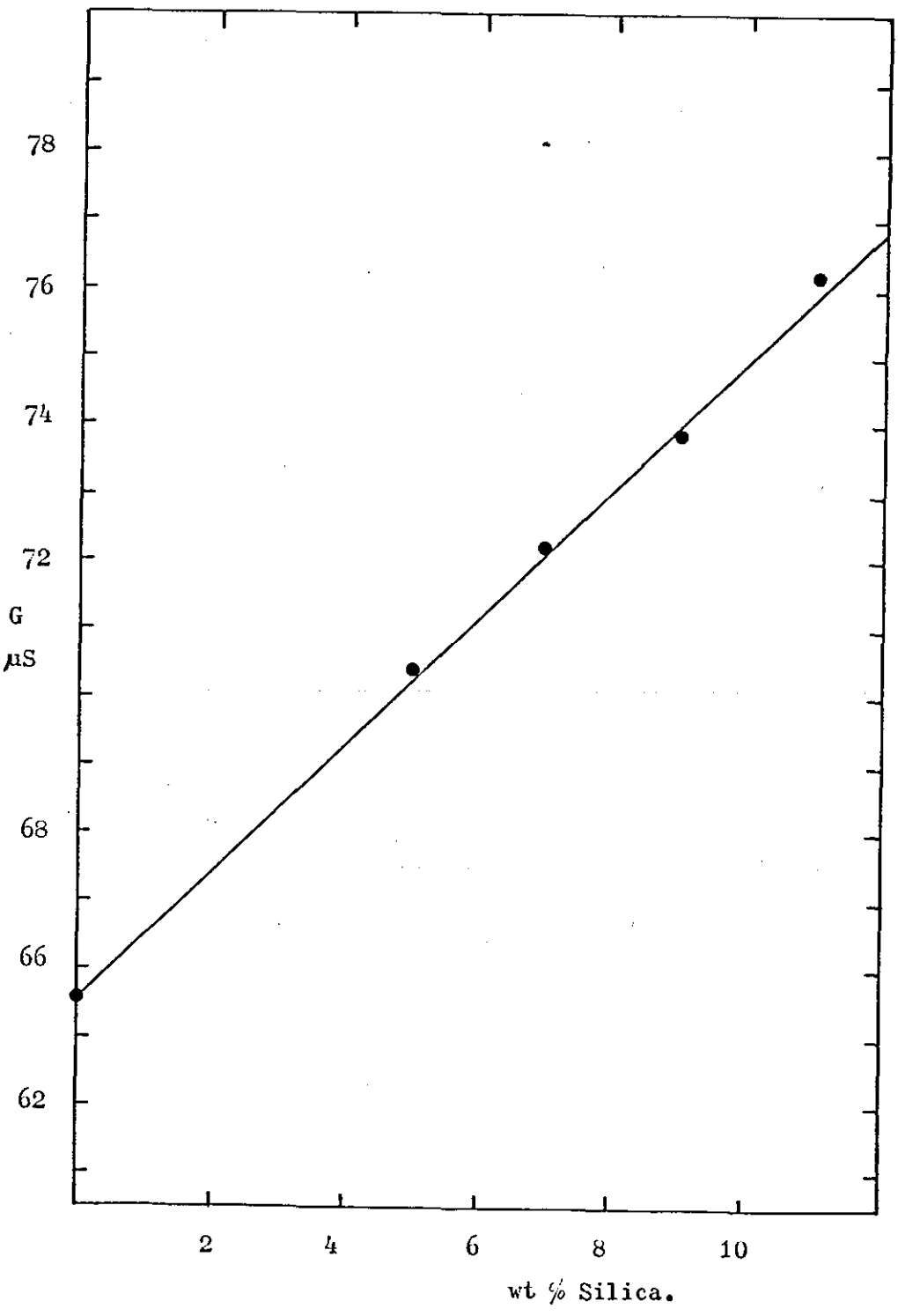

Fig. 5.34b Conductance vs wt % Silica,
EH5 Silica/0.001D H_2SO_4 in Cell I_r at 50°C.

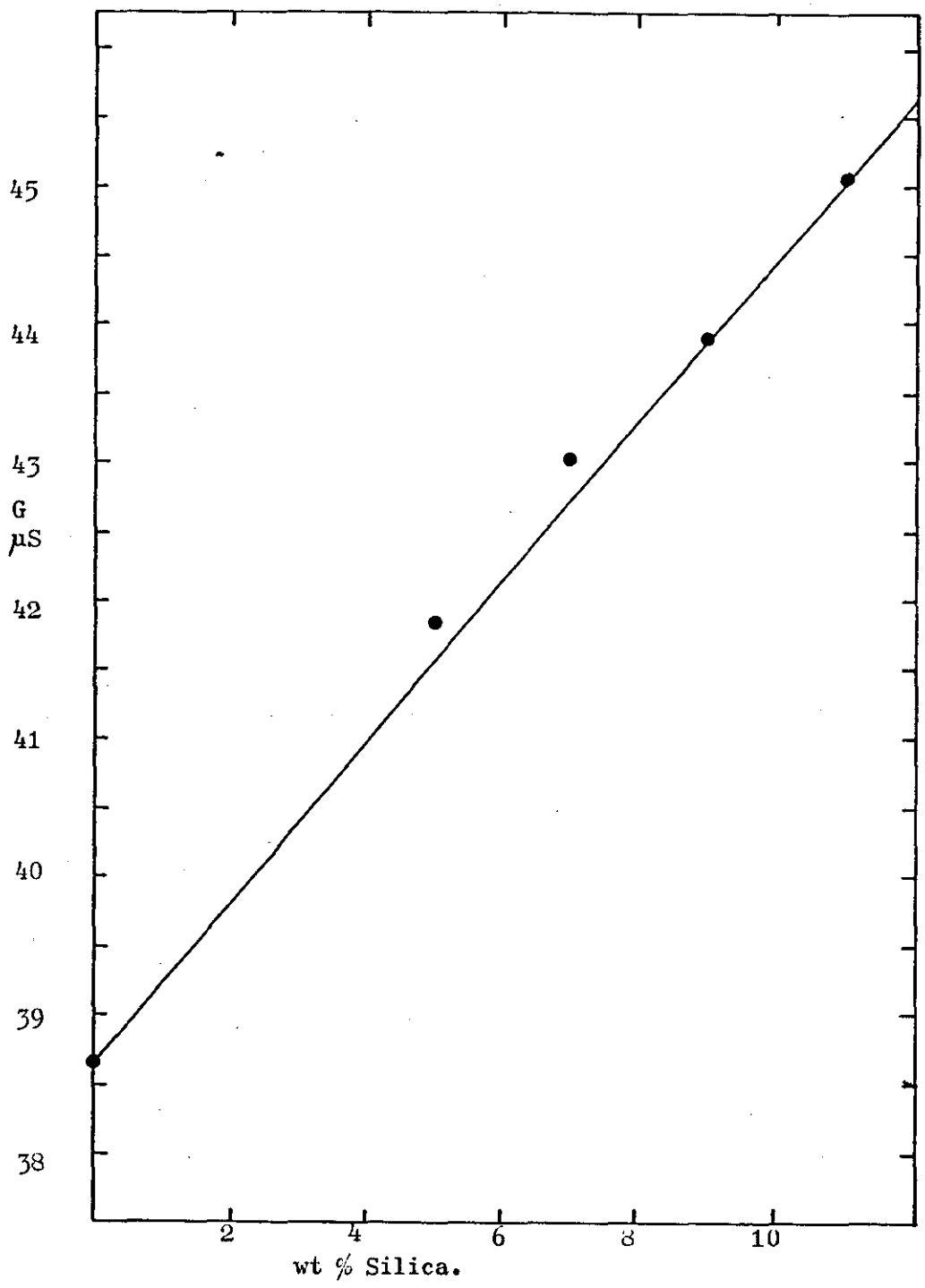

about 2 hours at 50°C. A slight settling could be detected at the gel meniscus in the filling arms of the cell (though not in the main part of the cell). The conductances were subject to a greater scatter than those for the 25°C measurements and the overall reproducibility of results was not as good. The most likely reason for this instability is the expulsion of dissolved air trapped within the silica and/or acid causing stress within the gel structure and changes in the network.

The most obvious difference between the 50° and 25° measurements was that the gradient of the conductance versus wt % silica had changed, and is shown more clearly by the normalized plots of conductivity versus weight per cent silica given in fig. 5.35. In fact the order of decreasing negative gradient at 50°C was 40%, (0.1D, 1.0D) 0.01D with 0.001 D giving a positive slope.

The lowest temperature that the oil bath could maintain with adequate control and without major alteration was 5°C, shown as before by the constant conductivity of 40% sulphuric acid in cell II.

The stability of gels at 5°C was much better than at 50°C and a greater reproducibility in the conductances of gels was observed. Only acid gels were examined at this temperature and very similar results compared to those observed at the other temperatures were obtained, i.e. good straight line plots of conductance versus wt. % silica lying below the lines predicted by the simple volume fraction theory were obtained for 40% (~5D), 1.0D, 0.1D and 0.01D sulphuric acid gels as shown in figs. 5.36, 5.37, 5.38 and 5.39. respectively.

The 0.001D acid gels differed from the previously observed behaviour in that they did not show a positive slope indicative

Fig. 5.35.

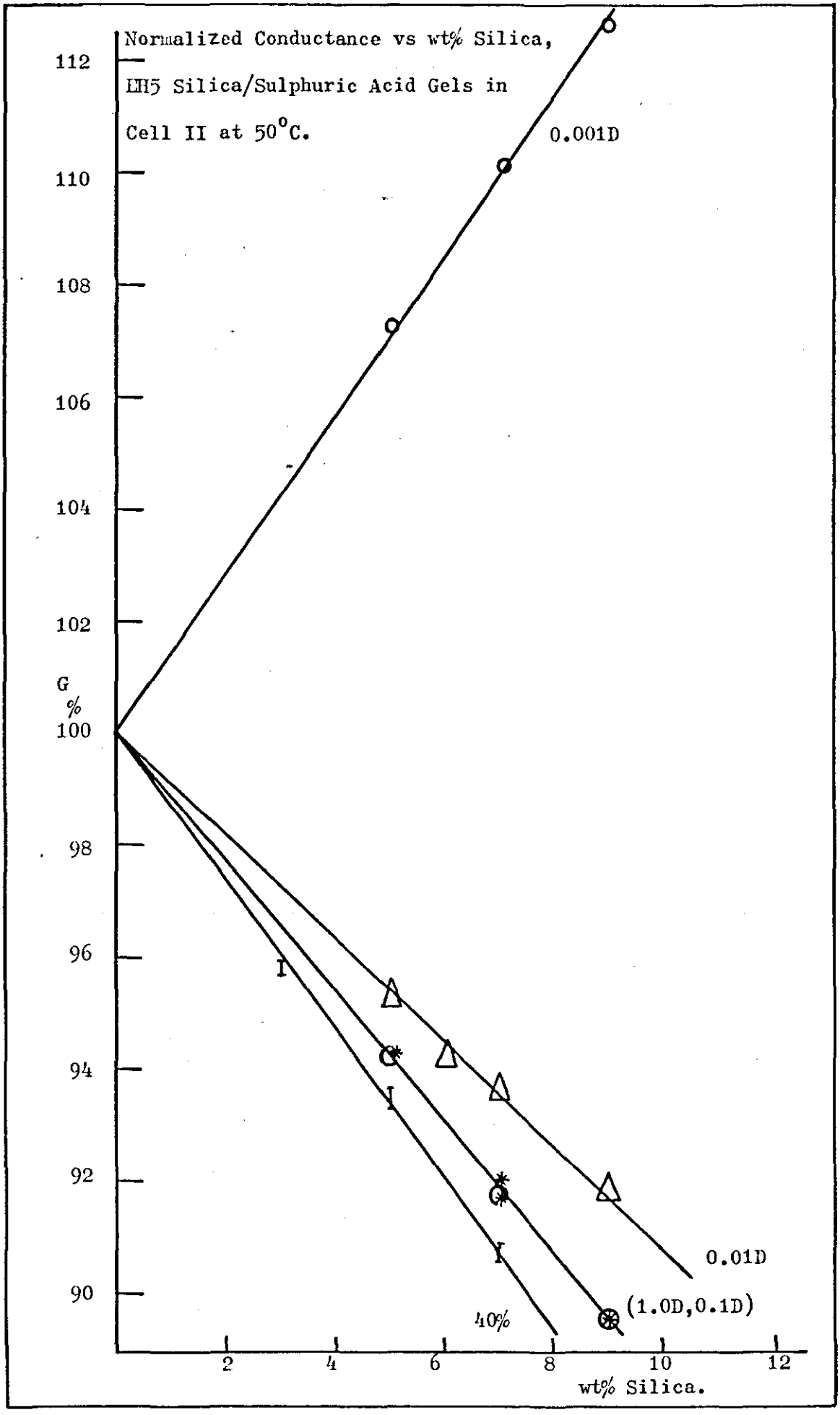
Normalized Conductance vs wt% Silica,
LH5 Silica/Sulphuric Acid Gels in
Cell II at 50°C.
0.001D
0.01D
(1.0D,0.1D)
40%
G %
112
110
108
106
104
102
100
98
96
94
92
90
2
4
6
8
10
12
wt% Silica.

Fig. 5 36a Conductance vs wt % Silica,
M5 Silica/40% H_2SO_4 in Cell II at 5°C.

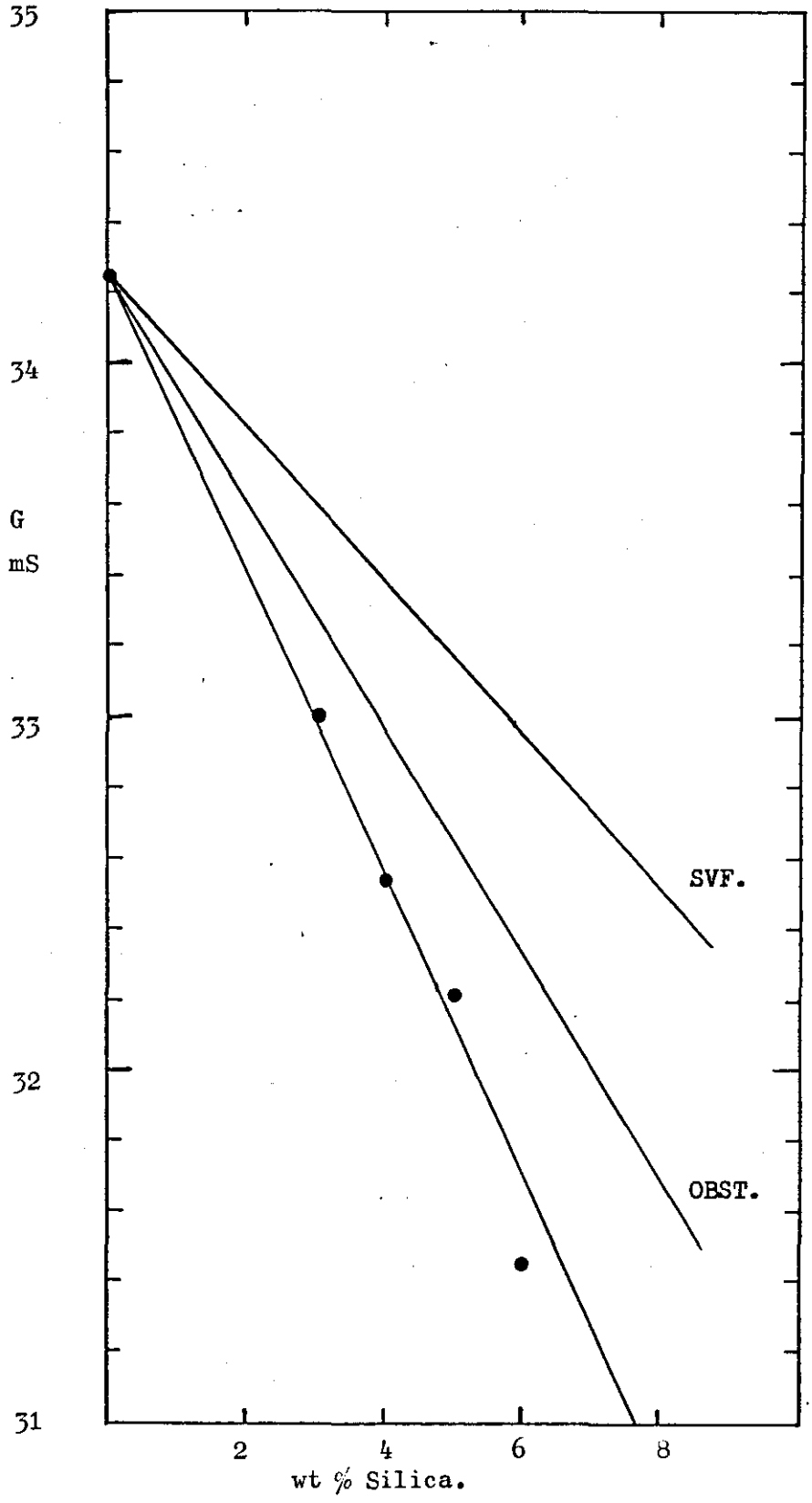

Fig. 5. 36b Conductance vs wt % Silica,
M5 Silica/40% H_2SO_4 in Cell I_r at 5°C.

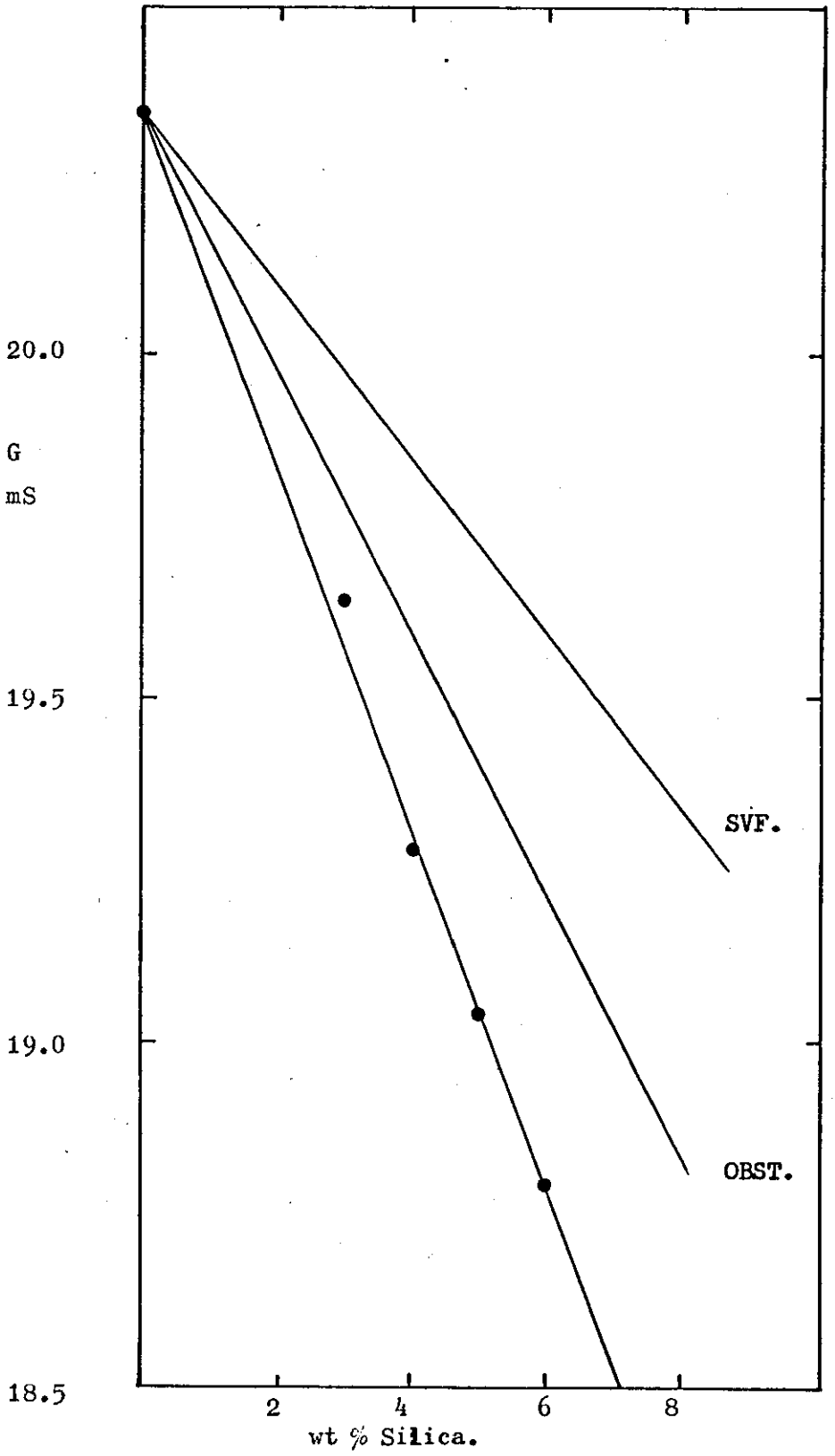

Fig. 5.37a Conductance vs wt % Silica,
M5 Silica/1.0D H_2SO_4 in Cell II at 5°C.

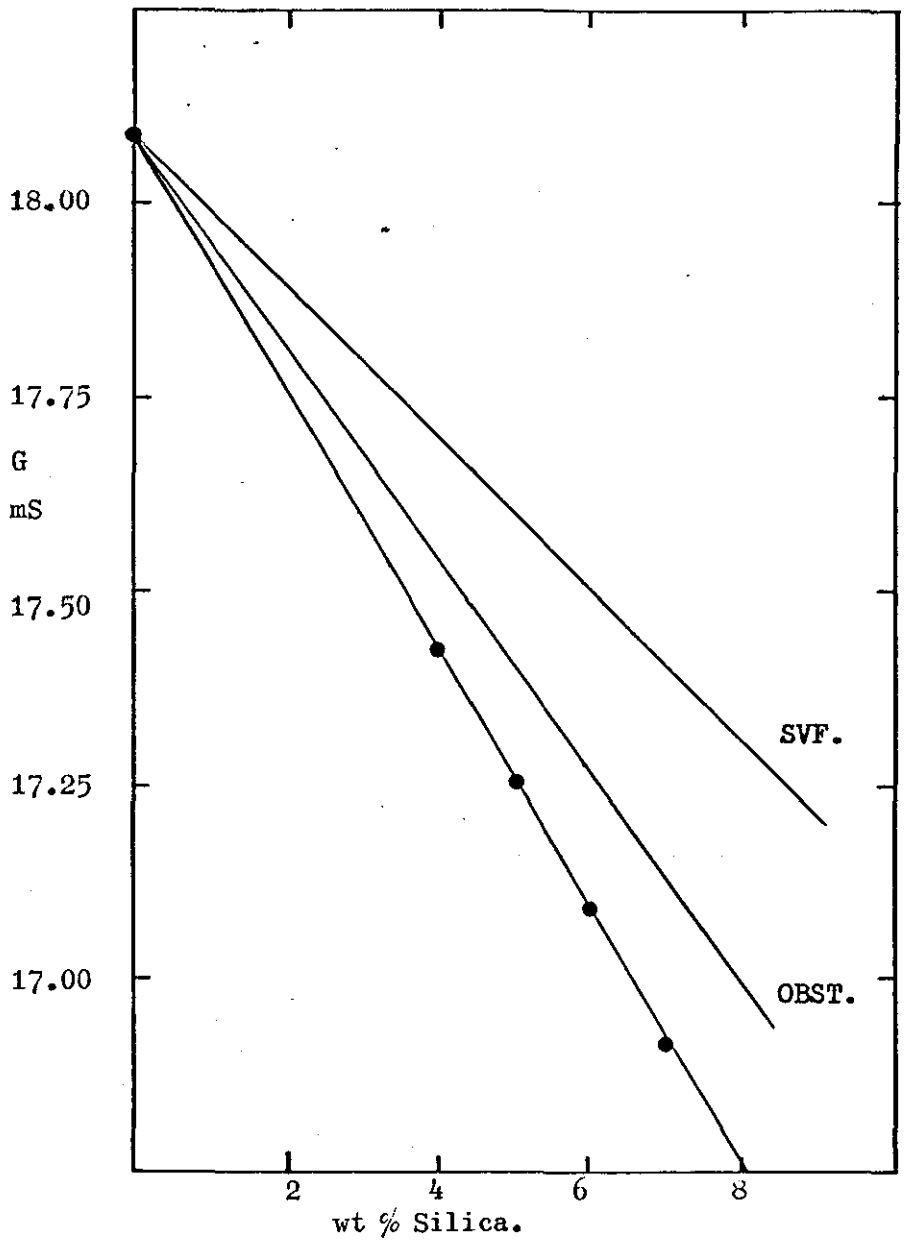

Fig. 5.37b Conductance vs wt % Silica,
M5 Silica/1.0D H_2SO_4 in Cell I_r at $5^{\circ}C$.

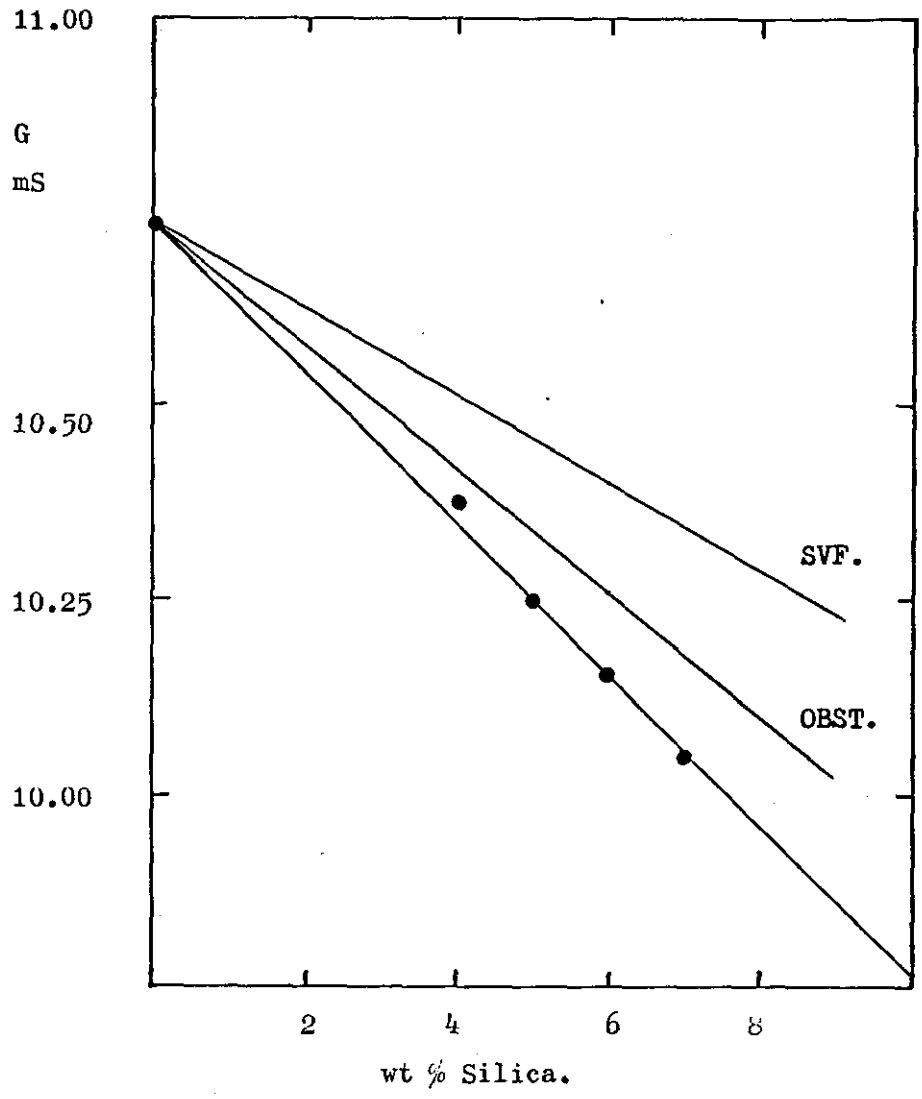

Fig 5. 38a Conductance vs wt% Silica,
M5 Silica/0.1D H_2SO_4 in Cell II at 5°C.

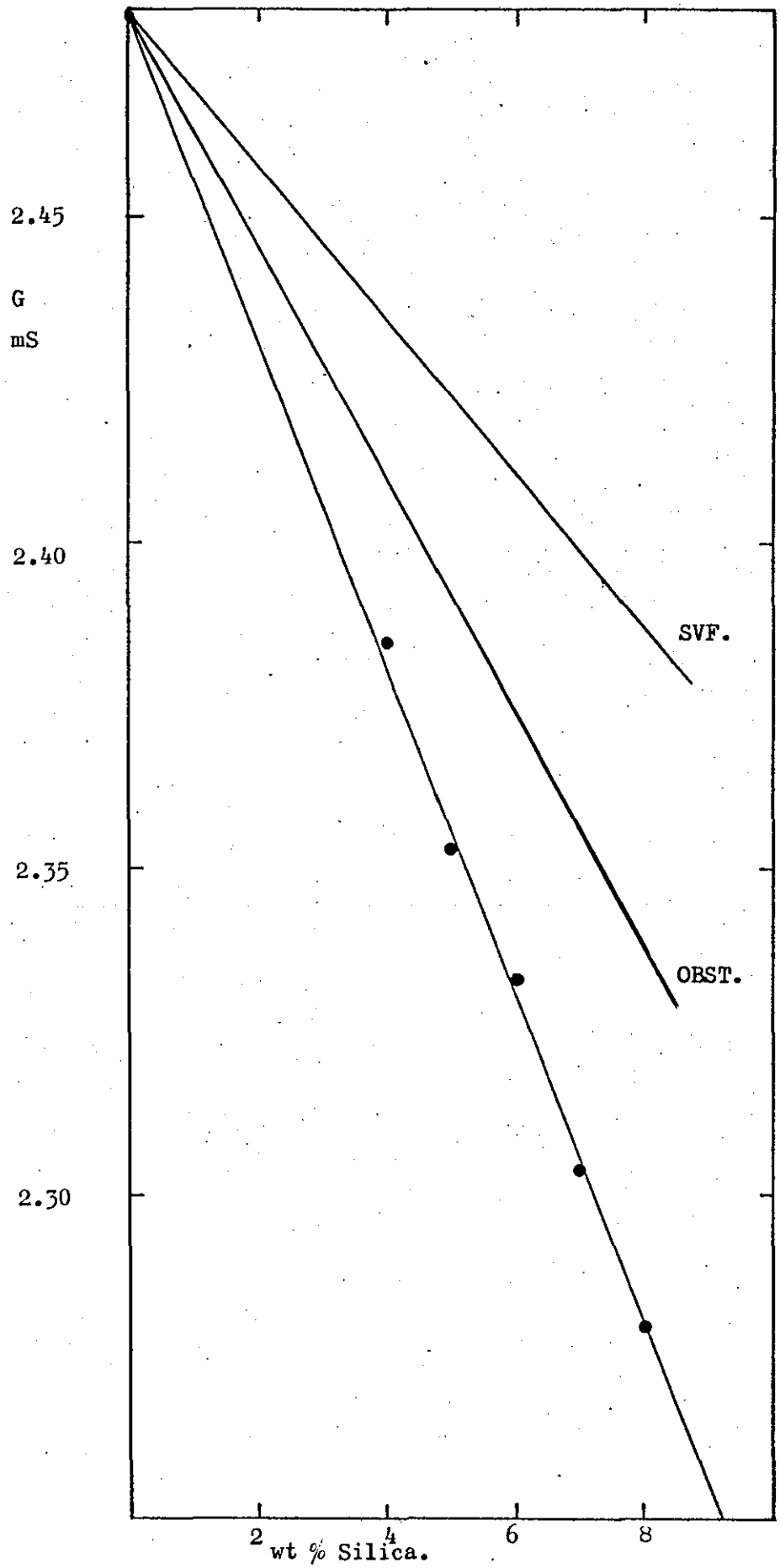

Fig. 5.38b Conductance vs wt% Silica,

M5 Silica/0.1D H_2SO_4 in Cell I_r at 5°C.

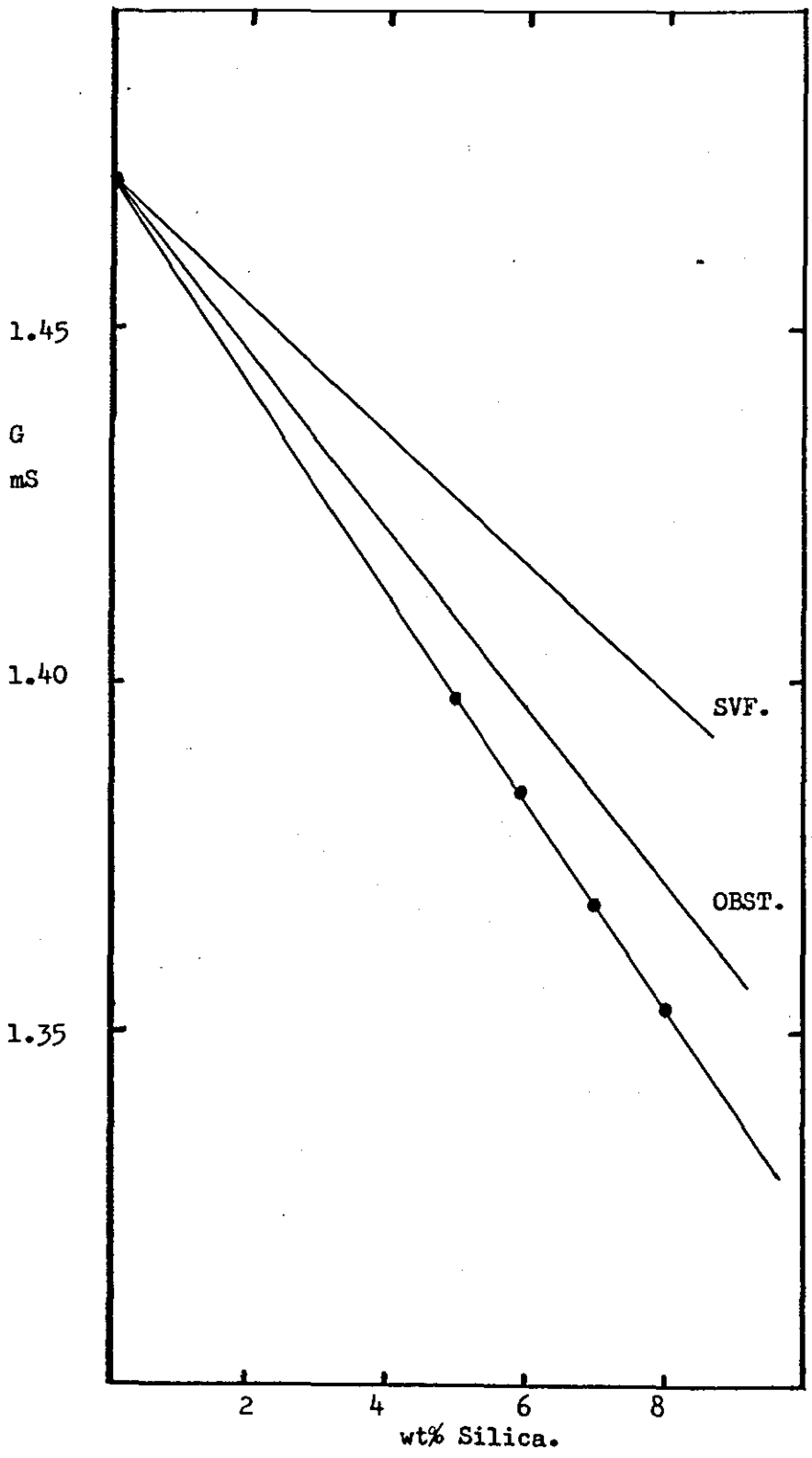

Fig. 5. 39a Conductance vs wt % Silica,
M5 Silica/0.01D H_2SO_4 in Cell II at 5°C.

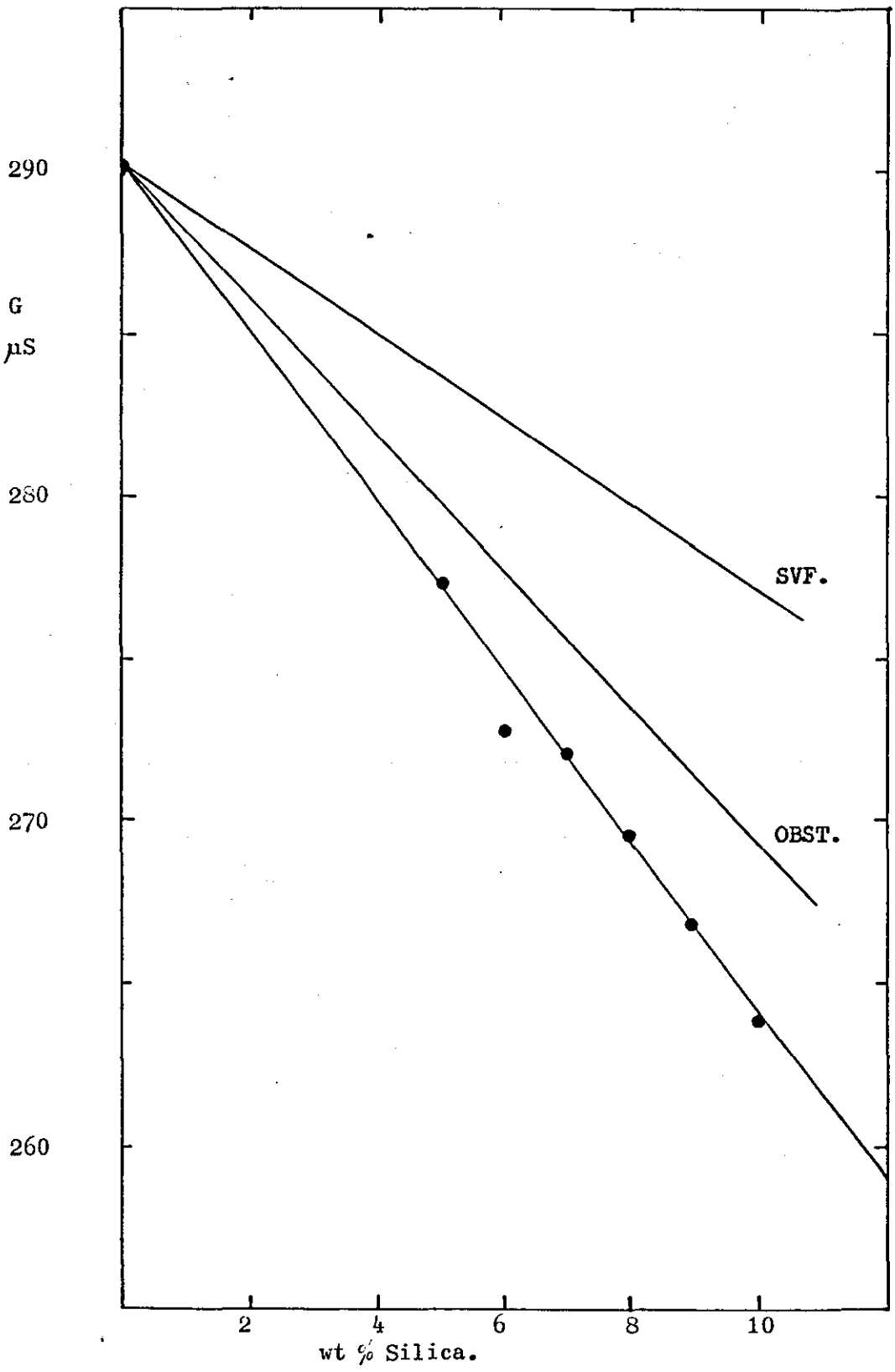

Fig. 5. 39b Conductance vs wt % Silica,
M5 Silica/0.01D H_2SO_4 in Cell I_r at 5°C.

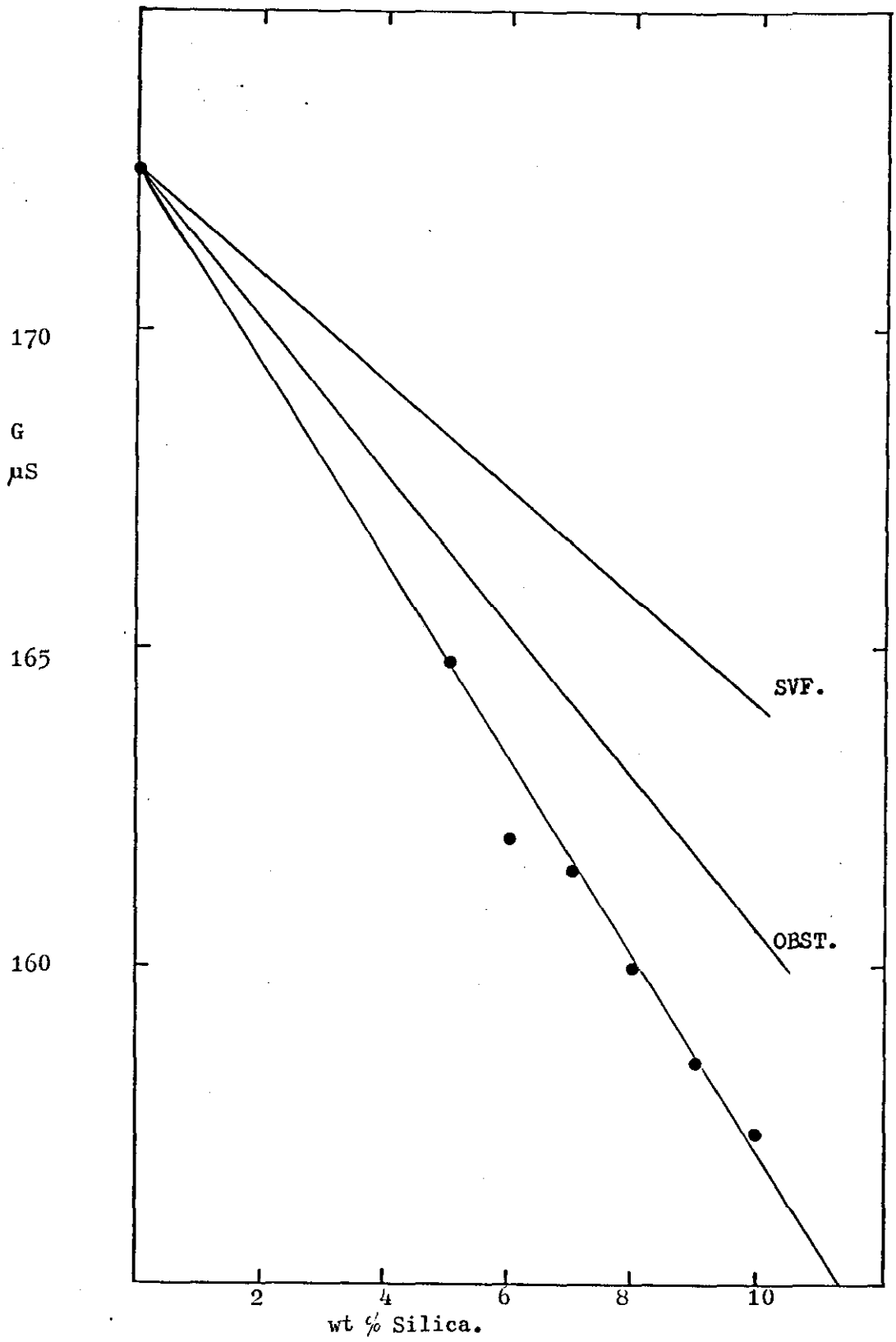

of surface conductance as shown in fig. 5.40. However the scatter of results was quite high and the gels were very unstable. It is likely that this behaviour was due to the two opposing contributions to the gel conductivity, namely the conductance through the solution and the surface conductance at the silica-solvent interface, were very nearly balanced at this temperature and concentration of acid. Further work at this temperature was not performed as the apparatus had to be dismantled due to building alterations within the Department of Chemistry.

5.16. Conductivity of M5 Silica/Potassium Chloride Gels.

The parallel series of measurements performed on silica/potassium chloride gels proved to be very useful.

The first measurements were made using cell III, the dilution cell. The conductivity of a 5% gel in 0.01D KCl at 25°C was measured, followed by measurements after successive additions of ~10 mls of 0.01D KCl solution. A plot of the conductivity versus the calculated weight per cent of silica given in fig. 5.41 shows the large scatter in the conductivities for the first five additions of 0.01D KCl solution. The conductivities of gels after the remaining additions lie on a straight line, but extrapolation of this line to zero per cent silica gives a conductivity below that measured for 0.01D KCl solution. This behaviour was reproduced several times for 0.01D KCl gels and also for gels with a lower concentration of KCl solution. It was observed that if the conductivity of a diluted gel was measured, then the cell shaken for a short time, and the conductivity remeasured, a higher value of conductivity was obtained which slowly reverted to the original value on standing as shown in fig. 5.42. Although no visible change in the appearance of the gel was observed, this behaviour

Fig 5.40a Conductance vs wt % Silica,
M5 Silica/0.001D H_2SO_4 in Cell II at 5°C.

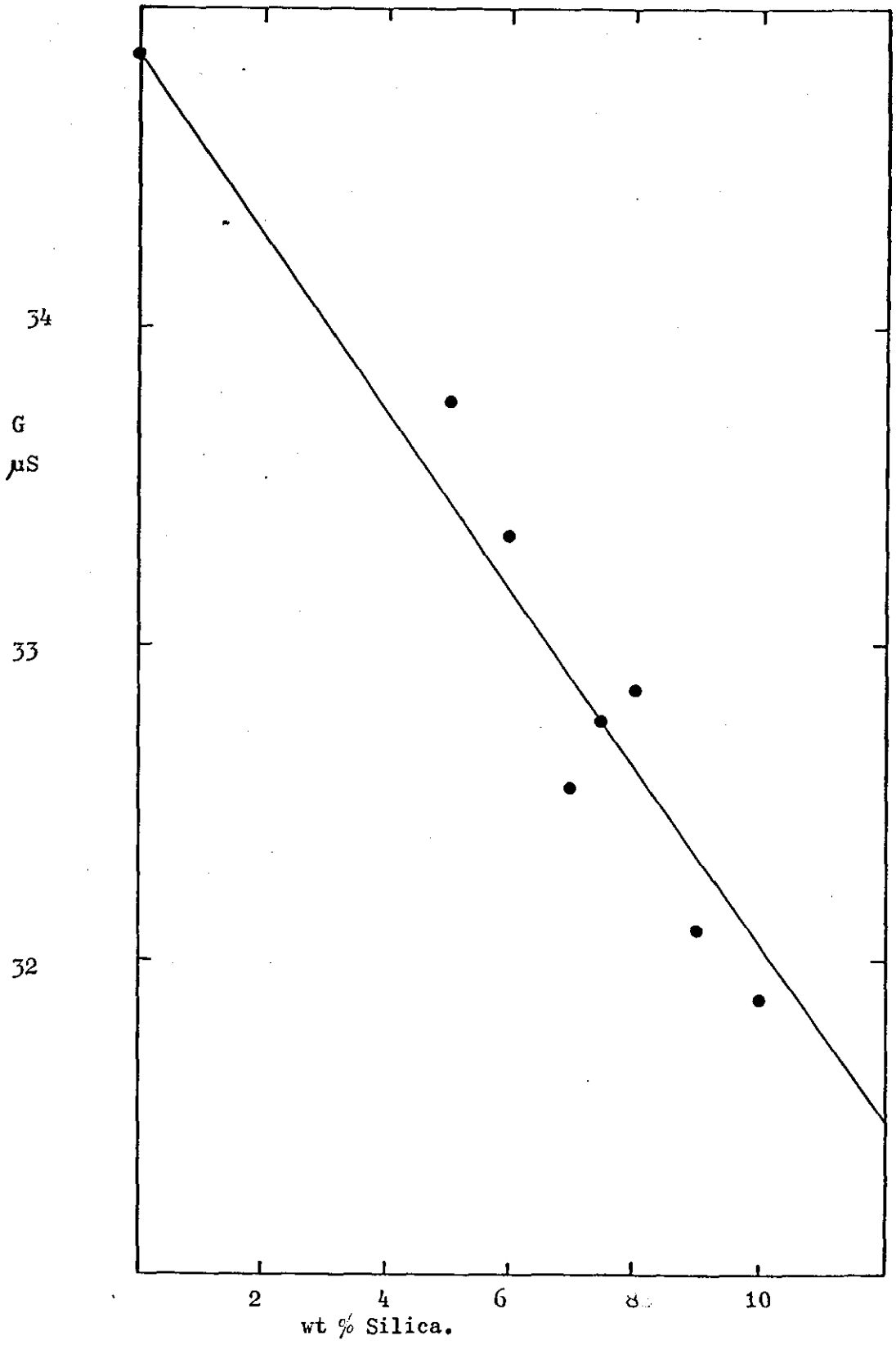

Fig. 5.40b Conductance vs wt% Silica,
M5 Silica/0.001D H_2SO_4 in Cell I_r at 5°C

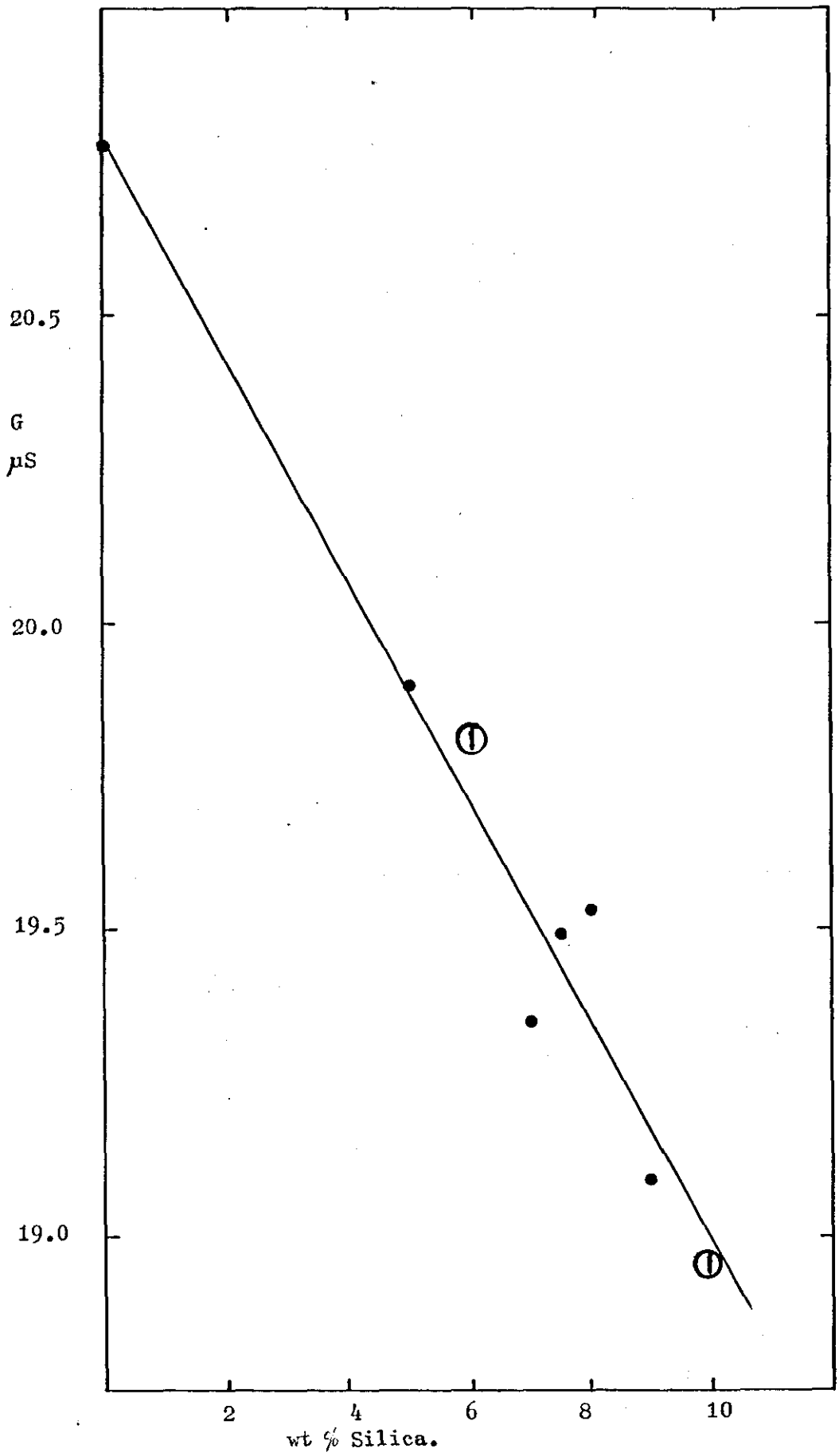

Fig. 5.41 Conductance vs wt % silica,
M5 Silica/0.01D KCl in cell III at 25°C.

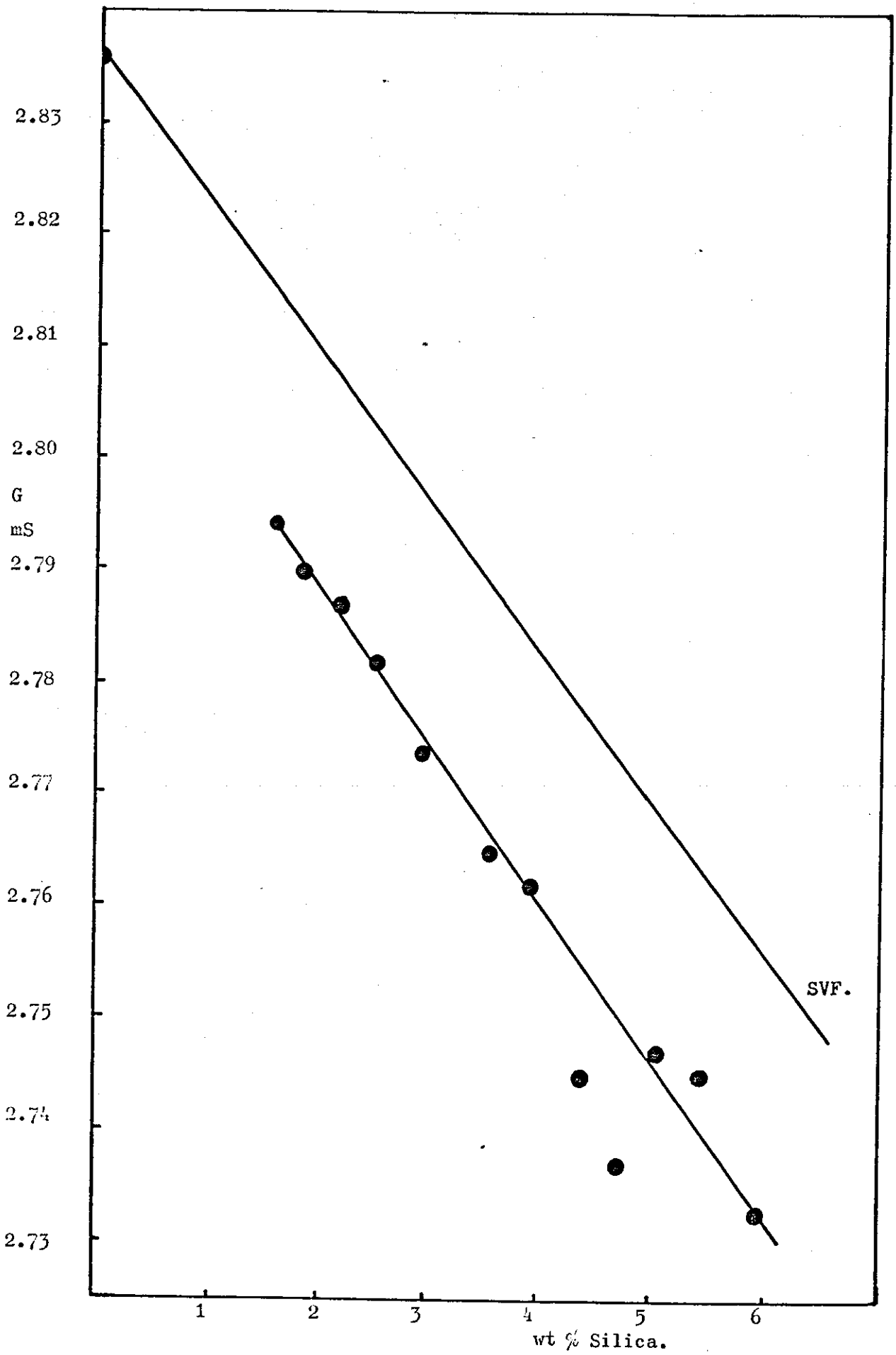

Fig. 5.42 Conductance vs wt % Silica,
M5 Silica/0.001D KCl in Cell III at 25°C,
showing the effect of agitation of the gel.

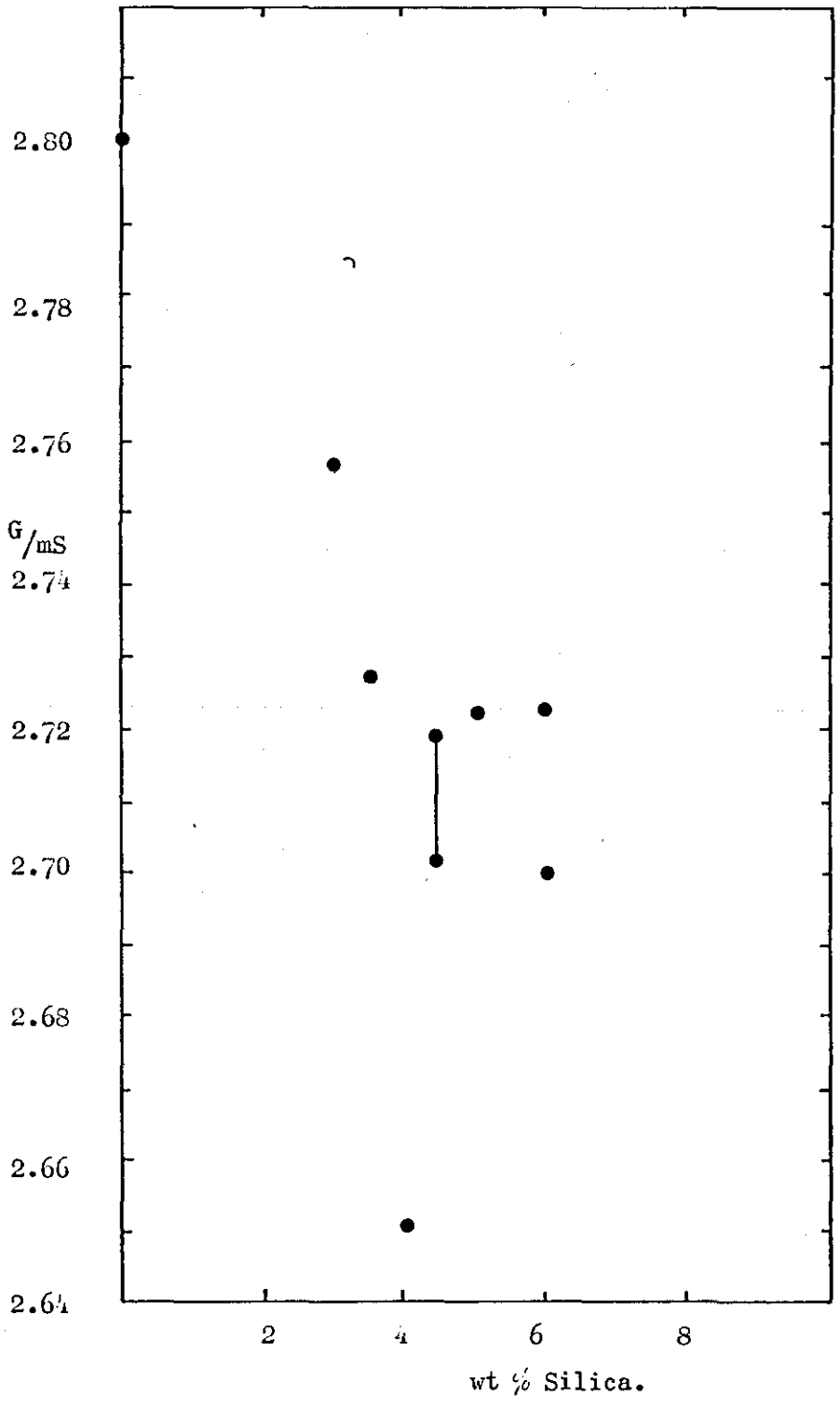

in conjunction with the difficulty that was experienced in obtaining a reproducible conductance for 6% gel in 40% sulphuric acid described earlier, led to the deduction that a mixing problem was involved.

The likely explanation of this conductivity behaviour in terms of gel structure is that the initial gel, which was prepared outside the cell by mixing with a single bladed stirrer at 100 r.p.m. for 10 minutes, contained reasonably well dispersed silica and a good degree of network formation. Addition of 10 mls of 0.01D KCl solution followed by shaking of the cell redispersed the silica very unevenly and gave relatively large "lumps" of the original network joined with a much lower degree of cross-linking. Shaking of the cell broke some of the network and hence the conductivity was higher, but fell again as the bonds reformed causing more hinderance to the mobility of ions. This pattern continued until sufficient 0.01D KCl solution had been added to dilute the gel such that shaking the cell produced a more complete redispersion of the gel. The most probable reason for extrapolation of the straight line not passing through the measured value for 0% silica is due to the fact that the addition of small quantities of electrolyte and shaking to disperse the silica allowed a far higher degree of solvation of the silica than is normally obtained with an associated loss of conducting ions from the potassium chloride solution.

Use of the standard mixing technique to prepare gels from 1.0D and 0.1D potassium chloride produced linear plots of conductivity versus weight % silica, the lines lying below those predicted by the simple volume fraction or obstruction theories as shown in figs. 5.43 and 5.44.

Fig. 5.43 Conductivity vs wt % Silica,
M5 Silica/1.0D KCl in Cell II at 25°C.

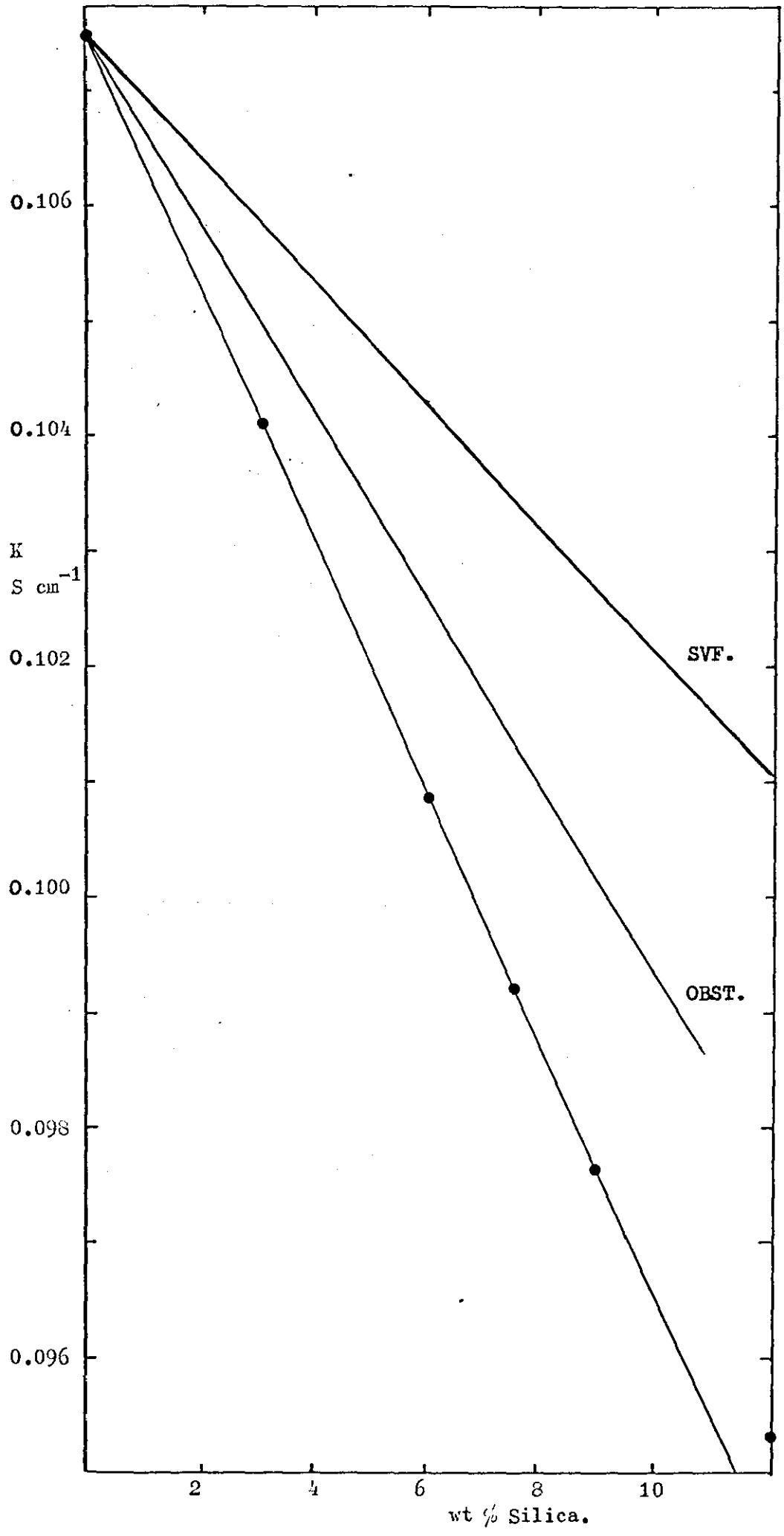

Fig. 5.44 Conductivity vs wt % Silica,
M5 Silica/0.1D KCl in Cell II at 25°C.

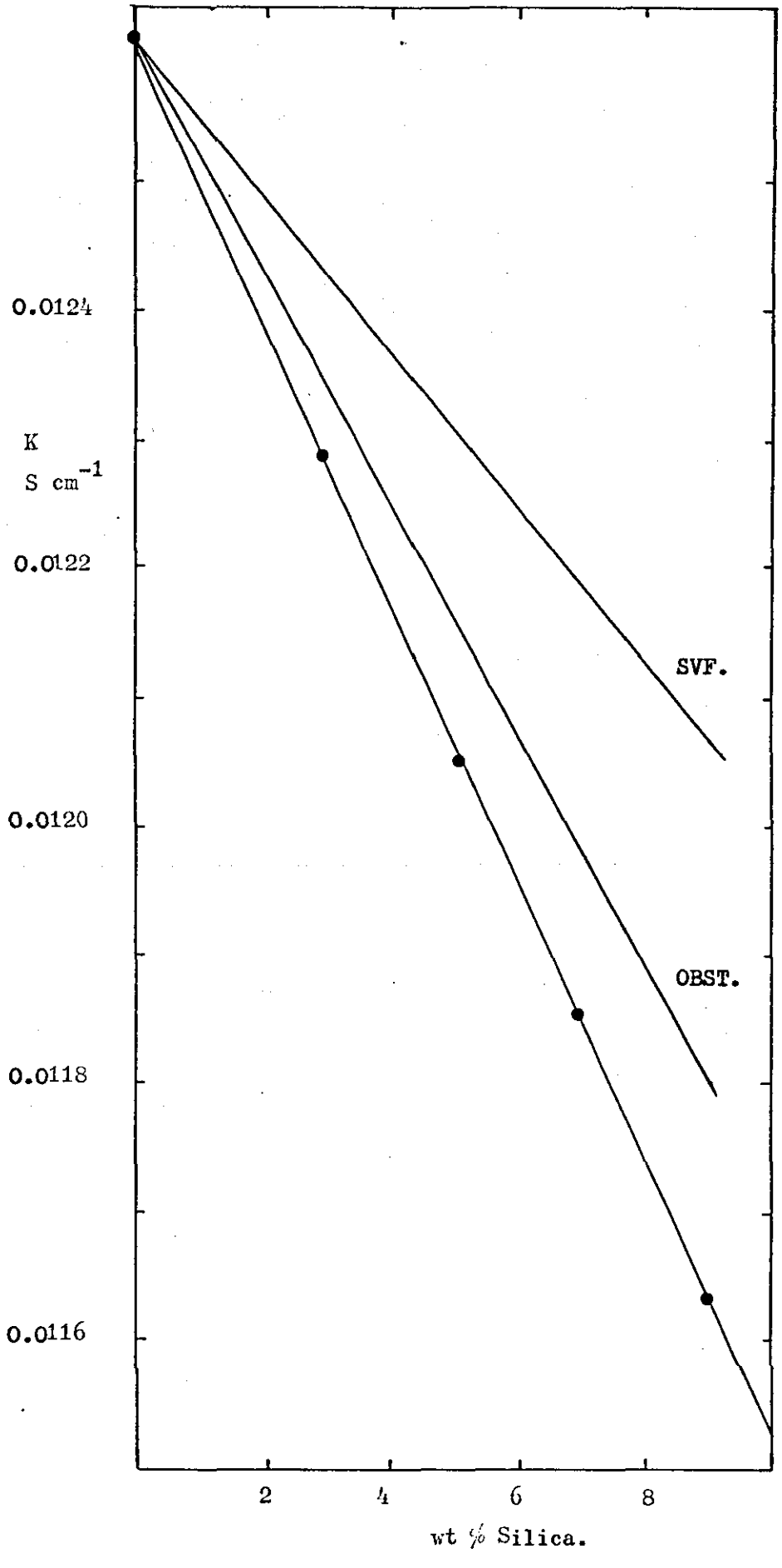

The 0.01D gels showed surface conductivity i.e. a positive gradient with increasing weight % silica as shown in fig. 5.45, similar to that observed with 0.001D acid gels. The surface conductivity is observed at this higher concentration because of the overall lower conductivity of potassium chloride compared to sulphuric acid solutions with the large excess of H^+. Gel stability of 0.01D gels was poor and for 0.001D gels containing 12% silica the conductivity fell rapidly with time as shown in fig. 5.46.

The conductance of potassium chloride gels at 50°C was very similar to that observed at 25°C, the experimental conductivities lying below that predicted by the theories as shown in fig. 5.47, 5.48, and 5.49 for 1.0D, 0.1D, and 0.05D M5 silica/ KCl gels. The 0.01D gels showed the expected increase in conductivity with increase in silica content due to surface conductance effects, but the gels were unstable and the conductance decreased with time quite rapidly, see fig. 5.50.

The normalized conductance versus weight % silica plots for 25°C and 50°C are given in figs. 5.51 and 5.52 respectively. Although the lines are of different gradient for each concentration, the order of decreasing gradient is the same as that of decreasing concentration of potassium chloride, which is a major difference in behaviour from that of sulphuric acid gels and indicating there is a fundamental difference between the two systems. Discussion of this result is delayed until the next section, 5.17.

5.17. A Method of Predicting Gel Conductivity.

The conclusions derived from measurements of the density of silica indicate that one possible reason for the large discrepancy between the values of gel conductivity predicted from the theory and those determined experimentally was the use of the value of 2.2 for the

Fig. 5.45 Conductivity vs wt % Silica,
EH5 Silica/0.01D KCl in Cell II at 25°C.

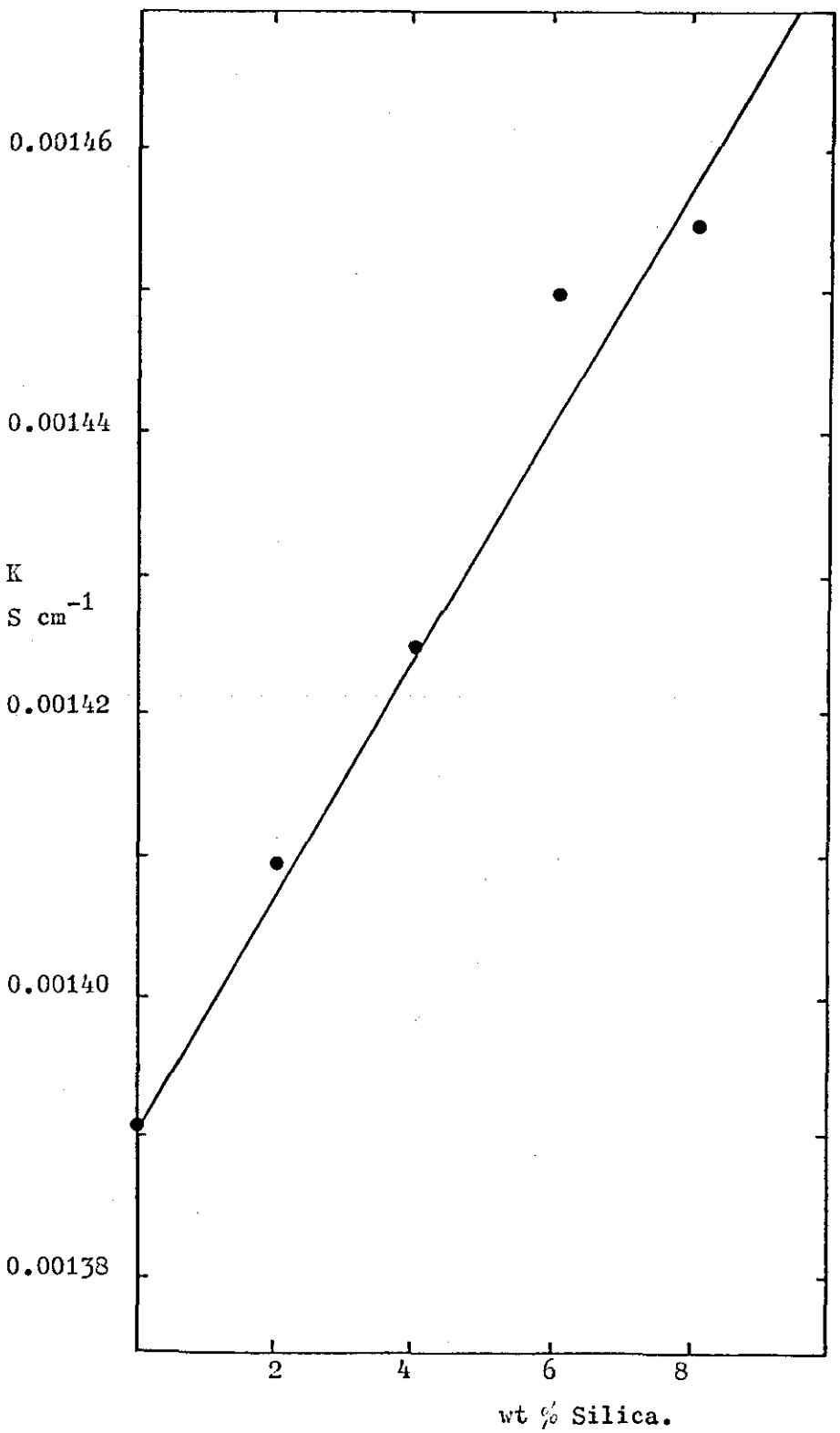

Fig. 5. 46 Conductance vs Time, 12% EH5 Silica/0.001D KCl in Cell II at 25°C.

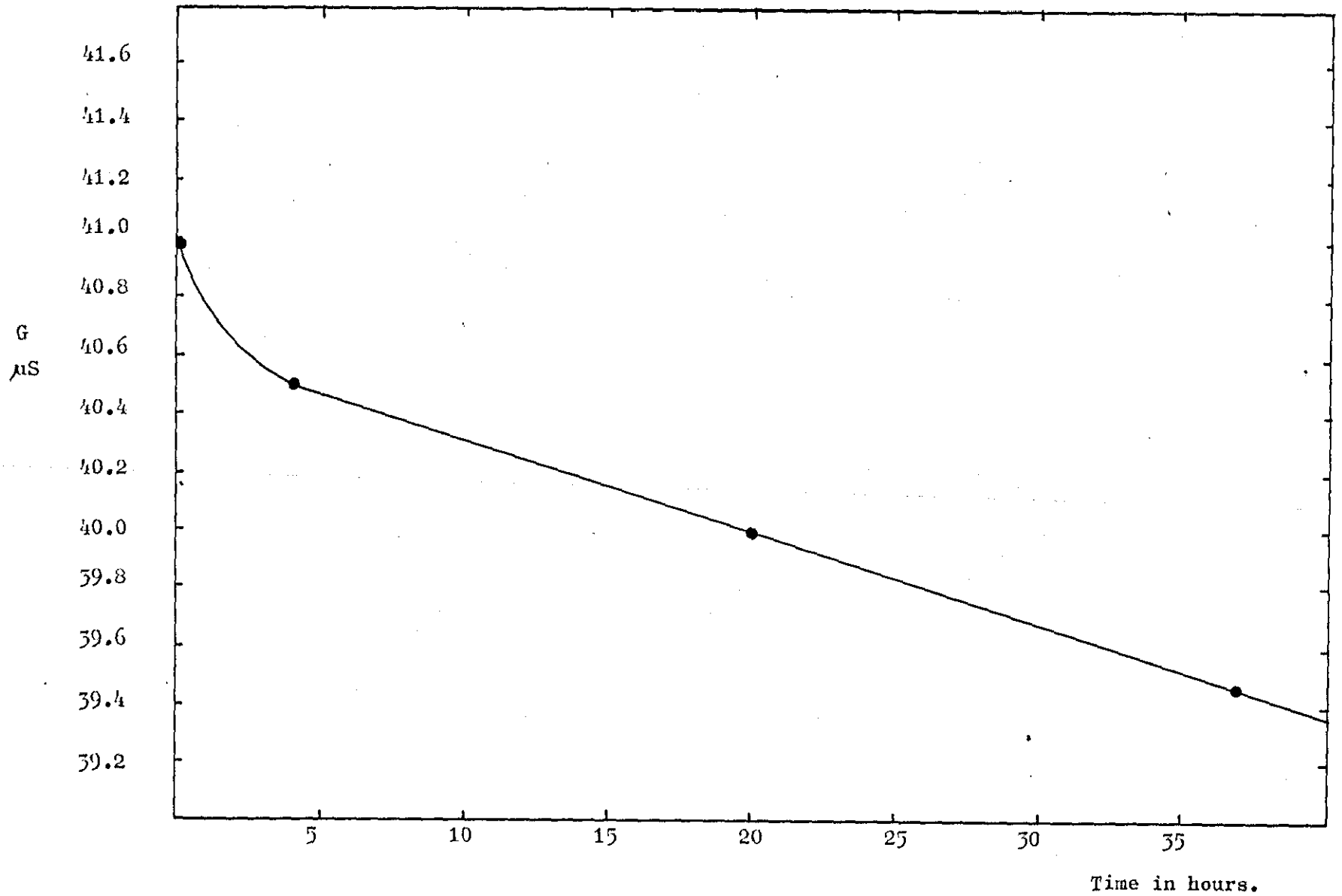

Fig. 5.47. Conductance vs wt% Silica, EH5 Silica/1.0D Potassium Chloride in Cell II at 50°C.

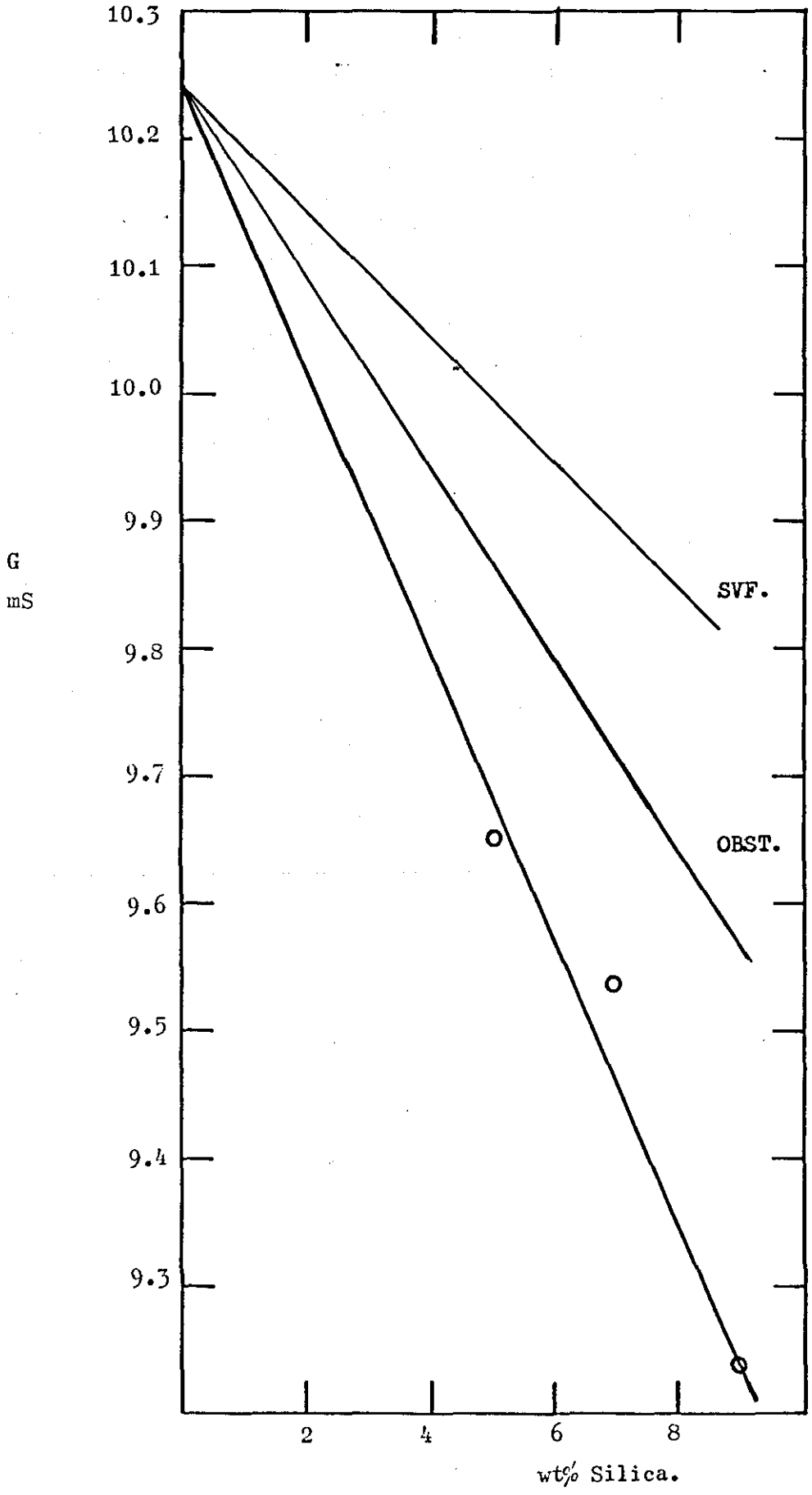

Fig. 5. 48a Conductance vs wt % Silica,
EH5 Silica/0.1D KCl in Cell II at 50°C

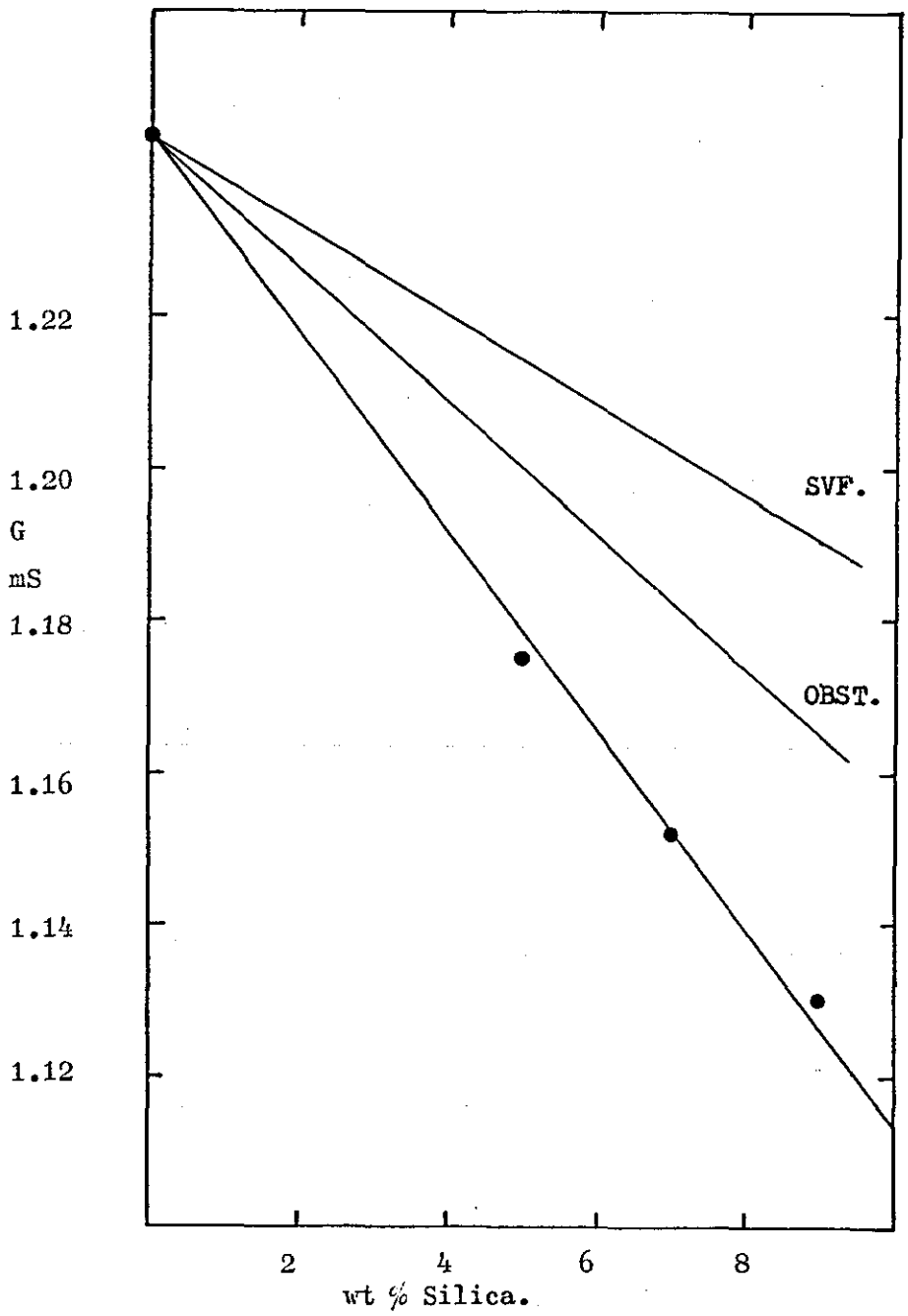

Fig. 5. 48b Conductance vs wt % Silica,
EH5 Silica/0.1D KCl in Cell I_r at 50°C.

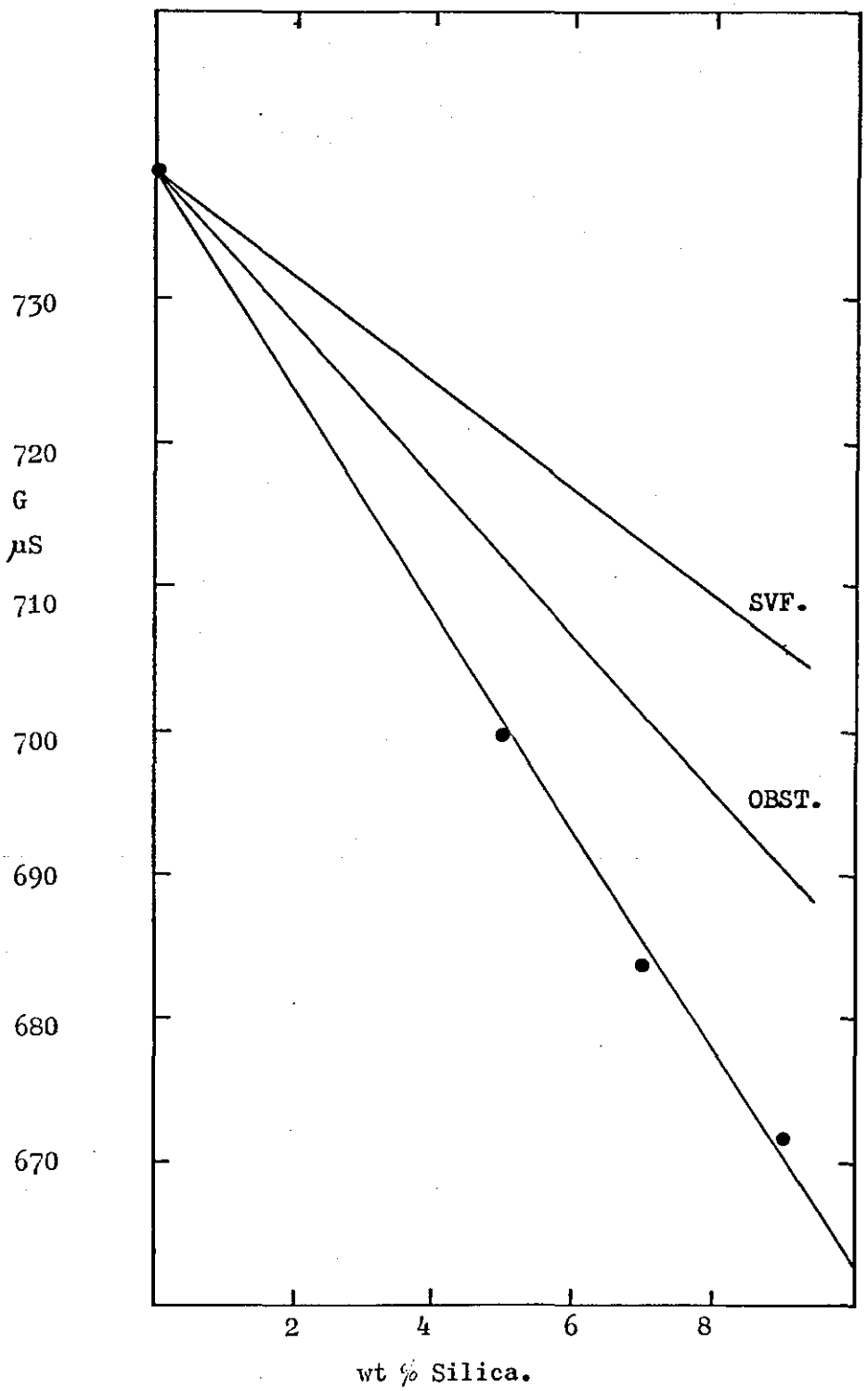

Fig. 5. 49a Conductance vs wt % Silica,
EH5 Silica/0.05D KCl in Cell II at 50°C.

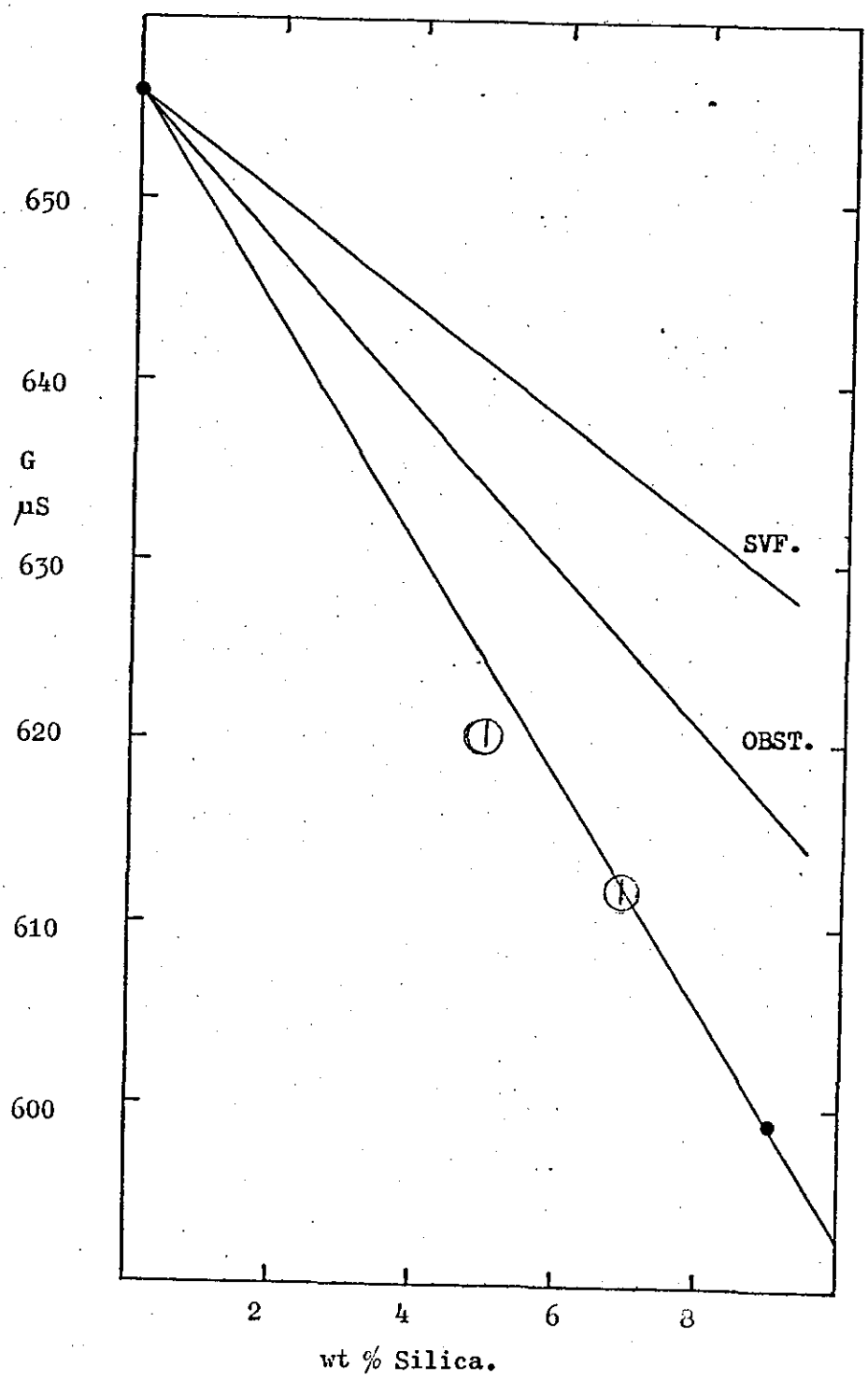

Fig. 5. 49b Conductance vs wt% Silica,
EH5 Silica/0.05D KCl in Cell I_r at 50°C.

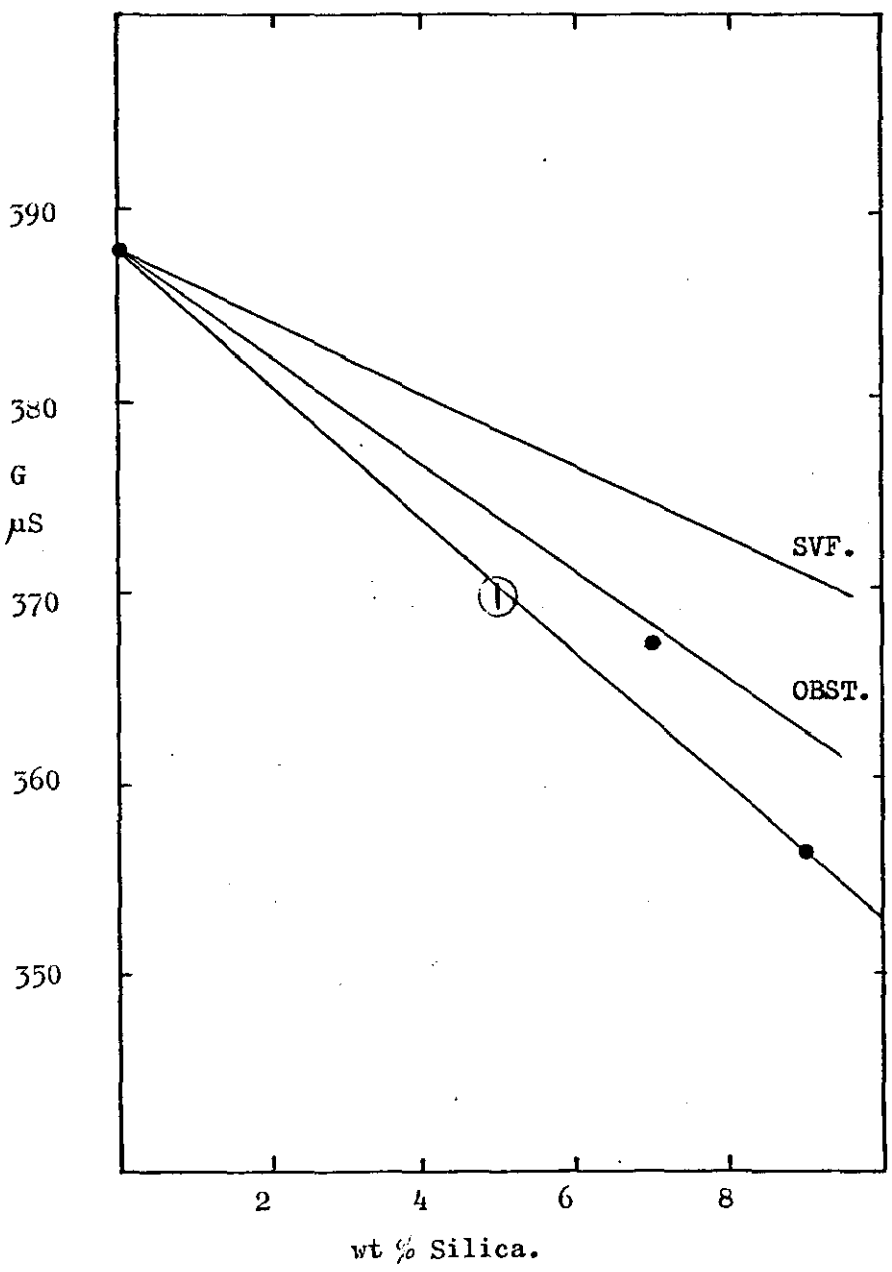

Fig. 5. 50a Conductance vs wt % Silica,
EH5 Silica/0.01D KCl in Cell II at 50°C.

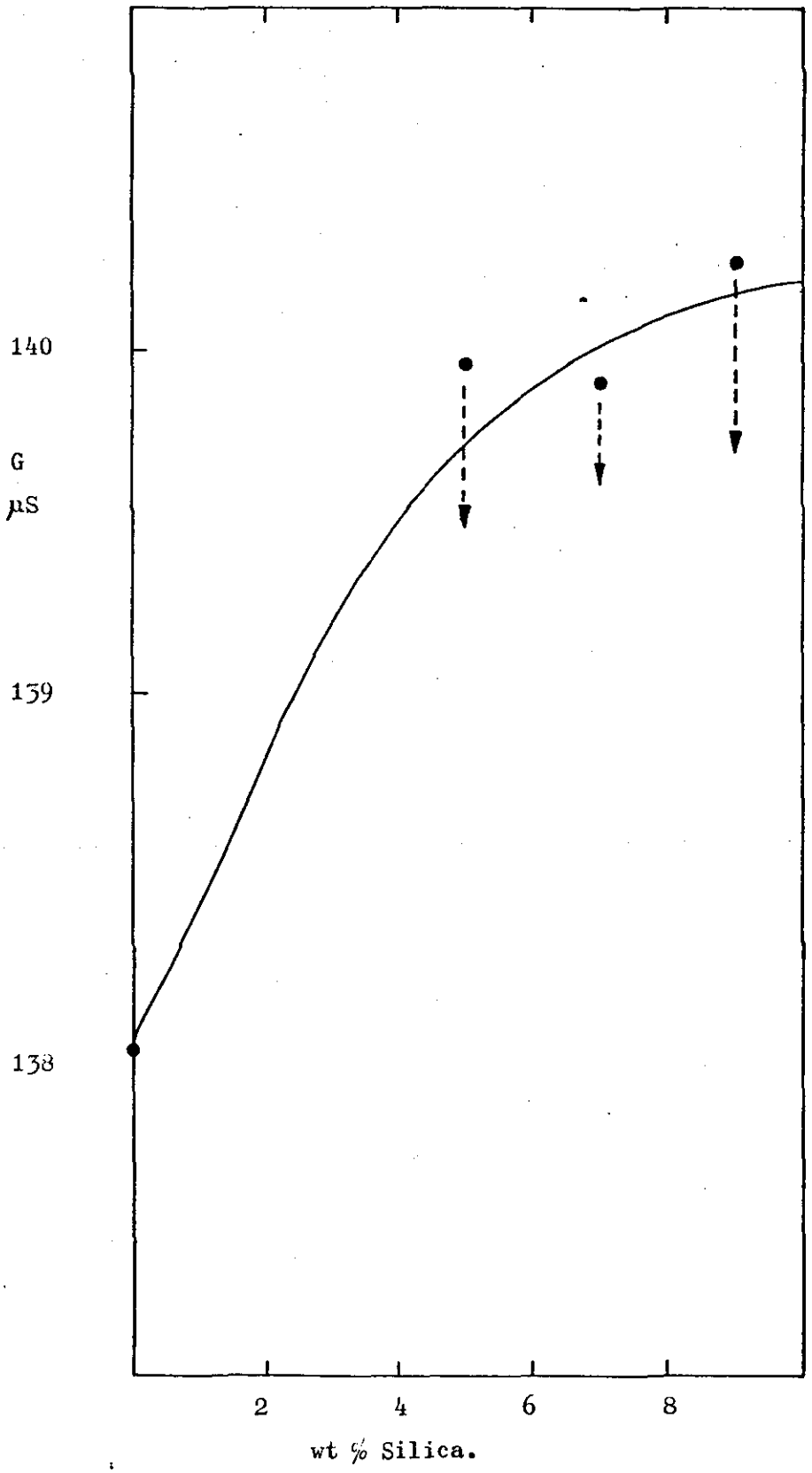

Fig. 5. 50b Conductance vs wt % Silica, EH5 Silica/0.01D KCl in Cell I_r at 50°C.

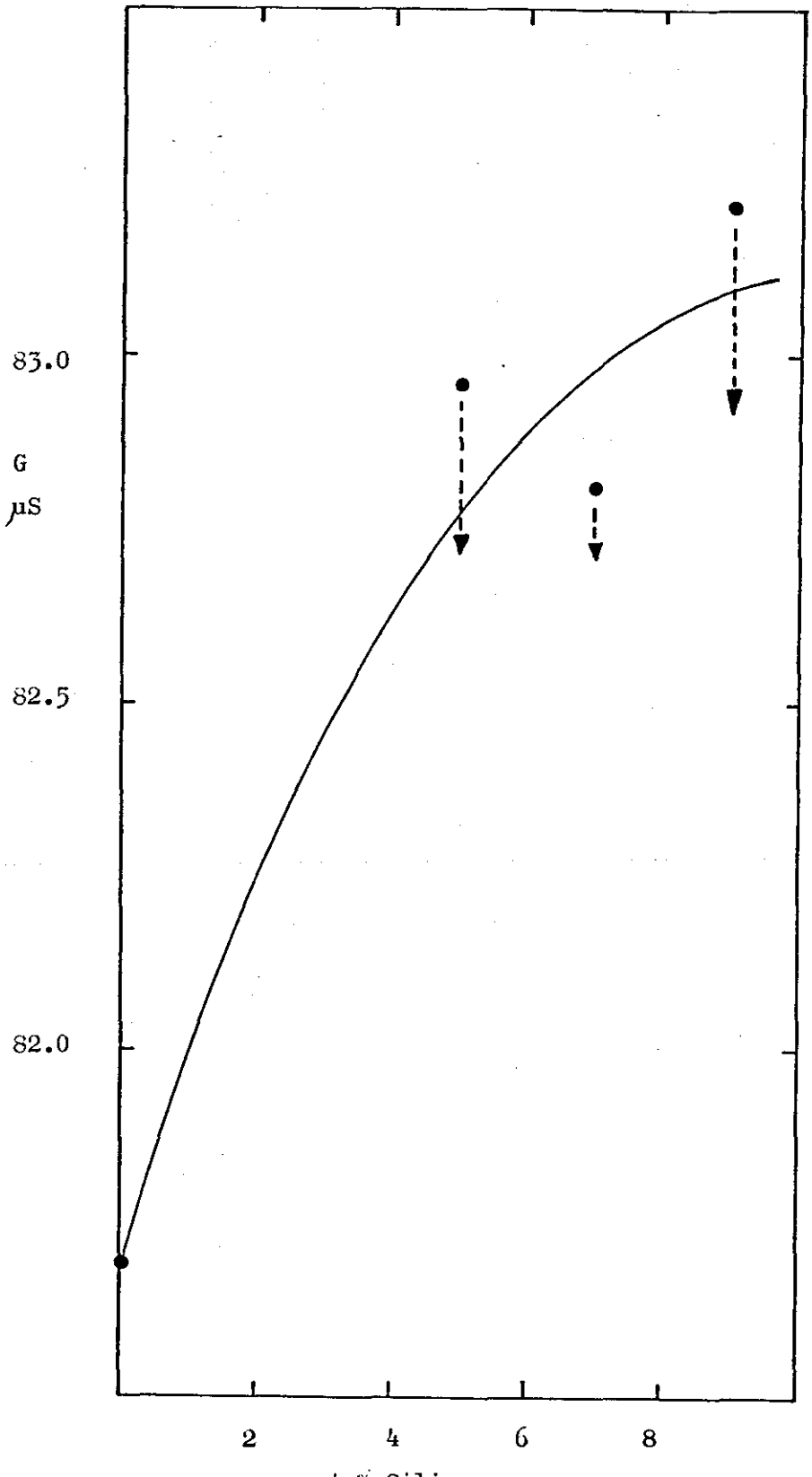

Fig. 5.51. Normalized Conductance vs wt% Silica, M5 Silica/Potassium Chloride Gels in Cell II at 25°C.

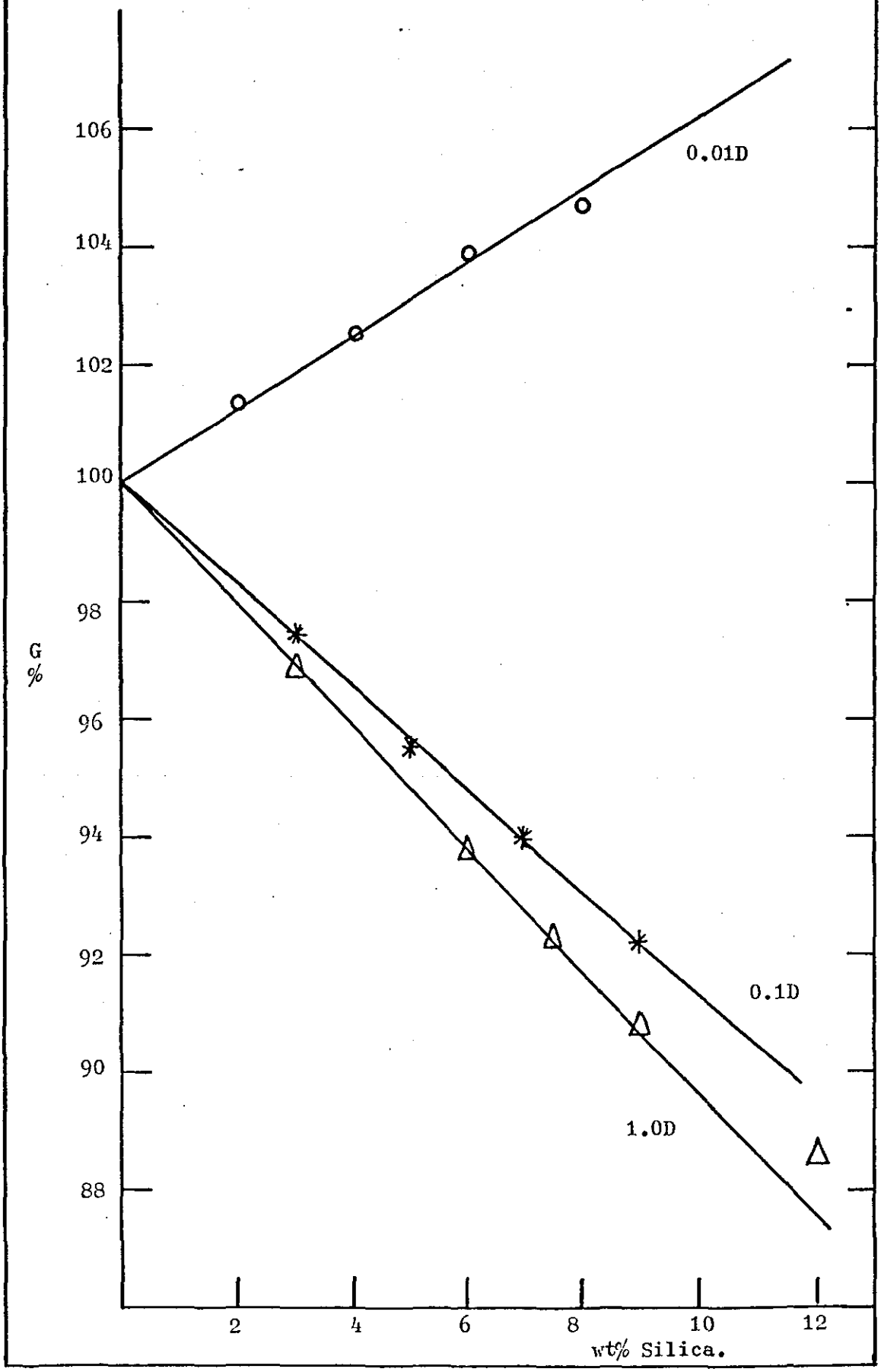

Fig. 5.52.

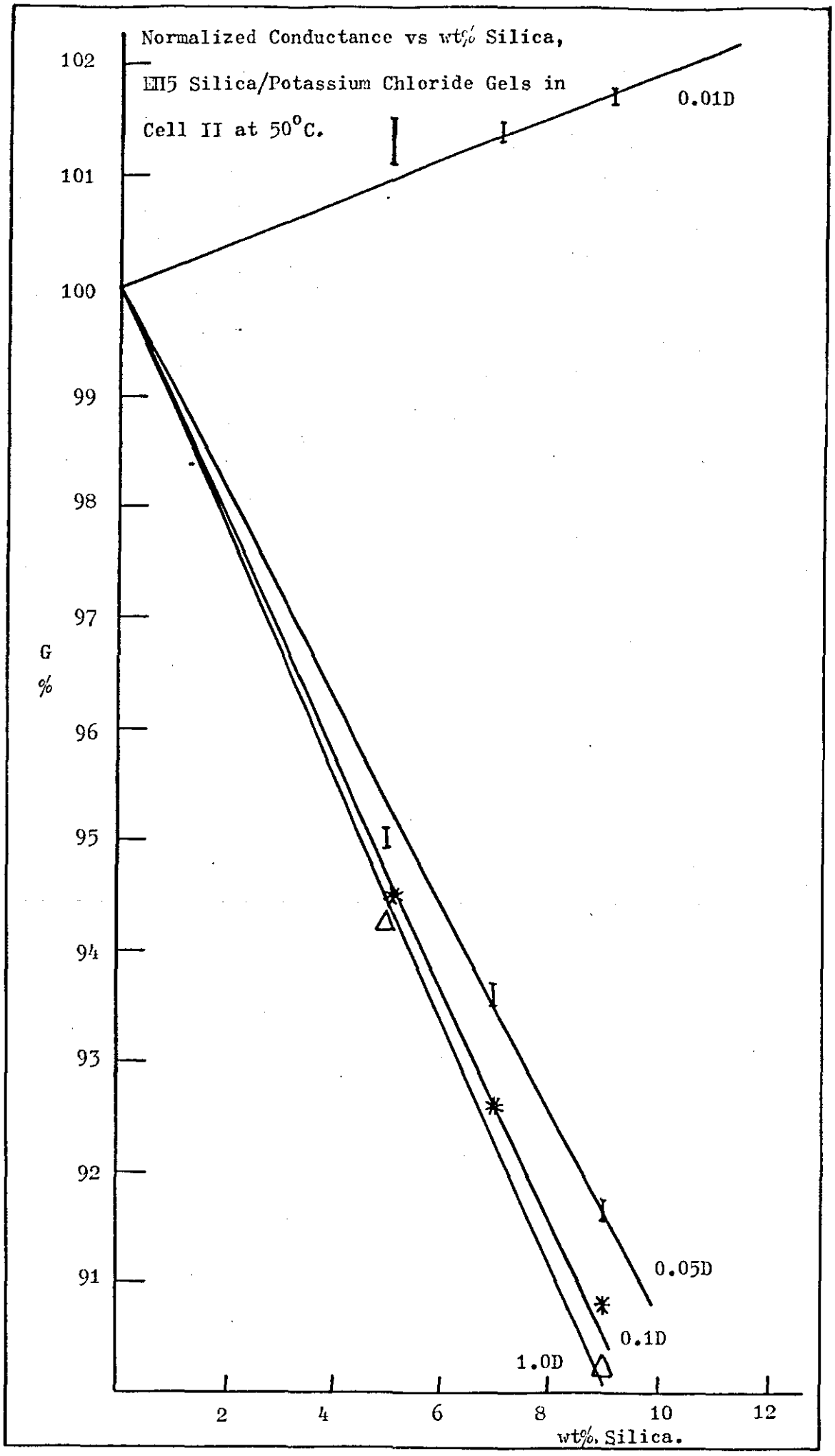
Normalized Conductance vs wt% Silica,
EH5 Silica/Potassium Chloride Gels in
Cell II at 50°C.
0.01D
0.05D
0.1D
1.0D
G
%
102
101
100
99
98
97
96
95
94
93
92
91
2
4
6
8
10
12
wt%. Silica.

density of silica in the calculation of the volume fraction of silica in the gel.

In order to develop a method of predicting the values of gel conductivity the following procedure was adopted:

The values of conductivity determined experimentally for gels of varying silica concentration in 40% sulphuric acid at 25°C were assumed to be accurately described by the conductivity equivalent of the Rayleigh (1892) expression for the obstruction effect, (see table 3. 4). This expression was then rearranged to allow the effective volume fraction, ϕ_s', of the silica in the various gels to be calculated:-

$$K_g = K_a \frac{(1 - \phi_s')}{(1 + \phi_s'/2)} \qquad \text{Rayleigh (1892)}$$

$$K_g (1 + \frac{\phi_s'}{2}) = K_a (1 - \phi_s')$$

$$K_g \cdot \frac{\phi_s'}{2} + K_a \phi_s' = (K_a - K_g)$$

$$\phi_s' \frac{(K_g + 2K_a)}{2} = (K_a - K_g)$$

$$\therefore \phi_s' = 2 \frac{(K_a - K_g)}{(K_g + 2K_a)} \qquad 5.\ 3.$$

The various values of ϕ_s' determined by substitution of the relevent conductivity data in equation 5. 3 were then used to calculate the effective density of the silica in the gel from equation 5. 5 which was derived as follows:

$$\phi_s' = \frac{W_s/\rho_s'}{W_s/\rho_s' + (100 - W_s)/\rho_a} \qquad 5.\ 4.$$

$$\therefore \quad \frac{\phi_{s'} W_s}{\rho_{s'}} + \phi_{s'} \frac{(100 - W_s)}{\rho_a} = \frac{W_s}{\rho_{s'}}$$

$$\therefore \quad \phi_{s'} \frac{(100 - W_s)}{\rho_a} = \frac{W_s}{\rho_{s'}} - \frac{\phi_{s'} W_s}{\rho_{s'}} = W_s(1 - \phi_{s'}). \frac{1}{\rho_{s'}}$$

$$\therefore \quad \rho_{s'} = W_s(1 - \phi_{s'}). \frac{\rho_a}{\phi_{s'} (100 - W_s)}$$

$$\therefore \quad \rho_{s'} = \frac{(W_s \rho_a)}{(100 - W_s)} \left\{ \frac{1}{\phi_{s'}} - 1 \right\} \qquad 5.5.$$

The values of $\rho_{s'}$ obtained were subject to a small spread due to the errors in the experimental gel conductivities. The values of $\rho_{s'}$ were averaged to give the value ρ_{sa}. The value ρ_{sa} was then used in equation 5.4 instead of ρ_s to calculate the volume fraction of silica in gels prepared from lower sulphuric acid concentrations. This value for the volume fraction obtained was substituted in the simple obstruction expression for conductivity:

$$K_g = K_a (1 - 1.5\phi) \qquad (3.25)$$

along with the conductivity of the bulk acid, K_a, to predict the conductivity of the gels.

The value of ρ_{sa} determined from the gels prepared from 40% sulphuric was 1.66 ± 0.03 gcm^{-3}. Use of this value to calculate the volume fractions for substitution in the obstruction equation 3.25 gave an accurate prediction of the gel conductivities for gels prepared from 23%, 1.0D, 0.1D and 0.01D sulphuric acid as shown in figures 5.53, 5.24, 5.25 and 5.26 respectively by the line drawn through the experimental points.

Similarly, for sulphuric acid and potassium chloride gels at 50°C and 5°C the same method gave a good prediction of the conductances which can be seen from figs. 5.30 to 5.35, 5.36 to 5.39, and 5.47 to 5.49 respectively, by the lines which pass through most of the experimental points.

This result is of great significance for several reasons: Firstly, two of the alternative explanations of the failure of the obstruction equations to predict the gel conductances may be discounted. If the solubility of silica in the electrolyte had been the cause of the additional decrease in conductances of the gels, then the effective density of the silica would be expected to vary with different electrolytes because the solubility of silica, although small, is known to be pH dependent, Iler (1973). Alternatively, had the additional decrease in conductance been due to specific changes in viscocity, then a constant effective density of silica would not be expected for differing electrolytes, nor for a range of silica concentrations.

Secondly, the failure of the plots of normalized conductances vs. volume fraction for a range of acid concentrations to be superimposed is explained because the use of the actual density of silica in its natural state instead of the effective density exhibited in the gels leads to an error in the calculated volume fractions. Use of the effective density of silica in the calculation of volume fractions does give superimposed lines within the experimental error for the electrolyte concentrations where surface conductance effects are negligible.

Thirdly, the suggestion that the effects of gel network in sulphuric acid produced a different result compared to potassium chloride advanced from the fact that the order of decreasing slopes of the normalized conductances varied for sulphuric acid but did not for potassium chloride is discounted because the same effective density

is found to be applicable to both systems, and also to the potassium nitrate and sodium sulphate silica systems as seen from figs. 5.54 and 5.55 respectively, where the predicted lines pass through most of the experimental points.

Fourthly, the effective density of silica can be used to calculate the number of primary silica particles in a silica aggregate, and hence the number of aggregates/unit volume of gel can be determined. The distribution of the aggregates within the gel can then be discussed.

1g of silica powder may be considered to consist of a number, n, of spherical primary particles of radius, r_p , density, ρ_p , in the form of N_s spherical aggregates of radius, r_a , density, ρ_a , containing N_a primary particles. The surface area of a sphere is $4\pi r^2$ where r is the radius of the sphere. Therefore the total surface area of the primary particles is $n4\pi r_p^2$, which may be equated to the value of $200 \pm 20\ m^2g^{-1}$ quoted by the Manufacturers for the surface area of M5 silica determined by the B.E.T. method (Brunauer, Emmett, and Teller 1938):

$$n.4\pi r_p^2 = 200 \times 10^4\ cm^2g^{-1}$$

This may be rearranged to give n :

$$n = \frac{2 \times 10^6}{4\pi r_p^2} \quad \text{primary particles} \qquad 5.6$$

The volume of a sphere is $\frac{4\pi r^3}{3}$, so the total volume of 1g of primary particles is $n.\frac{4\pi r_p^3}{3}$.

Using the relation density x volume = mass :

$$\rho_p.n.\frac{4\pi r_p^3}{3} = 1$$

Rearrange to give n :

$$n = \frac{3}{4\pi r_p^3 \rho_p} \quad \text{primary particles} \qquad 5.7$$

n can be eliminated from equations 5.6 and 5.7 to find r_p , which may be substituted back into either 5.6 or 5.7 to give n. The number of primary particles in an aggregate, N_a, can be determined by assuming various

Fig. 5. 53 Conductance vs wt % Silica,
M5 Silica/23% H_2SO_4 in Cell II at 25°C.

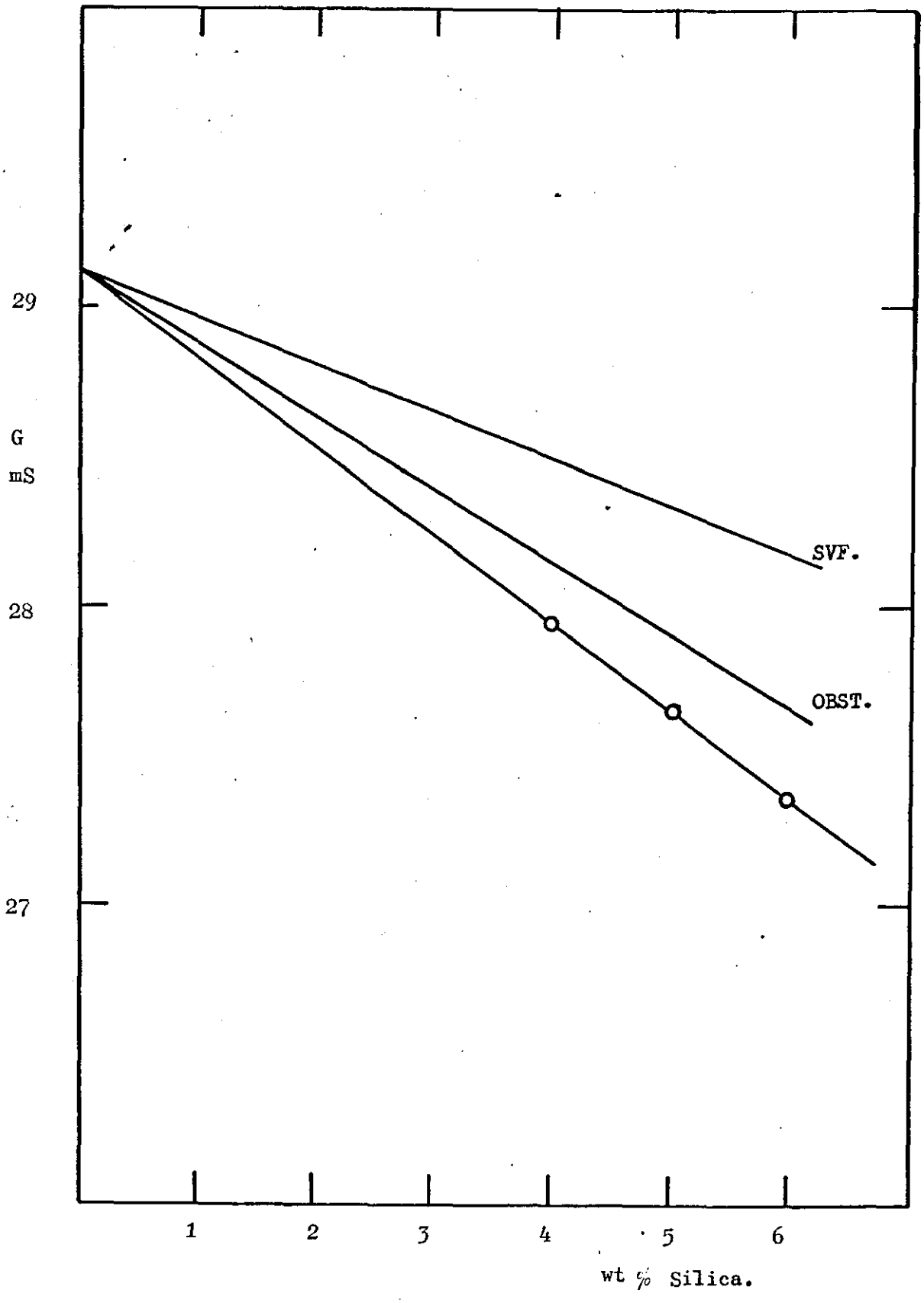

Fig. 5.54 Conductance vs wt % Silica,

M5 Silica/~1M KNO_3 in Cell I_r at 25°C.

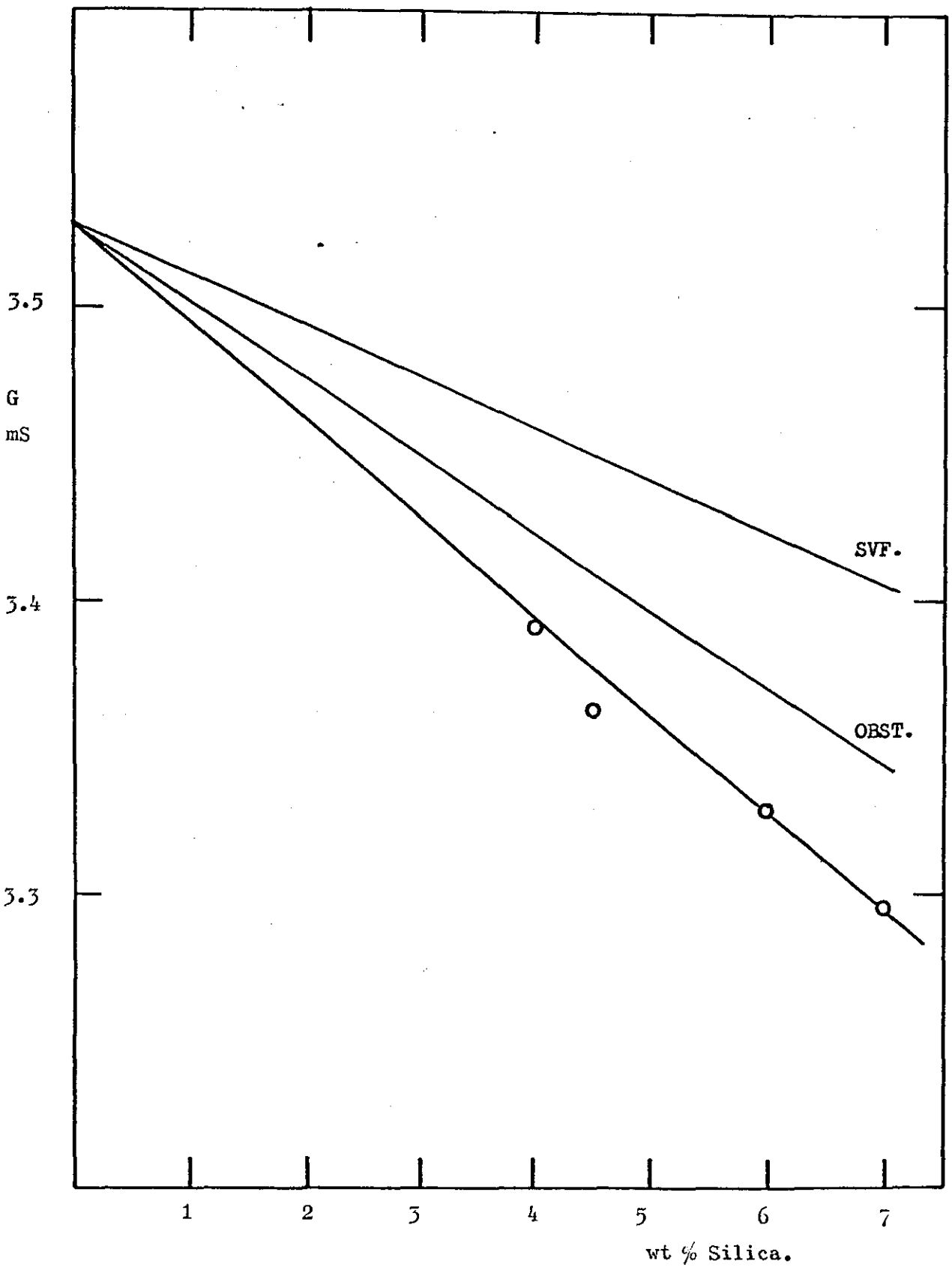

Fig. 5. 55 Conductance vs wt % Silica,
M5 Silica/1.0M Na_2SO_4 in Cell I_r at 25°C.

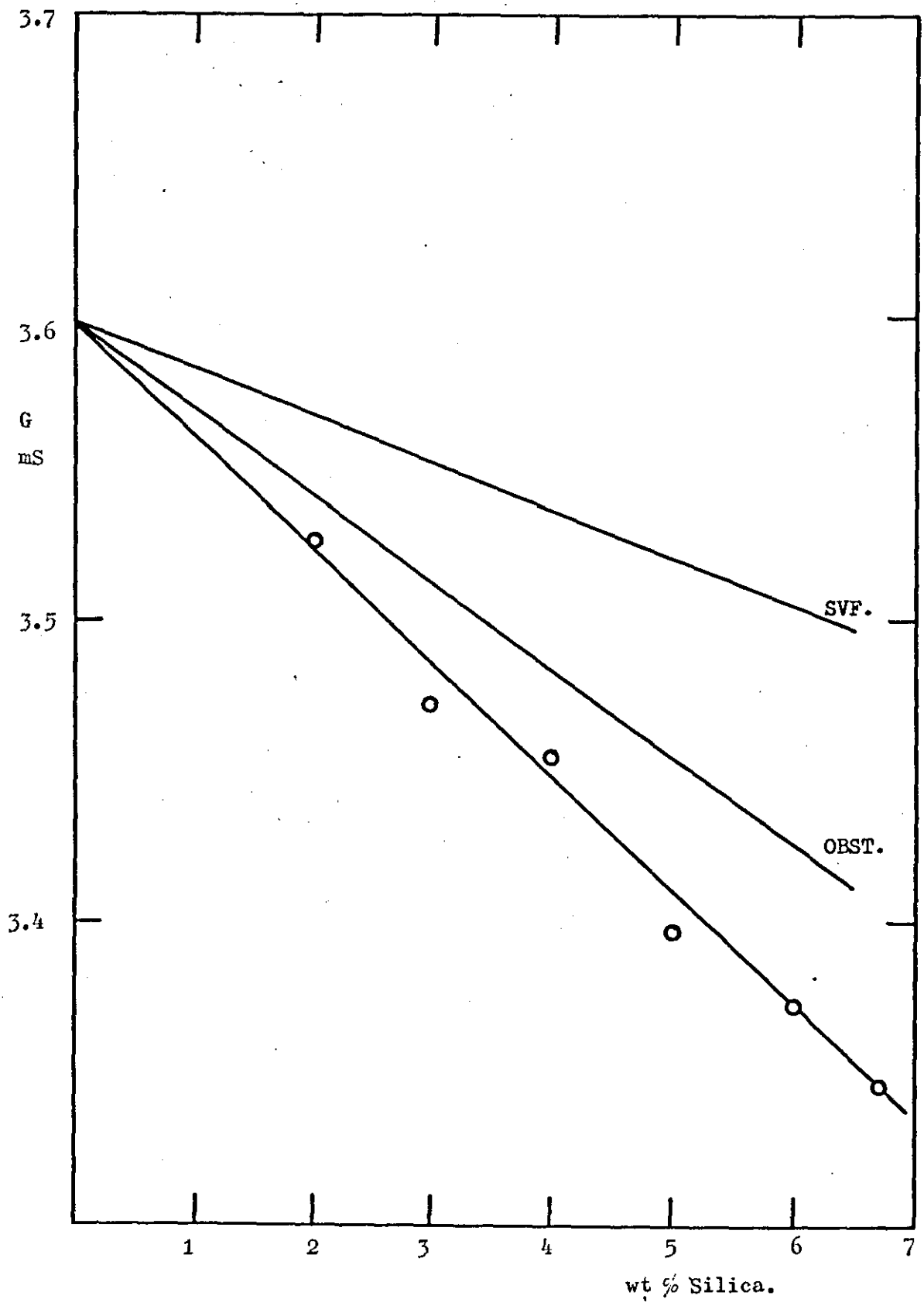

packing types and the manufacturers value of 6×10^{-4}cm for the mean radius of the aggregates, r_a . Primary particles have a density of 2.2 g cm^{-3} = ϱ_p, and the bulk density, ϱ_b, of the silica powder is 0.0369 g cm^{-3}.

The void volume, V, in the silica powder for any packing type is related to the bulk density ϱ_b by:

$$\varrho_b = (1 - V)\varrho_a \qquad 5.8$$

Using density x volume = mass, then for aggregates :

$$\text{volume} = \frac{4}{3}\pi r_a^3 \text{ , mass } = N_a . \frac{4}{3}\pi r_p^3 . \varrho_p$$

$\therefore$ the density of an aggregate ϱ_a will be given by :

$$\varrho_a = N_a . \frac{4}{3}\pi r_p^3 . \varrho_p / \frac{4}{3}\pi r_a^3$$

which reduces to :

$$\varrho_a = \frac{N_a r_p \varrho_p}{r_a^3} \qquad 5.9$$

Combining equations 5.8 and 5.9 gives :

$$\varrho_b = \frac{(1 - V) N_a r_p^3 \varrho_p}{r_a^3} \qquad 5.10$$

The void volumes for some of the common types of packing of spherical particles are given in table 3.1. The minimum void volume for close packing is 26% , and substitution of this value in equation 5.10 will allow evaluation of the minimum value of the other unknown, N_a , the number of primary particles per aggregate, giving a useful base line for comparison:

$$0.0369 = \frac{(1 - 0.26) r_p^3 \times 2.2 N_a}{(6 \times 10^{-4})^3} \qquad 5.11$$

where r_p is the value determined from equations 5.6 and 5.7, i.e. 6.82×10^{-7} cm. The value of N_a found from equation 5.11 is 5.043×10^8 primary particles per aggregate. Therefore the number of aggregates per gram, $N_s = n/N_a$, and yields a value of 6.789×10^8 aggregates per gram of silica powder.

Consider now the silica powder dispersed in the acid. The value of ρ_{sa}, the effective density of silica in electrolytes will be assumed to be that due to dispersed silica aggregates.

Substitution of the value of $\rho_{sa} = 1.66 \pm 0.03$ gcm^{-3} determined from the conductivity measurements into equation 5.9 leads to a value of 5.14×10^8 for the number of primary particles in an aggregate, N_a. A comparison of this value to that obtained for a close packed aggregate in the silica powder, 5.043×10^8, and bearing in mindthe various assumptions made and the accuracy of the value for ρ_a, the conclusion is reached that on dispersion of the silica powder in an electrolyte, the aggregates of close packed primary particles are dispersed with minimal loss of primary particles from the close packed condition. The suggestion could also be advanced that the inter-aggregate interactions in the powder must be weak compared to that between the close-packed primary particles.

The number of aggregates per gram N_s can be determined from the total number of primary particles calculated from equations 5.6 or 5.7 divided by Na, the number of primary particles per aggregate, and yields a value for N_s of 6.789×10^8 aggregates g^{-1}.

Using this value of N_s, the distributions of aggregates in a gel, and hence the gel structure, can be discussed. Particularly the two simple distributions where:

1. all aggregates are distributed evenly through the available volume (i.e. viscous solution).
2. all aggregates are linked in straight chains (gel).

(1) 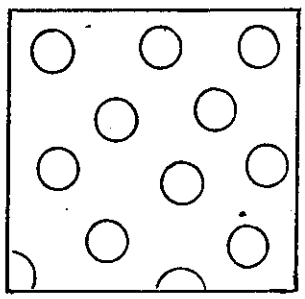 (2) 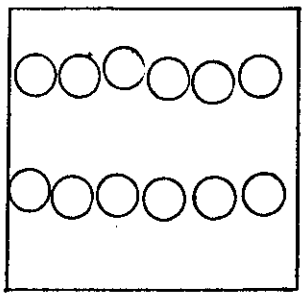

Consider a unit volume (1 cm^3) of a 6% M5 silica/40% sulphuric acid gel. The gel is made from 6 g silica + 94 g acid → 100 g gel, a total of $6N_s$ aggregates/100 g gel. Therefore the number of aggregates per cm^3, N_{sc} is:

$$N_{sc} = \frac{6N_s/100g}{\rho \text{ gel}} \qquad 5.12.$$

If there were sufficient aggregates to be close packed in the unit volume then the maximum number of sites, N_{cp}, would be given by:

$$\frac{1}{4/3\ \pi\ r_a^3} \times 0.74 = N_{cp} \qquad 5.13.$$

N_{sc}/N_{cp} will give the number of close packed sites filled. The values of N_{cp} and N_{sc} are 8.18×10^8 and 5.379×10^7 respectively, therefore only 6.6% of the sites are filled. The aggregate separation assuming a uniform distribution of aggregates would be 2.09×10^{-3} cm.

This clearly demonstrates that over-dispersion of the silica will cause irreversible network-breaking to give a distribution of aggregates that are sufficiently separated to be statistically unlikely to reform a gel network.

If the aggregates were distributed as straight chains the number of aggregates per 1 cm chain would be 1 cm/aggregate diameter, which is $1/12 \times 10^{-4}$ or 833 aggregates per 1 cm chain. Therefore, the number of such chains in 1 cm^3 of gel assuming no cross-linking is $N_{sc}/833$, which yields a value of 6.46×10^4 chains per 1 cm^3. A relaxation of the straight chain assumption and only a small degree of cross-linking of chains could produce an extensive 3 Dimensional gel network. This is presumably the case for the gels and is remarkable for a system with a volume fraction of solids of 0.0365.

5.18. The Influence of Gelled Electrolytes on Capacitor Performance.

A comparison of the performance of the fifty capacitors containing gels prepared by the Loughborough method with the performance of the fifty capacitors containing production gels showed very little difference between the two batches. This result is hardly surprising as both gels contain exactly the same concentration of silica and sulphuric acid. The variations in the anode and cathode, in the anode cathode spacing, and the amount of gel incorporated in the capacitor all contribute to the small differences between the various capacitors. The testing methods used to examine the capacitors are relatively insensitive to the effects due to the electrolyte compared to those due to the anodic oxide dielectric. The results of the measurements are given in Table 5.5 - 5.8 and are summarised for easy comparison in Table 5.9.

Table 5.5

Comparison of Initial Capacitor Parameters with those obtained after 1000 Hours Endurance Test for the two groups of Capacitors.

Capacitors with Production Gel.

Initial Cap. µF	Final Cap. µF	Initial Tan d. %	Final Tan d. %	Initial Leak 13. µA	Final Leak 13. µA	Initial Leak 15. µA	Final Leak 15. µA
223	222	8.9	7.8	1.0	0.6	0.7	0.4
226	226	6.6	6.1	0.8	0.5	0.8	0.4
222	220	6.5	6.1	0.8	0.6	0.7	0.4
210	210	6.4	6.0	0.8	0.5	0.6	0.3
226	225	6.9	6.4	0.8	0.5	0.7	0.4
220	220	6.8	6.4	0.8	0.5	0.6	0.4
222	221	6.7	6.3	0.8	0.5	0.7	0.4
217	216	6.4	6.1	0.7	0.5	0.8	0.6
Capacitors with Loughborough Gel.							
220	218	7.6	7.0	0.9	0.8	0.6	0.4
224	224	8.4	8.9	0.8	0.8	0.5	0.4
222	223	5.6	6.5	0.9	0.7	0.7	0.4
214	214	6.6	6.0	0.8	0.7	0.5	0.4
220	221	10.1	10.6	0.8	0.7	0.6	0.4
216	214	9.3	9.5	0.8	0.7	0.5	0.4
222	222	7.8	7.8	0.8	0.7	0.5	0.4
223	223	6.4	6.1	0.8	0.6	0.5	0.4

Table 56

Comparison of Capacitor Parameters of the two groups of Capacitors at -55 C, and after 5 Temperature Cycles (-55 C — +I25 C.).

-55 C Cap. µF	-55 C Impedance	-55 C Impedance	-55 C % C	After 5 Temperature Cycles. Cap. µF	Tan d. %	Leak I. µA
I76	2.0	2.2	20	22I	6.I	I.5
I70	2.8	3.0	24	225	7.2	2.I
I82	2.5	2.5	I8	224	6.6	I.0
I80	2.4	2.5	20	227	6.5	0.9
I85	2.3	2.3	I6	222	6.I	I.0
I58	2.5	2.5	27	2I8	8.6	0.9
I8I	I.8	I.8	I7	2I9	6.0	0.9
I84	2.5	2.5	I8	222	6.2	0.9
I79	I.6	I.6	I8			
I84	2.2	2.2	I5			
Capacitors with Loughborough Gel.						
I76	I.9	I.9	I9	2I9	5.9	I.0
I73	2.6	2.2	I9	2I4	6.I	0.9
I46	4.6	4.7	35	224	8.0	I.0
I75	4.8	5.2	22	224	8.I	22.0
I64	4.I	4.2	24	2I6	8.I	II.0
I76	3.2	3.4	I9	2I9	5.8	0.9
I70	5.I	5.3	24	226	7.4	0.9
I85	2.9	3.0	I6	22I	6.5	I.0
I80	2.4	2.6	I8			
I47	4.7	4.8	32			
I8I	2.7	2.7	I5			
I80	2.7	2.5	I8			

Table 5.7

Comparison of Capacitor Parameters of the two groups of Capacitors after a further 5 Temperature Cycles, and at +I25 C.

After a further 5 Cycles			+I25 C	+I25 C	+I25 C	+I25 C
Cap. µF	Tan d. %	Leak I. µA	Cap. µF	Tan d. %	Leak I. µA	C%
22I	6.8	I.4	230	II.8	3.2	4.5
224	8.I	I.8				
224	7.0	0.8	234	9.4	2.0	4.9
226	7.0	0.8				
222	6.9	0.9				
2I8	9.3	0.8	230	I0.0	I.8	6.0
220	6.5	0.9	230	I0.2	2.3	5.5
225	6.8	0.8	236	9.I	2.4	5.4
			230	9.0	I.8	5.5
			238	9.5	2.0	9.7
			235	9.5	I.9	5.9
Capacitors with Loughborough Gel.						
220	6.6	0.8	230	8.2	I.6	5.5
2I4	6.6	0.7	225	8.3	I.3	5.6
224	9.0	0.8	235	7.5	I.4	5.4
224	9.0	3.9				
2I7	8.I	8.9				
2I9	7.7	0.8				
226	8.8	0.8	237	7.8	I.2	5.3
22I	7.2	0.7				
			232	8.0	I.7	5.5
			230	9.3	I.6	6.0
			226	8.2	I.I	5.6
			23I	8.3	I.2	5.5

Table 5.8

Comparison of Initial Capacitor Parameters with those obtained after Temperature Cycling and Vibration Tests for the two groups of Capacitors.

Capacitors with Production Gel.

Initial Cap. µF	Final Cap. µF	Initial Tan d. %	Final Tan d. %	Initial Leak I3. µA	Final Leak I3. µA
220	22I	6.2	6.7	0.8	5.8
2I8	Failed	-	-	-	-
224	225	7.5	6.7	I.I	6.0
223	224	6.7	6.8	0.8	I.0
226	227	6.9	6.9	0.8	9.2
220	22I	6.5	9.I	0.8	2.4
2I7	2I8	5.6	9.2	0.8	0.9
2I8	220	6.2	6.5	0.7	I.0
224	225	6.4	9.8	0.9	I.I
2I8		6.4		0.9	
2I7		6.8		0.9	
222		6.6		0.9	

Capacitors with Loughborough Gel.

2I8	2I8	6.2	8.0	0.9	I.6
2I3	2I4	6.3	6.6	0.9	I.I
223	224	8.7	6.9	I.0	2.6
223	222	8.2	I2.I	I.0	I3.6
2I6	2I4	8.5	I2.0	0.9	4.6
2I8	2I8	7.9	8.5	0.9	I.0
225	226	8.0	8.3	0.9	I.6
220	22I	6.0	7.2	0.9	I.8
220		7.2		0.9	
2I7		9.5		I.0	
2I4		6.8		0.9	
2I9		6.8		0.9	

Table 5.9

Comparative Table of Mean Results.

Test		Capacitors with Production Gel.	Capacitors with Loughborough Gel.
Initial	Cap	221	220
	Tan d.	6.9	7.7
	Leak I. 3	0.81	0.82
	5	0.52	0.55
After 1000 Hours.	Cap.	220	220
	Tan d.	6.4	7.8
	Leak I. 3	0.75	0.71
	5	0.40	0.40
Initial	Cap.	220.6	219
	Tan d.	7.6	7.6
	Leak I.		
After Temp. Cycling and Vibration Tests.	Cap.	223	220
	Tan d.	7.7	8.7
	Leak I. 3	2.6	1.93
-55 C	Cap.	178	171
	Impedance.	2.23	3.5
	ΔC%	19.7	21.7
After 5 Cycles.	Cap.	221	220
	Tan d.	6.7	7.0
	Leak I.	1.15	1.1
After 5 more Cycles.	Cap.	222	220
	Tan d.	8.2	7.9
	Leak I.	1.0	0.8
+125 C	Cap.	233	231
	Tan d.	9.8	8.2
	Leak I.	2.18	1.39
	ΔC%	5.38	5.58

Bearing in mind that the differences between the two batches of capacitors are very small, there are some general comments which can be made. With reference to the initial room temperature measurements, the capacitance of the Loughborough gel capacitors was slightly lower and of smaller standard deviation compared to the production gel capacitors. After 1000 hours at 85°C with a potential of 50 Volts applied the Loughborough gel capacitors had suffered a smaller loss of capacitance than the production gel capacitors, but the standard deviation of the Loughborough gel capacitors had risen to that of the production gel capacitors.

This implies that the better dispersed Loughborough gels with their larger degree of network formation compared to the production gels had deteriorated after 1000 hours endurance test. A similar comment may be made with reference to the higher Tan d (%) of the Loughborough gel capacitors.

The results of the temperature cycling and vibration tests again show a smaller standard deviation of Capacitance, Tan d and leakage current for the Loughborough gel capacitors.

In terms of overall suitability for use in capacitors the Loughborough gels are not as useful, particularly with regard to the high impedance at -55°C and overall lower capacitance.

The changes in properties of capacitors as a function of gel concentration, all gels prepared by the Loughborough method, were very small and showed no general trend. In fact the only measurements of significance were the -55°C impedance and capacitance measurements.

The capacitance was much lower for 0% silica and the impedance was half that of the gel capacitors. Although there is a slight maximum in the plot of initial capacitance as a function of gel concentration, this is more probably attributable to problems in the dispensing of gels into the capacitors for the very much moreviscous 7 and 8% silica than to a real effect.

The results of the measurements are given in tables 5.10 - 5.12 and summarised in table 5.13.

The small anode-cathode spacing of the capacitors used for these comparitative tests is obviously not very suitable.

Further work of this type would be of more value if the spacing was considerably increased, possibly by mounting the anode and cathode in a tubular casing several centimetres in length.

Table 5.10

Comparison of Capacitor Parameters for Capacitors with different concentrations of Gel Electrolyte.

% Silica in Gel.	Initial Cap.	Final Cap.	Initial Tan d.	Final Tan d.	Initial Leak I.	Final Leak I.
0	210	209	5.4	6.4	1.7	1.2
	209	209	5.4	6.0	1.0	1.1
	210	210	6.1	5.8	1.0	1.0
	216	216	6.2	5.8	1.0	1.1
	200		5.5		0.9	
	210		5.6		0.9	
8	211	210	5.0	6.0	1.8	1.4
	207	206	5.0	7.6	1.0	1.3
	207	207	5.4	6.0	0.9	1.0
	209	210	5.0	5.5	0.9	1.0
	214		4.8		0.9	
	198		5.2		0.9	
7	204	204	5.2	5.6	0.9	2.5
	212	212	5.3	6.0	0.9	1.0
	202	202	5.5	8.1	1.4	1.2
	211	212	5.5	5.5	2.1	1.1
	206		5.3		0.9	
	200		5.5		0.9	
6	199	199	5.4	5.5	0.9	0.8
	212	212	5.6	6.2	1.0	3.4
	211	211	5.0	5.2	0.9	1.0
	219	219	5.4	5.4	0.9	1.3
	213		5.6		0.9	
5	216	216	5.6	5.9	0.9	5.1
	208	209	5.1	5.0	0.9	0.8
	210	211	5.1	5.7	0.9	1.9
	208	208	5.5	6.2	0.9	1.1
	214		5.3		0.8	

Table 5.11

Comparison of Capacitor Parameters for Capacitors with different concentrations of Gel Electrolyte.

% Silica in Gel.	-55 C Cap.	-55 C Impedance	-55 C Impedance	-55 C % C	After IO Temperature Cycles. Cap.	Tan d.	Leak I.
0	I52	0.8	I.0	27.6			I.I
	I75	0.8	0.7	I6.3			0.9
	I78	I.0	I.4	I5.2	2I0	6.2	I.2
	I64	I.2	I.2	24.0	2I6	6.0	I.2
	I68	0.7	0.9	I6.0	200	5.7	I.2
	I74	0.9	I.I	I7.0	2I0	5.7	I.I
8	I76	I.4	I.4	I6.6			I.5
	I74	I.8	I.8	I5.9			I.0
	I75	I.8	I.8	I5.5	208	5.6	I.3
	I77	I.6	I.7	I5.3	2I0	5.4	I.3
	I83	I.6	I.7	I4.5	2I4	5.I	I.3
	I69	I.9	I.7	I4.6	I99	5.3	I.2
7	I76	2.0	I.9	I3.7			I.0
	I83	2.4	2.5	I3.7			I.I
	I74	2.6	2.6	I3.9	202	5.8	I.3
	I82	2.7	2.7	I3.7	2I2	5.7	I.4
	I76	I.6	I.6	I4.6	207	5.4	I.3
	I70	2.0	2.0	I5.0	200	5.8	I.3
6	I70	I.8	I.8	I4.6			I.0
	I83	2.5	2.0	I3.7			I.I
	I80	2.2	I.8	I4.7	2II	5.2	I.2
	I88	I.8	I.6	I4.2	220	5.5	I.3
	I80	2.3	2.I	I5.5	2I4	5.6	I.2
	I80	2.0	I.8	I5.I	2I2	5.6	I.3
5	I8I	2.0	2.I	I6.2			0.9
	I80	I.8	I.6	I3.5			0.9
	I83	2.3	2.I	I2.9	2II	5.5	I.2
	I85	2.6	2.2	II.I	209	5.7	I.I
	I87	2.I	I.7	I2.6	2I4	5.5	I.I

Table 5.12

Comparison of Capacitor Parameters for Capacitors with different concentrations of Gel Electrolyte.

% Silica in Gel.	+I25 C Cap.	+I25 C Tan d.	+I25 C Leak I.	+I25 C % C
0	220	7.8	5.4	4.8
	220	6.8	I.5	5.3
	22I	7.I	2.0	5.2
	228	7.3	I.8	5.6
	2I0	6.8	I.6	5.0
	222	7.3	I.8	5.7
8	224	7.4	4.3	6.2
	2I8	6.8	I.6	5.3
	2I8	6.8	I.6	5.3
	220	6.5	I.6	5.3
	225	6.5	2.5	5.I
	2I0	6.7	2.7	6.I
7	2I2	8.0	I.6	3.9
	222	7.4	I.3	4.4
	2II	6.8	I.8	4.5
	222	7.5	I.5	5.2
	2I7	7.5	I.5	5.3
	2I0	9.3	I.2	5.0
6	2I0	7.3	I.7	5.6
	224	7.5	3.8	5.7
	224	7.2	I.9	6.2
	226	7.6	I.7	3.2
	225	7.8	I.6	5.6
	224	9.8	I.5	5.7
5	220	7.6	I.7	I.9
	223	7.6	I.7	7.2
	223	7.6	I.7	6.2
	220	8.3	2.I	5.8
	224	7.5	I.6	4.7

Table 5.13

Comparative Table of Mean Results of Capacitor Parameters for Capacitors with different concentrations of Gel Electrolyte.

		% Silica in Gel Electrolyte				
		0 %	8 %	7 %	6 %	5 %
Initial	Cap.	209.2	207.7	205.8	2II.0	2II.7
	Tan d.	5.7	5.I	5.4	5.4	5.4
	Leak I.	I.I	I.I	I.2	0.9	I.0
-55 C	Cap.	I68.5	I75.7	I76.8	I80.2	I83.8
	Impedance	I.0	I.7	2.2	2.0	2.I
	%ΔC	I9.4	I5.4	I4.I	I4.6	I3.2
After IO Temp. Cycles	Cap	209.0	207.8	205.3	2I4.3	2I2.0
	Tan d.	5.9	5.4	5.7	5.5	5.7
	Leak I.	I.2	I.3	I.3	I.3	I.I
-I25 C	Cap.	220.2	2I9.2	2I5.7	222.2	222.7
	Tan d.	7.2	6.8	7.8	7.9	7.9
	Leak I.	2.4	2.4	I.5	2.0	I.8
	%ΔC	5.3	5.6	4.8	5.3	5.2
After Vibr Test	Cap.	2II.0	208.3	207.5	2I0.3	2II.0
	Tan d.	6.0	6.3	6.3	5.6	5.7
	Leak I.	I.I	I.2	I.5	I.6	2.2

CHAPTER 6.

6.1. Conclusions.

The differential capacitance of the tantalum electrode in a number of aqueous electrolyte solutions containing simple inorganic anions is below 9 $\mu F\ cm^{-2}$ at all potentials in the experimentally accessible region. The low values are attributed to a thin layer of protective oxide which thickens at the more positive potentials. In oxalate solutions for a concentration range of at least 0.0135 to 0.5M, and over the polarizable region of -0.8 to -0.3V, the capacitance is much higher and corresponds to that expected for a clean metal surface in contact with an aqueous solution.

The point of zero charge potential must lie outside the experimental region because no concentration dependent diffuse layer capacity minimum was found.

Field recrystallization of tantalum pentoxide is considerably reduced during anodization in gelled electrolytes compared to that in silica free sulphuric acid electrolytes.

The onset of scintillation occurs at a higher voltage for the gelled electrolytes. Scintillation voltage increases with temperature of anodization for both electrolytes, the voltage always being higher for the gelled electrolytes.

The reduction in field recrystallization and higher scintillation voltage for the gelled electrolytes is beneficial for capacitors because the leakage current across the dielectric will be reduced.

The other properties of tantalum pentoxide are unaffected by anodizing in gelled electrolytes, and there is no evidence for silica incorporation in the oxide.

The addition of silica to sulphuric acid or to potassium chloride solutions leads to a reduction in conductivity except for 0.001D H_2SO_4 and 0.01D KCl where the conductivity increases, probably because there is a surface conductivity contribution at

these low electrolyte concentrations which is the major contribution.

For all silica and electrolyte concentrations the conductivity, and therefore the gel structure, are dependent on the method and degree of dispersion of the silica in the electrolyte. The use of a plunger mixer produces gels which exhibit a reproducible conductivity.

The reduction in conductivity of the electrolytes on addition of silica is due to the loss in conducting volume as silica is effectively an inert insulator, with a further reduction in conductivity due to the increase in path length of the moving ions as they move past the insulating obstructions.

The effective density of silica in the gelled electrolytes is 1.66 ± 0.03 g cm^{-3} compared to the value of 2.2 g cm^{-3} for the silica powder alone. Use of the effective density of silica in calculating the volume fractions of silica in the gel required to evaluate the conductivity obstruction equations allows the reduction in conductivity of silica/electrolyte systems to be predicted accurately from the conductivity of the silica free electrolyte and the wt% of silica in the gel.

Calculations are given which show that an extensive 3D gel structure is possible from well dispersed silica aggregates at 6% concentration in 40% sulphuric acid.

The influence of the mode of dispersion of silica in acid electrolyte on the properties of capacitors was very small, and the well dispersed gels produced by the standard method are possibly less useful than the poorly dispersed production gels because of their lower $-55^{\circ}C$ impedance.

The effect of gel concentration on capacitor performance was small, but 3.7% may be the optimum concentration for ease of handling and overall capacitor performance.

6.2 Further Work.

There is a considerable amount of further investigation required on many aspects of this work.

The tantalum and Ta/Ta_2O_5 electrodes should be examined in solutions containing other complexants of a similar type to oxalate where the experimentally accessible potential range might be wider, or possibly include the point of zero charge potential. The use of the new techniques of rapid measurement of impedance using computer control being developed at present would be of considerable advantage in this system where the protective oxide film is difficult to force off the metal.

The rheological properties of gelled electrolytes should be examined to determine the minimum quantity of silica required to gel the electrolyte at each electrolyte concentration, and the relative strength of the various gels. The effectiveness of the different methods of dispersing the silica should also be investigated in addition to the effect of the method of dispersion on the final conductivity of the gel. These measurements would be of use in explaining the influence of the gel structure on the conductivity, and may lead to a better understanding of the gel structure itself.

A cryostat should be constructed to enable accurate conductivity measurements to be made at $-55^{\circ}C$, and also to allow a more precise comparison of the $-55^{\circ}C$ impedance of capacitors containing various gelled electrolytes which is of commercial importance.

The design of capacitors with a longer conducting pathway through the electrolyte between the electrodes should be varied to allow an increase in the dependence of capacitor properties on the electrolyte to aid the formulation of the optimum gel composition.

REFERENCES.

Aerosil , GOST (All-Union State Standard) 14922-69 .

Alexander,G.B.,(1957) J.Amer.Chem.Soc. 61(1957)1563 .

Allgood,R.W., LeRoy,D.J., and Gordon,A.R.,(1940)
J.Chem.Phys. 8(1940)418 .

Allgood,R.W., and Gordon,A.R.,(1942)
J.Chem.Phys. 10(1942)124 .

Archie,G.E.,(1942) Trans.A.I.M.E. 146(1942)54 .

Atkins,P.W.,(1978) Physical Chemistry p727 Oxford University Press 1978 .

Bechtold,M.F., and Snyder,O.E.,(1951) U.S.Pat. 2,574,902 (E.I. du Pont de Nemours & Co.) 1951 .

Benson,G.C., and Gordon,A.R.,(1945)
J.Chem.Phys. 13(1945)473 .

Bernal,J.D., and Fowler,R.H.,(1939)
J.Chem.Phys. 1(1939)515 .

Bockris,J.O'M., and Parry-Jones, (1953)
Nature 171(1953)930 .

Bockris,J.O'M., Devanathan,M.A.V., and Muller,K.,(1963)
Proc.Roy.Soc. London A274(1963)55 .

Borisova,T.I., and Proskurnin,M.,(1936)
Acta Physicochim. 4(1936)819 .

Borisova,T.I., and Proskurnin,M.,(1940)
Acta Physicochim. 12(1940)371 .

Borisova,T.I., and Proskurnin,M.,(1947)
Zh.Fiz.Khim. 21(1947)463 .

Bottcher,C.J.F.,(1945) Rec.Trav.Chim. pays-bas 64(1945)47 .

Bouhard,G.C.,(1907) French Pat. 377931 30th April 1907 .

Brodd,R.J., and Hackerman,N.,(1957)
J.Electrochem.Soc. 104(1957)704

Brody,O.V., and Fuoss,R.M.,(1956)
J.Phys.Chem. 60(1956)177 .

Bruggeman,D.A.G.Von.,(1935) Ann. Physik 5(24)(1935)636 .

Brauner,S., Emmett,P.H., and Teller,E.,(1938)
J.Amer.Chem.Soc. 60(1938)309 .

Cabot Carbon Ltd., CAB-O-SIL, How to use it, where to use it (C GEN-6)
CAB-O-SIL, Properties and Functions (C GEN-8)

Campbell,A.N.,and Kartzmark,E.M.,(1952)
Canad.J.Chem. 30(1952)128 .

Campbell,A.N., Kartzmark,E.M., Bisset,D., and Bednas,M.E.,(1953)
Canad.J.Chem. 31(4)(1953)303 .

Campbell,D.S.,(1966) The Use of Thin Films inPhysical Investigations
p11, Ed. Anderson. Academic Press London,1966 .

Campbell,D.S.,(1971) The Radio and Electronic Eng. 41(1)(1971)5 .

Carman,P.C.,(1940) Trans.Farad.Soc. 36(1940)964

Chapman,D.L.,(1913) Phil.Mag.(6),25,(1913)475 .

Charlot,G.,(1957) L'analyse quantitative et les reactions en solution
4th Edition. Masson,Paris 1957 .

Cooper,I.L., and Harrison,J.A.,(1975)
J.Electroanal.Chem.66(1975)85 .

Cooper,I.L., and Harrison,J.A.,(1977a)
Electrochimica Acta 22(1977)519 .

Cooper,I.L., and Harrison,J.A.,(1977b)
Ibid. 22(1977)1361 .

Cooper,I.L., and Harrison,J.A.,(1977c)
Ibid. 22(1977)1365 .

Cooper,I.L., and Harrison,J.A.,(1978)
Ibid. 23(1978)545 .

Cotten,F.A., and Wilkinson,G.,(1966)
Advanced Inorganic Chemistry, 2nd Edition,
p919-930,Interscience 1966 .

Coursey,P.R.,(1937) Electrolytic Condensers, Chapman and Hall, London 1937 .

Daggett,H.M., Blair,E.J., and Kraus,C.A.,(1951) J.Amer.Chem.Soc. 73(1951)799 .

Damaskin,B.B., and Frumkin,A.N.,(1974) Electrochimica Acta 19(1974)173 .

Darling,H.E.,(1964) J.Chem. and Eng. Data 9(3)(1964)421 .

Debye,P., and Huckel,E.,(1923) Physik Zeits 24(1923)185 .

Deeley,P.M.,(1938) Electrolytic Capacitors, Cornell Dubilier Electric Corp.,1938 .

Delahay,P.,(1965) Double Layer and Electrode Kinetics, J.Wiley & Sons Inc, (Interscience) New York, London, Sydney, 1965 .

De Levie,R.,(1967) Adv.Electrochem. and Electrochem.Eng. 6(1967)329 .

Duclaux,J.,(1953) Colloides et Gels, Gauthiers-Villars, Paris 1953 .

Feates,F.S., Ives,D.J.G., and Pryor,J.H.,(1956) J.Electrochem.Soc. 103(1956)580 .

Franklin,R.W.,(1961) Inst.Elec.Eng. 3585(1961)525 .

Fricke,H.,(1924) Phys.Revs. 24(1924)575 .

Fricke,H.,(1931) Physics 1(1931)106 .

Fricke,H.,(1953) J.Phys.Chem. 57(1953)934 .

Frumkin,A.N., Gorodetzkaya,A., Kabanov,B.N., and Nekrassov,N.J.,(1932) Phys.Z.Sowjet. 1(1932)225 .

Frumkin,A.N.,(1937) Actualites sci.industr.,No.373 , Paris 1937 .

Frumkin,A.N.,(1955) Z.Elektrochem. 59(1955)807 .

Frumkin,A.N.,(1960) J.Electrochem.Soc. 107(1960)461 .

Frumkin,A.N.,(1963) Adv.Electrochem. and Electrochem.Eng. 13(1963)287.

Gaut,G.C.,(1957) Proceedings of the International Symposium on Electronic Components, Malvern 1957, paper no. 5 .

Georgiev,A.M.,(1945) The Electrolytic Capacitor,Murray Hill Books 1945.

Gerzhberg,Yu.I., Krumgal'z,B.S., Ryabikova,V.M., Traber,D.G., Kozlov,D.A., and Trepalin,A.I.,(1969) Elektrokhimiya 5(12)(1969)1457 .

Gibbs,J.W.,(1928) Collected Works Vol. 1,page429 2nd Edition, Longmans,Green,New York, 1928 .

Glasstone,S., Laidler,K.J., and Eyring,H.,(1941) The Theory of Rate Processes, Chapter 10, McGraw-Hill Book Co. Inc. 1941 .

Gordon,A.R.,(1940,1942, and 1945) See Allgood,R.W., et al (1940,1942) Benson,G.C.,and Gordon,A.R.,(1945) .

Gorodetzkaya,A., and Kabanov,B.N.,(1934) Phys.Z.Sowjet. 5(1934)418 .

Gouy,G.,(1910) J.Phys.Radium (4)9(1910)457 .

Gouy,G.,(1910) Compt.rend. 149(1910)654 .

Gouy,G.,(1917) Ann.Phys.Paris 7(1917)163 .

Grahame,D.C.,(1941) J.Amer.Chem.Soc. 63(1941)1207 .

Grahame,D.C., and Whitney,R.W.,(1942) J.Amer.Chem.Soc. 64(1942)1548 .

Grahame,D.C.,(1947) Chem.Revs. 41(1947)441 .

Grahame,D.C.,(1949) J.Amer.Chem.Soc. 71(1949)2975 .

Grahame,D.C.(1954) J.Amer.Chem.Soc. 76(1954)4819 .

Grahame,D.C.,(1955) Ann.Rev.Phys.Chem. 6(1955)346 .

Grahame,D.C.,(1957) J.Amer.Chem.Soc. 79(1957)2093 .

Hague,B., and Foord,T.R., (1971) Alternating Current Bridge Methods. 6th Edition, Pitman and Sons, London 1971.

Hamer,W.J.,(1959) Structure of Electrolyte Solutions, Chapter 4, Ed. Hamer, J.Wiley & Sons Inc. New York, Chapman & Hall Ltd. London 1959 .

Hampson,N.A.,(1972) Specialist Periodical Report on Electrochemistry, 2(1972)117 The Chemical Society London .

Hampson,N.A.,(1973) Specialist Periodical Report on Electrochemistry, 3(1973)41 The Chemical Society London .

Harris,L.F.,(1974) Electrocomponent Sci. and Technol. 1(1974)11 .

Heesch,H., and Laves,F.,(1933) Z.Krist. A85(1933)443.

Helfferich,F.,(1962) Ion Exchange, McGraw-Hill Book Co.Inc. 1962 .

Helmholtz,H.L.F.von.,(1879) Wiss.Abh.Phys.Tech.Reichsast 1(1879)925 .

Hermans,P.H.,(1949) Colloid Science Volume 2 Ed. Kruyt page 483 Elsevier Scientific Pub.Co. New York 1949 .

Hills,G.J., and Payne,R.,(1965) Trans.Farad.Soc. 61(1965)316 .

Hills,G.J., and Payne,R.,(1965) Trans.Farad.Soc. 61(1965)326 .

Hoar,T.P.,(1959) Modern Aspects of Electrochemistry Volume 2, page 262, Butterworth Scientific Pub. London 1954.

Iler,R.K.,(1952) J.Phys.Chem. 56(1952)680 .

Iler,R.K.,(1955) The Colloid Chemistry of Silica and Silicates, Cornell University Press,Ithaca,New York 1955 .

Iler,R.K.,(1973) Surface and Colloid Science Ed. Matijevic, 6(1973)1.

Isaacs,H.S., and Leach,J.S.L.,(1962-3) J.Inst.Metals 91(1962-3)80 .

Jackson,N.F.,(1973) J.Appl.Electrochem. 3(1973)91 .

Jones,G., and Josephs,R.C.,(1928) J.Amer.Chem.Soc. 50(1928)1049 .

Jones,G., and Bollinger,G.M.,(1931) J.Amer.Chem.Soc. 53(1931)411 .

Jones,G., and Bradshaw,B.C.,(1933) J.Amer.Chem.Soc. 55(1933)1780 .

Jones,G., and Christian,S.M.,(1935)
J.Amer.Chem.Soc. 57(1935)272 .

Jones,G., and Bollinger,D.M.,(1935)
J.Amer.Chem.Soc. 57(1935)280 .

Jones,G., and Prendergast,M.J.,(1937)
J.Amer.Chem.Soc. 59(1937)731 .

Jordon-Lloyd,D.,(1926) Colloid Science Volume 1, Ed. Alexander, page 767,
Chem.Cataloque Co., New York 1926 .

Kittaka,S., and Morimoto,T.,(1976)
J.Coll.Int.Sci. 55(1976)431 .

Kohlrausch,F.,(1897) Wied.Ann. 60(1897)315 .

Kruyt,H.R.,Ed.(1952) Colloid Science Volume 1, page 363,
Elsevier Scientific Pub.Co. New York 1952 .

Levine,S., Bell,G.M., and Smith,A.L.,(1969)
J.Phys.Chem. 75(1969)3534 .

Lippmann,G.,(1875) Ann.Chim.Phys. 5(5)(1875)494 .

Manegold.E.,(1941) Kolloid Z. 96(1941)186 .

McMullen,J.J., and Hackerman,N.,(1959)
J.Electrochem.Soc. 106(1959)341 .

Mead,P.H.,(1962) Inst.Elec.Eng. 3656(1962)537 .

Moller,H.,(1908) Z.Phys.Chem. 65(1908)226 .

Morley,A.R.,(1970) Proc.Inst.Elec.Eng. 117(8)(1970)1648 .

Morley,A.R., and Campbell,D.S.,(1973)
Radio and Electronic Eng. 43(7)(1973)421 .

Mysels,K.J.,(1959) Introduction to Colloid Chemistry Chapter XV,
Interscience New York 1959 .

Orkina,T.N., and Aguf,I.A.,(1975)
Kolloidnyi Zhurnal 37(3)(1975)579 .

Parker,H.C., and Parker,E.W.,(1924)
J.Amer.Chem.Soc. 46(1924)312 .

Parsons,R., and Devanathan,M.A.V.,(1953)
Trans.Farad.Soc. 49(1953)404 .

Parsons,R.,(1954) Modern Aspects of Electrochemistry Volume 1,
Ed. Bockris, page 103, Butterworth Scientific Pub.
London 1954 .

Parsons,R.,(1975) J.Electroanal.Chem. 59(1975)229 .

Pourbaix,M.,(1966) Atlas of Electrochemical Equilibria in Aqueous
Solutions, Chapter IV, Section9.3 page 252 .

Proskurnin,M., and Frumkin,A.N.,(1935)
Trans.Farad.Soc. 31(1935)110 .

Quincke,G.,(1861) Pogg.Ann. 113(1861)513 .

Radczewski,O.E., and Richter,H.,(1941)
Kolloid.Z. 96(1941)1 .

Randles,J.E.B.,(1947) Disc.Farad.Soc. 1(1947)11 .

Rauter,R.,(1965) U.S. Patent 3,180,760 (Marc Inc.) 1965 .

Lord Rayleigh.(1892) Phil.Mag. 5(34)(1892)481 .

Rehbinder,P.A., and Wenstrom, (1944)
Acta Physicochim. 19(1944)36 .

Robinson,R.A., and Stokes,R.H.,(1970)
Electrolyte Solutions 2nd Edition, 5th Impression,
(revised) Butterworths, London.

Rose,W., and Bruce,W.A.,(1949)
Trans.A.I.M.E. 186(1949)127 .

Roughton,J.E.,(1951) J.Appl.Chem. 1.,Supplement Issue 2,(1951)S141 .

Shedlovsky,T.,(1930) J.Amer.Chem.Soc. 52(1930)1793 .

Shedlovsky,T.,(1932) J.Amer.Chem.Soc. 54(1932)1411 .

Shedlovsky,T., and Brown,A.S.(1934)
J.Amer.Chem.Soc. 56(1934)1066 .

Spiegler,K.S.,(1953) J.Electrochem.Soc. 100(11)(1953)303C .

Stern,O.,(1924) Z.Elektrochem. 30(1924)508 .

Tegart,W.J.McG.,(1956) Electrolytic and Chemical Polishing of Metals . Pergamon Press London 1956 .

Thornton,O.F.,(1949) Trans.A.I.M.E. 186(1949)328 .

Udupa,H.V.K., and Venkatesan,V.K.,(1974) Electrochemistry of the Elements Chapter II(3), Ed. Bard, Marcel Dekker New York 1974 .

Vermilyea,D.A.,(1954) Acta Met. 2(1954)482 .

Vermilyea,D.A.,(1955) J.Electrochem.Soc. 102(1955)207 .

Vermilyea,D.A.,(1957) Ibid 104(1957)427 .
Ibid " " 485 .
Ibid " " 542 .

Wang,J.H.,(1954) J.Amer.Chem.Soc. 76(1954)4755 .

Wein,M., (1896) Ann.Phys.Lpz. 58(1896)37 .

Weiser,H.B.,(1950) Colloid Chemistry 2nd Edition, page 307 J.Wiley & Sons Inc. New York 1950 .

Winkel,P., and de Groot,D.G.,(1958) Phillips Research Reports 13(1958)489 .

Wittman,A.,(1961) Oesterr. Chemiker-Ztg. 62(1961)245 .

Wyllie,M.R.J.,(1950) Trans.A.I.M.E. 189(1950)105 .

Wyllie,M.R.J., and Rose,W.D.,(1950) Nature (london) 165(1950)972 .

Wyllie,M.R.J., and Spangler,M.B.,(1952) Bull.Amer.Assoc.Petroleum Geol. 36(2)(1952)359 .

Young,L.,(1955) Trans.Farad.Soc. 51(1955)1250 .

Young,L.,(1961) Anodic Oxide Films, Academic Press London and New York 1961 .